AD-A058 507 UNCLASSIFIED STATE UNIV OF NEW YORK AT STONY BROOK MARINE SCIENCES--ETC F/6 13/2
FIELD INVESTIGATIONS OF THE NATURE, DEGREE, AND EXTENT OF TURBI--ETC(U)
JUL 78 J R SCHUBEL, H H CARTER, R E WILSON DACW39-76-C-0129
WES-TR-D-78-30



ADA 0 58507

# LEVELY

DREDGED MATERIAL RESEARCH PROGRAM



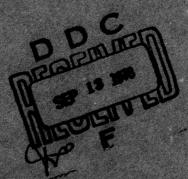
TECHNICAL REPORT D-78-30

FIELD INVESTIGATIONS OF THE NATURE DEGREE, AND EXTENT OF TURBIDITY GENERATED BY OPEN-WATER PIPELINE DISPOSAL OPERATIONS

J. R. Schubel, H. H. Corter, R. E. Wilson W. M. Wice, M. G. Heston, M. G. Green

Marine Sciences Research Conter State University of New York at Stony Break Stony Break, N. Y. 11794

> July 1978 First Parent



DOC FILE COPY



William D. C 20014

CHENNAL CALL COM

78 09 12 003



## DEPARTMENT OF THE ARMY WATERWAYS EXPERIMENT STATION, CORPS OF ENGINEERS

P. O. BOX 631 VICKSBURG, MISSISSIPPI 39180

IN REPLY REFER TO: WESYV

31 July 1978

SUBJECT: Transmittal of Technical Report D-78-30

TO: All Report Recipients

- 1. The technical report transmitted herewith represents the results of one research effort (Work Unit 6CO2) initiated as part of Task 6C, entitled "Turbidity Prediction and Control," of the Corps of Engineers' Dredged Material Research Program (DMRP). Task 6C, included as part of the Disposal Operations Project of the DMRP, was concerned with investigating the problem of turbidity and developing methods to predict the nature, extent, and duration of turbidity generated by dredging and disposal operations. Equal emphasis was also placed on evaluating both chemical and physical methods for controlling turbidity generation around dredging and disposal operations.
- 2. Although there are still questions about the direct and indirect effects of different levels of turbidity on various aquatic organisms, turbidity generated by dredging and disposal operations can be aesthetically displeasing. Therefore, regardless of the ecological effects associated with turbidity, it may be necessary under certain circumstances to be able to predict levels of turbidity that might be generated by a particular dredging or disposal operation. These predictions can then be used to evaluate the necessity for different control measures.
- This particular study was concerned with turbidity generated in the upper water column by open-water pipeline disposal operations. Based on plume characteristics measured at three estuarine sites along the Gulf Coast, a theoretical/empirical mathematical model was developed to predict suspended solids concentrations in and dimensions of a turbidity plume that might be generated by a typical open-water pipeline disposal operation. In addition to studying the dredged material suspended in the upper water column downcurrent of the operation, dissolved nutrients and heavy metals were also measured to determine the degree of release of these chemical constituents. Methodologies for predicting heavy metals/nutrient distributions and dissolved oxygen levels in the vicinity of a pipeline disposal operation were also developed as part of this research effort. This report is concerned only with the dredged material suspended in the upper water column and does not address the dispersion of the majority of the dredged material that forms a fluid mud layer over the bottom of the disposal area.

31 July 1978

WESYV

SUBJECT: Transmittal of Technical Report D-78-30

4. This study represents one of a series of reports on turbidity prediction and control. Other studies within Task 6C provide information on silt curtains, submerged pipeline discharge, and the generation of fluid mud dredged material. All research results from Task 6C are synthesized in a technical report entitled "Prediction and Control of Dredged Material Dispersion Around Dredging and Open-Water Pipeline Disposal Operations."

JOHN L. CANNON

as part of the Disposal Operations Protect of the DMAP, was concerned

2. Although their are still questions about the direct and indirect

Colonel, Corps of Engineers

Commander and Director

2

SECURITY CLASSIFICATION OF THIS PAGE (When Data Entered) READ INSTRUCTIONS
BEFORE COMPLETING FORM REPORT DOCUMENTATION PAGE I. REPORT NUMBER 3. RECIPIENT'S CATALOG NUMBER 2. GOVT ACCESSION NO. Technical Report D-78-30 TYPE OF REPORT & PERIOD COVERED 4. TITLE (and Subtitle) EIELD INVESTIGATIONS OF THE NATURE, DEGREE, AND EXTENT OF TURBIDITY GENERATED BY OPEN-WATER PIPELINE DISPOSAL OPERATIONS inal report PERFORMING ORG. REPORT NUMBER 8. CONTRACT OR GRANT NUMBER(\*) J. R. Schubel W. M. Wise Contract No. H. H. Carter DACW39-76-C-0129 R. E. Wilson Marine Sciences Research Center State University of New York at Stony Brook DMRP Work Unit No. 6C02 Stony Brook, N. Y. 11794 1. CONTROLLING OFFICE NAME AND ADDRESS July 1978 Office, Chief of Engineers, U. S. Army NUMBER OF Washington, D. C. 20314 297 14. MONITORING AGENCY NAME & ADDRESS(if different from Controlling Office) 15. SECURITY CLASS. (of this report) U. S. Army Engineer Waterways Experiment Station Unclassified Environmental Laboratory P. O. Box 631, Vicksburg, Miss. 39180 154. DECLASSIFICATION/DOWNGRADING 16. DISTRIBUTION STATEMENT (of this Report) Approved for public release; distribution unlimited. DISTRIBUTION STATEMENT (of the abstract entered in Block 20, If different from Report) Appendices B, C, and D were reproduced attached inside the back cover of this report. 19. KEY WORDS (Continue on reverse side if necessary and identify by block number) Dredged material Plumes Dredged material disposal Suspended solids Environmental effects Turbidity Field investigations Open water disposal 20. ABSTRACT (Continue on reverse stde if necessary and identity by block number) In response to the public's concern over the environmental effects of open-water disposal of dredged material, this study was undertaken to evaluate the characteristics of turbidity plumes in the vicinity of open-water pipeline disposal operations. In addition, the distribution and concentration of dissolved heavy metals, nutrients, and dissolved oxygen were evaluated. Based on field studies conducted in Corpus Christi Bay, Texas, Atchafalaya Bay, Louisiana,

(Continued)

DD FORM 1473 EDITION OF 1 NOV 65 IS OBSOLETE

Unclassified SECURITY CLASSIFICATION OF THIS PAGE (When Data Entered)

406 652

CON; 1

## SECURITY CLASSIFICATION OF THIS PAGE(When Data Entered)

20. ABSTRACT (Continued).

Cost '

and Apalachicola Bay, Florida, a simple model was developed to predict the spatial and temporal distributions of suspended solids in turbidity plumes.

Turbidity plume characteristics are primarily dependent on the discharge rate of the dredge, the settling velocity of the suspended dredged material, the water depth, the hydrodynamic regime (i.e., current velocity and diffusion velocity) of the disposal site, and the age of the plume. Several estimates of dredged material partitioning between the turbidity plume and the bottom layers indicate that 97 to 99 percent of the discharged slurry rapidly settles to the bottom of the disposal area within a few tens of meters of the discharge point. The remaining 1 to 3 percent is incorporated into the plume.

No well-defined plumes of dissolved metals were observed at any of the three sites, indicating that dissolution of metals from the suspended solids was limited. Increases in concentrations of suspended solids and particle-associated metals in the receiving waters were obviously associated with the discharge plume. Concentrations of dissolved ammonia and silica were locally increased near the discharge; however, no increases in dissolved phosphate were noted, despite high dissolved phosphate concentrations in interstitial water of the channel sediment being dredged.

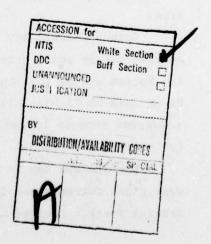
Elutriate test results using the channel sediment were found to have limited use in predicting changes in concentrations of dissolved metals during open-water disposal operations.

A simple model was developed to predict concentrations of particle-associated constituents.

Although large quantities of reduced sediment with a high oxygen demand are introduced into the water column during open-water pipeline disposal operations, only a small fraction of this material is reactive on a time scale comparable to that associated with the settling of the vast majority of the dredged material slurry. Dissolved oxygen levels in surface waters in the immediate vicinity of the pipeline discharge point are depressed by 1 to 2 mg/l with dissolved oxygen levels decreasing with depth due to increasing levels of suspended solids. Dissolved oxygen levels tend to increase with distance away from the discharge point primarily due to dilution within the mixing zone at the disposal site.

Unclassified
SECURITY CLASSIFICATION OF THIS PAGE(When Data Entered)

THE CONTENTS OF THIS REPORT ARE
NOT TO BE USED FOR ADVERTISING,
PUBLICATION, OR PROMOTIONAL
PURPOSES. CITATION OF TRADE
NAMES DOES NOT CONSTITUTE AN
OFFICIAL ENDORSEMENT OR APPROVAL
OF THE USE OF SUCH COMMERCIAL
PRODUCTS.



#### SUMMARY

Field investigations of open-water pipeline disposal operations were conducted in Corpus Christi Bay (Texas), Atchafalaya Bay (Louisiana), and Apalachicola Bay (Florida). The primary objectives of these studies were (1) to document the extent and intensity of plumes of suspended solids, (2) to relate these plumes to the texture of the dredged material, the discharge configuration, and to the characteristics of the receiving waters, (3) to develop a simple model to predict the areal extent, intensity, and persistence of turbidity plumes, (4) to assess the release of metals and nutrients from the dredged material and its interstitial waters to the receiving waters, (5) to document plumes of particleassociated metals, and (6) to develop a simple model to predict the extent and intensity of plumes of particle-associated metals. Secondary objectives were (1) to estimate the partitioning of the total mass of material discharged between the bottom layer near the discharge and the plume of suspended solids and (2) to estimate the short-term oxygen demand of the dredged material.

Corpus Christi is a shallow bar-built estuary with weak tidal currents and poorly developed estuarine circulation flow. Wind can be an important driving force. The dredged material was discharged through a submerged elbow normal to the sea surface. No well-defined plumes were observed. Concentrations of suspended solids greater than 100 mg/ $\ell$  were relatively rare and confined to puddles, usually less than 0.5 km $^2$  in area.

Corpus Christi Bay supports a productive shrimp fishery which is carried out by small otter trawlers. The weighted nets are dragged along the bottom and disturb the sediments to a depth of approximately 5 cm. Using data on fishing effort, it was estimated that each year shrimpers resuspend between 16 and 133 times more sediment than is dredged for channel maintenance.

Atchafalaya Bay is a shallow coastal embayment characterized by weak tidal currents and large river input. Wind can also be an important driving force. Dredged material was discharged above the water surface against a splash plate. The material was coarser than at the other two sites. Natural background concentrations of suspended solids varied over a period of three days from about 30 mg/ $\ell$  to more than 500 mg/ $\ell$  as bottom sediments were resuspended by strong northwest winds. When background levels were between 30 and 100 mg/ $\ell$ , maximum total concentrations within the plume were about 1500 mg/ $\ell$ , but were confined to a relatively small area, less than 0.03 km $^2$ . The area of the plumes with concentrations greater than 300 mg/ $\ell$  never exceeded 0.85 km $^2$  and in two of the four plume realizations it was less than 0.02 km $^2$ . The maximum linear extent of the 300 mg/ $\ell$  field was less than 1.0 km.

Apalachicola Bay is a shallow bar-built estuary characterized by relatively weak tidal currents. The major forces that drive the circulation pattern throughout most of the year are the wind and fresh water input from the Apalachicola River--the largest river on the west coast of Florida. Dredged material was discharged through a variety of discharge configurations to permit an assessment of the effects of the discharge configuration on the plumes of suspended solids. The maximum linear extent of the plume, as defined by the 50 mg/L isopleth, was less than 2.5 km and in only 2 of the 12 plume realizations did it exceed 2 km. In 7 of the 12 plume realizations the maximum linear extent was less than 1 km. The maximum areal extent of the plume, as defined by the 50 mg/& isopleth, ranged from less than 0.02 km<sup>2</sup> to more than 0.40 km<sup>2</sup>. The use of a deflector plate reduced the surface plume, but there was no substantial difference between the surface plumes associated with abovewater and below-water discharge. When no deflecting plate was used the near-surface plume, as defined by the 50 mg/l isopleth, was more extensive when the material was discharged into the air than when discharged below water. The area with concentrations greater than 100 mg/k iecreased with an above-water discharge, however.

If the objective is to minimize the areal extent of the nearsurface plume, the authors' limited data indicate that discharge below and normal to the water surface is better than discharge below or above and parallel to the water surface. If the discharge pipe is approximately parallel to the water surface, the extent of the near-surface plume can be reduced by discharge against a deflector plate, either above or below water.

Several independent estimates of the partitioning of dredged material between the bottom layer and the plume indicated that between 97-99 percent of the total mass of sediment discharged went rapidly to the bottom layer within a few tens of meters of the point of discharge. The remaining 1-3 percent was incorporated into the plume.

A model was developed to predict, from graphs, the spatial and temporal distributions of the concentration of suspended solids produced by open-water pipeline disposal of dredged material. The model is based on a relationship for horizontal turbulent diffusion for a vertical line source which assumes that the time rate of change of local variance of a small, radially symmetric diffusing patch of substance (the horizontal eddy diffusivity) is porportional to a characteristic velocity, ω, called the diffusion velocity and the time, t, since release. Conceptually, a continuous source of diffusing material can be considered as a superposition of a large number of small patches of material released at a constant rate from a fixed point and whose centers of mass move with the ambient flow. After modifying the basic patch model to include particle settling, it was integrated numerically over time and the results presented in graphical form to provide estimates of (1) the centerline concentration distribution of suspended solids and (2) the variance of the suspended solids plume as a function of distance from the point of discharge. Estimation of these variables from the graphs requires only two physical parameters; one proportional to the settling velocity and age of the plume, the other proportional to the ratio of the diffusion velocity to the ambient flow. Instructions are included for estimating the required input parameters and for applying the set of graphs to actual dredging and disposal operations.

No well-defined plumes of dissolved metals (manganese, iron, zinc, copper, chromium, cadmium, lead) were observed at any of the three sites indicating that dissolution of metals from suspended solids was limited. Concentrations of dissolved iron and manganese in the water were, in fact, reduced in the plumes of dredged material.

Concentrations of dissolved ammonia and silica species were locally increased near the discharge. No increases in dissolved phosphate levels were observed in the discharge plumes despite high dissolved phosphate concentrations in interstitial waters of channel deposits dredged. The particle-associated metals studied (iron, manganese, zinc, copper chromium, cadmium, lead, mercury) remained associated with particles during dredging and disposal except for cadmium. Increases in concentrations of suspended solids and particle-associated metals in receiving waters were obviously associated with the discharge plume. Such increases affected only small areas and were short-lived.

A simple model was developed to predict concentrations of particle-associated constituents. The model was tested using data from the three study sites and found to provide useful predictions within the plume of excess turbidity from the dredged material discharge. The model worked best in the plume of excess turbidity in well mixed systems. The model was least successful at near-background concentrations of suspended solids in a system receiving industrial waste discharges—Corpus Christi Bay.

Elutriate test results from deposits to be dredged were compared with field results and found to have limited utility in predicting changes in concentrations of dissolved metals during open-water disposal operations. Elutriate test results indicated release of dissolved ammonia and silicate which was observed near the discharge pipe in Apalachicola.

Although large quantities of reduced particulate matter with a high potential oxygen demand are introduced into the water during open-water pipeline disposal, only a small fraction of this material is reactive on a time scale comparable to that associated with settling of the bulk of the mass. Utilization of dissolved oxygen during open-water pipeline disposal results primarily from reduced dissolved species in the interstitial waters of the dredged material. The principal components are reduced sulfur species, reduced iron, and reduced manganese. For typical fine-grained estuarine sediments with water contents of 80 percent (by volume), the oxygen demand of interstitial waters is

approximately 0.4 mg  $0_2/g$  of dry sediment. This means that the dissolved oxygen demand of 1 m<sup>3</sup> of material designated for dredging would require 21 m<sup>3</sup> of water with an oxygen concentration of 9 mg/ $\ell$  to satisfy the demand.

Distributions of dissolved oxygen were mapped in Apalachicola Bay in the receiving waters off the discharge and clearly show a depression in the levels of dissolved oxygen. The oxygen depression increased with depth and the area with depressions greater than 1.0 mg/l ranged from less than 0.04 km² to about 0.80 km². Estimates were made of the total oxygen consumption within these areas and related to the amount of dredged material discharged over the period required to produce the plume, approximately  $10^5$  sec. These calculations resulted in apparent oxygen demands of approximately 0.3-0.6 mg  $\rm O_2/g$  of dry sediment which agree closely with oxygen demands estimated from analyses of interstitial waters and support the argument that observed oxygen sags are largely the result of oxidation of reduced species in interstitial waters, and to a lesser extent to oxidation of surfaces of sulfide minerals.

#### PREFACE

The work described in this report was conducted under Contract DACW39-76-C-0129 entitled "Field Investigations of Nature, Degree, and Extent of Turbidity Generated by Open-Water Pipeline Disposal Operations" between the U. S. Army Engineer Waterways Experiment Station (WES), Vicksburg, Miss., and the Research Foundation of the State University of New York. Part of the study was performed under subcontract to the Chesapeake Bay Institute, Johns Hopkins University. The study was sponsored by the Dredged Material Research Program (DMRP) as part of Task 6C, Turbidity Prediction and Control, of the Disposal Operations Project (DOP).

The authors thank Blair Kinsman, William S. Reeburgh, David J. Hirschberg, George Carroll, William Carter, William Cronin, Andrew Hamilton, Alan Robbins, John Lekan, Jeffrey Parker, Edmund Schiemer, and Christopher Zeppie for their advice and assistance. The authors thank Carol Cassidy, Marie Eisel, and Eileen Quinn for the graphic arts, and are particularly indebted to Jeri Schoof and Hirlsa White for typing and editorial assistance. Grateful acknowledgments are extended to the U. S. Army Corps of Engineers District personnel of the Corpus Christi, Morgan City, and Apalachicola field offices.

The DMRP was administered by the WES Environmental Laboratory (EL). This study was managed by Dr. William D. Barnard, Manager of Task 6C, under the direct supervision of Mr. Charles C. Calhoun, Jr., Manager of the DOP, and Dr. John Harrison, Chief, EL. Contracting Officer was COL John L. Cannon, CE. Mr. F. R. Brown was the WES Technical Director.

## CONTENTS

<u>P</u>	age
NOTICE CONCERNING USE OF TRADE NAMES AND MANUFACTURERS	1
SUMMARY	2
PREFACE	7
LIST OF FIGURES	10
LIST OF TABLES	17
CONVERSION FACTORS, METRIC (SI) TO U.S. CUSTOMARY UNITS OF	
MEASUREMENT	19
PART I: INTRODUCTION	20
PART II: TURBIDITY PLUMES	22
Site Descriptions and Field Data	22
Discussion	91
PART III: A SUSPENDED SOLIDS PLUME MODEL AND ITS APPLICATION	102
The Model	102
Applying the MSRC Plume Model to an Example Problem	137
PART IV: CHEMICAL ASPECTS OF OPEN-WATER PIPELINE DISPOSAL-	
DISSOLVED NUTRIENTS AND METALS AND PARTICLE-	
ASSOCIATED METALS	153
Introduction	153
	153
Dissolved Metals and Nutrients	159
Particle-Associated Metals	192
PART V: OPEN-WATER PIPELINE DISPOSAL AND DISSOLVED OXYGEN	
DEMAND	223
Turundunadan	224
Introduction	225
A Simple Method for Estimating Short-Term Oxygen Demand	226
	230
reer observations or onlygen and in reportant and it is	
Discussion	230
REFERENCES	241

## CONTENTS

Pag	ge
APPENDIX A: SUSPENDED SOLIDS MEASUREMENTS	<b>A1</b>
	A1 A3
Suspended Solids	A7 A9 11
APPENDIX B: GRAIN-SIZE ANALYSIS OF BOTTOM SEDIMENTS	В1
	В1
그리고 얼마나 살아나 살아보는 이렇게 빠른데 그리는 살이 살아 살아 살아 살아 살아 살아 살아가지 않는데 그렇게 살아	B1 B2
Computations	B2 B3
	C1
Navigation	C1
	C2
	C3 C4
APPENDIX D: CHEMICAL ANALYTICAL METHODS AND MODEL CONTOURS	D1
	D2
	D4 D4
	D5
	D6
Heavy Metals Analyses	D6
Determination of Interstitial and Elutriate Cadmium and Lead . Di	13
Analysis of Dissolved Nutrient Samples DI Contours-Model for Prediction of Particle-Associated	17
	23

NOTE: Appendices B, C, and D were reproduced on microfiche and are enclosed in an envelope attached inside the back cover of this report.

## LIST OF FIGURES

No.	<u> </u>	age
1	Map of Corpus Christi Bay study area	23
2	Discharge configuration used in Corpus Christi Bay	25
. 3	Map of portion of study area showing locations of current meters and discharge pipe	25
4	Progressive vector diagram of winds at Corpus Christi International Airport	27
5	Distribution of total suspended solids (mg/l)	29
6	Distribution of total suspended solids (mg/l)	29
7	Distribution of total suspended solids $(mg/l)$	32
8	Distribution of total suspended solids (mg/l)	32
9	Distribution of total suspended solids (mg/l)	33
10	Distribution of total suspended solids $(mg/l)$	33
11	Map of Atchafalaya BayGulf of Mexico study area	34
12	The Dredge GEORGE A. MC WILLIAMS	35
13	Map of study area showing locations of current meters and discharge pipe	36
14	Progressive vector diagram of winds measured at Baton Rouge, LA	37
15	Distribution of total suspended solids $(mg/l)$	40
16	Distribution of total suspended solids $(mg/l)$	41
17	Distribution of total suspended solids (mg/l)	43
18	Distribution of total suspended solids (mg/l)	44
19	Size distributions of suspended solids within and near the plume of dredged material in Atchafalaya Bay	46
20	Size distributions of suspended solids within and near the plume of dredged material in Atchafalaya Bay	46
21	Map of Apalachicola Bay study area	48
22	Summary of discharge configurations used in Apalachicola Bay	49
23	One of discharge configurations used in Apalachicola Bay	50
24	Map of study area showing locations of current meters and discharge pipe	50
25	Progressive vector diagram of winds measured at Apalachicola	52

No.		Page
26	Distribution of total suspended solids (mg/l) before start of dredging	55
27	Distribution of total suspended solids (mg/l) before start of dredging	56
28	Distribution of total suspended solids $(mg/l)$	57
29	Distribution of total suspended solids (mg/l)	57
30	Distribution of total suspended solids (mg/l)	58
31	Distribution of total suspended solids (mg/l)	59
32	Distribution of total suspended solids (mg/l)	64
33	Distribution of total suspended solids (mg/l)	65
34	Distribution of total suspended solids (mg/l)	66
35	Distribution of total suspended solids (mg/l)	67
36	Distribution of total suspended solids (mg/l)	68
37	Distribution of total suspended solids (mg/l)	69
38	Distribution of total suspended solids (mg/l)	71
39	Distribution of total suspended solids (mg/l)	72
40	Distribution of total suspended solids (mg/l)	73
41	Distribution of total suspended solids (mg/l)	74
42	Distribution of total suspended solids (mg/l)	75
43	Distribution of total suspended solids (mg/l)	76
44	Distribution of total suspended solids (mg/l)	77
45	Distribution of total suspended solids (mg/l)	78
46	Distribution of total suspended solids (mg/l)	79
47	Distribution of total suspended solids (mg/l)	80
48	Distribution of total suspended solids (mg/l)	81
49	Distribution of total suspended solids (mg/l)	82
50	Distribution of total suspended solids (mg/l)	83
51	Distribution of total suspended solids (mg/l)	84
52	Distribution of total suspended solids (mg/l)	85
53	Distribution of total suspended solids (mg/l)	86
54	Size distributions of suspended solids within and near the	
	plume of dredged material in Apalachicola Bay	88

No.		Page
55	Size distributions of suspended solids within and near the plume of dredged material in Apalachicola Bay	89
56	Size distributions of suspended solids within and near the plume of dredged material in Apalachicola Bay	89
57	Size distributions of suspended solids within and near the plume of dredged material in Apalachicola Bay	90
58	Aerial photograph showing trails of suspended solids produced by shrimp trawlers	100
59	Distribution of total suspended solids $(mg/\ell)$ in wake of shrimp trawler	100
60	Normalized centerline concentration of suspended solids versus normalized centerline distance from source for $\gamma = 10^{-2}$ with $\omega/u$ as a parameter	107
61	Normalized centerline concentration of suspended solids versus normalized centerline distance from source for $\gamma = 10^{-1}$ with $\omega/u$ as a parameter	108
62	Normalized centerline concentration of suspended solids versus normalized centerline distance from source for $\gamma$ = 100 with $\omega/u$ as a parameter	109
63	Normalized centerline concentration of suspended solids versus normalized centerline distance from source for $\gamma$ = $10^1$ with $\omega/u$ as a parameter	110
64	Normalized centerline concentration of suspended solids versus normalized centerline distance from source for $\gamma = 10^2$ with $\omega/u$ as a parameter	111
65	Normalized concentration of suspended solids to plume front x* = 1 versus $\omega/u$ with $\gamma$ as a parameter	112
66	Normalized second moment of lateral distribution of concentration of suspended solids versus normalized centerline distance from source for $\gamma = 10^{-2}$ with $\omega/u$ as a parameter	114
67	Normalized second moment of lateral distribution of concentration of suspended solids versus normalized centerline distance from source for $\gamma=10^{-1}$ with $\omega/u$ as a	
68	parameter	115
	parameter	116

No.		Page
69	Normalized second moment of lateral distribution of concentration of suspended solids versus normalized centerline distance from source for $\gamma=10^1$ with $\omega/u$ as a parameter	117
70	Normalized second moment of lateral distribution of concentration of suspended solids versus normalized centerline distance from source for $\gamma=10^2$ with $\omega/\upsilon$ as a parameter	118
71	Normalized second moment of lateral distribution of concentration of suspended solids at plume front $x^* = 1$ versus $\omega/u$ with $\gamma$ as a parameter	119
72	Suspended solids $(mg/l)$ plume observed in Atchafalaya Bay .	121
73	Suspended solids $(mg/l)$ plume observed in Apalachicola Bay .	122
74	Suspended solids (mg/ $\ell$ ) plume observed in Apalachicola Bay .	123
75	Suspended solids (mg/ $\ell$ ) plume observed in Corpus Christi Bay	124
76a	Comparison of observed plume structure in Atchafalaya Bay with theoretical structure predicted from model for values of $\omega/u$ and $\gamma$ indicated. (a) Centerline concentration of suspended solids versus distance	125
76Ъ		126
77a		127
77Ъ	Comparison of observed plume structure in Apalachicola Bay with theoretical structure predicted from model for values of $\omega/u$ and $\gamma$ indicated. (b) Second moment of lateral distribution of concentration of suspended solids versus distance	128
78a	Comparison of observed plume structure in Apalachicola Bay with theoretical structure predicted from model for values of $\omega/u$ and $\gamma$ indicated. (a) Centerline concentration of	
	suspended solids versus distance	129

No.		Page
78ъ	Comparison of observed plume structure in Apalachicola Bay with theoretical structure predicted from model for values of $\omega/u$ and $\gamma$ indicated. (b) Second moment of lateral distribution of concentration of suspended solids versus distance	130
79a	Comparison of observed plume structure in Corpus Christi Bay with theoretical structure from model for values of $\omega/u$ and $\gamma$ indicated. (a) Centerline concentration of suspended solids versus distance	131
79Ъ	Comparison of observed plume structure in Corpus Christi Bay with theoretical structure from model for values of $\omega/u$ and $\gamma$ indicated. (b) Second moment of lateral distribution of concentration of suspended solids versus distance	132
80	Typical lateral distribution of concentration of suspended solids at different distances from source used to compute second moment for Atchafalaya Bay, 19 October 1976	133
81	Typical lateral distributions of concentration of suspended solids at different distances from source used to compute second moment for Apalachicola Bay, 6 April 1977	134
82	Characteristic plume shapes predicted by the model for different $\omega/u$	139
83	Graph for determining dimensionless concentration of suspended solids at unit dimensionless distance when $\omega/u$ is known	144
84	Graph for determining the dimensionless distance at which a given dimensionless concentration of suspended solids occurs	145
85	Graph for determining the dimensionless second moment of lateral distribution of concentration of suspended solids at unit dimensionless distance when $\omega/u$ is known	148
86	Graph for determining the dimensionless distance at which a given dimensionless second moment occurs	149
87	Plan view of hypothetical plume as delimited by the 50 mg/ $\ell$ isopleth for $\omega/u = 10^{-1}$ , $\gamma = 10^{-1}$ , $\sigma^2(1) = 0.9$	151
88	Fe and Mn in interstitial water, Apalachicola Bay	189
89	Comparison of turbidity plumes measured optically with concentrations of particle-associated Fe, Corpus Christi Bay	194
90a	Comparison of turbidity plumes measured optically with concentrations of particle-associated Fe. Atchafalaya Bay .	195

No.	<u> </u>	age
90ъ	Comparison of turbidity plumes measured optically with concentrations of particle-associated Fe, Atchafalaya Bay .	196
91a	Comparison of turbidity plumes measured optically with concentrations of particle-associated Fe, Apalachicola Bay	197
91ь	Comparison of turbidity plumes measured optically with concentrations of particle-associated Fe, Atchafalaya Bay .	198
92	Concentration of total suspended solids versus combustible organic matter, Apalachicola Bay	207
93	Correlations among particle-associated Fe and other metals on plume suspended solids, Corpus Christi Bay	,211
94	Correlations among particle-associated Fe and other metals on plume suspended solids, Atchafalaya Bay	,213
95	Correlations among particle-associated Fe and other metals on plume suspended solids, Apalachicola Bay	,215
96	Sketch of apparatus used to measure short-term $0_2$ -demand of sediments	228
97	Depletion of dissolved oxygen versus time measured in the apparatus shown in Figure 96	229
98	Depletion of dissolved oxygen versus time measured in the apparatus shown in Figure 96	229
99	Depletion of dissolved oxygen versus time measured in the apparatus shown in Figure 96	229
100	Distribution of dissolved oxygen depression (mg/l)	231
101	Distribution of dissolved oxygen depression (mg/l)	231
102	Distribution of dissolved oxygen depression $(mg/l)$	232
103	Distribution of dissolved oxygen depression (mg/l)	232
104	Distribution of dissolved oxygen depression (mg/l)	233
105	Distribution of dissolved oxygen depression (mg/l)	233
106	Distribution of dissolved oxygen depression (mg/l)	234
107	Distribution of dissolved oxygen depression (mg/l)	234
108	Distribution of dissolved oxygen depression (mg/l)	235
109	Distribution of dissolved oxygen depression (mg/l)	235
110	Distribution of dissolved oxygen depression (mg/l)	236
111	Distribution of dissolved oxygen depression (mg/l)	236

## LIST OF FIGURES (concluded)

No.		Page
112	Distribution of dissolved oxygen depression $(mg/l)$	237
A1	Typical nephelometer calibration curves from Apalachicola Bay suspended solids	A2
A2	Comparison of sensitivities of transmissometer and nephelometer	A4
A3	Sketch of underwater unit of transmissometer	A5
A4	Spectral response of transmissometers used in study	A6
A5	Typical transmissometer calibration curves used to predict concentrations of suspended solids	A8
A6	Total suspended solids $(mg/l)$ versus combustible organic matter (%) for samples from Apalachicola Bay	A10
B1	Particle size distributions of channel sediments	В4
D1	Sketch of sampling system for analyses of nutrients, suspended solids, and metals	D3
D2	Sketch of microfiltration system	D9
D3	Sketch of mercury analysis system	D11
D4	Comparison of turbidity plumes measured optically with concentrations of particle-associated Fe, Corpus Christi Bay	D24
D5	Comparison of turbidity plumes measured optically with concentrations of particle-associated Fe, Apalachicola Bay .	D25
D6	Comparison of turbidity plumes measured optically with concentrations of particle-associated Fe, Apalachicola Bay .	D26
D7	Comparison of turbidity plumes measured optically with concentrations of particle-associated Fe, Apalachicola Bay .	D27
D8	Comparison of turbidity plumes measured optically with concentrations of particle-associated Fe, Apalachicola Bay .	D28
D9	Comparison of turbidity plumes measured optically with concentrations of particle-associated Fe, Apalachicola Bay .	D29
D10	Comparison of turbidity plumes measured optically with concentrations of particle-associated Fe, Apalachicola Bay .	D30
D11	Comparison of turbidity plumes measured optically with concentrations of particle-associated Fe, Apalachicola Bay.	D31

## LIST OF TABLES

No.		Page
1	Summary of Sampling Program in Corpus Christi Bay	26
2	Current Speed and Direction in Corpus Christi Bay at 1.1 m near "55" from 24 August 1977-25 August 1977	28
3	Summary of Extent of Suspended Solids Plumes in Corpus Christi Bay	31
4	Current Speed and Direction in Atchafalaya Bay at 1.1 m Near "C27"	38
5	Summary of Sampling Program in Atchafalaya Bay	39
6	Summary of Extent of Suspended Solids Plumes in Atchafalaya Bay	42
7	Summary of Particle Size Data for Selected Samples of Suspended Solids from Atchafalaya Bay	47
8	Summary of Sampling Program in Apalachicola Bay	51
9	Current Speed and Direction in Apalachicola Bay at Depth of 1 m Near "N68"	52
10	Summary of Extent of Suspended Solids Plumes in Apalachicola Bay	60
11	Summary of Particle Data for Selected Samples of Suspended Solids	87
12	Total Mass of Excess Suspended Solids within the Plumes for Selected Runs in Apalachicola Bay	95
13	Computation of Plume Structure Defined by an Isoline of Concentration	138
14	Values of $\omega$ for Different Environments	141
15	Parameter Values for Application of Model to Case Study	142
16	Estimate of Lateral Extent of Plume	150
17	Estimate Rate of Dissipation of Plume By Settling and Turbulent Diffusion	152
18	Metals in Interstitial Waters in Sediments from Dredged Channels	154
19	Nutrients in Interstitial Waters in Sediments from Dredging Channels	155
20	Elutriate Test Results	156
21	Grain Size of Sediments from Dredged Channels	158
22	Metals and Other Constituents in Sediments from Dredged	158

## LIST OF TABLES (concluded)

No.		Page
23	A. Corpus Christi Dissolved Metals; B. Atchafalaya Dissolved Metals; C. Apalachicola Dissolved Metals	161
24	A. Corpus Christi Dissolved Nutrients; B. Atchafalaya Dissolved Nutrients; C. Apalachicola Dissolved Nutrients	168
25	Summary of Data on Particle-Associated Metals in Suspended Sediment and in Channel Sediment Deposits	175
26	Particle-Associated Metals, Corpus Christi Bay (TX), 25 August 1976	176
27	Particle-Associated Metals, Atchafalaya Bay (LA), 21 October 1976	179
28	Particle-Associated Metals, Apalachicola (FL), 4-7 April 1976	181
29	Particle-Associcated Iron on Suspended Solids Samples	200
30	Predicted Particle-Associated Metal Concentrations	204
31	Settling Velocity and Particle Size of Plume Suspended Solids	220
32	Summary of Oxygen Sag Expected for Different Dilutions of Interstitial Water Release during Dredging and Disposal	226
33	Short-Term Oxygen Demand of Apalachicola Bay Sediments	227
34	Areas of Oxygen Depression in Apalachicola Bay	238
D1	Analytical Parameters for Suspended Metals	D14
D2	Analytical Parameters for Dissolved Metals	D15
D3	Analytical Coefficients of Variation for Dissolved and Suspended Metals	D16

## CONVERSION FACTORS, METRIC (SI) TO U.S. CUSTOMARY UNITS OF MEASUREMENT

Metric (SI) units of measurement used in this report can be converted to U.S. customary units as follows:

Multiply	Ву	To Obtain_
centimeters	0.393700787	inches
meters	3.28083989	feet
meters	1.0936133	yards
kilometers	0.53995680	nautical miles
square meters	10.76391042	square yards
square meters	$2.471054 \times 10^4$	acres
cubic meters	35.31466247	cubic feet
cubic meters	13.07950547	cubic yards
kilograms	2.20462248	pounds (mass)
centimeters per second	$3.28083939 \times 10^2$	feet per second
meters per second	2.17917676	knots (nautical
		miles per hour)
kilowatts	1.34	horsepower

## FIELD INVESTIGATIONS OF THE NATURE, DEGREE, AND EXTENT OF TURBIDITY GENERATED BY OPEN-WATER PIPELINE DISPOSAL OPERATIONS

## PART I: INTRODUCTION

Large volumes of material must be dredged each year to maintain and enlarge navigable waterways and harbors. In the past, open-water pipeline disposal has been employed frequently for disposal of material from large projects because of economic reasons. Environmental concerns, however, have decreased the popularity of this method of disposal in many sections of the country. Opponents of open-water pipeline disposal contend that it produces large-scale dispersal of dredged material and promotes the release of associated contaminants from the particles and the interstitial waters. This study was designed to assess these effects.

The primary goals of this study were (1) to document the extent, intensity, structure, and persistence of plumes of suspended solids produced by open-water pipeline disposal of dredged material in a variety of coastal environments, and (2) to develop a simple model to predict the extent and intensity of these plumes for coastal environments with a range of physical oceanographic characteristics. A secondary goal was to document the extent and intensity of the plumes of dissolved and particle-associated species of selected metals and dissolved nutrients.

For each of three sites--Corpus Christi Bay (Texas), the lower Atchafalaya estuary (Louisiana), and Apalachicola Bay (Florida)--the following questions were addressed:

- What are the extent and intensity of plumes of suspended solids in three dimensions, over a limited range of oceanographic and meteorologic conditions?
- 2. What is the internal structure of the plumes of suspended solids—the distributions of (a) optical properties, (b) concentration of suspended solids, and (c) size distribution of

particles suspended within the plume?

- 3. What is the character of the material being dredged, particularly its texture, water content, and chemical composition (including that of the interstitial water)?
- 4. What are the important physical properties of the receiving waters that affect the behavior of plumes of suspended solids, and how do they affect them?
- 5. What are the extents of the plumes of selected dissolved and particle-associated constituents?

## PART II: TURBIDITY PLUMES

## Site Descriptions and Field Data

## Corpus Christi Bay

Physical geography. Corpus Christi Bay is located on the south Texas coast about 290 km southwest of Galveston and 209 km north of the mouth of the Rio Grande, Figure 1. The Bay is a shallow estuarine system about 22 km long (northwest-southwest) and 18 km wide at its widest part, and is roughly elliptical in outline. It has natural depths of 3 to 4 m.1

Mustang Island separates Corpus Christi Bay from the Gulf of Mexico on the east. Tributary embayments include Redfish Bay to the northeast, Nueces Bay to the west, and Oso Bay to the south. Laguna Madre, a narrow lagoon, extends along the coast southward from Corpus Christi Bay. The Nueces River is the prime source of fresh water to Corpus Christi Bay. The Neuces and its tributaries, the Frio and Atascosa Rivers, drain about 481 km<sup>2</sup> of south central Texas and discharges into Nueces Bay near Corpus Christi. The average discharge of the Neuces River is approximately 24 m<sup>3</sup>/s and it carries a substantial sediment load.<sup>1</sup>

Sediments in the central portion of Corpus Christi Bay consist of silt and clay. Sands, composed primarily of carbonate shell fragments occur widely around the Bay in the shallow areas. Some carbonate sediment and evaporite material from Laguna Madre may also be present in the Bay deposits. Recently deposited materials in the navigation channels are therefore derived primarily from river discharge, shell materials, carbonate-evaporite deposits, and polluted sediment from the nearby industrial complex.

In Corpus Christi Bay the mean tidal range is about 15 cm. The water surface may be depressed as much as 25 cm below mean low tide level by strong north winds in winter. Between June and October the

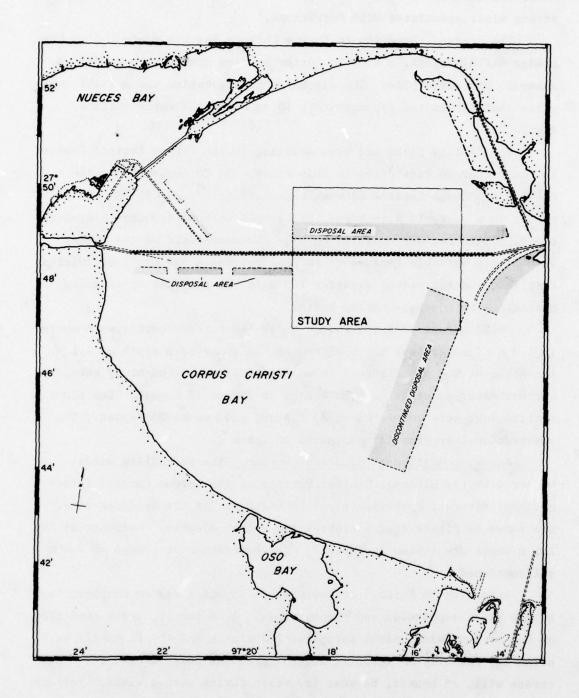


Figure 1. Map of Corpus Christi Bay study area.

water surface may be raised as much as 45 cm above mean low tide by strong winds associated with hurricanes. 1

The dredge. Dredging in Corpus Christi Bay was conducted by the Dredge CAPTAIN CLARK, a 4500 kw cutter suction dredge with a 76.2 cm diameter discharge pipe. The discharge configuration was a right angle elbow that terminated approximately 30 cm below the water surface, Figure 2.

The CAPTAIN CLARK had been dredging in the Corpus Christi Channel for more than 30 days prior to this study. On 20 August 1976, the CAPTAIN CLARK was located between beacons "49-50" and "55-56" and was moving in a westerly direction. Background suspended solids concentrations, concentrations measured outside the near-field of the plume, were highly variable because of natural processes and man's activities. Far field concentrations exceeded 100 mg/l, as a result of trawling operations by numerous shrimp boats.

On 22 August 1976 two Endeco Model 105 current meters were moored in 4.3 m of water just south of beacon "55"; one at a depth of 1.1 m, the other at 2.4 m. Figure 3 shows the location of the study area, the current meter moorings and the dredge on 25 and 26 August. Two plume realizations were completed on 25 August, and one on 26 August. The observational program is summarized in Table 1.

Survey conditions: wind and current. The prevailing winds measured by the National Weather Service at the Corpus Christi International Airport, approximately 8 km northwest of the dredging site, are shown in Figure 4 as a progressive vector diagram. Currents at the 1.1 m depth are listed in Table 2. The current meter placed at 2.4 m malfunctioned.

According to Smith, 4 Corpus Christi Bay is a region characterized by low tidal amplitudes and strong winds. As a result, under conditions of no, or low, wind, tidal forces will dominate and the flow will be primarily easterly or westerly depending on the phase of the tide. Wind stress will, of course, be most important during strong winds. Periods of low to moderate wind from directions other than the east or west will produce a very complicated current pattern.

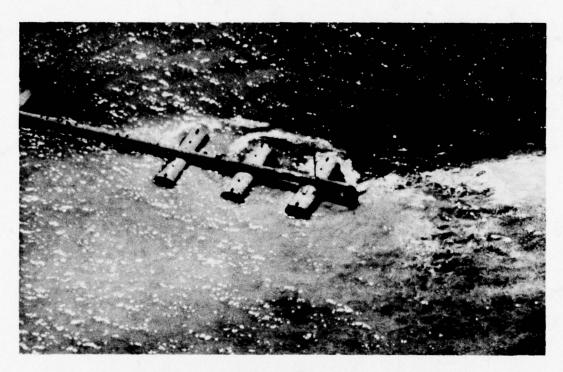


Figure 2. Discharge configuration used in Corpus Christi Bay.

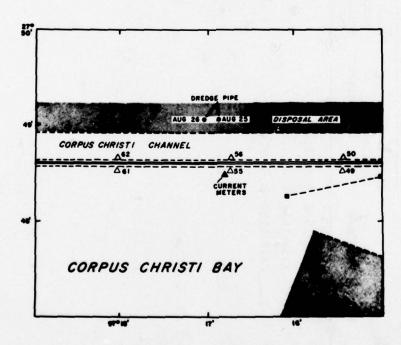


Figure 3. Map of portion of study area showing locations of current meters and discharge pipe.

Table 1 Summary of Sampling Program in Corpus Christi Bay

	Dredge Operating	Yes	Yes	Yes
	02			
	Metals	1		
Measurements	Nutrients	`		
	Susp. of Size Dists. Solids Susp. Solids Nutrients Metals 0 <sub>2</sub> Operating	,	`	,
	Conc. of Susp. Solids	`	,	`
	Optical	`	1	1
	Sampling Depths (m)	0.6, 2.4	0.6, 2.4	158 0.6, 2.4
	Times	0738-1058 0.6, 2.4	1355-1459 0.6, 2.4	0848-1158
	Run #	1	2	1
	Date	25 Aug'77		26 Aug'77

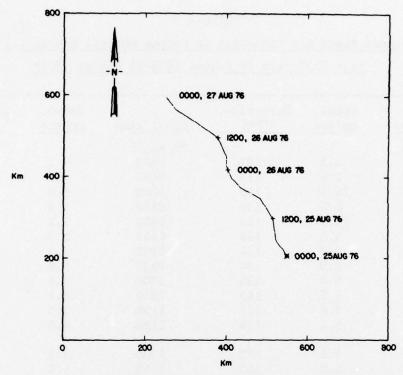


Figure 4. Progressive vector diagram of winds at Corpus Christi International Airport.

Plumes of suspended sediment. Optical measurements for suspended solids concentrations were made on two days--25 and 26 August 1976. On 25 August two runs were completed; on 26 August, one run. Measurements were made continuously at 0.6 m and 2.1 m with transmissometers and nephelometers. The two transmissometers were hung on a hydrographic wire with a heavy (50 kg) weight at the bottom; a line was run forward from the lower unit to reduce the wire angle. The nephelometer intakes (1/2 inch polyflo tubing) were attached to a fixed streamlined strut at the same depths.

On Run 1 of 25 August 1976, the background concentration of suspended solids varied from 15 to 25 mg/ $\ell$ . The near-surface plume was poorly developed; maximum concentrations were between 50-75 mg/ $\ell$  and were observed in "puddles," Figure 5. At the lower sampling depth (2.1 m) the plume of new material was much better developed than nearer the surface and trended westerly with the ambient current flow, Figure 6. An older plume field extended to the east, presumably the result of an

Table 2 Current Speed and Direction in Corpus Christi Bay at 1.1 m near "55" from 24 August 1976-25 August 1976\*

Local time	Speed, cm/sec	Direction,  °T**	Local time	Speed, cm/sec	Direction,  T**
24 Aug'76			25 Aug'76		
1800	5.3	107	0600	9.3	281
1830	7.4	113	0630	7.7	310
1900	10.6	116	0700	9.8	317
1930	8.8	136	0730	9.8	314
2000	10.6	124	0800	7.2	322
2030	8.5	128	0830	6.9	313
2100	8.2	134	0900	4.2	294
2130	9.0	134	0930	5.8	295
2200	6.4	135	1000	6.6	295
2230	7.2	142	1030	6.1	307
2300	5.6	177	1100	5.3	314
2330	5.3	154	1130	4.0	281
25 Aug '76					
0000	5.6	173	1200	3.2	269
0030	5.0	185	1230	1.6	251
0100	4.8	201	1300	0.8	206
0130	2.9	224	1330	1.8	248
0200	3.7	233	1400	0.5	205
0230	3.4	273	1430	5.6	262
0300	4.0	271	1500	6.9	277
0330	7.7	278	1530	4.0	283
0400	8.5	273	1600	3.2	275
0430	9.6	277	1630	2.4	278
0500	8.8	274	1700	1.8	282
0530	8.8	272	1730	2.4	303

<sup>\*</sup> No current data for 26 August 1976 \*\* Degrees relative to true north

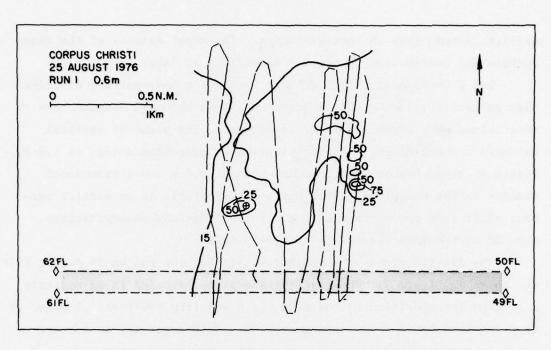


Figure 5. Distribution of total suspended solids (mg/l). Dashed lines traversing plumes indicate track lines.

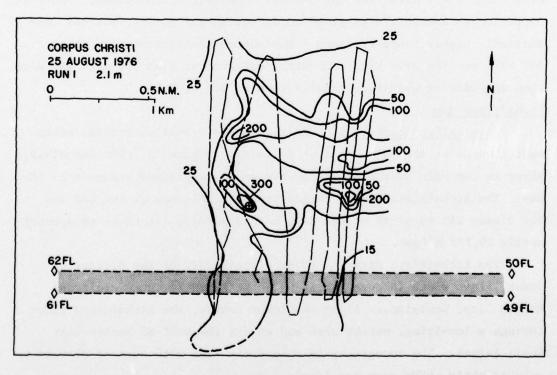


Figure 6. Distribution of total suspended solids (mg/l).

THE PROPERTY OF THE PARTY OF TH

earlier current flow in that direction. The areal extents of the nearsurface and near-bottom plumes are summarized in Table 3.

Run 2 on 25 August 1976, Figure 7, shows a near-surface distribution pattern similar to that observed on Run 1 although maximum concentrations were somewhat lower, 25-40 mg/ $\ell$ . The plume of material extended southwesterly. The distribution of suspended solids at 2.2 m, Figure 8, shows higher concentrations than at 0.6 m and a pronounced meander in the new plume. This may be attributable to an earlier current shift from the northeast to the south. Maximum concentrations were 85 mg/ $\ell$  and background levels 10-15 mg/ $\ell$ .

The distributions of suspended solids for the run on 26 August 1976 are shown in Figure 9. The near-surface plume extended in an easterly direction in opposition to the wind which was from  $180^{\circ}T$  at 4.1 m/sec at 0900 and from  $140^{\circ}T$  at 6.2 m/sec at 1200. Unfortunately, no current meter record was obtained for this period. Maximum concentrations of suspended solids at 0.6 m were about 225 mg/ $\ell$  and were confined to a relatively small area near the source. The near-bottom plume, Figure 10, conformed to the shallower plume in direction and extent, but had considerably higher concentrations. Maximum concentrations were about 500 mg/ $\ell$  and the area with concentrations greater than 100 mg/ $\ell$  was more than an order of magnitude greater than at 0.6 m, Table 3.

## Atchafalaya Bay

Physical geography. Atchafalaya Bay is a shallow coastal embayment located on the Gulf Coast of Louisiana, Figure 11. The Atchafalaya River is the main source of freshwater and fine-grained sediment to the Bay. The Atchafalaya River, formed by the confluence of the Red and Old Rivers 243 km north of the Bay, has an average discharge of approximately 10,735 m<sup>3</sup>/sec.

The Atchafalaya River, a major distributary of the Mississippi River, flows south through the Atchafalaya Basin to the vicinity of Morgan City, Louisiana. Along its lower course, the Atchafalaya flows through a low-lying, marshy area and enters the Gulf of Mexico near Shell Island. The topography is relatively flat with surface elevations only slightly above mean sea level.

Table 3

Summary of Extent of Suspended Solids Plumes
in Corpus Christi Bay

Date	Run #	Depth (m)	Suspended Solids (mg/l)	Area (m²)	Max. Linear Extent (km)*
25 Aug'76	1	0.6	> 25 > 50 > 75	1,789,625 105,567 5,027	
	1	2.1	> 25 > 50 > 100 > 200 > 300	3,493,790 1,417,624 547,947 30,162 5,027	
25 Aug'76	2 2	0.6	> 25 > 25 > 50 > 75	346,865 1,151,191 256,379 75,405	
26 Aug'76	1	0.6	> 25 > 50 > 100 > 200	2,005,787 135,730 25,135 10,054	
	1	2.1	> 25 > 50 > 100 > 150	5,082,333 1,477,948 281,514 25,135	

<sup>\*</sup> Not applicable because of the absence of well defined plumes.

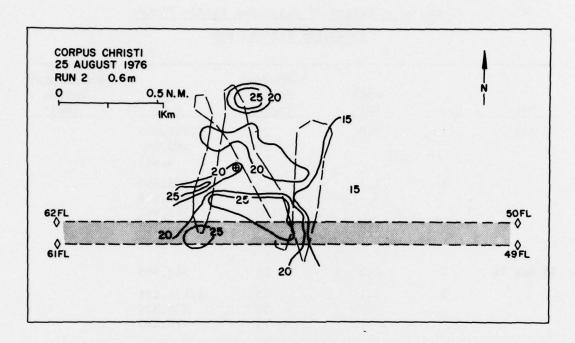


Figure 7. Distribution of total suspended solids (mg/l).

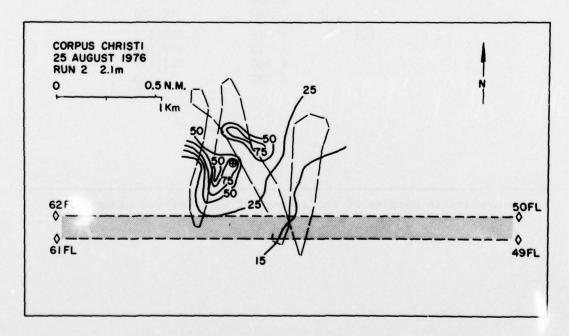


Figure 8. Distribution of total suspended solids (mg/l).

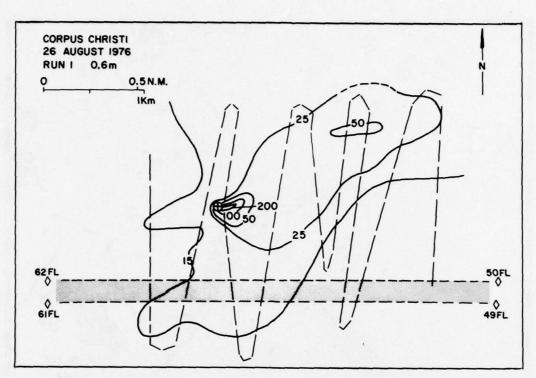


Figure 9. Distribution of total suspended solids (mg/l).

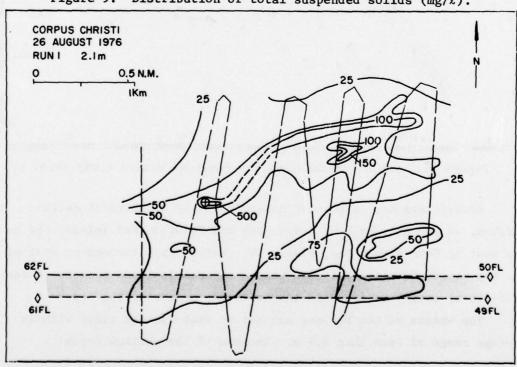


Figure 10. Distribution of total suspended solids (mg/l).

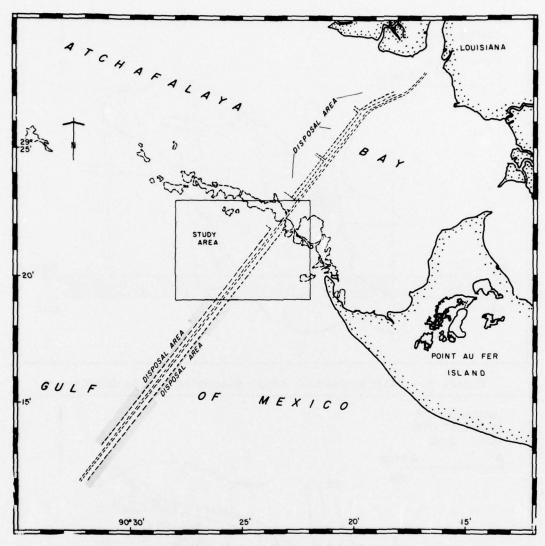


Figure 11. Map of Atchafalaya Bay--Gulf of Mexico study area.

Atchafalaya Bay is bounded on the north by a series of deltaic marshes, on the east by Four League Bay and Point Au Fer Island, and on the west by Cote Blanch Bay, Figure 11. Water depth throughout most of the Bay ranges from 1.4-2.1 m, although several isolated pockets of deeper (2.5-3.5 m) water are found in the southwest corner of the Bay.

The waters of the Bay are subject to weak diurnal tides with an average range of less than  $0.6\ m.$  Because of the shallow depth

and relatively wide expanse of the Bay, wind is a major driving force of hydrodynamic processes within the Bay.

The study area lies within the Deltaic Plain of the Gulf Coastal Plain just seaward of Atchafalaya Bay. Sediments are derived from fluvial and marine sources and are complexly interfingered both laterally and vertically. The primary source is the Atchafalaya River but the sediments have been intensively reworked by waves. The Deltaic Plain deposits are the result of seaward extension of the land surface; i.e. prograding and aggrading deltaic-marine sedimentary processes.

The dredge. Dredging in Atchafalaya Bay was conducted by the GEORGE A. MC WILLIAMS, a 3950 kw cutter suction dredge with 71 cm diameter discharge line. The material was discharged above the water surface against a splash plate, Figure 12.

During the study period, 15-21 October 1976, the dredge was operating south of Point Au Fer shell reef near buoys "26"-"27" and "28"-"29," Figure 13.

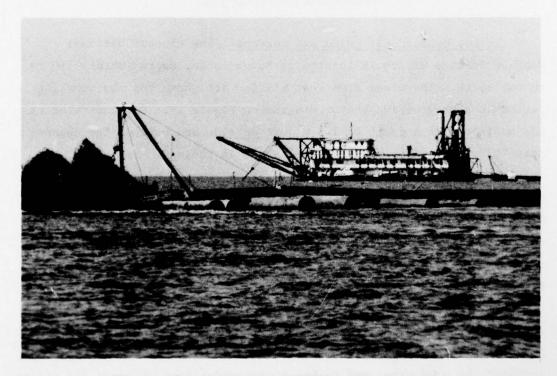


Figure 12. The Dredge GEORGE A. MC WILLIAMS.

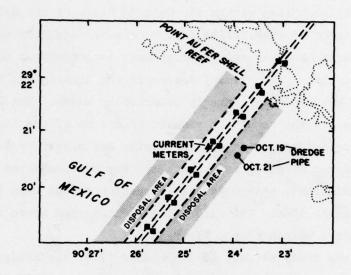


Figure 13. Map of study area showing locations of current meters and discharge pipe.

Survey conditions: wind and current. The closest National Weather Service Office is located at Baton Rouge, approximately 110 km to the north. The winds from that station are shown for the sampling period as a progressive vector diagram on Figure 14. Current velocity was monitored at a depth of 1.1 m just outside and west of the channel near "C27." The data collected are shown in Table 4.

Plumes of suspended sediment. Optical measurements were made continuously underway at 0.6 m and 1.2 m with transmissometers, and at 0.9 m with a nephelometer. Because of the shallow depths, 1.2-2.1 m in the disposal area, only one sampling depth was used for nephelometer measurements to avoid damage to the rigid sampling strut. The observational program is summarized in Table 5.

Plume measurements were made on 19 and 21 October 1976. On 19 October 1976 the background was only about 30-40 mg/L at 0.9 m. On 20 October 1976 strong northwesterly winds resulted in resuspension of sediments by wind waves and raised background levels of suspended solids

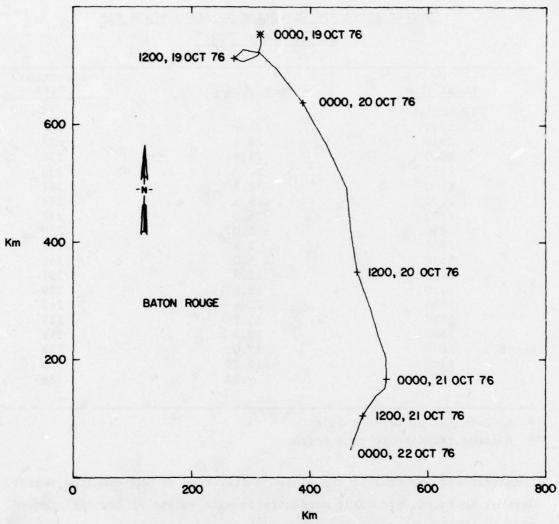


Figure 14. Progressive vector diagram of winds measured at Baton Rouge, LA.

to > 500 mg/ $\ell$  masking the plume from the dredge. By 21 October 1976 background levels of suspended solids had dropped to about 100 mg/ $\ell$ .

On 19 October data were obtained during two runs; Run 2 between 1334 and 1509 and Run 3 from 1536 to 1734. Figures 15 and 16 show the distribution of suspended solids in mg/l for these two runs. On Run 2 a near-field plume was absent which was believed to be due to a temporary interruption in the dredging between 1350 and 1420 which apparently

Table 4
Current Speed and Direction in Atchafalaya Bay
at 1.1 m Near "C27"

Ī	ocal Time	Speed, cm/s	Direction °T**
1	19 Oct'76*		
	0900	21.6	237
	0930	24.5	237
	1000	21.9	238
	1030	24.7	239
	1100	18.2	241
	1130	9.1	239
	1200	6.0	237
	1230	5.0	239
	1300	2.1	239
	1330	5.0	240
Run # 2	1400	12.2	237
un # 2	1430	18.8	239
	1500	22.4	243
	1530	23.2	239
	1600	20.6	241
Run # 3	1630	19.0	238
	1700	12.24	239
	1730	9.12	236

<sup>\*</sup> No data for 21 October 1976

coincided with several of the close-in traverses of the sampling vessel. Several isolated patches of concentrations in excess of 100 mg/l tended in a southwesterly direction in general agreement with the current meter data shown in Table 4. The isolated patch with concentrations in excess of 150 mg/l midway between the end of the pipe and the channel is probably due to a leak in the pipe. The near-field may be seen to be superimposed on a far-field of approximately 35-50 mg/l. The area of the plume as defined by the 100 mg/l isopleth was about  $0.14 \text{ km}^2$ ; the linear extent of the plume was about 0.48 km. The geometry of the plumes is summarized in Table 6.

On 21 October data were also obtained on two runs; Run 1 between 0931 and 1155 and Run 2 between 1302 and 1449. Figures 17 and 18 show

<sup>\*\*</sup> Degrees relative to true north

Summary of Sampling Program in Atchafalaya Bay Table 5

						Measurements				
Date	Run #	Times	Sampling Depth (m) Optical	Optical	Conc. of Susp. Solids	Conc. of Size Dists. Susp. of Susp. Solids Nutrients Metals $0_2$ Operating	Nutrients	Meta1s	02	Dredge Operating
19 Oct'76 2*	6 2*	1334-1509	6.0 6	1	1	1				Yes**
	3	1536-1734	6.0 4	`	`	,				Yes
21 Oct '76	1 9,	0931-1155	6.0 9	`	1	`	`	`		Yes
	2	1302-1449	6.0 6	`	,	,	`~	`		Yes

\* Run 1 was aborted when ship ran aground. \*\* Dredge stopped pumping for approximately 20 min (1400-1420) during run. Dredge stopped pumping for approximately 12 min (1622-1634) during run.

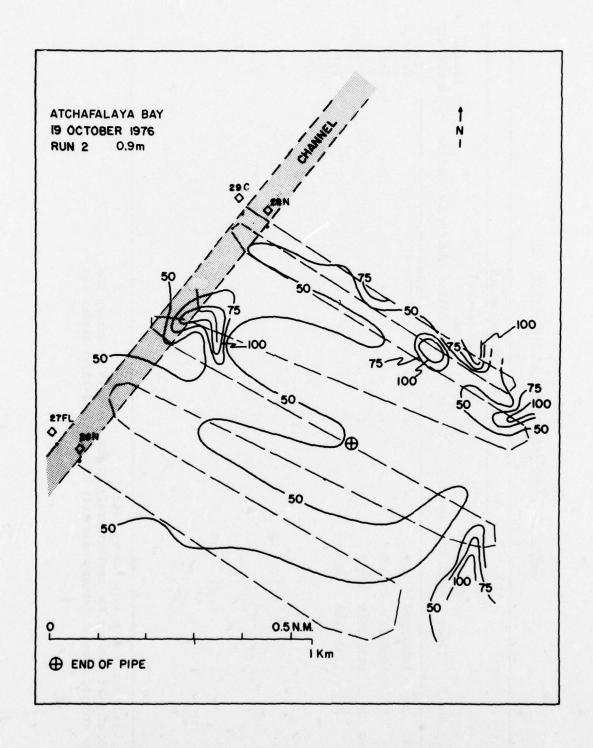


Figure 15. Distribution of total suspended solids (mg/L).

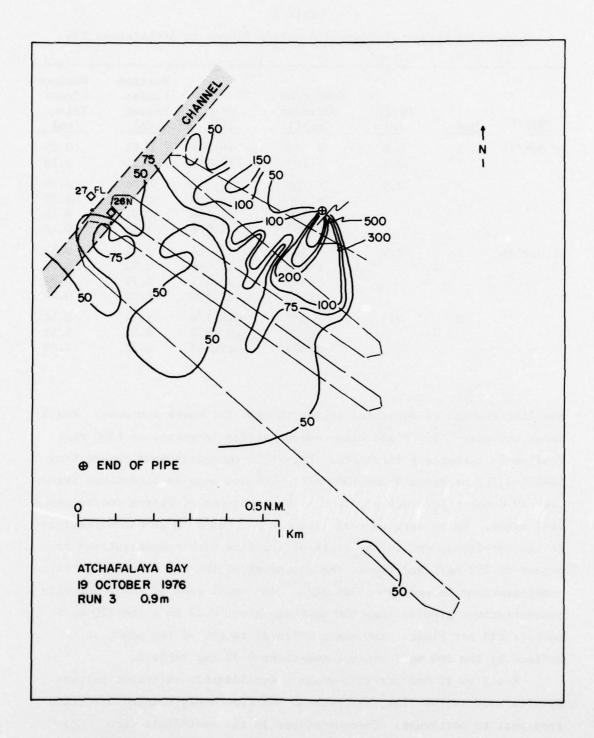


Figure 16. Distribution of total suspended solids (mg/l).

Table 6
Summary of Extent of Suspended Solids Plumes in Atchafalaya Bay

Date	Run #	Depth (m)	Suspended Sediment (mg/l)	Area (m²)	Maximum Linear Extent (Km)	Maximum Linear Extent (nm)
19 Oct'76	2	0.9	> 75 > 100	46,005 17,353	0.43 0.30	0.23 0.16
	3	0.9	> 100 > 200 > 300 > 500	141,110 42,333 21,166 9,878	0.48 0.41 0.32 0.19	0.28 0.22 0.17 0.10
21 Oct'76	1	0.9	> 300 > 400 > 500 >1500	372,214 194,199 83,471 27,256	0.97 0.82 0.71 0.32	0.52 0.44 0.38 0.17
	2	0.9	> 300 > 500 >1000	848,776 200,376 69,849	1.64 0.95 0.71	0.88 0.51 0.38

the distribution of suspended solids in mg/ $\ell$  for these two runs. Run 1 shows the near-field plume with concentrations in excess of 1500 mg/ $\ell$  tending in a westerly direction. Far-field concentrations ranged from 10-200 mg/ $\ell$ ; background was 100 mg/ $\ell$ . The increase in background levels over 19 October 1976 was produced by resuspension of bottom sediments by wind waves. There were several isolated patches of high concentrations in the far-field, one to the south of the pipe with concentrations in excess of 200 mg/ $\ell$  and two to the southeast of the end of the pipe with concentrations in excess of 300 mg/ $\ell$ . The total area of the plume with concentrations greater than 300 mg/ $\ell$  was about 0.37 km<sup>2</sup>; the 200 mg/ $\ell$  contour did not close. The maximum linear extent of the plume as defined by the 300 mg/ $\ell$  contour was about 0.97 km, Table 6.

Run 2 on 21 October 1976 shows a considerably different pattern. By afternoon on the 21st, the current had apparently changed direction from west to northeast. Concentrations in the near-field were comparable to those measured during Run 1 (% 1400 mg/ $\ell$ ) but the near-field

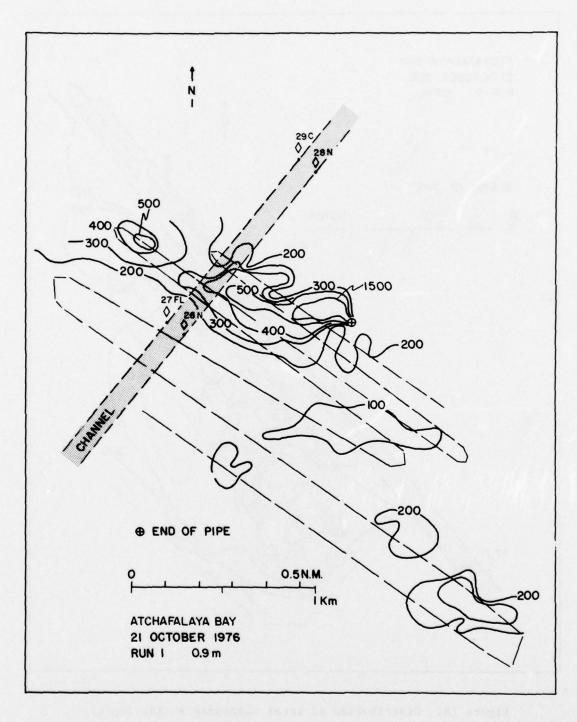


Figure 17. Distribution of total suspended solids (mg/l).

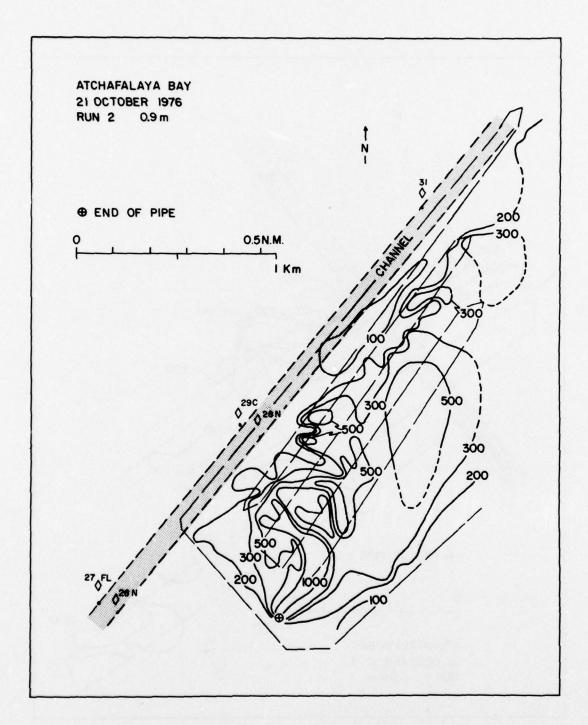


Figure 18. Distribution of total suspended solids  $(mg/\ell)$ .

was somewhat larger in extent (see Table 6). Background ( $\ell$  100 mg/ $\ell$ ) was little changed from that measured during Run 1. The area with concentrations greater than 300 mg/ $\ell$  had increased from about 0.37 km $^2$  on Run 1 to approximately 0.85 km $^2$  on Run 2. The maximum linear extent of the plume, as defined by the 300 mg/ $\ell$  isopleth, had increased from 0.97 km to 1.64 km, Table 6.

Size distributions of selected samples of suspended sediment are presented in Figures 19 and 20 and selected statistical parameters are summarized in Table 7. See Appendix A for a complete description of methods of analysis and data reduction.

## Apalachicola Bay

Physical geography. Apalachicola Bay is a shallow bar-built estuary located along the Gulf coast of northwest Florida's Franklin and Gulf counties, Figure 21. The Apalachicola River is the primary source of freshwater and fine-grained sediment to the Bay. The drainage basin of the Apalachicola River extends approximately 644 km north to the mountains of northern and western Georgia and includes southeastern Alabama and southwest Georgia, an area of over 49,735 km². The Apalachicola is the only major river of northwest Florida and the largest river on the entire west coast of Florida. It is formed by the confluence of its two major tributaries, the Chattahoochee and the Flirt Rivers and has an average annual discharge of about 700 m³/sec.

Apalachicola Bay is essentially a smooth, featureless, gently seaward sloping plain. Water depths range from about 2 m near the bridge on the north side of the Bay to 4 m along the north side of St. George Island. The eastern end of the Bay is marked by Bulkhead Shoal which extends from Cat Point to St. George Island. According to Kofoed and Gorsline<sup>5</sup> this shoal acts as a major barrier to the eastward migration of sediment. Beyond Bulkhead Shoal in St. George Sound the irregular bottom is characterized by three distinct basins bounded by bars and shoals. To the west St. Vincent Sound is a shallow continuation of Apalachicola Bay with an average depth of about 2 m.

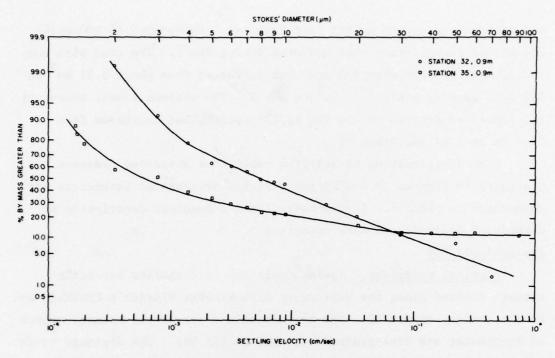


Figure 19. Size distributions of suspended solids within and near the plume of dredged material in Atchafalaya Bay.

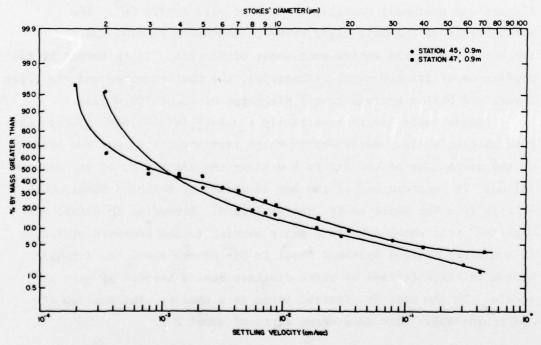


Figure 20. Size distributions of suspended solids within and near the plume of dredged material in Atchafalaya Bay.

Table 7

<u>Summary of Particle Size Data for Selected Samples of Suspended Solids from Atchafalaya Bay. See</u>

Figures 19 and 20 for Size Distributions.

Date	Run #	Station	Depth (m)	Susp. Solids	Median Settling Velocity (cm/sec)	Mean Settling Velocity (cm/sec)
21 Oct'76	1	32*	0.9	1104	$3.8 \times 10^{-3}$	$5.2 \times 10^{-3}$
	1	32*	0.9	1104	$2.2 \times 10^{-3}$	$2.5 \times 10^{-3}$
	1	32**	0.9	1104		$6.9 \times 10^{-3}$
	1	35	0.9	251	$6.6 \times 10^{-4}$	$1.4 \times 10^{-3}$
	1	45	0.9	131	$1.1 \times 10^{-3}$	$1.6 \times 10^{-3}$
21 Oct'76	2	47*	0.9	408	$2.2 \times 10^{-3}$	$2.7 \times 10^{-3}$
	2	47**	0.9	408	$1.0 \times 10^{-3}$	$1.6 \times 10^{-3}$
	2	47*	0.9	408	$1.9 \times 10^{-3}$	$2.5 \times 10^{-3}$
	2	57	0.9	124	$1.2 \times 10^{-3}$	$1.4 \times 10^{-3}$

<sup>\*</sup> Replicate Samples

As in most other estuaries and lagoons of the Gulf coast, wind has a pronounced effect on mixing and circulation processes in Apalachicola Bay. Wind frequently dominates the astronomical tides which are of low amplitude.

Apalachicola Bay is connected with the open Gulf of Mexico by two natural inlets (Indian Pass and West Pass), a dredged inlet (Bob Sikes Cut), and the eastern end of St. George Sound. West Pass, the largest in cross-sectional area, probably has the greatest exchange of water with the Gulf over a tidal cycle. Except during periods of strong easterly winds, West Pass is also the most significant inlet in terms of the amount of sediment discharged to the Gulf. 5

<sup>\*\*</sup> Plotted

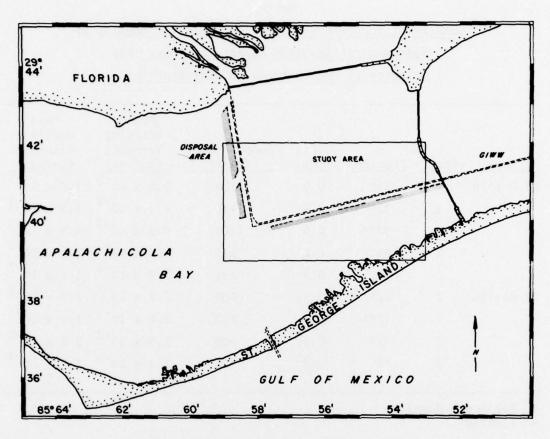


Figure 21. Map of Apalachicola Bay study area.

The distribution of sediments in Apalachicola Bay is determined primarily by topography.<sup>5</sup> The bulk of the fine-grained material discharged by the Apalachicola River is deposited on the smooth portions of Apalachicola Bay and the eastern half of St. Vincent Sound. Fine sand and shell inter-mixed with mud occur along the borders of the Bay. Silt predominates where water depths are greater than about 2 m.

The dredge. Dredging in Apalachicola Bay was conducted by the Dredge W. I. GUTHRIE, a 950 kw cutter suction dredge with a 41 cm diameter discharge pipe. During the period of observation several discharge configurations were used. These are shown schematically in Figure 22. The configuration for Run 4, 8 April, is also shown in Figure 23.

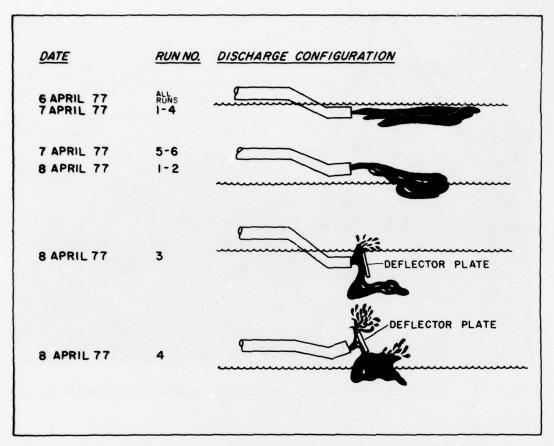


Figure 22. Summary of discharge configurations used in Apalachicola Bay.

The GUTHRIE began dredging on 5 April 1977 near Beacon "70."

During the period of observation it was located between buoys N68 and C71 just to the east of the dog leg in the channel south of the mouth of the Apalachicola River, Figure 24. The observational program is summarized in Table 8.

Survey conditions: wind and current. The prevailing winds as measured by the National Weather Service Office at the Municipal Airport at Apalachicola, Florida, approximately 10.2 km to the northwest of the dredging site, are shown on Figure 25 as a progressive vector diagram. On 2 April 1977 two current meters were set—one near buoy "N4," the other near "N70."



Figure 23. One of the discharge configurations used in Apalachicola Bay.

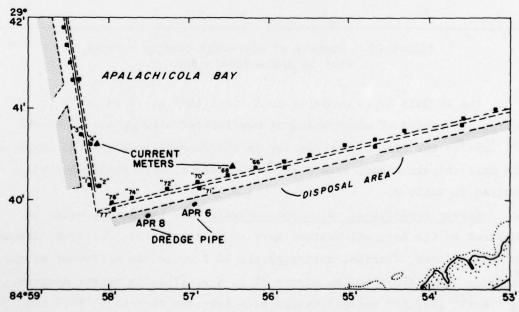


Figure 24. Map of study area showing locations of current meters and discharge pipe.

Table 8 Summary of Sampling Program in Apalachicola Bay

Date   Run #   Times   Depth (m)   Optical   Solids   Susp. Solids   Susp. Solids   Susp. Solids   Susp. Solids   Susp. Solids   Solids   Susp. Solids   S							Measurements	r.s			
1 1137-1431 0.6, 2.1	Date	Run #		Sampling Depth (m)	Optical	Conc. of Susp. Solids	Size Dists. of Susp. Solids	Nutrients		02	Dredge Operating
1 1447-1716 0.9, 2.7	2 Apr'77	1	1137-1431	1	-	-				1	No
1 0654-0736 0.6, 2.1	4 Apr'77	1	1447-1716		`	,					No
2 0742-0938 0.6, 2.1	6 Apr '77	1	0654-0736	0.6, 2.1	,	<b>,</b>	1				Yes
3 0947-1006 0.6, 2.1		7	0742-0938	0.6, 2.1	`	`	,				Yes
4 1030-1201 0.6, 2.1		3	0947-1006	0.6, 2.1	`						Yes
5 1450-1611 0.6, 2.1		4	1030-1201	0.6, 2.1	`	`	,				Yes
6 1635-1708 0.6, 2.1 / / / / / / / / / / / / / / / / / / /		2	1450-1611	0.6, 2.1	`	`	,	,	`		Yes
1 0716-0918 0.6, 2.1		9	1635-1708	0.6, 2.1	`						Yes
2 0927-1044 0.6, 2.1	7 Apr'77	1	0716-0918	0.6, 2.1	`	,	,	`	1	>	Yes
3 1210-1239 0.6, 2.1		2	0927-1044	0.6, 2.1	,	`	1			>	Yes
4 1315-1358 0.6, 2.1 /* / 5 1458-1516 0.6, 2.1 /* / 6 1525-1620 0.3, 2.1 /* / 1 0658-0753 0.6, 1.8 /* / / 3 1334-1512 0.6, 1.8 /* / / 4 1636-1735 0.6, 1.8 /* /		3	1210-1239	0.6, 2.1	,	`			`		Yes
5 1458-1516 0.6, 2.1		4	1315-1358	0.6, 2.1	`	`				>	Yes
6 1525-1620 0.3, 2.1 / / / / / / / / / / / / / / / / / / /		2	1458-1516	0.6, 2.1	*						Yes
1 0658-0753 0.6, 1.8		9	1525-1620	0.3, 2.1	,	`	`			>	Yes
2 0758-1051 0.6, 1.8 / / / / / / / / / / / / / / / / / / /	8 Apr'77	1	0658-0753	0.6, 1.8	1	1	1			>	Yes
0.6, 1.8 / / / / / / / /		7	0758-1051	0.6, 1.8	,	`	,			>	Yes
0.6, 1.8 / / / /		3	1334-1512	0.6, 1.8	•	`				>	Yes
		4	1636-1735	0.6, 1.8	`	`	,			>	Yes

\* Transmissometers only

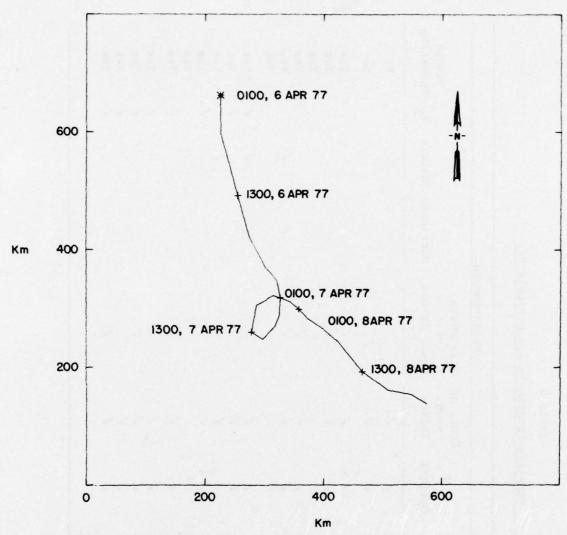


Figure 25. Progressive vector diagram of winds measured at Apalachicola Municipal Airport.

On 5 April 1977 the meter near "N70" was moved to a position about 15 m north of buoy "N68." The meter near "N4" failed. The currents at % 1 m near "N68" are listed in Table 9.

<u>Plumes of suspended sediment.</u> Dredging was initiated on 5 April 1977. Pre-dredging (background) observations were made in the designated dredging and disposal areas on 2, 4, and 5 April 1977. The optical measurements were made continuously underway at two depths, 0.6 m and 2.1 m, with both transmissometers and nephelometers.

Table 9

Current Speed and Direction in Apalachicola Bay at Depth

of 1 m Near "N68"

Local Time	Speed cm/s	Direction °T	Local Time	Speed cm/s	Direction °T
5 Apr'77			6 Apr'77		02.80
1545	7.7	254	1015	13.5	022
1615	14.5	241	1045	15.5	049
1645	12.0	246	1115	18.5	038
1715	10.2	250	1145	16.3	039
1745	8.2	308	1215	15.5	023
1815	6.0	261	1245	16.8	018
1845	9.2	254	1315	13.8	024
1915	3.7	211	1345	10.2	023
1945	2.7	192	1415	11.5	012
2015	6.0	202	1445	11.5	335
2045	4.7	209	1515	13.4	310
2115	3.5	299	1545	15.4	302
2145	4.5	346	1615	17.3	306
2215	6.2	353	1645	10.7	281
2245	8.2	020	1715	14.5	249
2315	13.3	018	1745	11.2	223
2345	13.3	009	1815	11.5	224
6 Apr'77			1845	9.0	213
0015	15.5	011	1915	8.7	214
0145	15.8	018	1945	7.2	196
0215	13.5	020	2015	5.2	220
0245	14.3	017	2045	5.0	188
0315	10.7	013	2115	1.2	245
0345	8.5	349	2145	4.0	312
0415	7.5	315	2215	2.5	340
0445	7.0	275	2245	6.0	351
0515	3.5	272	2315	5.7	352
0545	4.0	310	2345	11.7	352
0615	5.7	353	7 Apr'77		
0645	7.0	033	0015	8.0	352
0715	14.0	028	0045	5.2	021
0745	11.5	035	0115	9.5	028
0815	13.5	070	0145	9.0	039
0845	16.3	053	0215	9.2	041
0915	18.8	072	0245	11.2	032
0945	15.0	061	0315	5.2	030

(continued)

Table 9 (concluded)

Local Time	Speed cm/s	Direction T	Local Time	Speed cm/s	Direction T
7 Apr'77			7 Apr'77		
0345	6.2	347	2215	5.2	351
0415	6.2	324	2245	4.7	353
0445	2.7	323	2315	3.7	354
0515	6.7	330	2345	4.7	355
0545	8.0	343	8 Apr'77		333
0615	6.5	355	0015	3.5	357
0645	9.7	350	0045	5.7	355
0715	8.7	016	0115	8.2	012
0745	12.2	020	0145	8.0	017
0815	12.5	041	0215	10.5	020
0845	12.7	045	0245	13.3	023
0915	18.5	038	0315	11.5	020
0945	13.0	041	0345	15.8	018
1015	16.3	029	0415	12.7	025
1045	15.5	051	0445	10.2	016
1115	15.4	044	0515	8.2	347
1145	15.3	023	0545	5.7	328
1215	16.8	017	0615	8.2	318
1245	15.0	058	0645	7.7	320
1315	10.2	018	0715	3.0	338
1345	13.5	019	0745	5.5	348
1415	12.5	025	0815	2.7	345
1445	9.5	163	0845	6.0	357
1515	15.0	221	0915	8.7	015
1545	12.0	244	0945	9.5	021
1615	13.8	238	1015	12.5	027
1645	17.8	216	1045	8.5	016
1715	10.7	243	1115	13.0	047
1745	15.5	247	1145	14.3	017
1815	17.0	242	1215	13.0	026
1845	15.3	237	1245	13.8	052
1915	14.5	239	1315	16.0	053
1945	10.5	250	1345	15.3	048
2015	9.5	264	1415	11.0	057
2045	7.0	299	1445	7.2	029
2115	8.0	313	1515	2.7	067
2145	4.7	320	1545	1.2	316

The pre-dredging observations, Figures 26-29, show a north-south gradient in suspended solids with concentrations increasing to the north of the channel as one approaches the mouth of the Apalachicola River. There is evidence of a plume of unknown origin extending easterly, Figures 28-29. The range in concentration of suspended solids on 2 April 1977 was from < 25 mg/ $\ell$  to > 75 mg/ $\ell$ . On 4 April 1977 the range was from < 25 mg/ $\ell$  to > 150 mg/ $\ell$ .

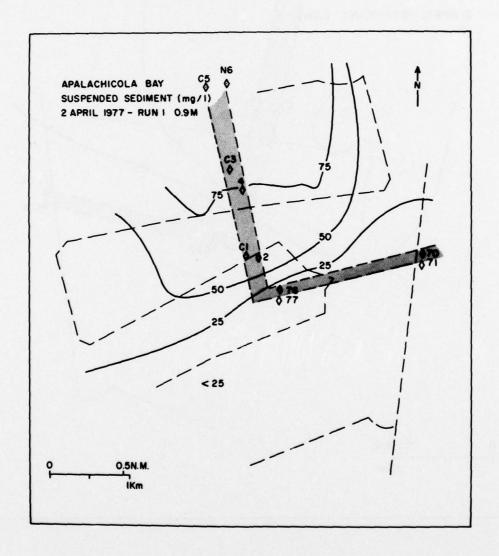


Figure 26. Distribution of total suspended solids (mg/l) before start of dredging.

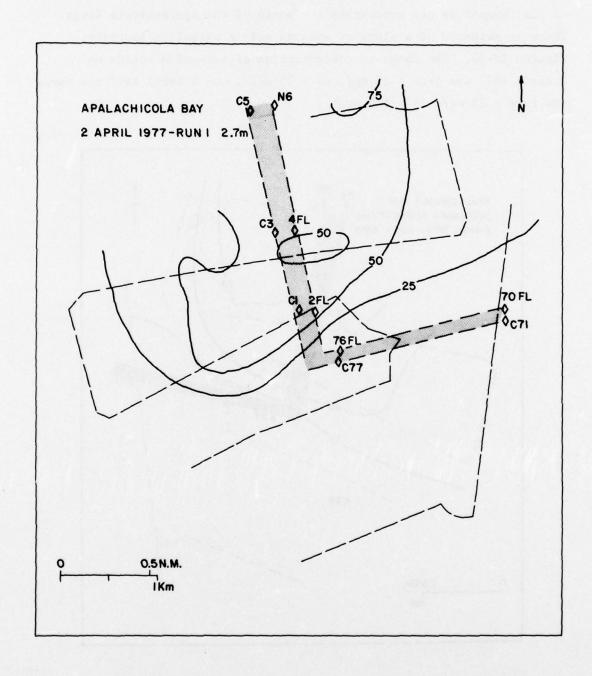


Figure 27. Distribution of total suspended solids (mg/l) before start of dredging.

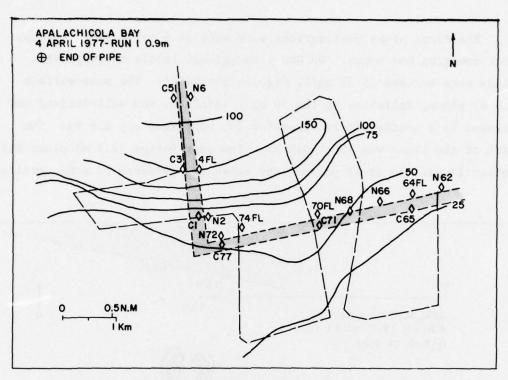


Figure 28. Distribution of total suspended solids (mg/l).

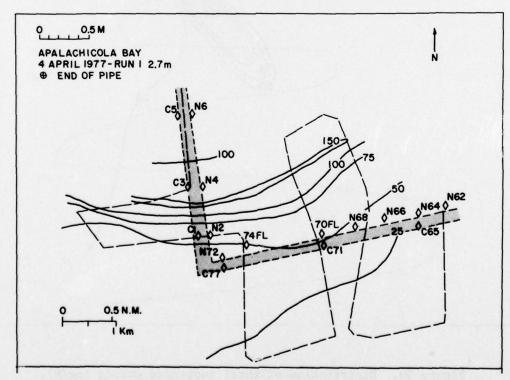


Figure 29. Distribution of total suspended solids (mg/l).

The first plume realizations were made on 6 April 1977, the day after dredging had begun. On Run 1 background levels of suspended solids were between 25-50 mg/ $\ell$ , Figures 30 and 31. The near-surface (0.6 m) plume, delimited by the 50 mg/ $\ell$  isopleth, was well-defined and extended in a southwesterly direction for approximately 0.6 km. The width of the plume was about 0.2 km. The near-bottom (2.1 m) plume had similar linear and areal extents and there was evidence of some vertical

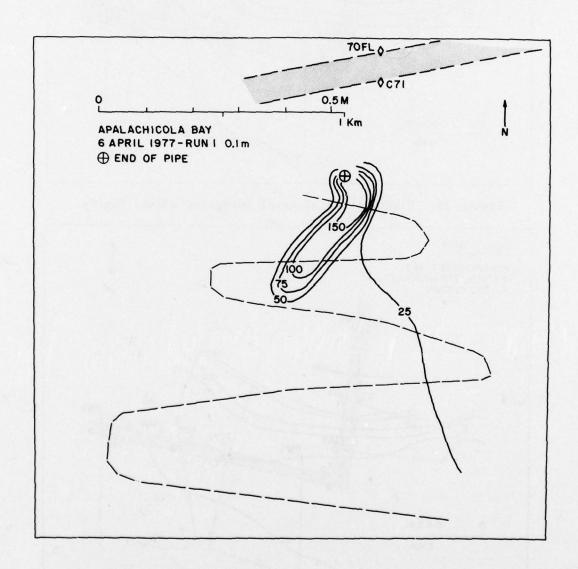


Figure 30. Distribution of total suspended solids (mg/l).

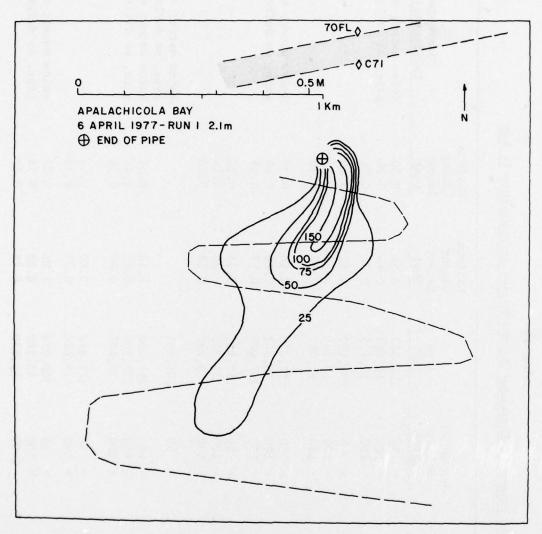


Figure 31. Distribution of total suspended solids (mg/l).

shear with the near-bottom plume displaced slightly to the east of the near-surface plume. The total surface area of the plume with concentrations of suspended solids greater than 50 mg/ $\ell$  was 0.10 km $^2$  at 0.6 m and 0.11 km $^2$  at 2.1 m. The areas exceeding 150 mg/ $\ell$  were 0.02 km $^2$  at 0.6 m and 0.02 km $^2$  at 2.1 m. The areal extents of the plumes on all runs are summarized in Table 10.

Table 10 Summary of Extent of Suspended Solids Plumes in Apalachicola Bay

Date         Number of Area         Linear Li		02				Maximum	Maximum	
Apr'77         1         0.6         > 50         101,887         0.56         0.30           1         2.1         > 150         46,463         0.44         0.24           1         2.1         > 50         109,112         0.52         0.28           2         100         18,282         0.37         0.20           3         150         18,282         0.37         0.20           4         5         100         17,630         0.46         0.23           2         2         2         100         18,282         0.37         0.20           3         100         18,282         0.37         0.20           4         5         100         17,630         0.46         0.25           5         100         27,342         0.37         0.09           6         100         27,345         0.28         0.14           7         150         27,345         0.28         0.14           8         150         100,441         0.16         0.58           9         150         10,441         0.48         0.26           9         150         100,441         0.48	Date	Run #		Solids (mg/l)	Area (m <sup>2</sup> )	Linear Extent (km)	Linear Extent (nm)	Discharge Configuration
2 0.6	6 Apr'77	1	9.0		101,887	0.56	0.30	Below water: open
1 2.1 > 150 15,175 0.21 0.11  1 2.1 > 50 109,112 0.52 0.28  > 100 50,799 0.43 0.23  > 150 109,112 0.52 0.28  0.20 0.6 > 50 77,630 0.46 0.25  > 150 19,802 0.26 0.14  > 150 27,345 0.28 0.14  4 0.6 > 50 100,441  4 2.1 > 100 294,460 1.16 0.63  > 200 25 200 0.81 0.46  > 200 294,460 1.16 0.63  > 200 200 0.81 0.46  > 200 200 0.81 0.46  > 200 200 0.81 0.46  > 200 200 0.81 0.46  > 200 200 0.81 0.46  > 200 200 0.81 0.86  > 200 200 0.81 0.86  > 200 200 0.81 0.86  > 200 200 0.81 0.86  > 200 200 0.81 0.86  > 200 200 0.81  > 200 200 0.81  > 200 200 0.81  > 200 200 0.81  > 200 200 0.81  > 200 200 0.81  > 200 200 0.81  > 200 200 0.81  > 200 200 0.81					46,463	0.44	0.24	pipe, no deflector
1 2.1 > 50 109,112 0.52 0.28					15,175	0.21	0.11	
2 0.6 > 50 77,630 0.45 0.23 0.20			2.1		109,112	0.52	0.28	
2 0.6				> 100	50,799	0.43	0.23	
2 0.6 > 50 77,630 0.46 0.25				> 150	18,282	0.37	0.20	
2 2.1 > 100 19,802 0.26 0.14   > 150 7,009 0.17 0.09   2 2.1 > 50 62,402 0.37 0.20   2 2.1 > 100 27,345 0.28 0.14   4 0.6 > 50 100,441   4 2.1 > 100 294,460 1.16 0.63   2 2.0 > 50 100,441   2 2.1 > 100 294,460 0.18 0.44   2 2.0 > 100 125,500 0.81 0.44   2 2.0 > 100 125,500 0.81 0.45   2 2.0 > 50 122,842 0.80 0.45   2 2.1 > 50 100 16,620 0.28 0.15   2 2.1 > 50 309,273 1.06 0.57   2 2.0 > 100 45,162 0.28 0.15   2 2.0 > 100 45,162 0.28 0.15   2 2.0 > 100 45,162 0.28 0.15   2 2.0 > 100 10,839 0.24 0.13			9.0	> 50	77,630	97.0	0.25	Below water; open
2 2.1 > 50 62,402 0.17 0.09 4 0.6 > 50 62,402 0.37 0.20 7,345 0.28 0.14				> 100	19,802	0.26	0.14	pipe, no deflector
2 2.1 > 50 62,402 0.37 0.20 > 100 27,345 0.28 0.14 4 0.6 > 50 100,441 4 2.1 > 100 294,460 1.16 0.63 > 200 35,407 0.48 0.26 5 0.6 > 50 122,842 0.80 0.45 > 100 45,162 0.28 0.15 > 200 10,839 0.24 0.13 > 200 45,162 0.80 0.15 > 100 45,162 0.80 0.15 > 100 45,162 0.28 0.15 > 200 10,839 0.24 0.13				> 150	7,009	0.17	0.09	
27,345 0.28 0.14  4 0.6 > 50 100,441  4 2.1 > 100 294,460 1.16 0.63  4 2.1 > 150 294,460 0.81 0.44  > 200 35,407 0.48 0.26  5 0.6 > 50 122,842 0.80 0.43  > 100 16,620 0.28 0.15  > 200 45,162 0.28 0.15  > 200 45,162 0.28 0.15  > 200 45,162 0.28 0.15  > 200 45,162 0.28 0.15  > 200 45,162 0.28 0.15		2	2.1	> 50	62,402	0.37	0.20	
4       0.6       > 50       100,441         4       2.1       > 100       294,460       1.16       0.63         4       2.1       > 100       294,460       1.16       0.63         5       150       105,500       0.81       0.44         5       2.0       35,407       0.48       0.26         5       2.1       > 50       122,842       0.80       0.43         6       > 50       122,842       0.80       0.43         7       100       16,620       0.28       0.15         8       100       45,162       0.28       0.15         9       200       10,839       0.24       0.15         9       100       45,162       0.28       0.15         9       10,839       0.24       0.13				> 100	27,345	0.28	0.14	
4 2.1 > 100 294,460 1.16 0.63				> 150	9,290	0.18	0.10	
4 2.1 > 100 294,460 1.16 0.63 > 150 105,500 0.81 0.44 > 200 35,407 0.48 0.26 5 0.6 > 50 122,842 0.80 0.43 > 100 16,620 0.28 0.15 > 2.1 > 50 309,273 1.06 0.57 > 2000 10,839 0.24 0.13		4	9.0		100,441			Below water; open
5 0.6		,	, 1	100	057 700	1.16	67 0	pipe, no deflector
5 0.6 > 50 122,842 0.80 0.45 > 100 16,620 0.28 0.15 5 2.1 > 50 309,273 1.06 0.57 > 2000 10,839 0.24 0.13			77	150	105 500	1.10	0.03	below water; open
5 0.6 > 50 122,842 0.80 0.43 > 100 16,620 0.28 0.15 5 2.1 > 50 309,273 1.06 0.57 > 100 45,162 0.28 0.15 > 2000 10,839 0.24 0.13				> 200	35,407	0.48	0.26	pipe, no dellector
5 2.1 > 50 309,273 1.06 0.57 > 100 45,162 0.28 0.15 > 2000 10,839 0.24 0.13		5	9.0	> 50	122,842	0.80	0.43	
5 2.1 > 50 309,273 1.06 0.57 > 100 45,162 0.28 0.15 > 2000 10,839 0.24 0.13					16,620	0.28	0.15	
> 100 45,162 0.28 0.15 > 2000 10,839 0.24 0.13 (continued)		2	2.1	> 50	309,273	1.06	0.57	Below water; open
(continued)				> 100 > 2000	45,162	0.28	0.15	pipe, no deflector
					(continued)			

Table 10 (continued)

Area Extent (m <sup>2</sup> ) (km)  31,453 0.61  13,007 0.39  210,227 1.39  74,428 0.83  54,566 0.52  39,743 0.39  26,736 0.50  91,048 0.46  53,111 0.33  33,420 0.31  No surface plume detected  73,344 0.63  48,414 0.55  22,032 0.35  15,604 0.22  11,412 0.20  3,214 0.09  1,630 0.07				Sus	Suspended		Maximum Linear	Maximum Linear	
1 0.6	Date	Run #	Depth (m)	100	olids mg/k)	Area (m <sup>2</sup> )	Extent (km)	Extent (nm)	Discharge Configuration
2.1	Apr'77	H	9.0	^ ^	50	31,453	0.61	0.33	Below water; open pipe; no deflector
0.6 > 100 54,566 0.52 0.28 0.28		1	2.1	۸	50	210,227	1.39	0.75	
0.6				^ ^	100	74,428 54,566	0.83	0.45	
0.6				^	2000	39,743	0.39	0.21	
2.1 > 50		2	9.0	^ /	0.5	26,736	0.20	0.11	Below water; open
2.1		,		١.	200	160,4	60.0	60.0	pipe, no deilector
> 250 53,111 0.33 0.18 > 2000 33,420 0.31 0.17 No surface plume detected > 100 128,623 0.76 0.41 > 200 73,344 0.63 0.34 > 200 48,414 0.55 0.19 > 25 22,032 0.35 0.19 > 50 15,604 0.22 0.12 > 150 11,412 0.20 0.11 > 150 3,214 0.09 0.05 > 500 11,630 0.07 0.04		7	1.7	^ ^	100	91,048	0.50	0.27	
> 2000 33,420 0.31 0.17  No surface plume detected  > 100 128,623 0.76 0.41  > 200 73,344 0.63 0.34  > 2000 48,414 0.55 0.30  > 25 22,032 0.35 0.19  > 50 15,604 0.22 0.12  > 150 11,412 0.09 0.05  > 50 1,630 0.07 0.04				۸	250	53,111	0.33	0.18	
No surface plume detected  > 100					2000	33,420	0.31	0.17	
> 100 128,623 0.76 0.41 > 200 73,344 0.63 0.34 > 2000 48,414 0.55 0.30 > 25 22,032 0.35 0.19 > 50 15,604 0.22 0.12 > 150 11,412 0.20 0.11 > 150 3,214 0.09 0.05 > 500 1,630 0.07 0.04		4	9.0			No surface p.	lume detected		Below water; open
> 200 73,344 0.63 0.34 > 2000 48,414 0.55 0.30 > 25 22,032 0.35 0.19 > 50 15,604 0.22 0.12 > 150 11,412 0.20 0.11 > 150 3,214 0.09 0.05 > 500 1,630 0.07 0.04		7	2.1	^	100	128,623	0.76	0.41	pipe, no deflector
> 2000 48,414 0.55 0.30 > 25 22,032 0.35 0.19 > 50 15,604 0.22 0.12 > 100 11,412 0.20 0.11 > 150 3,214 0.09 0.05 > 500 1,630 0.07 0.04				۸	200	73,344	0.63	0.34	
> 25 22,032 0.35 0.19 > 50					2000	48,414	0.55	0.30	
15,604 0.22 0.12 11,412 0.20 0.11 3,214 0.09 0.05 1,630 0.07 0.04		9	0.3	^ /	25	22,032	0.35	0.19	Above water; open
11,412 0.20 3,214 0.09 1,630 0.07				. ^	3 %	15 60%	0 33	0 13	pipe, no deflector
3,214 0.09 1,630 0.07				^	100	11,412	0.20	0.11	
1,630 0.07				^	150	3,214	0.0	0.05	
				^	200	1,630	0.07	0.04	

Table 10 (continued)

	Discharge Configuration					Below water; open	pipe, no deflector					Below water; open	pipe, no deflector				Above water; open	pipe, no deflector					Above water; open	pipe, no deflector				
Maximum Linear	Extent (Nm)													0.41	0.34	0.30	0.19		0.12	0.11	0.05	0.04	0.32		0.29		0.22	0.04
Maximum Linear	Extent (km)	210,227 1.39	0.83	0.52	0.39	0.20	0.09	0.50	97.0	0.33	0.31	lume detected		0.76	0.63	0.55	0.35		0.22	0.20	0.09	0.07	0.59		0.54		0.41	0.07
	Area (m <sup>2</sup> )	210,227	74,428	54,566	39,743	26,736	4,697	130,068	91,048	53,111	33,420	No surface p		128,623	73,344	48,414	22,032		15,604	11,412	3,214	1,630	91,090		49,660		23,070	4,940
Suspended	Solids (mg/l)	> 50	> 75					> 50						> 100	> 200	> 2000	> 25	^ 20	> 75	> 100		> 200	> 25	> 20	> 75	100	> 150	> 200
	Depth (m)	2.1				9.0		2.1				9.0		2.1			0.3						1.8					
	Run #	1				7		2				4		4			9						9					
	Date	7 Apr'77																										

(continued)

Table 10 (concluded)

Discharge	Above water; open pipe, no deflector				Above water; open	pipe, no deflector			Above water; open	pipe, no deflector			Below water,			Above water, deflector plate				
Maximum Linear Extent (nm)	0.32	0.29	0.22	0.04	1.30	0.62	0.34		1.34	0.23	0.43	0.32	0.08	0.25	0.17	0.21	0.32	0.24	0.17	0.14
Maximum Linear Extent (km)	0.59	0.54	0.41	0.0	2.41	1.15	0.63	ume detected	2.48	0.43	08.0	0.59	0.15	0.46	0.31	0.39	0.59	0.44	0.31	0.26
Area (m <sup>2</sup> )	91,090	49,660	23,070	4,940	201,244	60,337	10,116	No bottom plume detected	408,960	25,002	150,011	28,574	11,923	138,739	40,827	15,897	869,09	50,582	28,904	16,620
Suspended Solids (mg/l)	> 25 > 50	> 75 > 100	> 150	> 200	> 50	> 75	7 100		> 50		> 100	> 2000	> 50	> 75	> 100	> 50	> 75	> 100	> 200	> 2000
Depth (m)	1.8				9.0			1.8	9.0		1.8		9.0	1.8		9.0	1.8			
Run #	9				1			1	2		2		က	6		4	7			
Date	7 Apr'77				8 Apr 77															

On Run 2 on 6 April 1977 the plume was well-defined at both sampling depths--0.6 m and 2.1 m--and the plume had swung around more to the east, Figures 32 and 33. There was still some evidence of shear. The near-surface and near-bottom plumes, as defined by the 50 mg/ $\ell$  isopleth, had linear extents of approximately 0.4 km. The total area with concentrations exceeding 50 mg/ $\ell$  at 0.6 m was 0.08 km<sup>2</sup> and at 2.1 m was 0.06 km<sup>2</sup>. The areas exceeding 150 mg/ $\ell$  were less than 0.01 km<sup>2</sup> at both depths.

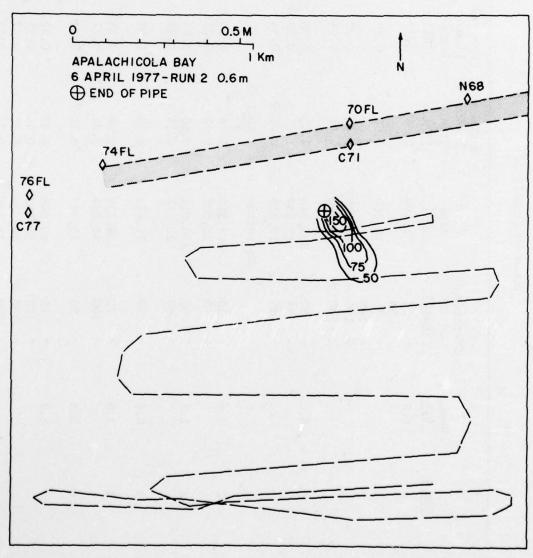


Figure 32. Distribution of total suspended solids (mg/l).

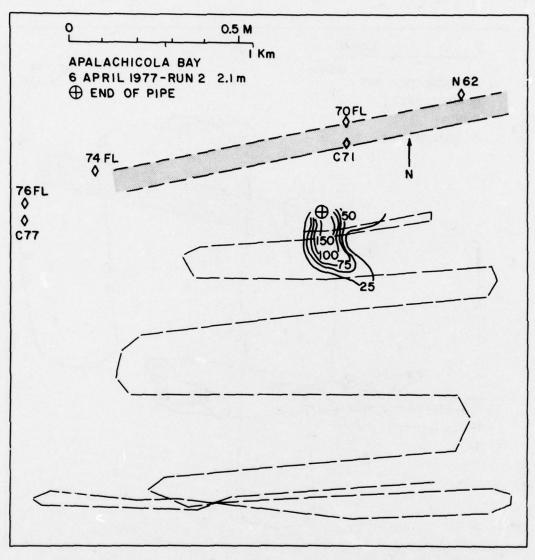


Figure 33. Distribution of total suspended solids (mg/l).

On Run 4 on 6 April 1977 (Figures 34 and 35) the near-surface plume was poorly defined; a series of three "puddles" was oriented in an easterly direction off the discharge. A fourth "puddle" of concentrations greater than  $50~\text{mg/}\ell$  was observed approximately 0.9 km farther north. The near-bottom plume was better defined and extended in a northeasterly direction. The maximum extent of the near-bottom plume as defined by the  $50~\text{mg/}\ell$  isopleth was about 1.1 km at 2.1 m. The total

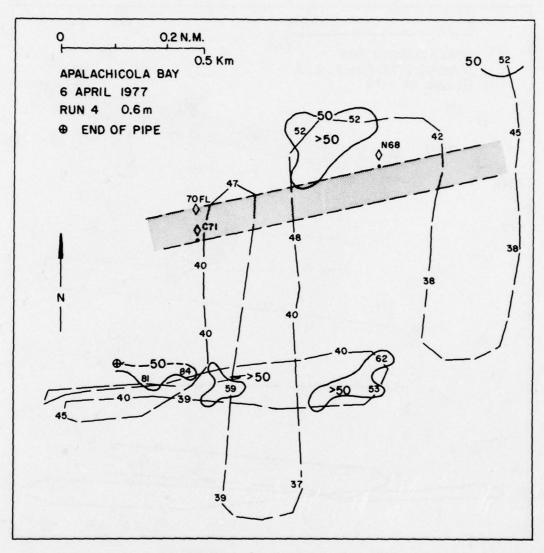


Figure 34. Distribution of total suspended solids (mg/l).

area with concentrations exceeding 50 mg/ $\ell$  was 0.10 km<sup>2</sup> at 0.6 m; the 50 mg/ $\ell$  contour did not close at 2.1 m. The total area at 2.1 m with concentrations greater than 150 mg/ $\ell$  was less than 0.01 km<sup>2</sup>. At 0.6 m the concentration of suspended solids did not exceed 100 mg/ $\ell$ . Because of the orientation of the plume and the positions of the cables holding the end of the discharge it was not possible to get closer than about 0.3 km from the end of the pipe.

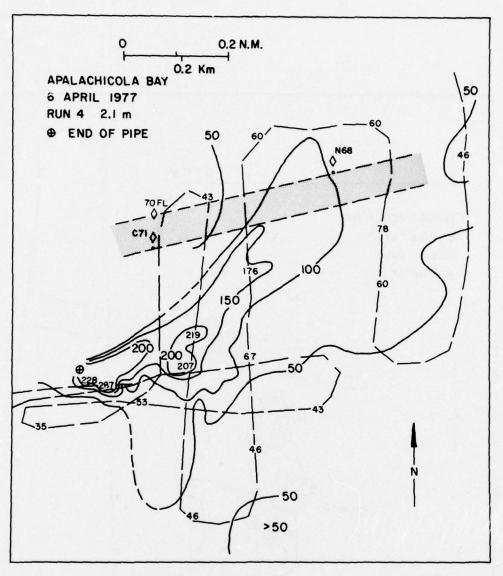


Figure 35. Distribution of total suspended solids (mg/l).

By Run 5 on 6 April 1977 (Figures 36 and 37) the surface plume had swung back around to the southeast. The near-bottom plume was still oriented in a northeasterly direction, but was beginning to be displaced to the south. The plume was well-defined at both depths. The maximum linear extent of the near-surface plume, as defined by the 50 mg/ $\ell$  contour, was about 0.7 km; the near-bottom plume, about 1.1 km. The areas with concentrations exceeding 50 mg/ $\ell$  were about 0.12 km<sup>2</sup> at 0.6 m

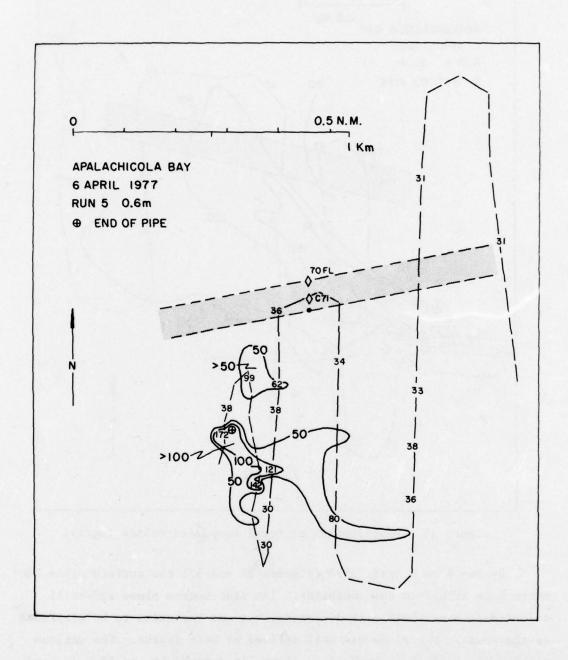


Figure 36. Distribution of total suspended solids (mg/l).

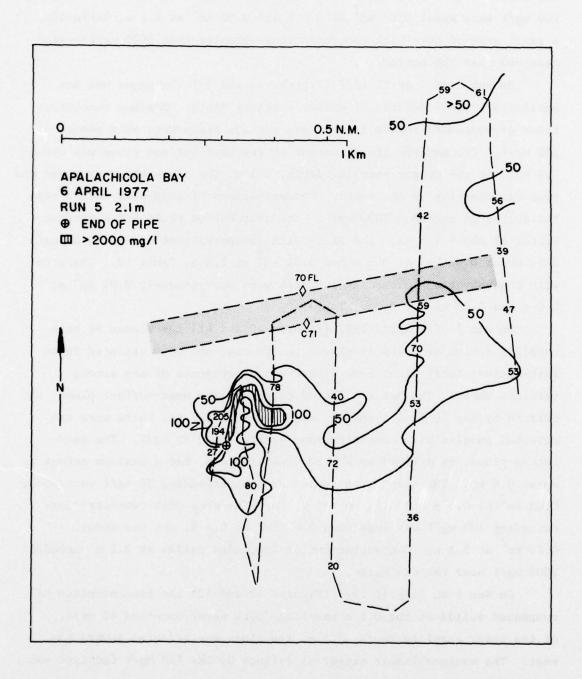


Figure 37. Distribution of total suspended solids (mg/1).

and 0.31 km<sup>2</sup> at 2.1 m, Table 10. The areas with concentrations exceeding 100 mg/ $\ell$  were about 0.02 km<sup>2</sup> at 0.6 m and 0.05 km<sup>2</sup> at 2.1 m, Table 10. A small area of very high concentrations—greater than 2000 mg/ $\ell$ \*—was observed near the bottom.

On Run 1 of 7 April 1977 (Figures 38 and 39) the plume was not particularly well-defined at either sampling depth. Maximum concentrations of suspended solids in the near-surface plume were only about 150 mg/ $\ell$ . The maximum linear extent of the near-surface plume was about 0.6 km. At the deeper sampling depth, 2.1 m, the plume was very broad and trended generally to the south. Concentrations of suspended solids near the discharge exceeded 2000 mg/ $\ell$ . The near-bottom plume had a maximum extent of about 1.5 km. The areas with concentrations exceeding 50 mg/ $\ell$  were about 0.03 km $\ell$  at 0.6 m and 0.21 km $\ell$  at 2.1 m, Table 10. The areas with concentrations exceeding 100 mg/ $\ell$  were approximately 0.01 km $\ell$  at 0.6 m and 0.05 km $\ell$  at 2.1 m, Table 10.

On Run 2 of 7 April 1977 (Figures 40 and 41) the plumes at both sampling depths had been displaced to the east and were oriented in an east-southeasterly direction. There was no evidence of any strong vertical shear. The maximum linear extent of the near-surface plume, as defined by the 50 mg/ $\ell$  isopleth, was less than 0.2 km; there were two detached puddles with concentrations greater than 50 mg/ $\ell$ . The near-bottom plume, as defined by the 50 mg/ $\ell$  isopleth, had a maximum extent of about 0.6 km. The areas with concentrations exceeding 50 mg/ $\ell$  were about 0.03 km<sup>2</sup> at 0.6 m and 0.13 km<sup>2</sup> at 2.1 m. The area with concentrations exceeding 100 mg/ $\ell$  was less than 0.01 km<sup>2</sup> at 0.6 m, and was about 0.10 km<sup>2</sup> at 2.1 m. Concentrations of suspended solids at 2.1 m exceeded 2000 mg/ $\ell$  near the discharge.

On Run 4 on 7 April 1977 (Figures 42 and 43) the concentration of suspended solids at the 0.6 m sampling depth never exceeded 42 mg/ $\ell$ . At the lower sampling depth, 2.1 m, the plume was oriented toward the east. The maximum linear extent as defined by the 100 mg/ $\ell$  isopleth was

<sup>\*</sup> The nephelometers "go blind" at 2 2000 mg/l; the transmissometers at about 500 mg/l with a 5 cm path length.

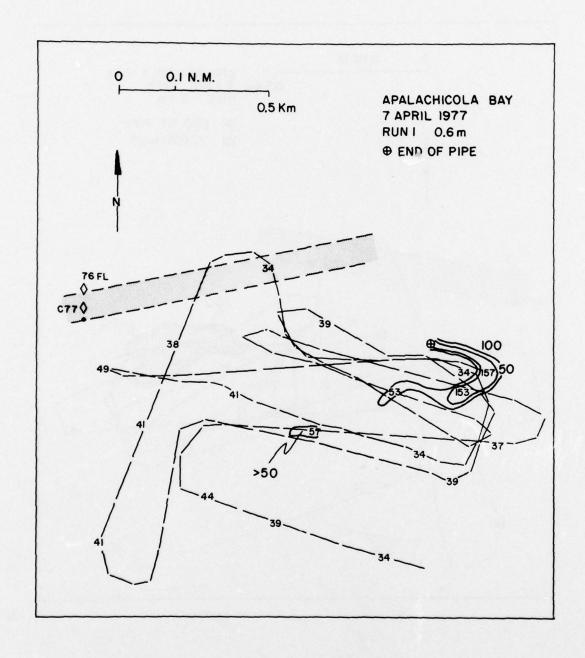


Figure 38. Distribution of total suspended solids (mg/l).

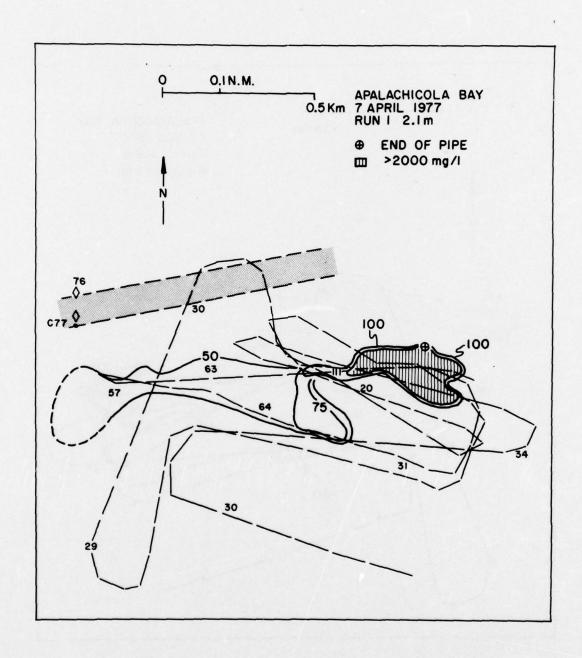


Figure 39. Distribution of total suspended solids (mg/l).

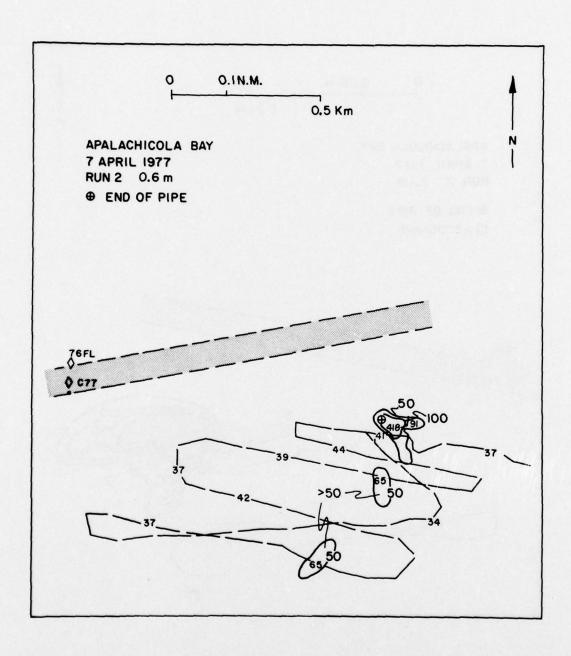


Figure 40. Distribution of total suspended solids (mg/1).

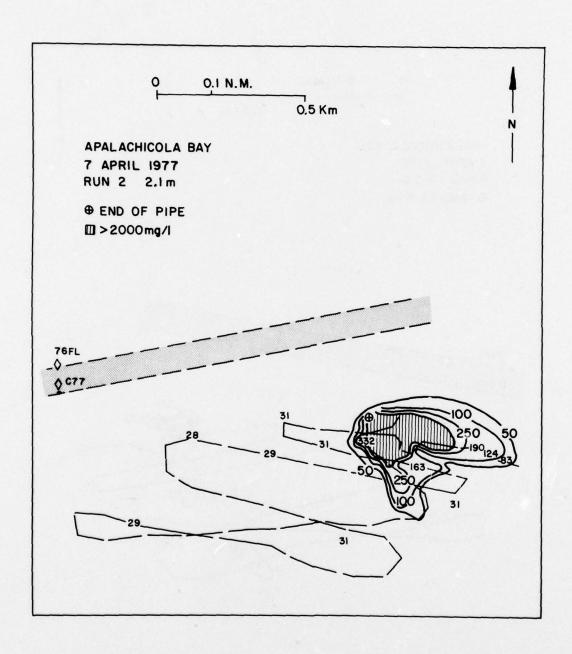


Figure 41. Distribution of total suspended solids (mg/1).

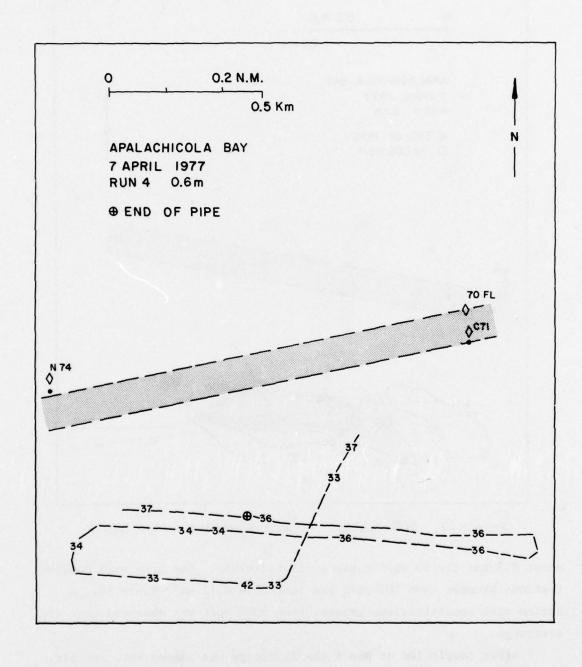


Figure 42. Distribution of total suspended solids (mg/l).

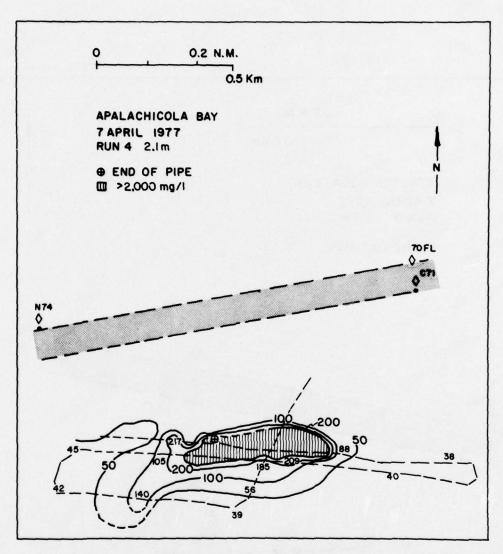


Figure 43. Distribution of total suspended solids (mg/l).

about 0.7 km; the 50 mg/ $\ell$  contour did not close. The area with concentrations greater than 100 mg/ $\ell$  was less than 0.13 km<sup>2</sup>, Table 10. A region with concentrations greater than 2000 mg/ $\ell$  was observed near the discharge.

After completion of Run 4 the discharge was raised into the air. The material was discharged directly through the open pipe without any deflector.

On Run 6 on 7 April 1977 the plume was well-developed at both sampling depths and was oriented generally in a southwesterly direction. There was evidence of some vertical shear, Figures 44 and 45. The maximum linear extent of the plume at both sampling depths, as defined by the 50 mg/ $\ell$  contour, was less than 0.4 km. The areas with concentrations exceeding 75 mg/ $\ell$  were less than 0.02 km<sup>2</sup> at 0.3 m and less than 0.05 km<sup>2</sup> at 1.8 m, Table 10. The area with concentrations exceeding 150 mg/ $\ell$ 

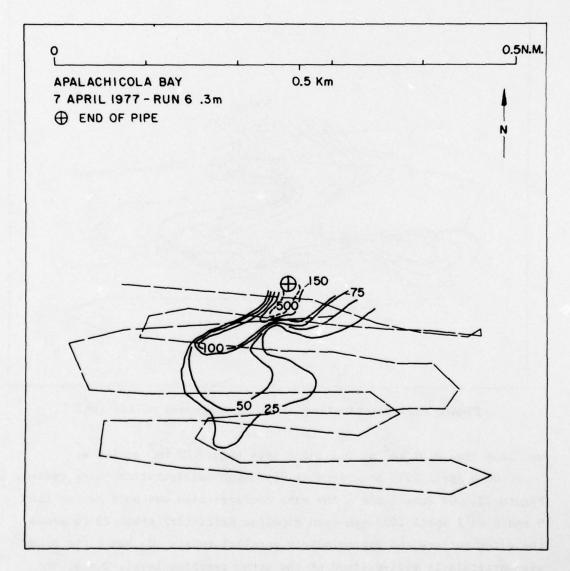


Figure 44. Distribution of total suspended solids (mg/l).

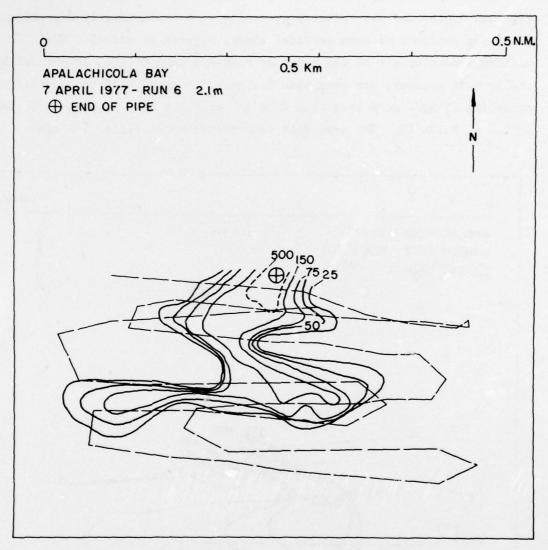


Figure 45. Distribution of total suspended solids (mg/l).

was less than 0.01  $\mathrm{km}^2$  at 0.3 m and less than 0.02  $\mathrm{km}^2$  at 1.8 m.

On 8 April 1977 a variety of discharge configurations were tested, Figure 22. On Runs 1 and 2 the same configuration was used as for Runs 5 and 6 on 7 April 1977—an open pipe (no deflector) about 25 cm above the water surface and approximately parallel to it. On Run 1 the plume was particularly well—defined at the upper sampling level, 0.6 m, and

was oriented in a southeasterly direction. A near-bottom plume was not observed. The maximum linear extent of the near-surface plume, as defined by the 50 mg/ $\ell$  isopleth, was greater than 2.4 km; the transect farthest from the discharge was about 2.4 km from the end of the pipe, Figures 46 and 47. The area at 0.6 m with concentrations greater than 50 mg/ $\ell$  was 0.20 km<sup>2</sup>; the area with concentrations greater than 100 mg/ $\ell$  was about 0.01 km<sup>2</sup>. At the lower sampling depth the maximum concentration was 66 mg/ $\ell$ .

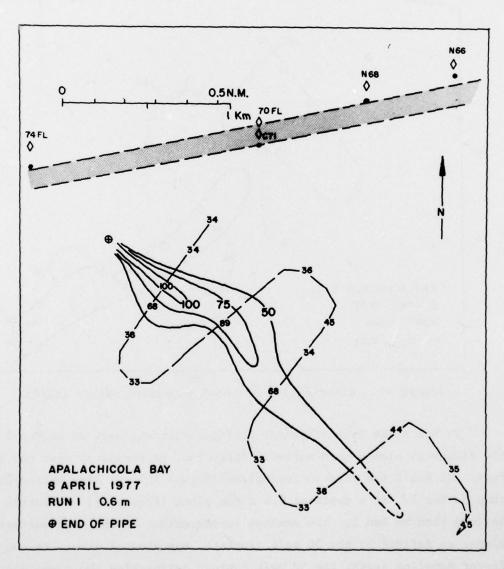


Figure 46. Distribution of total suspended solids (mg/l).

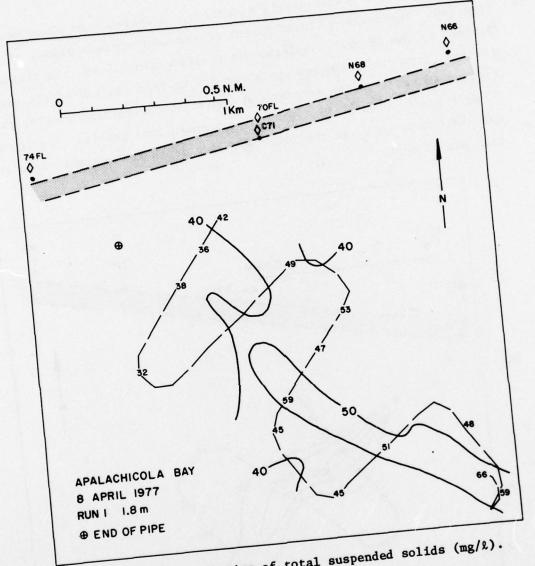


Figure 47. Distribution of total suspended solids (mg/l).

On Run 2 the same discharge configuration was used as on Run 1 but the discharge plumes were markedly different, particularly near the surface. On Run 2 the near-surface plume (Figure 48) was less well-defined than on Run 1. At a depth of 1.8 m the plume (Figure 49) was better defined than on Run 1. The maximum linear extent of the near-surface plume, as defined by the 50 mg/L isopleth, was about 2.4 km. At the deeper sampling depth, the 50 mg/2 contour delineating the plume did

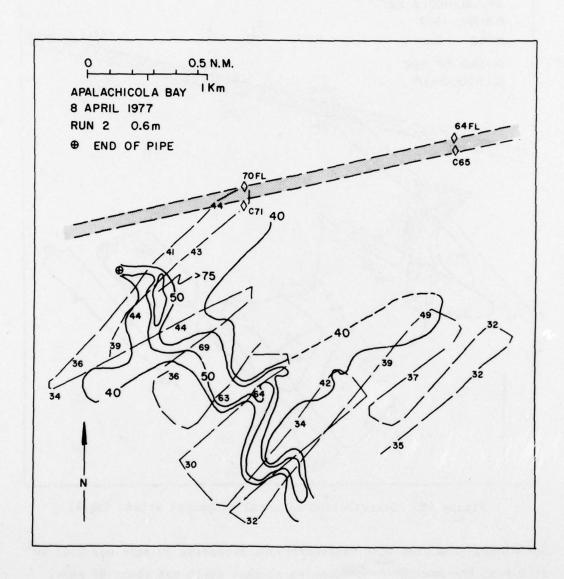


Figure 48. Distribution of total suspended solids (mg/l).

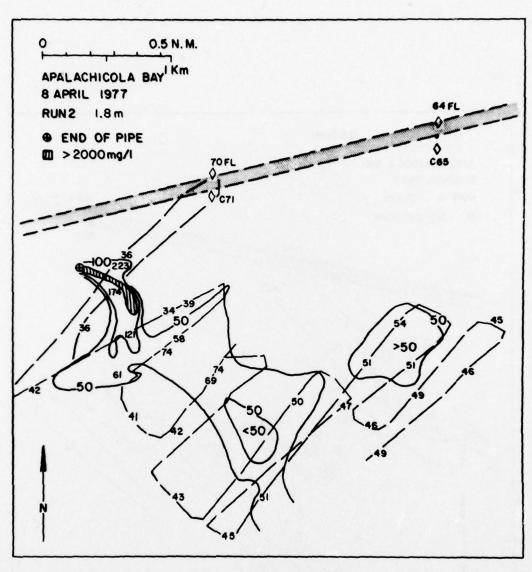


Figure 49. Distribution of total suspended solids (mg/l).

not close. The area with concentrations exceeding 50 mg/ $\ell$  was 0.41 km<sup>2</sup> at 0.6 m; the maximum concentration at that depth was about 80 mg/ $\ell$ . The area with concentrations exceeding 100 mg/ $\ell$  at 1.8 m was about 0.15 km<sup>2</sup>; maximum near-bottom concentrations exceeded 2000 mg/ $\ell$  in a relatively small area (< 0.03 km<sup>2</sup>) near the source.

For Run 3 the discharge was lowered just below the water surface and a deflector plate was added, Figure 22. The dredge pumped for more

than 100 min before the run was made. The plume was relatively well-defined at both depths, but limited in areal extent, Figures 50 and 51. The plume was oriented in an east-northeasterly direction and there was no evidence of strong vertical shear. The maximum linear extent of the plume at 0.6 m, as defined by the 50 mg/ $\ell$  contour, was about 0.2 km; at 1.8 m the 50 mg/ $\ell$  contour did not close. The maximum extent of the plume at 1.8 m as defined by the 75 mg/ $\ell$  isopleth was less than 0.6 km. The

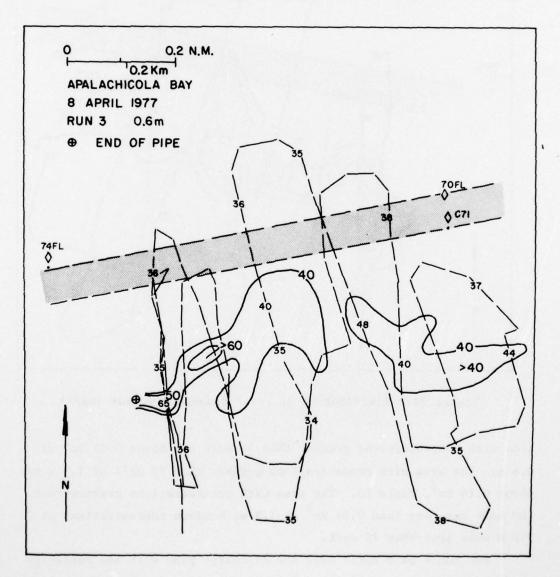


Figure 50. Distribution of total suspended solids (mg/l).

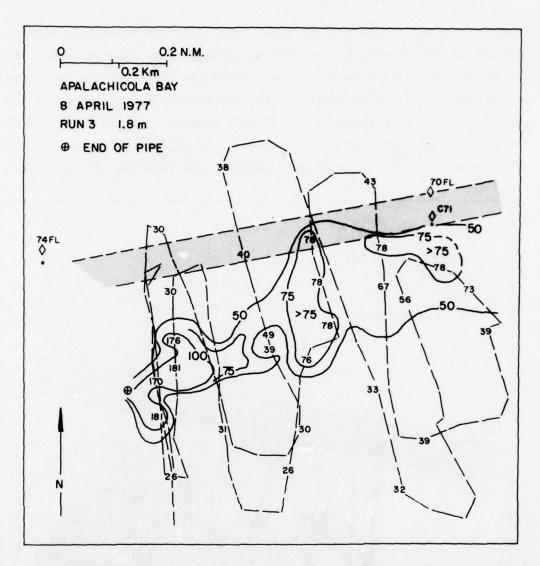


Figure 51. Distribution of total suspended solids (mg/l).

area with concentrations greater than 50 mg/ $\ell$  was about 0.01 km $^2$  at 0.6 m. The area with concentrations greater than 75 mg/ $\ell$  at 1.8 m was about 0.14 km $^2$ , Table 10. The area with concentrations greater than 100 mg/ $\ell$  was less than 0.04 km $^2$  at 1.8 m; maximum concentrations at 0.6 m were less than 70 mg/ $\ell$ .

For Run 4 on 8 April 1977 the discharge pipe with the deflector plate was raised into the air. Plumes were observed at both sampling

depths but they were limited in areal extent, Figures 52 and 53. The near-surface plume was oriented in a northeasterly direction; the near-bottom plume in an easterly direction. The maximum linear extent of the near-surface plume, as defined by the 50 mg/ $\ell$  isopleth, was 0.4 km; the maximum observed concentrations were less than 60 mg/ $\ell$ . The maximum linear extent of the near-bottom plume, defined by the 75 mg/ $\ell$  isopleth, was 0.6 km; the 50 mg/ $\ell$  contour did not close. The area with

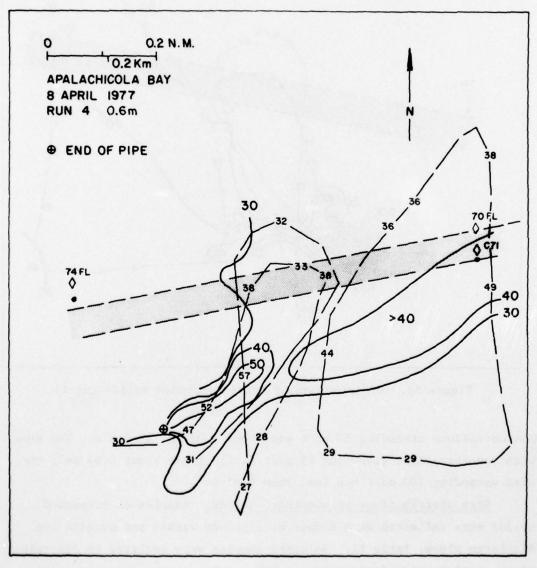


Figure 52. Distribution of total suspended solids (mg/l).

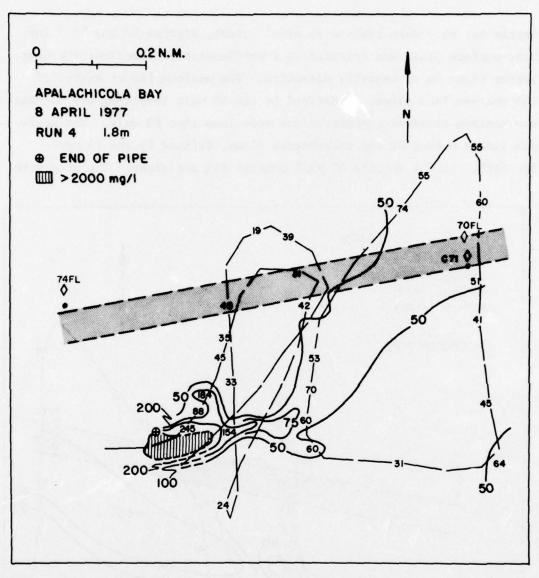


Figure 53. Distribution of total suspended solids (mg/l).

concentrations exceeding 50 mg/ $\ell$  was about 0.02 km $^2$  at 0.6 m. The area with concentrations exceeding 75 mg/ $\ell$  at 1.8 m was about 0.06 km $^2$ ; the area exceeding 200 mg/ $\ell$  was less than 0.03 km $^2$ .

Size distributions of suspended solids. Samples of suspended solids were collected at a number of stations within and outside the discharge plume, Table 11. Selected samples were analyzed to determine their particle size distributions. The analyses were made primarily

Summary of Particle Data for Selected Samples of Suspended Solids

See Figures 54-57 for Size Distributions

Date	Run #	Station	Depth (m)	Suspended Solids (mg/l)	Median Settling Velocity (cm/sec)	Mean Settling Velocity (cm/sec)
2 Apr.	1	A3	2.4		$1.1 \times 10^{-2}$	$2.0 \times 10^{-2}$
6 Apr.	4	A39	2.1	278.9	$8.0 \times 10^{-4}$	9.4 x 10 <sup>-4</sup>
7 Apr.	1	A55	2.1	74.8	$1.0 \times 10^{-3}$	$1.4 \times 10^{-3}$
7 Apr.	1	A56	9.0	30.5	$1.1 \times 10^{-3}$	$1.4 \times 10^{-3}$
7 Apr.	1	A60	2.1	44.5	1.1 × 10 <sup>-3</sup>	$1.5 \times 10^{-3}$
7 Apr.	2	A64	9.0	19.0	$6.2 \times 10^{-4}$	7.9 x 10 <sup>-4</sup>
7 Apr.	2	A68	2.1	17.0	$2.4 \times 10^{-3}$	$7.2 \times 10^{-3}$
8 Apr.	1	A81	9.0	68.4	4.0 × 10 <sup>-4</sup>	$5.2 \times 10^{-4}$
8 Apr.	2	A91	2.1	not filtered	7.5 x 10 <sup>-4</sup>	$1.2 \times 10^{-3}$

to provide inputs to the plume model described in Part III.

Size distributions of selected samples of suspended solids are presented in Figures 54-57, and several of their statistical parameters are summarized in Table 11. See Appendix A for a complete description of methods of analysis and data reduction.

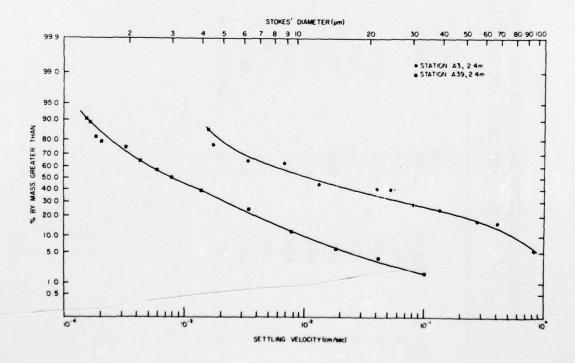


Figure 54. Size distributions of suspended solids within and near the plume of dredged material in Apalachicola Bay.

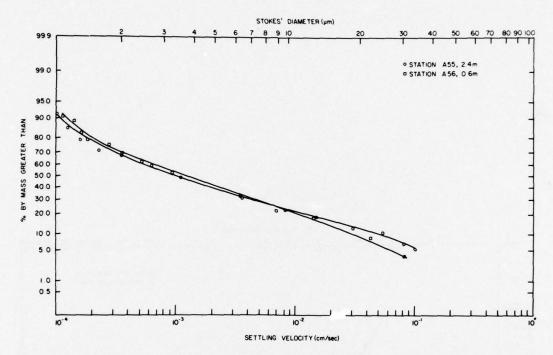


Figure 55. Size distributions of suspended solids within and near the plume of dredged material in Apalachicola Bay.

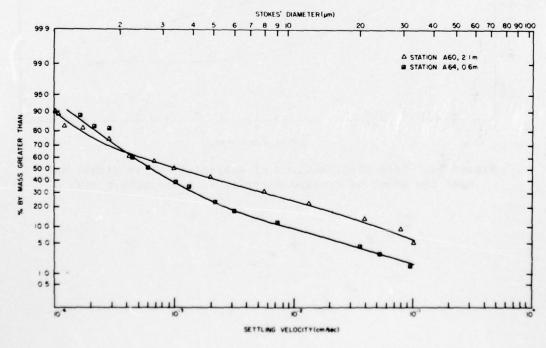


Figure 56. Size distributions of suspended solids within and near the plume of dredged material in Apalachicola Bay.

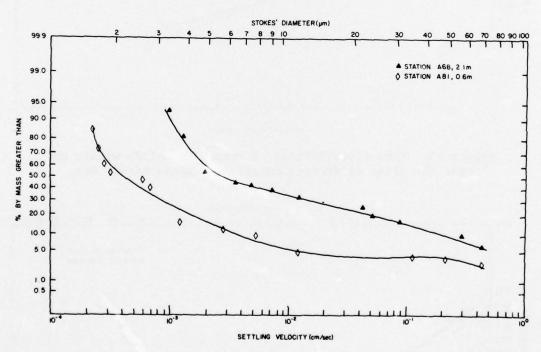


Figure 57. Size distributions of suspended solids within and near the plume of dredged material in Apalachicola Bay.

#### Discussion

## Inferring Plume Orientation from Currents and Wind

A detailed examination of all the plumes for Apalachicola Bay reveals little correspondence between the current directions as measured at 1.2 m near 'N68" and the principal axes of the plumes. Only Run 4 on 6 April and Run 3 on 8 April show any agreement at all. In retrospect it is not surprising that the current as measured at 1.2 m should be at variance with the plume observations for this area. The Apalachicola River which enters Apalachicola Bay several kilometers north of the dredging site significantly influences the vertical distribution of salinity in the area where our measurements were made. At times the water column was highly stratified with the fresher river water ( $^{\mathcal{H}}$  l ppt) causes a decoupling of the lower layers from the surface waters by inhibiting vertical mixing which in turn confines any wind effects primarily to the surface layers. Since the area is also characterized by low tidal amplitudes, the bottom waters of the stratified areas will be primarily influenced by the astronomical tides whereas the surface layers will be influenced by both tide and wind. The result is an extremely complicated vertical distribution of velocity which will exhibit considerable vertical shear. The current meters, which were located at mid-depth, were not properly located to define motions in the surface or the bottom layer where the plumes were measured.

An analysis of the effect of local winds on the surface plumes is also complicated by the fact that the winds shown on Figure 25 recorded by the National Weather Service Office at the Municipal Airport, Apalachicola are apparently not representative of winds in the vicinity of the dredging site. For example, at 1540 on 8 April the wind direction in the study area was observed as southwest and its speed estimated at 8.5-10 m/sec; the value reported by the NWS for 1600 was west at 4.5 m/sec. Again on 6 April at 1400, the estimate of the wind in the

AD-A058 507 UNCLASSIFIED

STATE UNIV OF NEW YORK AT STONY BROOK MARINE SCIENCES--ETC F/6 13/2 FIELD INVESTIGATIONS OF THE NATURE, DEGREE, AND EXTENT OF TURBI--ETC(U) JUL 78 J R SCHUBEL, H H CARTER, R E WILSON DACW39-76-C-0129 WES-TR-D-78-30 NL



dredging area was southwest at 7.5-10 m/sec compared to  $350^{\circ}T$  at 6 m/sec at 1300 by the NWS.

For reliable predictions of plume directions in shallow systems from measurements of current and wind, the current meters must adequately define the vertical distribution of velocity and the winds used must be appropriate to the disposal area. In many cases, this will mean that local winds must be measured.

# Partitioning of the total mass of solid material discharged between the bottom layer and the plume

An estimate of the partitioning of the total mass of sediment discharged by a pipeline dredge between the bottom (fluid mud?) layer and the plume would be useful. The authors have done this in several ways with the data from Apalachicola Bay and Atchafalaya Bay.

The simplest approach is to compare the concentration of total suspended solids in the pipe, which was calculated, with the maximum concentration observed in the plume very close to the source. One then assumes that any decrease of concentration is attributable entirely to rapid deposition of the slurry—and not at all to dilution. If the slurry in the pipe is about 15% solids, by mass\*, the concentration of solids in the pipe would have been about 150,000-200,000 mg/l. The maximum vertically averaged concentration of suspended solids determined from gravimetric and optical measurements was less than 1500 mg/l. Thus:

$$\frac{\text{Conc. Susp. Solids in Plume}}{\text{Conc. Susp. Solids in Pipe}} = \frac{1500 \text{ mg/} 2}{150,000 \text{ mg/} 2} = 0.01 = 1\%$$

This simple calculation suggests that about 1% of the mass of solid material discharged by a pipeline dredge is incorporated into the plume and that the other 99% goes rapidly into the bottom (fluid mud?) layer very close to the source.

A second estimate of the partitioning of the total mass of solid

<sup>\*</sup> W. Barnard, personal communication, November 1977.

material discharged was obtained as follows. In Part III it is shown that in the steady state part of the plume when there is no settling, the concentration of excess suspended sediment varies as

$$\frac{q}{\sqrt{\pi}\omega XD}$$
 for small  $\frac{\omega}{u}$ 

and

$$\frac{q}{2\sqrt{\pi}\omega XD}$$
 for large  $\frac{\omega}{u}$ 

where

 $q \equiv rate \ of \ addition \ of \ solid \ material \ not \ deposited \ near \ the \ discharge$ 

 $\omega \equiv diffusion velocity$ 

u = mean flow speed of the receiving waters

D = average thickness of the layer of water containing the plume

X ≡ distance along the axis of plume.

Even for very high settling, the concentrations of excess suspended solids in the steady state part of the plume would be reduced at most by  $10^{-0.5}$  from what they would be for no settling at small  $\frac{\omega}{u}$ . The correction for settling vanishes for large  $\frac{\omega}{u}$ . The above expressions would, for high settling, be:

$$\frac{q}{\sqrt{10\pi}\omega XD}$$
 for small  $\frac{\omega}{u}$ 

$$\frac{q}{2\sqrt{\pi}\omega XD}$$
 for large  $\frac{\omega}{u}$ 

Since most of the authors' data are for relatively small  $\frac{\omega}{u}$  , the first expression will be used to estimate q.

For Atchafalaya Bay (see Figure 72 in Part III) we have

w ₹ 1 cm/sec

$$C(X) \approx 10^{2.6} \text{ mg/}10^3 \text{ cm}^3 \text{ at } X = 185 \text{ x }10^2 \text{ cm}$$

Using these data one obtains

$$q = C(X)\sqrt{\pi\omega}XD$$

$$q = (10^{2.6} \text{ mg/}10^3 \text{ cm}^3)(\sqrt{\pi})(1 \text{ cm/sec})(1.85 \text{ x } 10^4 \text{ cm})(10^2 \text{ cm})$$

$$q \approx 1305 \times 10^3 \text{ mg/sec} \sim 1.3 \times 10^6 \text{ mg/sec}$$

This is the value q would have to have to produce the C(X) observed in Atchafalaya Bay if there were no settling. With high settling the value of q required to produce the observed distribution increases to about  $4.1 \times 10^6$  mg/sec. Thus, q might range between about 1.3 and  $4.1 \times 10^6$  mg/sec. The rate of discharge of total mass of solids by the pipe, Q, was about 0.39 metric tons/sec (3.9 x  $10^8$  mg/sec). For Atchafalaya Bay then, q/Q was probably between 0.3 x  $10^{-2}$  and  $1.0 \times 10^{-2}$ . This means that between 0.3 and 1.0% of the total mass of solid material discharged by the dredge was incorporated into the plume, the remainder settled rapidly to the bottom as a density flow very near the source.

Using the same arguments for data from Apalachicola Bay (see Figures 73 and 74 in Part III), one has

ω % 1 cm/sec

$$C(X) \approx 10^{2.2} \text{ mg/}10^3 \text{ cm}^3 \text{ at } X = 185 \times 10^2 \text{ cm}$$

$$q = (10^{2.2} \text{ mg}/10^3 \text{ cm}^3)(\sqrt{\pi})(1 \text{ cm/sec})(1.85 \times 10^4 \text{ cm})(2 \times 10^2 \text{ cm})$$

$$q = 1.04 \times 10^6$$
 mg/sec for no settling and small  $\frac{\omega}{u}$ .

It was found that for high settling,  $q = 3.28 \times 10^6$  mg/sec. The Q estimated for Apalachicola Bay was about 0.13 metric tons/sec. The value is much smaller than for Atchafalaya Bay because the area of the discharge pipe used in Apalachicola Bay was only about 1/3 of that used in Atchafalaya Bay. For the authors' Apalachicola Bay data  $q/Q \approx 0.8 \times 10^{-2}$  to 2.5 x  $10^{-2}$ . This means that about 0.8 to 2.5% of the total amount of material discharged was incorporated into the plume, and that the remainder went into the bottom (fluid mud?) layer very close to the discharge.

A third approach to estimate the partitioning of the total mass of solid material discharged between the plume and the bottom layer is to compare the mass of solids suspended within the plume to the total mass of solids discharged during the time required to generate the plume. The total mass of solids suspended within the plume of excess suspended solids for four runs in Apalachicola Bay are summarized in Table 12. The method is described in the Dissolved Oxygen Section of Part IV.

Table 12

Total Mass of Excess Suspended Solids within the

Plumes for Selected Runs in Apalachicola Bay.

(The Natural, Background, Concentration was

Assumed to be 20 mg/l).

		Mass		
		$_{\rm kg} \times 10^{-3}$		
Run	Date	Upper 1.3 m	Lower 0.7 m	Total
6	7 Apr'76	6.1	6.5	12.7
1	8 Apr'76	60.8	24.5	85.3
2	8 Apr'76	57.4	44.9	102.3
3	8 Apr'76	8.4	5.5	13.9

The range in total mass of solids suspended within the plume is  $1 \times 10^4$  kg to  $1 \times 10^5$  kg, Table 12. The next step is to compare these totals with the amount of material discharged during the time, t, equal to the age of the plume. The authors have estimated that t is of order  $10^5$ sec--1 day. The total mass of sediment discharged by the dredge in Apalachicola Bay during time, t, can be estimated from:

If one assumes that  $Q \approx 0.13$  metric tons/sec =  $0.13 \times 10^3$  kg/sec, then

 $M_D = (0.13 \times 10^3 \text{ kg/sec})(10^5 \text{ sec}) = 0.13 \times 10^8 \text{ kg} \% 1 \times 10^7 \text{ kg}.$ 

Using this value for M<sub>D</sub> and the data in Table 12, it is apparent that between about 0.1% and 1.0% of the total mass of material discharged during the time it took for the plume to develop was incorporated into the plume. This estimate of the mass of material within the plumes may be somewhat low since our bottom sensor was located at 2.1 m and the average depth in the disposal area was about 2.7 m. Based on the gradients of suspended material near the bottom, determined by lowering a transmissometer very close to the bottom, the authors estimate that the computed masses of solids in the plumes may be low by as much as a factor of 2, but not more than this. This would increase the estimate of the amount of material in the plume by this factor. The value for t may be low which would also decrease the estimate.

In summary, all three estimates indicate that 1% is the correct order of magnitude for the fraction of the total mass of solids discharged by a pipeline dredge that is incorporated into the plume.

### Effects of discharge configuration on plumes

The effects of different discharge configurations have been analyzed from the data presented in Table 10. Although the data are few, some general conclusions can be drawn. Only two runs were made while the material was discharged against a deflector plate—one with the discharge below water, and one with it above. The use of a deflector reduced the surface plume, but there was no significant difference between the surface plumes associated with the above—water and below—water discharge. When no deflecting plate was used the near—surface plume, as defined by the 50 mg/l isopleth, was more extensive when the material was discharged into the air than when discharged below water. The area with concentrations greater than 100 mg/l decreased with an above—water discharge, however. The one low value of the 50 mg/l area for an above—water discharge without a deflector plate was obtained on the first run approximately 20-30 min after the discharge was elevated and probably indicates that the plume had not had time to develop fully.

If the objective is to minimize the areal extent of the near-surface plume, the authors' limited data for four discharge configurations tested in Apalachicola Bay indicate that discharge against a deflector plate, either above or below water, is better than discharge without a deflector plate. The data also suggest that if a discharge plate is not used, discharge below water is probably preferable to discharge above water if one wants to minimize the areal extent of the surface plume.

Observations at Corpus Christi suggest that discharge below and normal to the water surface is more effective in reducing the surface plume than discharge below and parallel to the water surface.

The data for the near-bottom plume are, as might be expected, more variable. This results in part because natural background concentrations are more variable because of local resuspension. In part, it also reflects variations in the levels of the lower sensor above the bottom; relatively minor changes in elevation near the bottom can result in relatively large changes in the concentration of suspended solids because vertical gradients are strong.

## Shrimping as a source of suspended solids in Corpus Christi Bay

Corpus Christi Bay supports a productive shrimp fishery and the method of harvesting with weighted nets may be a significant source of suspended solids to the waters of the Bay. This hypothesis was tested.

The shrimp fishery in Corpus Christi Bay is conducted by small, 10-15 m, otter trawlers. Brown shrimp, *Penaeus aztecus*, is the dominant species in the catch. Total fishing effort in 1975 amounted to about 5800 boat days\*. Trawls vary in width at the footrope from about 6-20 m and are towed 30-100 m astern at a speed of about 1 m/sec. A smaller net, called a "try-net," is towed ahead of the main trawl and is used to locate and keep the main net in areas of commercial concentrations of shrimp.

J. Morgan, National Marine Fisheries Service, personal communication, November 1977.

The "try-net" is put over the side and towed until frequent haul-backs reveal a concentration of shrimp, whereupon the main trawl is set out. The weighted footrope of the main net disturbs approximately the upper 5 cm of the sediment, forcing the shrimp into the overlying water where they are entrapped in the advancing net. The main trawl is hauled back when inspection of the try-net reveals decreasing numbers of shrimp. The vessel then frequently reverses course and attempts to fish the same school again. Main trawls are fished an average of 5-10 hr/day.

Using the data furnished by the National Marine Fisheries Service, an estimate was made of the minimum and maximum amounts of sediment resuspended by shrimping activity each year in Corpus Christi Bay. The pertinent data are presented below.

Number of boat days/yr	5800
Number of hours worked/day	4-10
Towing speed	1 m/sec
Width of trawl at footrope	6-20 m
Depth of disturbance of bottom	5 cm

Making the appropriate calculations one finds that between  $25 \times 10^6$  m<sup>3</sup> and  $209 \times 10^6$  m<sup>3</sup> of in-place sediment are disturbed by shrimping activity in a typical year (1975).

The total maintenance dredging in Corpus Christi Bay between 1971-1976 was 9.7 x  $10^6\ \mathrm{m}^3$  and was distributed as follows:

No dredging was conducted in 1972, 1973, and 1975. The average maintenance dredging for the six year period, 1971-1976, was then about  $1.6 \times 10^3 \, \mathrm{m}^3/\mathrm{yr}$ . Therefore, the amount of sediment resuspended each year by shrimpers is approximately 16-131 times that dredged for channel maintenance.

It is useful to estimate how much of the material disturbed by shrimping activity is added to the overlying water column.

Approximately 75-85 percent of the 26.5-215.5 x  $10^6$  m<sup>3</sup> of material resuspended by shrimpers is probably accounted for by interstitial waters, and therefore the *volume of sediment* (solid material) resuspended by shrimping activity may be between 4 and 54 x  $10^6$  m<sup>3</sup>. This would be equivalent to a total mass of dry sediment of between  $11 \times 10^6$  and  $143 \times 10^6$  metric tons, assuming a density of 2.65 gm/cm<sup>3</sup> (quartz).

Assuming that a trawl cuts into the bottom to a depth of 5 cm and that the in-place sediments are 15 percent by volume solid material, the mass of dry sediment resuspended by shrimping activity per meter of trawl travel ranges from about 0.1 metric ton for a 6 m trawl to 0.4 metric ton for a 20 m trawl. If this mass of material were distributed uniformly throughout a 4 m water column—the "average" depth in the area studied—the concentration of total suspended solids immediately behind the trawl would be more than 5000 mg/l.

Observations were made of the concentrations of suspended solids in the trails of a number of shrimp boats. Because of the uncertainty of the position of the trawl and other factors, the observations were never made closer than 100 m astern of the estimated position of the trawl. Observations were made continuously and underway at 2 depths--0.6 m and 2.1 m--with transmissometers and nephelometers. Concentrations of suspended solids in the shrimper trails, Figure 58, were typically between 100 and 500 mg/l, Figure 59. While much lower than the calculated mean value of 5000 mg/l based on the assumption that the resuspended material was uniformly distributed vertically, these concentrations of 100-500  $mg/\ell$  are comparable to those observed off the discharge off the dredge, Figures 30-53. Nor are they discordant with the total mass of sediment disturbed by shrimping activity. The discrepancy between the calculated and measured values of suspended solids in shrimper trails is attributable primarily to the assumption of uniform dispersal of resuspended material throughout the water column and to the sampling depths for the optical measurements of suspended solids. The resuspended material is, of course, not uniformly distributed throughout the water column; concentrations increase exponentially near the bottom. Since the mean depth in the area was between 3 and 4 m,



Figure 58. Aerial photograph showing trails of suspended solids produced by shrimp trawlers.

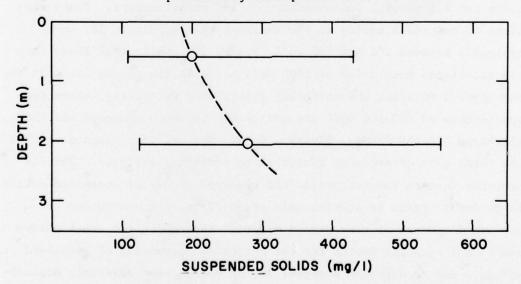


Figure 59. Distribution of total suspended solids (mg/l) in wake of shrimp trawler. The horizontal bars indicate the observed range in concentration; the circles the arithmetric mean.

the deepest observations were 1 m, or more, above the bottom and well above the layer of maximum concentrations of total suspended solids.

Settling of disturbed bottom material between the time of resuspension and the time of observation accounts for a smaller fraction of the apparent discrepancy between calculated and observed values. Shrimper trails were crossed at least 100 m astern of the trawl. At a shrimp boat speed of about 1 m/sec, the trail was crossed at least 100 sec after passage of the trawl. Since the mean settling velocity of the agglomerated bottom sediments is probably  $^{\sim}$  10<sup>-2</sup> to 10<sup>-1</sup> cm/sec, in 100 sec particles would settle  $^{\sim}$  1-10 cm. Near the bottom where concentrations of total suspended solids reach thousands of mg/ $\ell$ , particles do not settle as individual particles and effective settling velocities may be increased by several orders of magnitude.

In summary, not only is the total amount of sediment disturbed each year by shrimping activity greater than that removed by maintenance dredging, but the total area of the Bay affected is much greater. This is not to suggest that the increased suspended solids levels resulting from shrimping are deleterious to the biota of Corpus Christi Bay.

# PART III: A SUSPENDED SOLIDS PLUME MODEL AND ITS APPLICATION

## The Model

# Introduction

The model presented here was developed to describe the characteristics of suspended solids plumes which form in shallow estuarine or coastal waters during dredging operations involving open-water pipeline disposal. The objective has been to develop a predictive model which would provide maximum information on the spatial distribution of suspended solids concentrations from minimum information on local hydrography, the intensity of advective and dispersive processes, the configuration of the discharge, and the characteristics of the material being discharged. The emphasis has been on simplicity. Results are for a steady and spatially uniform ambient flow field, and they relate to vertically averaged concentrations only.

### Formulation

The material in suspension is not homogeneous; it consists of various size particles with each size fraction characterized by a different settling velocity. The transport equation which governs the distribution of total suspended sediment of all fractions may be written  $^6$  as

$$\frac{\partial}{\partial \mathbf{t}} \Sigma \mathbf{c}_{\mathbf{i}} = -\frac{\partial}{\partial \mathbf{x}} \mathbf{u} \Sigma \mathbf{c}_{\mathbf{i}} - \frac{\partial}{\partial \mathbf{y}} \mathbf{v} \Sigma \mathbf{c}_{\mathbf{i}} - \frac{\partial}{\partial \mathbf{z}} \Sigma \left[ \mathbf{w} + \mathbf{w}_{\mathbf{i}} \right] \mathbf{c}_{\mathbf{i}} + \frac{\partial}{\partial \mathbf{x}} K_{\mathbf{H}} \frac{\partial}{\partial \mathbf{x}} \Sigma \mathbf{c}_{\mathbf{i}}$$

$$+ \frac{\partial}{\partial \mathbf{v}} K_{\mathbf{H}} \frac{\partial}{\partial \mathbf{v}} \Sigma \mathbf{c}_{\mathbf{i}} + \frac{\partial}{\partial \mathbf{z}} K_{\mathbf{z}} \frac{\partial}{\partial \mathbf{z}} \Sigma \mathbf{c}_{\mathbf{i}} , \qquad (1)$$

where  $c_i$  is the concentration of the size fraction whose settling velocity in still water is  $w_i$ ; t is time; x, y, z are Cartesian coordinates (z is positive downward with origin in the free surface),

and u, v, w, are components of water velocity in directions, x, y, z.  $K_H$  and  $K_Z$  are, respectively, horizontal and vertical eddy diffusion coefficients for the suspended solids. It is assumed that the same diffusion coefficients apply to each size fraction. Note that equation (1) is applicable only to those regions away from the bottom where the water volume displaced by the suspended particles is negligible.

Of primary concern here are plumes which develop in very shallow water; as a consequence only vertically averaged concentrations will be examined. If it is assumed that u, v and  $K_H$  are independent of depth, that w vanishes at the bottom (z=D), and that there is no flux of suspended solids through the surface (z=0), equation (1) may be integrated to obtain:

$$\frac{\partial C}{\partial t} = -\frac{\partial}{\partial x} uC - \frac{\partial}{\partial y} vC + \frac{\partial}{\partial x} K_H \frac{\partial C}{\partial x} + \frac{\partial}{\partial y} K_H \frac{\partial C}{\partial y} + \frac{1}{D} \left( K_z \frac{\partial}{\partial z} \Sigma c_i - \Sigma w_i c_i \right)_{z=D}$$
(2)

where C is the vertically averaged solids concentration defined by

$$C = \frac{1}{D} \int_{0}^{D} \Sigma c_{i} dz \qquad . \tag{3}$$

The expression in parenthesis on the right side of equation (2) represents the flux of sediment into the bottom. In the model it has been assumed that this flux may be related to the vertically averaged concentration C associated with an effective settling velocity W:

$$\frac{1}{D} \left( K_{z} \frac{\partial}{\partial z} \Sigma c_{i} - \Sigma c_{i} w_{i} \right)_{z=D} \simeq - \frac{WC}{D} . \tag{4}$$

If the sediment does not experience significant resuspension at the bottom then a practical estimate for W might be obtained from:

$$W \simeq \frac{\int_{0}^{D} \Sigma w_{i} c_{i} dz}{\int_{0}^{D} \Sigma c_{i} dz} \qquad (5)$$

It is desired to simulate a plume which results from a continuous discharge into shallow water of depth D. For this purpose therefore, a solution to equation (2) for C(x,y,t) for a continuous vertical line source has been selected. Okubo and Pritchard<sup>7</sup> proposed a relationship for horizontal diffusion from an instantaneous vertical line source which could be integrated to give the concentration distribution for a continuous line source:

$$\tilde{C}(x,y,t) = \frac{m}{\pi\omega^2 Dt^2} \exp \left[-\frac{\left(x - \int_0^t u(t')dt'\right)^2}{\omega t}\right]^2 \exp \left[-\frac{\left(y - \int_0^t v(t')dt'\right)^2}{\omega t}\right]^2.$$
(6)

 $\tilde{C}(x,y,t)$  is the concentration from an instantaneous release of a mass m distributed over a depth D,  $\omega$  is the diffusion velocity, and t is the elapsed time since the release. The relationship (6) describes a diffusing patch whose variance in either the x or y direction equals  $\frac{\omega^2 t^2}{2}$ . It is easy to integrate (6) for a continuous source<sup>7,8</sup> and to extend it to incorporate a first order reaction such as particle settling. The result is

$$C(x,y,t) = \frac{q}{\pi\omega^2 D} \int_0^t \frac{1}{t^{\frac{1}{2}}} \exp{-\left[\frac{x-ut'}{\omega t'}\right]^2} \exp{-\left[\frac{y}{\omega t'}\right]^2} \exp{-\left[\frac{Wt'}{D}\right]} dt' ,$$
(7)

where q is the rate of release of material in mass per unit time. The relation (7) represents a solution to equation (2) for a continuous vertical line source release initiated at t=0 if we identify  $K_H$  as  $\omega^2 t$ . It incorporates particle settling as described by equation (4), and includes the assumption that the ambient flow is constant in time and directed along the x axis. It will serve as a basis for our description of suspended solids plumes.

# Predicted results

In order to examine the structure which the solution (7) represents, the independent variables, x, y, and t, have been nondimensionalized as follows:

It is important to realize that t is the time since initiation of the discharge, and that ut is the distance from the origin to the center of mass of a "patch" which was released at t=0. The distance ut marks the front of the plume<sup>8</sup>, and material can advance past this point only by dispersive processes. In terms of the nondimensional variables the equation (7) becomes

$$C(x,y,t) = \frac{q}{\pi\omega^2 Dt} \int_0^1 \frac{1}{t^{*2}} \exp{-\left(\frac{u}{\omega}\right)^2 \left(\frac{x^* - t^*}{t^*}\right)^2} \exp{-\left(\frac{u}{\omega}\right)^2 \left(\frac{y^*}{t^*}\right)^2} \exp{-\gamma t^* dt^*}, \quad (8)$$

where  $\gamma = \frac{Wt}{D}$  is a ratio of the plume age to a settling time.

The integral on the right side of (8) contains all of the information on the structure of the suspended solids plume. It is a function of x\*, y\*,  $\gamma$ , and  $\frac{\omega}{u}$ , the ratio of the diffusion velocity to the advective velocity. If y\* is set equal to zero in equation (8) an expression for centerline concentration is obtained:

$$C(x,o,t) = \frac{q}{\pi\omega^2 Dt} G(x^*, \frac{\omega}{u}, \gamma) , \qquad (9)$$

where  $G(x^*,\frac{\omega}{u},\gamma)$  represents the integral in (8). Normalizing by the concentration at the front, G(ut,o,t), a general expression for centerline concentration is obtained which is independent of q and t:

$$\frac{C(x,o,t)}{C(ut,o,t)} = \frac{G(x^*,\omega/u,\gamma)}{G(1,\omega/u,\gamma)} \qquad (10)$$

Figures 60 through 64 show the function  $\frac{G(x^*,\omega/u,\gamma)}{G(1,\omega/u,\gamma)}$  plotted versus  $x^*$  for the range of the parameters  $\omega/u$  and  $\gamma$  indicated. The figures show that the position of the front  $x^*=1$  separates the plume into two rather distinct regions. Upstream of the front the rate of decrease of concentration with  $x^*$  is generally much less than downstream of the front and the sharpness of the front increases with decreasing  $\omega/u$ . It is apparent that settling enhances the rate of decrease in concentration with  $x^*$ , and that the effect of settling is most pronounced at small  $\omega/u$ .

Upstream of the front, for small  $\gamma$  and small  $\omega/u$ , concentrations vary as  $2/x^*$ , and for large  $\omega/u$  they vary as  $1/x^*$ . In Figure 65  $G(1,\omega/u,\gamma)$  has been plotted as a function of  $\omega/u$  with  $\gamma$  as a parameter. For small  $\gamma$  this function varies as  $\frac{\sqrt{\pi}}{2}(\omega/u)$ . Referring to equation (9), it can be seen that for small  $\gamma$  and  $\omega/u$ , centerline concentrations upstream of the front vary as

$$C(x,o,t) = \frac{q}{\pi\omega^2 Dt} \frac{2}{x^*} \frac{\sqrt{\pi}}{2} \frac{\omega}{u} = \frac{q}{\sqrt{\pi} \omega D}, \qquad (11)$$

and as

$$C(x,o,t) = \frac{q}{\pi\omega^2 Dt} \frac{1}{x^*} \frac{\sqrt{\pi}}{2} \frac{\omega}{u} = \frac{q}{2\sqrt{\pi} \omega x D} , \qquad (12)$$

for large  $\omega/u$ . Note that centerline concentrations upstream of the front are, therefore, independent of u in this model.

Consider now the lateral structure of the plume. Rather than examine this structure in detail, the second moment  $\overline{y^2}$  of the concentration distribution will be computed from (6). The second moment or variance characterizes the lateral spread of the plume, and it can be determined as a function of x\*,  $\omega/u$  and  $\gamma$ . The second moment is defined by:

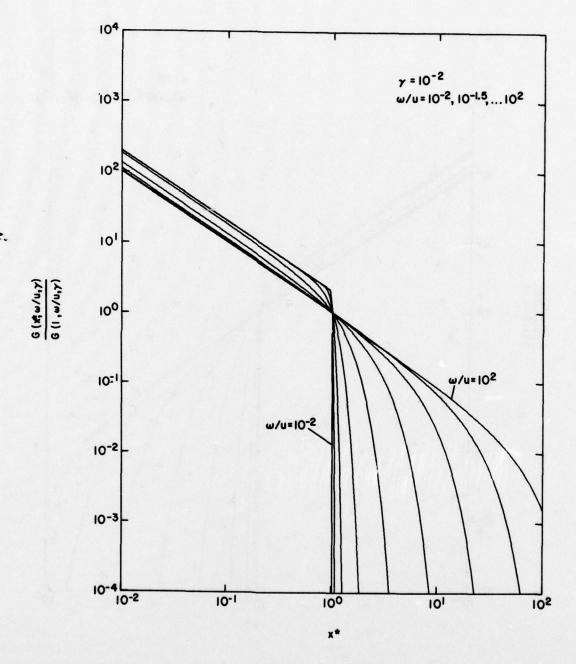


Figure 60. Normalized centerline concentration of suspended solids versus normalized centerline distance from source for  $\gamma = 10^{-2} \text{ with } \omega/u \text{ as a parameter.}$ 

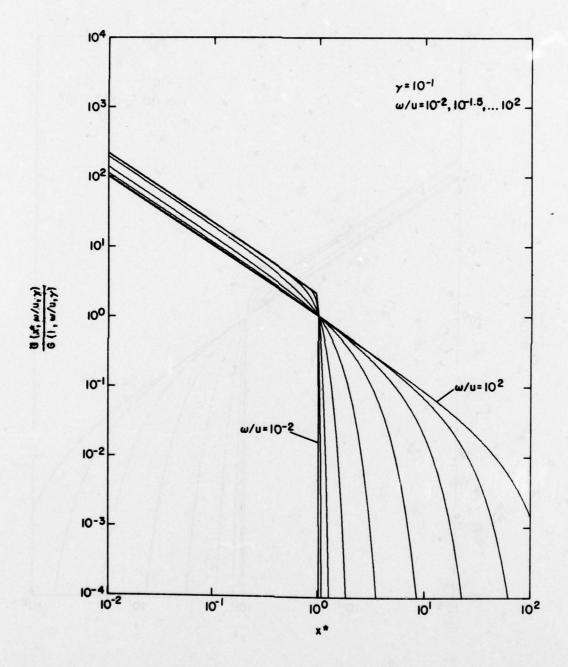


Figure 61. Normalized centerline concentration of suspended solids versus normalized centerline distance from source for  $\gamma = 10^{-1} \text{ with } \omega/u \text{ as a parameter.}$ 

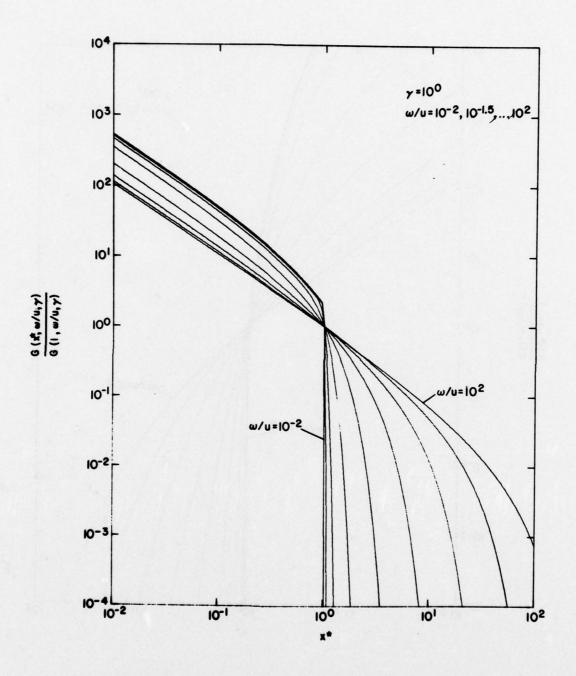


Figure 62. Normalized centerline concentration of suspended solids versus normalized centerline distance from source for  $\gamma \,=\, 10^0 \text{ with } \omega/u \text{ as a parameter.}$ 

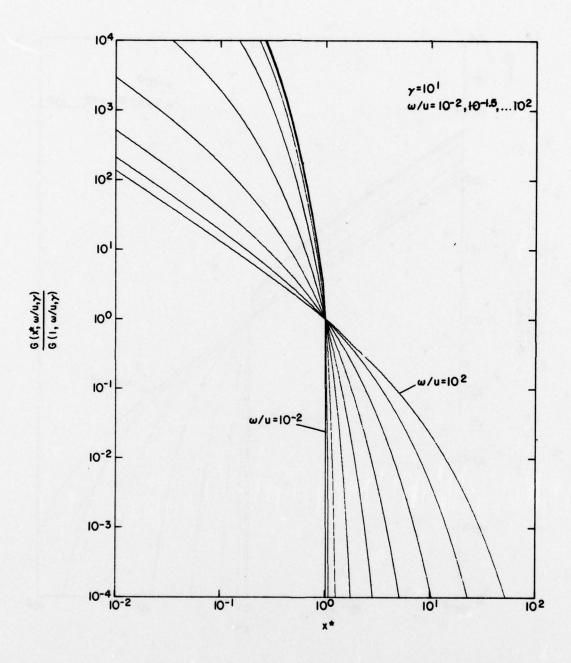


Figure 63. Normalized centerline concentration of suspended solids versus normalized centerline distance from source for  $\gamma \, = \, 10^1 \, \text{ with } \omega/u \, \text{ as a parameter.}$ 

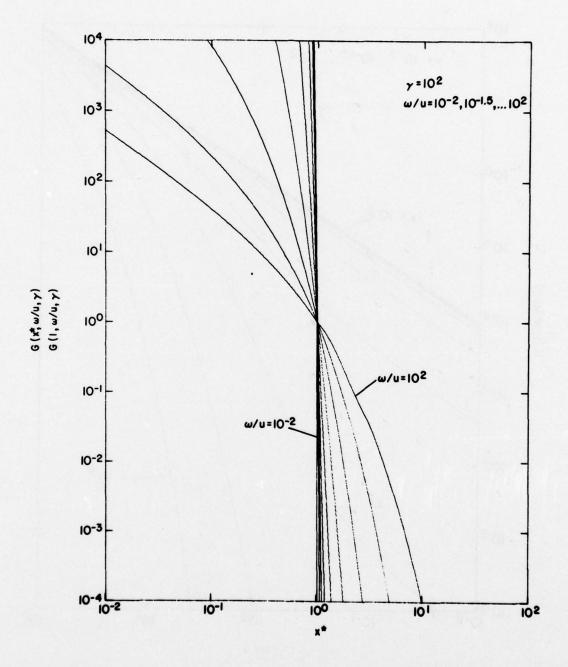


Figure 64. Normalized centerline concentraton of suspended solids versus normalized centerline distance from source for  $\gamma \,=\, 10^2 \text{ with } \omega/u \text{ as a parameter.}$ 

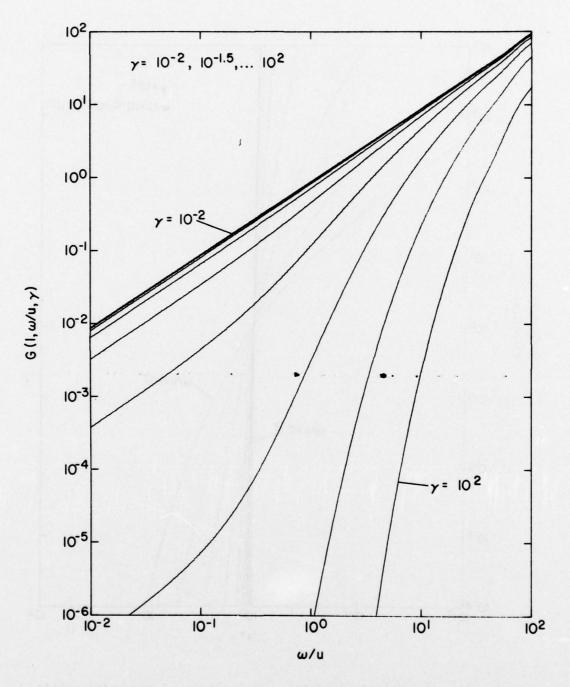


Figure 65. Normalized concentration of suspended solids to plume front  $x^* = 1$  versus  $\omega/u$  with  $\gamma$  as a parameter.

$$\overline{y^{2}}(x,t) = \frac{\Gamma\left(\frac{3}{2}\right)}{\Gamma\left(\frac{1}{2}\right)} \omega^{2} t^{2} \int_{0}^{1} t^{*} \exp{-\left(\frac{u}{\omega}\right)^{2} \left(\frac{x^{*} - t^{*}}{t^{*}}\right)^{2} \exp{-\gamma t^{*} dt^{*}}}} \int_{0}^{1} \frac{1}{t^{*}} \exp{-\left(\frac{u}{\omega}\right)^{2} \left(\frac{x^{*} - t^{*}}{t^{*}}\right)^{2} \exp{-\gamma t^{*} dt^{*}}}}$$
(13)

= 
$$\frac{\omega^2 t^2}{2}$$
  $F\left(x*,\frac{\omega}{u},\gamma\right)$  where  $F\left(x*,\frac{\omega}{u},\gamma\right)$  represents the integral

expression in (13).

In expression (13)  $\frac{\omega^2 t^2}{2}$  is simply the second moment of a single patch released at t=0. The function  $F\left(x^*,\frac{\omega}{u},\gamma\right)$  describes the variation of  $\overline{y^2}$  with  $x^*$ ,  $\frac{\omega}{u}$  and  $\gamma$ , and as before will be normalized by the second moment at the front, i.e.,  $x^*=1$ , in order to examine this function:

$$\frac{\overline{y^{2}}(x,t)}{\overline{y^{2}}(ut,t)} = \frac{F\left(x^{*}, \frac{\omega}{u}, \gamma\right)}{F\left(1, \frac{\omega}{u}, \gamma\right)}$$
(14)

Shown in Figures 66 through 70 is  $F(x^*,\frac{\omega}{u},\gamma)/F(1,\frac{\omega}{u},\gamma)$  plotted versus  $x^*$  with  $\frac{\omega}{u}$  and  $\gamma$  as parameters. It can be seen that for small values of  $\frac{\omega}{u}$  the function increases as  $x^{*2}$  up to the front, and then remains approximately constant. For larger  $\frac{\omega}{u}$  it increases more slowly with  $x^*$  reaching a maximum value somewhat past the front.

The effect of settling is to cause the function to increase relatively more rapidly with x\*. This effect is most pronounced for large  $\frac{\omega}{u}$ . Figure 71 shows  $F(1,\frac{\omega}{u},\gamma)$  plotted as a function of  $\frac{\omega}{u}$  with  $\gamma$  as a parameter. Note that for small  $\frac{\omega}{u}$ 

$$\overline{y^2}(x,t) = \frac{\omega^2 t^2}{2} x^{*2} 1 = \frac{1}{2} \left( \frac{\omega}{u} \right)^2 x^2$$
 (15)

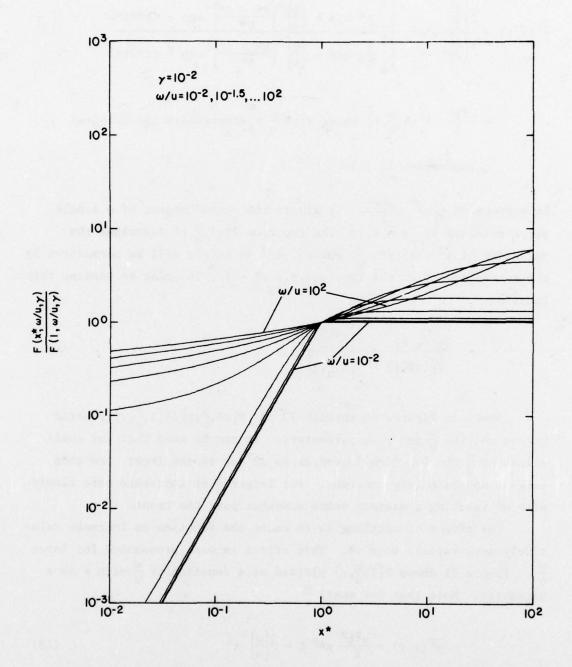


Figure 66. Normalized second moment of lateral distribution of concentration of suspended solids versus normalized centerline distance from source for  $\gamma$  =  $10^{-2}$  with  $\omega/u$  as a parameter.

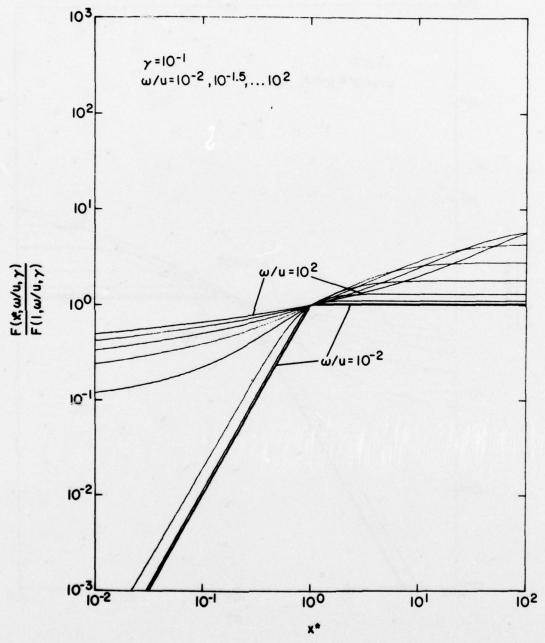


Figure 67. Normalized second moment of lateral distribution of concentration of suspended solids versus normalized centerline distance from source for  $\gamma$  =  $10^{-1}$  with  $\omega/u$  as a parameter.

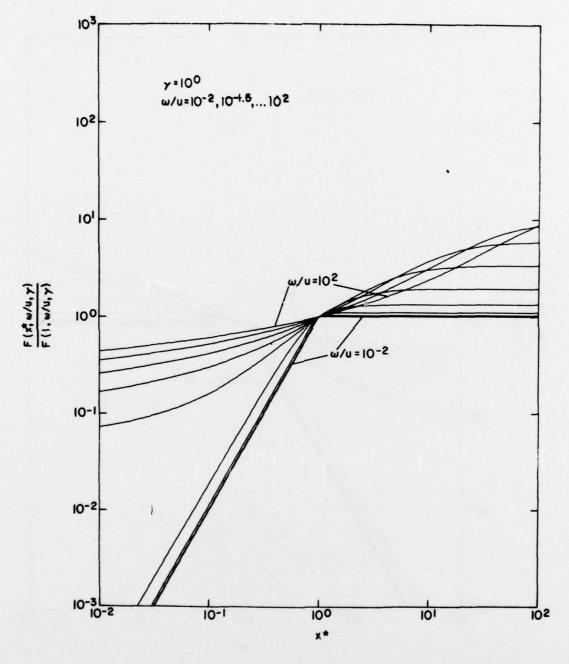


Figure 68. Normalized second moment of lateral distribution of concentration of suspended solids versus normalized centerline distance from source for  $\gamma$  =  $10^0$  with  $\omega/u$  as a parameter.

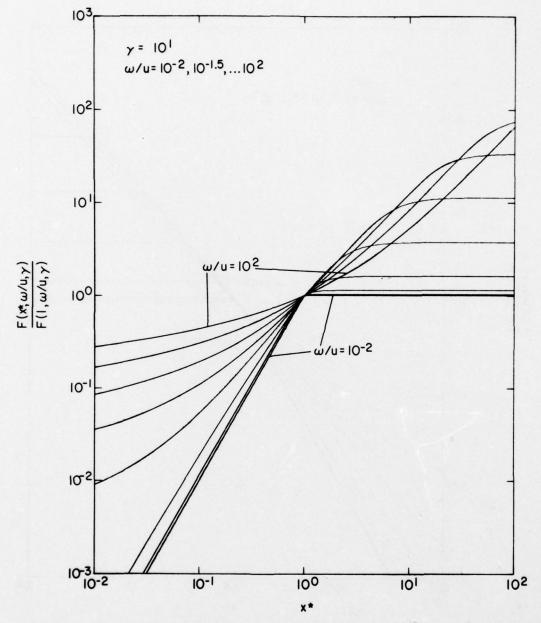


Figure 69. Normalized second moment of lateral distribution of concentration of suspended solids versus normalized centerline distance from source for  $\gamma$  =  $10^1$  with  $\omega/u$  as a parameter.

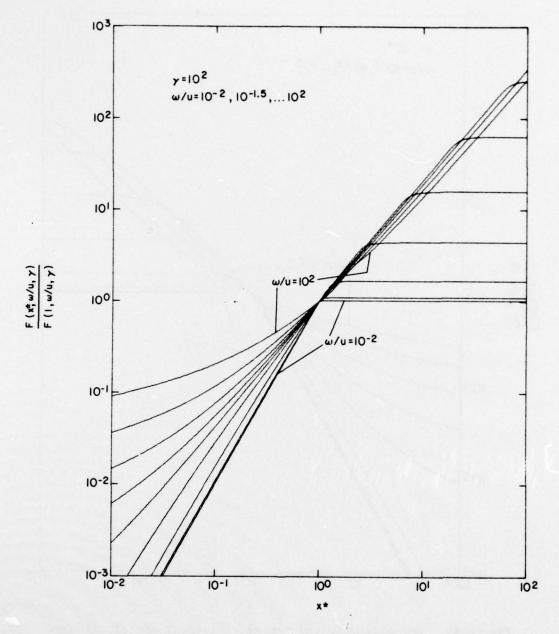


Figure 70. Normalized second moment of lateral distribution of concentration of suspensed solids versus normalized centerline distance from source for  $\gamma$  =  $10^2$  with  $\omega/u$  as a parameter.

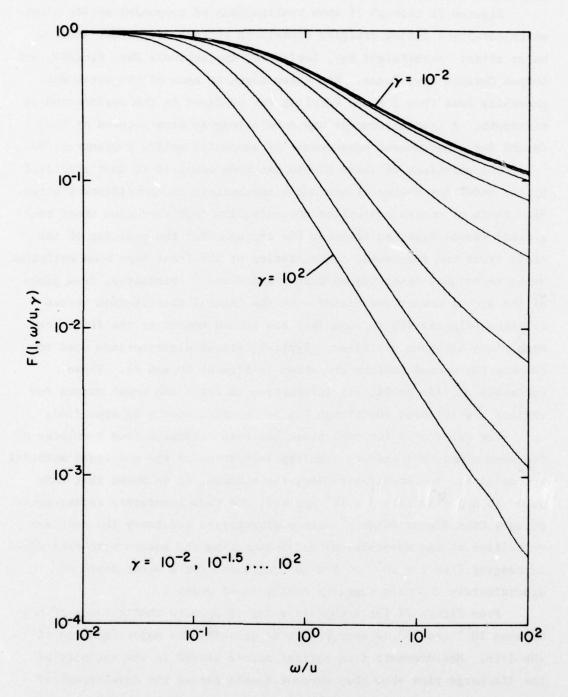


Figure 71. Normalized second moment of lateral distribution of concentration of suspended solids at plume front  $x^* = 1$  versus  $\omega/u$  with  $\gamma$  as a parameter.

### Comparison with Observations

Figures 72 through 75 show realizations of suspended solids plumes which developed during dredging operations at three different shallow water sites: Atchafalaya Bay, Louisiana, Apalachicola Bay, Florida, and Corpus Christi Bay, Texas. The water depth at each of the sites was generally less than 3 m and sampling was confined to the surface and to mid-depth. A transmissometer and a nephelometer were located at both depths for simultaneous measurement of suspended solids concentrations.

The structure of these plumes has been compared to that predicted by the model for values of  $\omega/u$  and  $\gamma$  appropriate to the different sites. From plots of excess centerline concentration (concentration above background) versus distance (Figures 76a through 79a) the position of the plume front and the excess concentration at the front have been estimated using techniques described by Carter and Okubo. Similarly, from plots of the second moment associated with the lateral distribution versus distance (Figures 76b through 79b) the second moment at the front for each plume has been estimated. Typical lateral distributions used to compute the second moments are shown in Figures 80 and 81. These estimates provide sufficient information to scale the model curves for various  $\omega/u$  (Figures 60 through 70) to our data once  $\gamma$  is specified.

The value of  $\gamma$  for each plume has been estimated from knowledge of its approximate age and the settling velocities of the suspended material it contains. For Atchafalaya Bay, for example, it is known that this plume is approximately 5 x 10<sup>4</sup> sec old, and from laboratory measurements using a Cahn Electrobalance<sup>R</sup> with sedimentation accessory the settling velocities of the suspended material away from the source were determined as ranging from 2 x 10<sup>-3</sup> to 5 x 10<sup>-3</sup> cm/sec. For a water depth of approximately 2 m this suggests that  $\gamma$  is of order 1.

From Figure 72 for Atchafalaya Bay it appears that a value of  $\omega/u$  between  $10^{-1}$  and  $10^{0}$  is appropriate to describe the major features of the data. Measurements from current meters moored in the vicinity of the discharge pipe show that current speeds during the development of this plume were very low, less than 5 cm/sec. Work by Okubo<sup>9</sup> suggests that a diffusion velocity of the order 1 cm/sec adequately describes

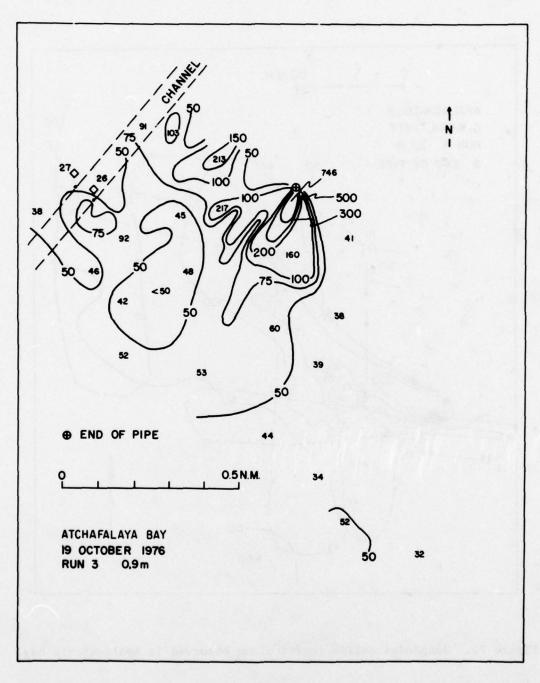


Figure 72. Suspended solids (mg/l) plume observed in Atchafalaya Bay.

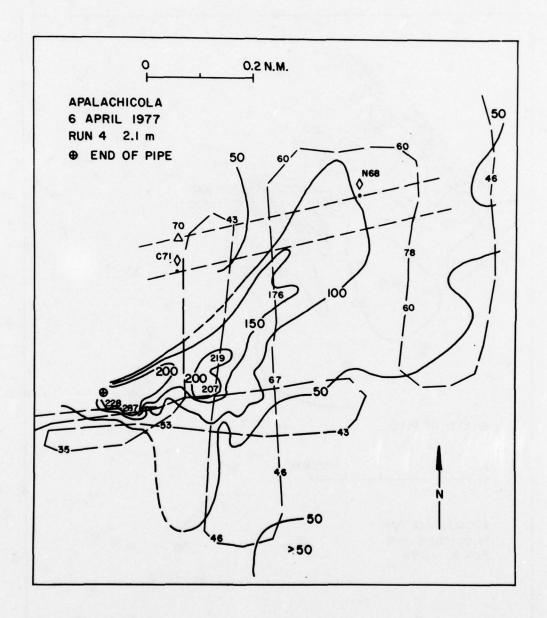


Figure 73. Suspended solids (mg/l) plume observed in Apalachicola Bay.

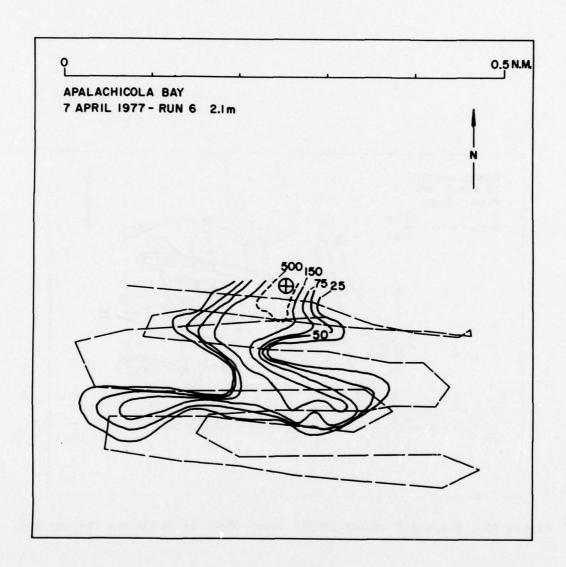


Figure 74. Suspended solids (mg/ $\ell$ ) plume observed in Apalachicola Bay.

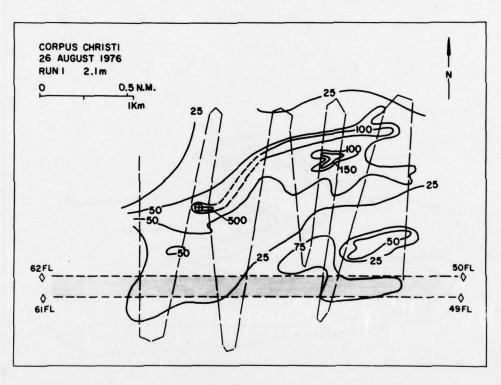


Figure 75. Suspended solids (mg/l) plume observed in Corpus Christi Bay.

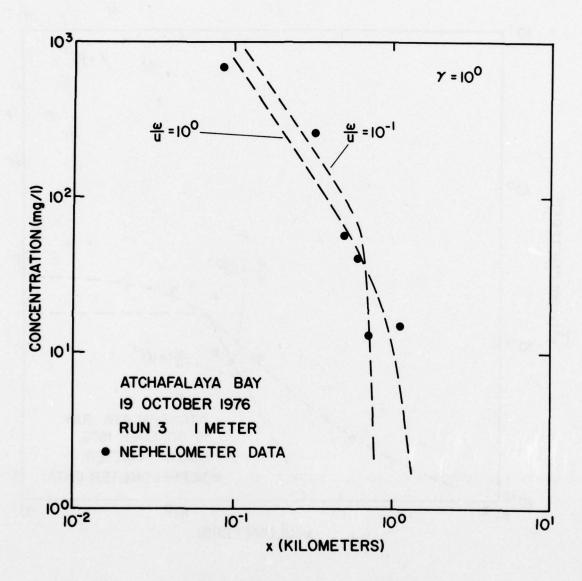


Figure 76a. Comparison of observed plume structure in Atchafalaya Bay with theoretical structure predicted from model for values of  $\omega/u$  and  $\gamma$  indicated. (a) Centerline concentration of suspended solids versus distance.

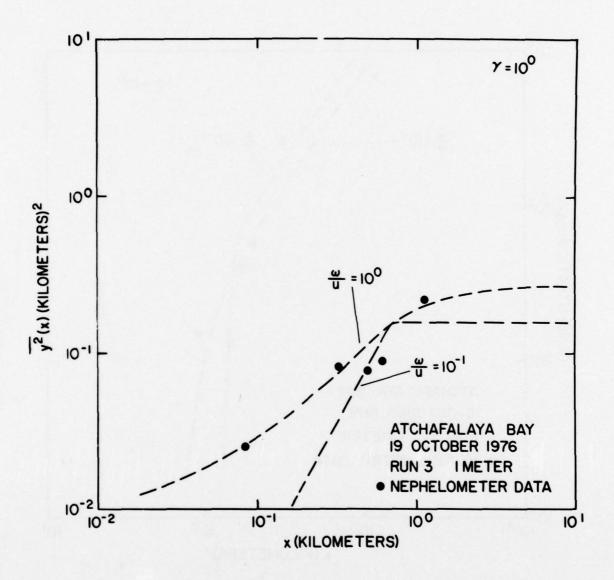


Figure 76b. Comparison of observed plume structure in Atchafalaya Bay with theoretical structure predicted from model for values of  $\omega/u$  and  $\gamma$  indicated. (b) Second moment of lateral distribution of concentration of suspended solids versus distance.

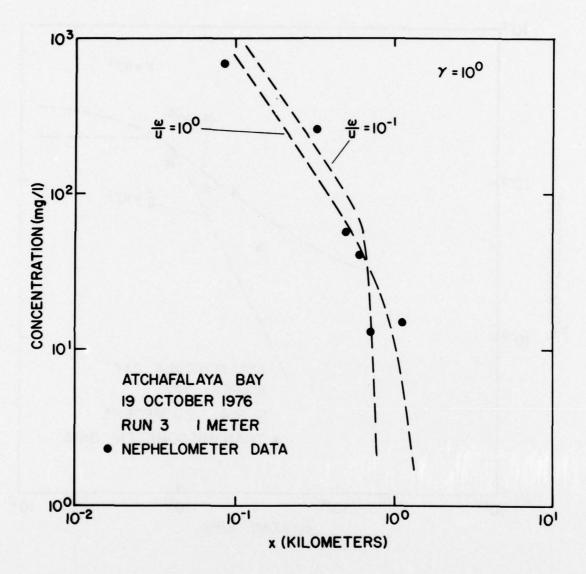


Figure 77a. Comparison of observed plume structure in Apalachicola Bay with theoretical structure predicted from model for values of  $\omega/u$  and  $\gamma$  indicated. (a) Centerline concentration of suspended solids versus distance.

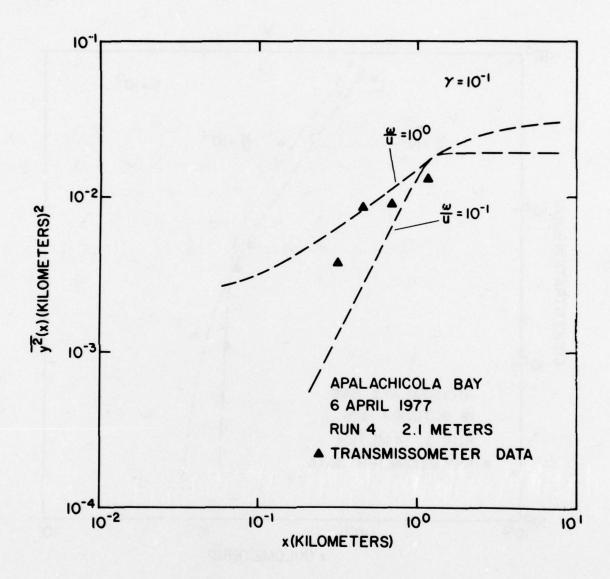


Figure 77b. Comparison of observed plume structure in Apalachicola Bay with theoretical structure predicted from model for values of  $\omega/u$  and  $\gamma$  indicated. (b) Second moment of lateral distribution of concentration of suspended solids versus distance.

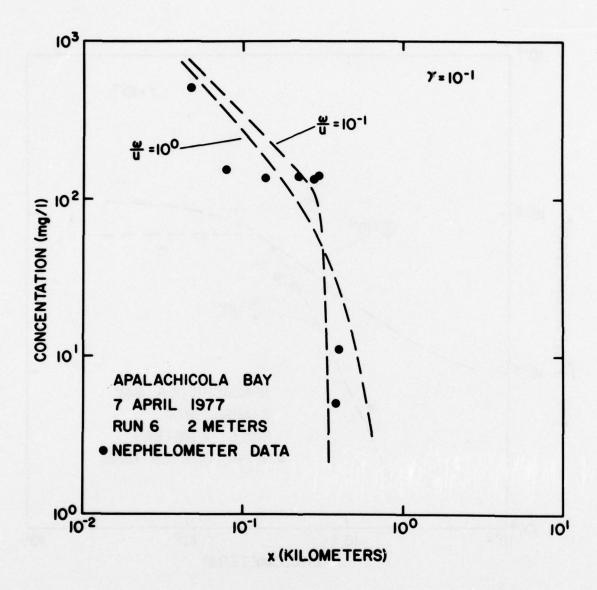


Figure 78a. Comparison of observed plume structure in Apalachicola Bay with theoretical structure predicted from model for values of  $\omega/u$  and  $\gamma$  indicated. (a) Centerline concentration of suspended solids versus distance.

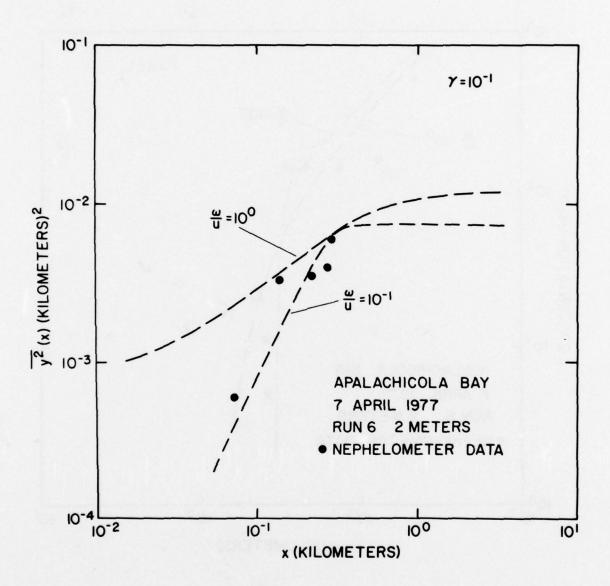


Figure 78b. Comparison of observed plume structure in Apalachicola Bay with theoretical structure predicted from model for values of  $\omega/u$  and  $\gamma$  indicated. (b) Second moment of lateral distribution of concentration of suspended solids versus distance.

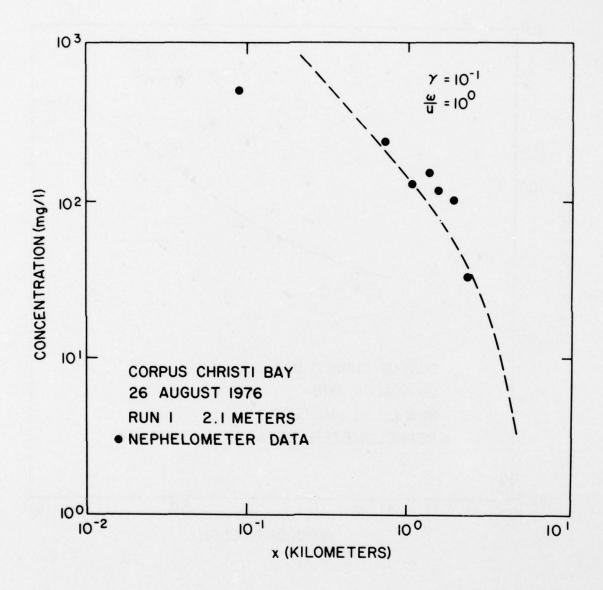


Figure 79a. Comparison of observed plume structure in Corpus Christi Bay with theoretical structure from model for values of  $\omega/u$  and  $\gamma$  indicated. (a) Centerline concentration of suspended solids versus distance.

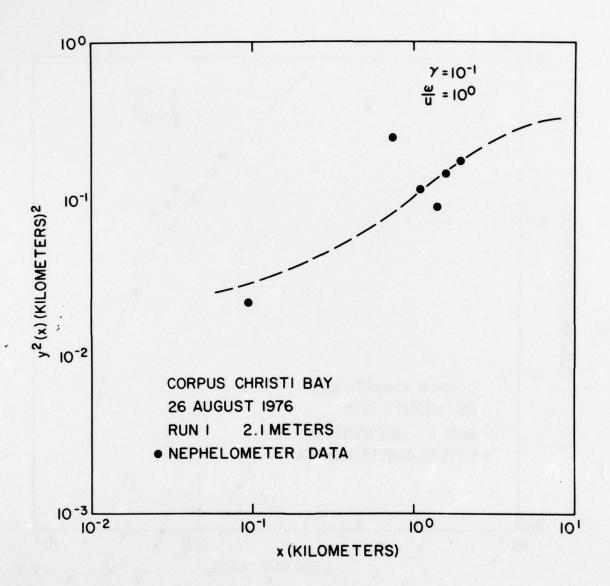


Figure 79b. Comparison of observed plume structure in Corpus Christi Bay with theoretical structure from model for values of  $\omega/u$  and  $\gamma$  indicated. (b) Second moment of lateral distribution of suspended solids versus distance.

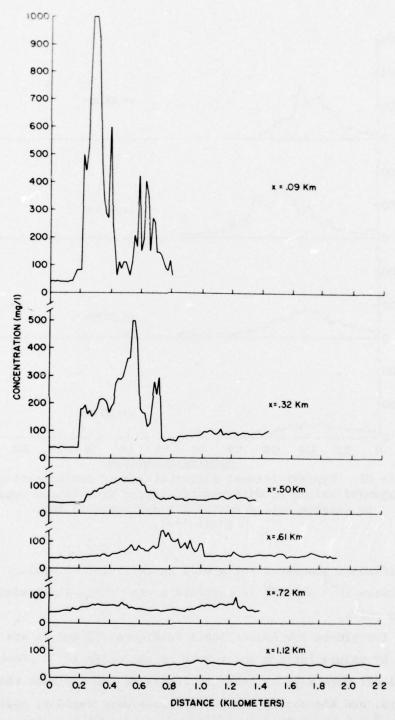


Figure 80. Typical lateral distribution of concentration of suspended solids at different distances from source used to compute second moment for Atchafalaya Bay,

19 October 1976.

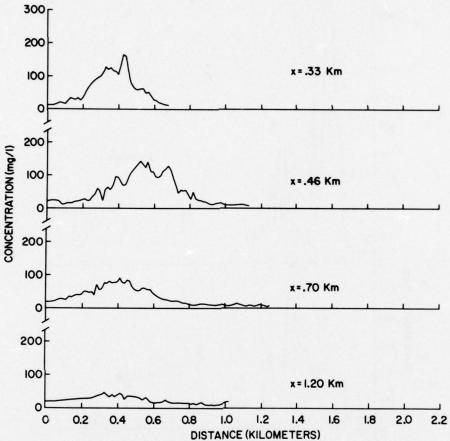


Figure 81. Typical lateral distributions of concentration of suspended solids at different distances from source used to compute second moment for Apalachicola Bay, 6 April 1977.

oceanic diffusion processes for a wide range of length scales. A value of  $\omega/u$  between  $10^{-1}$  and  $10^{0}$  is consistent with these independent estimates of u and  $\omega$ .

The two plumes for Apalachicola in Figures 73 and 74 are best described by values for  $\omega/u$  and  $\gamma$  both of the order  $10^{-1}$ . Concentrations fall off more rapidly past the fronts of these plumes than at Atchafalaya, and the second moments increase more rapidly, approximately as  $x^2$  up to the front. Both of these tendencies suggest that a value of  $\omega/u$  smaller than that for Atchafalaya is appropriate. Current speeds measured at Apalachicola were, in fact, of the order 10 cm/sec

during the development of these plumes. At Apalachicola the decrease of centerline concentration upstream of the front with distance is less rapid than at Atchafalaya suggesting a reduced value for  $\gamma$ . The measured settling velocities of the material at Apalachicola were definitely less than at Atchafalaya.

At Corpus Christi Bay settling velocities were of the order  $1 \times 10^{-3}$  cm/sec, comparable to those measured at Apalachicola Bay. Mean current speeds measured during the period of plume development were extremely low, only a few centimeters per second. As a result the appropriate value for  $\omega/u$  is of the order  $10^{0}$  or possibly higher (Figure 75).

#### Discussion

The reliability of predictions made with this model will depend primarily on prudent selection of values for the input parameters, and some discussion of these parameters is in order. The source strength q appearing in the defining equation (7) and (8) is the source for the suspended material. In Part III of this report it has been shown that for a number of different dredge sites q is consistently 1 to 5% of the mass rate of discharge of solid material from the pipe. This fraction was obtained both by estimating the mass of suspended material contained within different plumes of different ages and calculating the q required to produce this mass, and by using equation (11) to calculate q from observed centerline concentrations.

Reasonable estimates for the time t are crucial. Since t represents the expected age of a plume, unless the source is quite intermittent t will be determined by the characteristic periods of fluctuation in the ambient flow field. In a reversing tidal current, for example, t would be one-half of the tidal period. With each change in current direction a new plume would form and the old plume would disperse rapidly under the combined effects of horizontal diffusion and particle settling. Equations (6) and (7) show that concentrations in the old plume would decrease with time as:

$$\frac{1}{t^2} \exp \left(-Wt/D\right) \qquad . \tag{16}$$

In situations where tidal currents are not dominant, such as in the shallow water bays described in Part II, wind will often be responsible for inducing major changes in current direction and t can be of the order one day or longer.

Having determined t, the current speed should represent a mean over the period t. Without information to the contrary, a diffusion velocity of the order 1 cm/sec should be appropriate in most cases<sup>7</sup>. Most plumes will be adequately represented by a value for  $\omega/u$  in the range  $10^{-1}$  to  $10^{0}$ .

The lateral structure of a plume as described by the model is approximately Gaussian for values of  $\omega/u$  less than one with standard deviation given formally by equation (13). The validity of this approximation improves rapidly as  $\omega/u$  decreases. Assuming that the lateral distribution is Gaussian, it is possible to use Figures 66-71 to estimate the lateral extent of any given isoline of concentration as a function of centerline distance.

Consider a plume corresponding to some  $\omega/u$  and  $\gamma$  to be defined by an isoline of concentration. The shape of the plume and the ratio of length to width can be discussed using the model curves for centerline concentration and second moment. If the plume is indeed Gaussian then using the notation defined earlier:

$$C(x,y,t) = \frac{q}{\pi\omega^2 Dt} \frac{G(x^*)}{G(1)} G(1) \exp - \left(\frac{u}{\omega}\right)^2 \frac{y^{*2}}{\frac{F(x^*)}{F(1)}} F(1)$$
 (17)

The shape of two plumes, one for  $\omega/u=10^{-1}$ ;  $\gamma=10^{-1}$  and one for  $\omega/u=10^{0}$ ;  $\gamma=10^{-1}$ , can be compared using (17). For simplicity assume that the scaling factor  $\frac{q}{\pi\omega^2 Dt}$  is the same for both plumes so that the isoline will be defined by

$$\frac{C(x,y,t)}{q/\pi\omega^2Dt} = \frac{G(x^*)}{G(1)} G(1) \exp -\left(\frac{u}{\omega}\right)^2 \frac{y^{*2}}{\frac{F(x^*)}{F(1)}} = CONSTANT$$
 (18)

Consider specifically the isoline defined by

$$\frac{C(x,y,t)}{q/\pi\omega^2Dt} = 0.01 \qquad . \tag{19}$$

 $G(x^*)/G(1)$ , G(1),  $F(x^*)/F(1)$  and F(1) may be estimated from Figures 61, 65, 67 and 71 respectively. Having made these estimates it is possible to calculate y as a function of x for this isoline from the formula

$$y^* = -\left(\frac{\omega}{u}\right)^2 \frac{F(x^*)}{F(1)} F(1) \left[ \ln \frac{.01}{\frac{G(x^*)}{G(1)}} \right]^{1/2}$$
 (20)

The results of these calculations for the two plumes under consideration are tabulated in Table 13. Figure 82 shows the plumes for different  $\omega/u$  as defined by the isoline 0.01. That the plume becomes less elongated and more circular as  $\omega/u$  increases is obvious. The position of the front is also relatively closer to the source for larger  $\omega/u$ . As  $\omega/u$  increases still further, the plume will approach a circular patch and the "front," now very poorly defined, will be very close to the source.

#### Applying the MSRC Plume Model to an Example Problem

District Engineer: We have a maintenance dredging project scheduled that calls for open-water pipeline disposal of  $1 \times 10^6 \text{ m}^3$  of fine-grained material. The dredge is a cutterhead suction dredge with a 75 cm diameter pipeline. It will take us about 30 days and we will be discharging in an area of relatively strong semi-diurnal tidal currents. Can your plume model tell me anything useful with enough certainty so that I can depend on it?

Consultant: To use our plume model there are six parameters that you must know. The first is q defined as the rate of addition of solid dredged material discharged to the receiving water and not deposited

Table 13
Computation of Plume Structure Defined by an
Isoline of Concentration

	_x*	<u>y*</u>	$G(x^*)/G(1)$	$F(x^*)/F(1)$
$\omega/u = 10^{-1}; \gamma = 10^{-1}$	1.3		0.1	
$G(1) \simeq .09$	1.1	.123	0.5	1.05
$F(1) \simeq .9$	1.0	.143	1.0	1.0
	0.43	.088	2.0	0.22
	0.22	.046	10.0	0.053
	0.043	.035	50.0	0.022
	1			
$\omega/u = 10^{0}; \gamma = 10^{-4}$	2.4		.01	
$G(1) \simeq .9$	2.1	1.13	.05	1.5
$F(1) \simeq .53$	1.9	1.25	.01	1.3
	1.3	1.57	.05	1.2
	1.0	1.56	1.0	1.0
	.31	1.19	5.0	.43
	.17	1.04	10.0	.30
	.04	0.82	50.0	.15

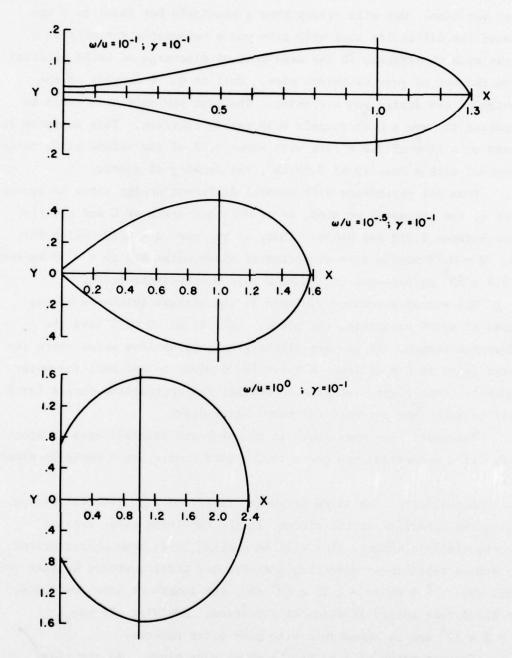


Figure 82. Characteristic plume shapes predicted by the model for different  $\omega/u$ . These plumes are defined by the isoline 0.01 for dimensionless concentration (see text). x and y are, respectively, the dimensionless longitudinal and lateral coordinates; x = 1 marks the front of each plume.

near the point of discharge. The parameter q will have dimensions of mass per time. One will seldom know q precisely but there is a way around the difficulty that will give you a reasonable estimate of q. Begin with an estimate of the mass rate of discharge of solid material from the end of your discharge pipe. Call it Q. Q depends on the design of the dredge you are using. The type you mentioned could be expected to have a Q of roughly 0.39 metric tons/sec. This estimate is based on a flow of 2.2 m<sup>3</sup>/sec with about 6.5% of the volume being solid material with a density of 2.65 cm<sup>3</sup>, the density of quartz.

From our experience with several different dredge sites it appears that q, the parameter we need, is at most one-tenth of Q and usually lies between 0.01Q and 0.05Q. Thus, if you use q = 0.1Q--which for the Q = 0.39 metric tons we estimated above works out to q = 39 kg/sec =  $3.9 \times 10^7$  mg/sec--you will have a safe overestimate for q.

The second parameter you need is the average thickness of the layer of water containing the plume. Call it D. D will have the dimension length. If you are discharging into shallow areas where the water depth is 8 m or less, a value for D equal to one-half the water depth is about right. At greater depths, the appropriate choice for D will be less than one-half the total water depth.

Engineer: The mean depth in the proposed disposal area is about  $4\ \mathrm{m.}$  If I understand you correctly, a good choice for D would be about  $2\ \mathrm{m.}$ 

Consultant: The third parameter is t, the time interval during which the *direction* of the current in the receiving water remains substantially constant. You will be working in an area characterized by strong rectilinear reversing semi-diurnal tidal currents so that you will use  $t \stackrel{\sim}{\sim} 6$  hours = 2.16 x  $10^4$  sec, the length of time any one ebb or flood runs before it reverses direction. Rounding off use  $t = 2 \times 10^4$  sec as compatible with your other numbers.

You can think of t as the "age" of your plume. As the tide begins to ebb the plume is carried seaward from your discharge pipe and continues until the end of ebb. As flood sets in the seaward plume established during ebb is "abandoned" and a "new" plume streams

landward during flood.

The fourth parameter is  $\omega$ , the diffusion velocity. The dimensions of  $\omega$  are those of speed, length per time. In coastal waters we find that  $\omega$  usually ranges from 0.2 cm/sec to 1.6 cm/sec (Table 14) and is characteristically of order 1 cm/sec.

Environment	ω (cm/sec)
Lakes and Rivers	0.2 - 0.5
Estuaries (Small to Medium, e.g. Corpus Christi Bay)	0.8 - 1.2
Estuaries (Large, e.g. main body of Chesapeake Bay)	1.2 - 1.6

<sup>\*</sup> Values supplied by A. Okubo, personal communication.

Since your bay is a medium sized estuary,  $\omega$  = 1 cm/sec is a reasonable value to use.

The fifth parameter you need is u, the mean flow speed of the receiving water during the interval t when the flow direction is steady. Being a speed, u has dimensions of length per time. It is obvious that u depends on t so that to get u you must first decide on t. We've agreed that in your bay the half tidal period is appropriate for t. Do you have any data from current meters or other kinds of water velocity probes?

Engineer: No. I don't think anyone has ever made direct current measurements there.

Consultant: That's unfortunate, but we can fall back on the NOAA Tide and Current Tables which say that maximum tidal currents are about 25 cm/sec. Using a formula from the theory of tides we can say that the mean tidal current, u, will be  $u \stackrel{\sim}{\sim} (2/\pi)u_{max} = (2/\pi)(25) = 16$  cm/sec. Therefore, use u = 16 cm/sec.

The sixth, and final parameter we need is the effective mean settling velocity of suspended material in the plume, w. Again, w is a speed with dimensions of length per time. Have you any idea of the mean settling velocity of the material you plan to dredge?

Engineer: Pipette analysis of some samples from the area gave a mean Stokes' particle diameter of about 4  $\mu\text{m.}$ 

Consultant: Good! We know that a Stokes' diameter of 4  $\mu m$  corresponds to a settling velocity of 1 x  $10^{-3}$  to 2 x  $10^{-3}$  cm/sec. Since the slower the settling velocity the longer the plume, and since we want to guard ourselves with a "worst case" estimate, let's assume w = 1 x  $10^{-3}$  cm/sec. For your bay we have:

Table 15
Parameter Values for Application of Model to Case Study

Parameter	Value	Unit
P	$3.9 \times 10^{7}$	mg/sec
D	$2 \times 10^2$	cm
t	$2 \times 10^4$	sec
ω	1	cm/sec
u	16	cm/sec
W	$1 \times 10^{-3}$	cm/sec

What, specifically, is it that you would like to predict about your dredge plume?

Engineer: I'd like to be able to predict how far the plume is likely to extend before I start operations. What I'd like is some idea of how far from the discharge point it will be before the concentration of total excess suspended matter drops to some specified value, say, 50 mg/l. Can your model predict this?

Consultant: Yes. The first thing we must do is to gather our known parameters into two dimensionless ratios:  $\omega/u$  which compares the diffusive processes with the advective processes and  $v_g$ t/D, called  $\gamma$ ,

which compares the age of the plume with the time it takes the settling material to reach the bottom boundary of the plume. The model and its graphs are expressed in terms of these dimensionless ratios. The advantage is that one set of graphs covers you no matter what system of units you choose so long as you keep them consistent. The disadvantage is that at the end of the analysis you must make one small extra calculation to recover your answer in physical units.

For the values of the six parameters for your bay we have:

$$\omega/u = (1 \text{ cm/sec})/(16 \text{ cm/sec}) = 1/16 = 0.0625$$
 (21)

and

$$\gamma = \text{wt/D} = (1 \times 10^{-3} \text{ cm/sec})(2 \times 10^{4} \text{ sec})/1200 \text{ cm}) = 0.1$$
 (22)

Since, some of the values for our parameters are fairly crude estimates, and since we will be reading from graphs, it will be good enough to round  $\omega/u$  to the nearest tenth and use  $\omega/u \stackrel{\sim}{\sim} 0.1$  and  $\gamma$  = 0.1 for your Bay.

The results of the plume model are contained in a series of non-dimensional graphs. We select the ones for which  $\omega/u$  and  $\gamma$  show the values we found, Figures 83 and 84.

Figure 83 shows the nondimensional concentration at nondimensional unit distance,  $C(1,\omega/u,\gamma)$ , the ordinate, as a function of  $\omega/u$ , the abcissa. Enter Figure 83 with your value of  $\omega/u=10^{-1}$ . Go up to the curve for your  $\gamma=10^{-1}$ . Then go over to the ordinate to get the concentration at unit distance,  $C(1;\omega/u,\gamma)=8\times10^{-2}$ . This is the value of the concentration,  $C(x;\omega/u,\gamma)$ , shown on Figure 83 when x=1. To find the value of  $C(1;\omega/u,\gamma)=8\times10^{-2}$  in physical units you must know the scale-factor which was used to nondimensionalize the graph. It was  $C_{\sigma}=q/(\pi\omega^2Dt)$ . Thus, for your bay the concentration scale-factor is

$$C_{\sigma} = \frac{(3.9 \times 10^7 \text{ mg/sec})}{(\pi)(1^2 \text{ cm}^2/\text{sec}^2)(2 \times 10^2 \text{ cm})(2 \times 10^4 \text{ sec})} = 3.10 \text{ mg/cm}^3$$
 (23)

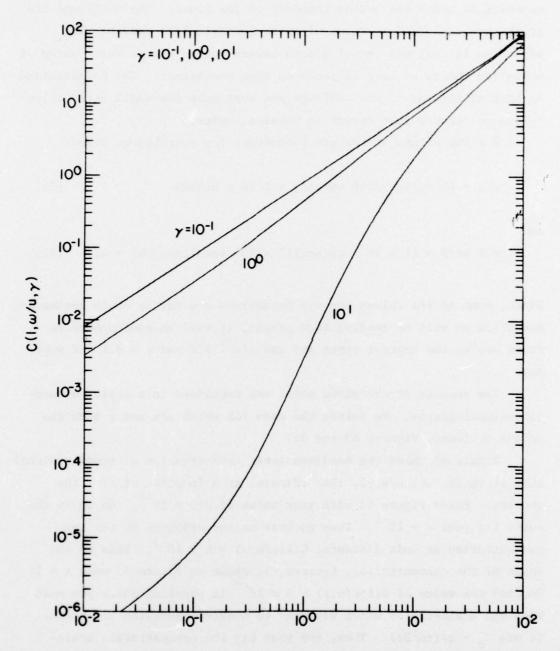


Figure 83. Graph for determining dimensionless concentration of suspended solids at unit dimensionless distance when  $\omega/u$  is known. The example shown is for  $\omega/u=10^{-1}$  and  $\gamma=10^{-1}$ .

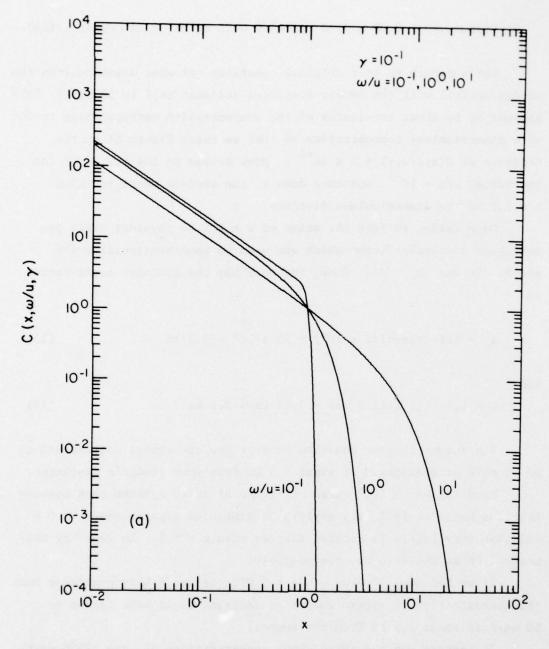


Figure 84. Graph for determining the dimensionless distance at which a given dimensionless concentration of suspended solids occurs. The example shown is for  $\omega/u \, = \, 10^{-1} \quad \text{and} \quad \gamma \, = \, 10^{-1} \quad .$ 

and at x = 1

$$C(x;\omega/u,\gamma) \sim 0.08 \times 3.10 \text{ mg/cm}^3 \stackrel{\sim}{\sim} 0.25 \text{ mg/cm}^3 = 250 \text{ mg/l}$$
 . (24)

Let's return to your original question: At what distance from the dredge outfall will the excess suspended sediment fall to 50 mg/l? This happens to be about two-tenths of the concentration corresponding to our unit dimensionless concentration so that we enter Figure 84 on the ordinate at  $C(x;\omega/u,\gamma)=2\times 10^{-1}$ . Move across to the curve for the bay value,  $\omega/u=10^{-1}$ , and then down to the abcissa where you find x=1.1 as the dimensionless distance.

Once again, to find the value of x=1.1 in physical units you must know the scale-factor which was used to nondimensionalize the graph. It was  $x_{\sigma} \equiv \text{ut}$ . Thus, for your bay the distance scale-factor is

$$x_g = (16 \text{ cm/sec})(2 \times 10^4) = 32 \times 10^4 = 3.2 \text{ km}$$
 (25)

and

$$x = 1.1 \sim (1.1)(3.2 \text{ km}) = 3.52 \text{ km}^{\circ} 3.5 \text{ km}$$
 (26)

The answer to your question is that you can expect concentrations of 50 mg/l at a distance of about 3.5 km from your dredge's discharge.

From the  $\omega/u = 10^{-1}$  curve on Figure 84 it is evident that concentrations begin to fall very rapidly at distances greater than x = 0.8 and that very little is carried farther than x = 1.3. In your bay this means 2.56 km and 4.16 km, respectively.

If we had used a value of q = 0.01Q, we would have predicted that the concentration of excess suspended sediment would have fallen to 50 mg/ $\ell$  at about 1.9 km from the source.

If instead you had asked about concentrations of, say, 2500 mg/ $\ell$ , (2500 mg/ $\ell$ )/(250 mg/ $\ell$ ) = 10 = C(x; $\omega$ /u, $\gamma$ ). Using Figure 84 in the same way, you would have found x  $\sim$  0.22 or 0.7 km.

Engineer: That seems straight forward but can I depend upon the estimates?

Consultant: I think they are pretty good. Your parameters are about the same as those which characterized the upper Chesapeake Bay north of Tolchester, 39°14'N, during a pipeline dredging operation in 1966. During that operation direct measurements were made of the turbid plume by  $\operatorname{Biggs}^{10}$  who found that the total suspended sediment in the plume fell to about 50 mg/ $\ell$  at roughly 3.1 km from the discharge point. The dredge used for the operation was the PITTSBURGH, a 69 cm cutterhead suction dredge. The Q for the PITTSBURGH was about 0.33 metric tons/sec so that the q was roughly 3.3 x  $10^{\ell}$  mg/sec if q = 0.1Q. Of course, this is total, not excess, suspended sediments but it does indicate that the plume-model is probably not far off.

Engineer: Can you predict the lateral extent of the plume from your model?

Consultant: Yes, let's define the plume by the 50 mg/ $\ell$  isopleth as we did to estimate the longitudinal extent. Previously, we saw that 50 mg/ $\ell$  is represented on our model curve (Figure 84) by a value of C(x) = 0.2 at a distance x of approximately 1.1. Let's now look upstream of x = 1.1 where centerline concentrations become very high and see how far off the centerline we have to move to have the concentration of suspended sediment drop to 50 mg/ $\ell$ . We can do this using curves for the second moment—the variance shown in Figures 85 and 86 in conjunction with Figure 84.

The easiest way to estimate plume width is to plot a few points. You'll need only a hand calculator to determine y—the distance one has to go away from the centerline of the plume to reach a concentration of suspended sediment of 50 mg/ $\ell$ . One can calculate y from:

$$y = \sqrt{\sigma^2(x) \ \sigma^2(1) (\frac{\omega}{u})^2 \left[ -\ln \frac{0.2}{C(x)} \right]}$$
 (27)

This equation was derived in the previous section on the model. We can estimate  $\sigma^2(1)$  from the curves in Figure 85 and  $\sigma^2(x)$  from

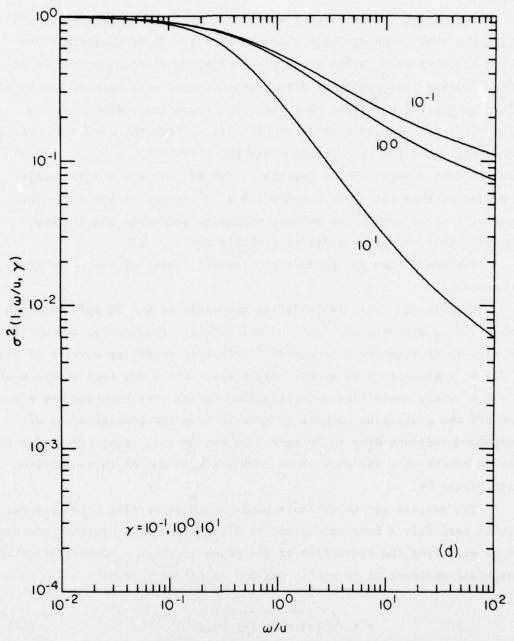


Figure 85. Graph for determining the dimensionless second moment of lateral distribution of concentration of suspended solids at unit dimensionless distance when  $\omega/u$  is known.

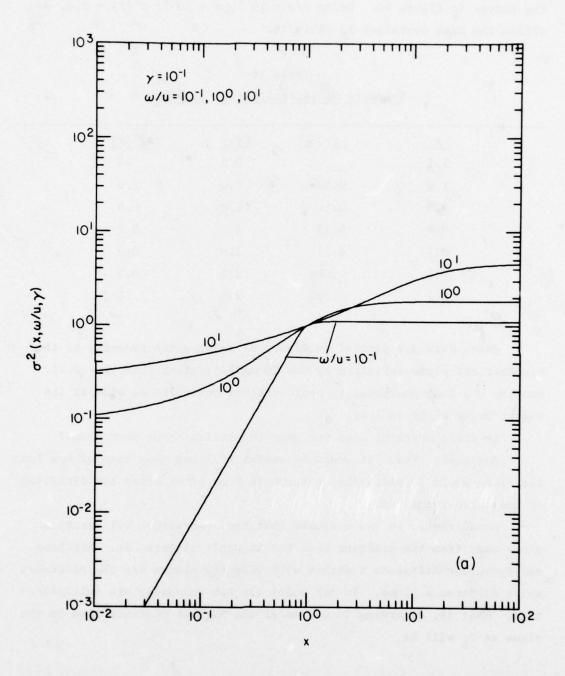


Figure 86. Graph for determining the dimensionless distance at which a given dimensionless second moment occurs.

the curves in Figure 86. Using  $\omega/u = 10^{-1}$ ,  $\gamma = 10^{-1}$ ,  $\sigma^2(1) = 0.9$ , we obtain the data contained in Table 16.

Table 16
Estimate of Lateral Extent of Plume

<u>x</u>	у	<u>C(x)</u>	$\sigma^2(\mathbf{x})$	
1.1		0.2		
1.0	0.12	1.0	1.0	
0.9	0.14	2.0	0.9	
0.8	0.13	2.5	0.7	
0.7	0.11	2.9	0.5	
0.6	.086	3.2	0.3	
0.1	.022	2.3	.012	

These data are plotted in Figure 87 to show the geometry of the hypothetical plume delimited by the 50 mg/ $\ell$  isopleth [C(x,y) = 0.2]. One can see that the plume is approximately one-third as wide at its widest point as it is long.

Is there anything else you want to predict about your plume?

Engineer: Yes. It would be useful if I had some idea of how long
the plume would persist after pumping is stopped or after the direction
of the current changed.

Consultant: We can estimate that too. Advection will carry a plume away from the dredging area but it won't disperse it. Settling and turbulent diffusion together with velocity shears are the processes which disperse a plume. In our model the two processes are multiplicative. That is, according to our model the highest concentration in the plume at to will be

$$C_{p}(t_{o}) \stackrel{\sim}{\sim} \frac{qt_{o}}{\pi\omega^{2}\left[\frac{t_{o}}{2}\right]^{2}} \exp\left\{-\frac{w}{D}\frac{t_{o}}{2}\right\}$$
 (28)

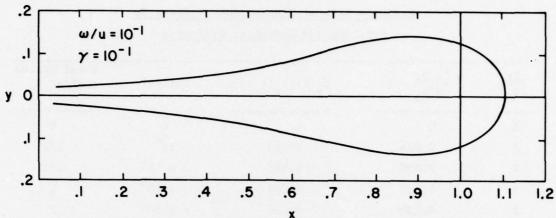


Figure 87. Plan view of hypothetical plume as delimited by the 50 mg/ $\ell$  isopleth for  $\omega/u = 10^{-1}$ ,  $\gamma = 10^{-1}$ ,  $\sigma^2(1) = 0.9$ .

and at some later time t it will be

$$C_{p}(t) = \frac{qt_{o}}{\pi\omega^{2}t^{2}D} \exp\left\{-\frac{w}{D}t\right\} \qquad (29)$$

We can estimate the percentage reduction in the highest concentration that was present in the plume at  $t = t_0$  from the ratio  $C_p(t)/C_p(t_0/2)$  or from the formula

$$C_p(t)/C_p(t_o/2) = \left(\frac{t_o}{2t}\right)^2 \exp\left\{-\frac{w}{D} \cdot \frac{t_o}{2}(\frac{2t}{t_o} - 1)\right\}$$
 (30)

For our example we have assumed that  $t_0 = 2 \times 10^4$  sec,  $w = 10^{-3}$  cm/sec and D is  $4 \times 10^4$  cm. Therefore,  $\frac{w}{D} \frac{t_0}{2} = 2.5 \times 10^{-2}$  and we can tabulate  $C_D(t)/C_D(t_0/2)$  as shown in Table 17.

That is, one-half tidal cycle  $(2 \times 10^4 \text{ sec})$  after dredging is stopped the highest concentration observed in the plume at t<sub>o</sub> will have been reduced by a factor of 0.106 and after one complete tidal cycle by 0.036.

Table 17

Estimate Rate of Dissipation of Plume By

Settling and Turbulent Diffusion

$(\frac{2t}{t_o})$	$\frac{w}{D} \frac{t_o}{2} (\frac{2t}{t_o} - 1)$	$C_p(t)/C_p(t_0/2)$	Δt(sec)	Tidal Cycles After t
1	0	1	0	0
2	0.025	0.244	104	1/4
3	0.050	0.106	$2 \times 10^4$	1/2
5	0.100	0.036	4 x 10 <sup>4</sup>	1
9	0.200	0.010	$8 \times 10^4$	2

# PART IV: CHEMICAL ASPECTS OF OPEN-WATER PIPELINE DISPOSAL--DISSOLVED NUTRIENTS AND METALS AND PARTICLE-ASSOCIATED METALS

## Introduction

To assess short-term changes in the levels of metals and nutrients in the water column resulting from the release and dispersal of dredged materials, a study was conducted of plumes associated with the openwater pipeline disposal operations at the three sites.

The research was designed: (1) to determine short-term changes in the levels of dissolved metals and nutrients and particle-associated metals associated with open-water pipeline disposal, and (2) to develop and test a model to predict elevated concentrations of particle-associated constituents in the plume of suspended dredged material.

### Description of channel sediments

Samples of sediments taken from the channels to be dredged were analyzed for: (1) interstitial metals (Table 18) and nutrients (Table 19), (2) release or uptake of metals and nutrients on mixing of sediment with site water using the elutriate test (Table 20), (3) grain size distribution (Table 21), (4) total metals (Table 22), and (5) carbonate and organic carbon content of bulk samples (Table 22). Methods for the analyses are given in Appendix D.

Sediments from Corpus Christi Bay, Texas, were light to dark gray in color and had a strong hydrogen sulfide odor. The material was extremely fine-grained (Table 21) and approximately 60% water by wet mass. Sediment temperatures were all about 28°C at the time of collection, August 1976.

Atchafalaya Bay, Louisiana, channel sediments were gray above 10 to 15 cm and streaked with what appeared to be black organic matter below this level in the sediment. The intense black color occurred in

Table 18 Metals in Interstitial Waters in Sediments from Dredged Channels

									Samula
		ъ	Ã	3	ង	25	Pb		Depth
	Sample	(ng/mg)	(µg/mg)	(ng/g)	(ng/g)	(ng/g)	(ng/g)	Core	(cm)
Corpus Christi	CCI-1	1.6	9.0	1	1			CC-1	4-24
	CCI-2	1.2	3.9	١	1	•	1	CC-1	24-44
	CCI-3	0.5	3.6	1	1		1	CC-1	79-77
	CCI-4	1.5	1.2	1	•	•		cc-1	64-84
Atchafalaya	IMC4-1	16.0	24.9	10.5	8.0			MC-4	8-0
	IMC4-2	51.8	22.6	14.4	2.6	1		MC-4	8-16
	IMC4-3	51.8	22.2	24.9	1.4			MC-4	16-24
	IMC7-1	3.8	18.5	1.3	1.9	4.5	0.5	MC-7	8-0
	IMC7-2	51.8	20.2	2.8	5.8	< 0.2	1.0	MC-7	8-16
	IMC7-3	20.7	31.9	10.5	3.6	0.5	1.0	MC-7	16-24
Apalachicola	AI-1	7.8	11.2	< 0.2	0.3	6.2	2.0	A-2	8-0
	AI-2	2.8	3.7	< 0.2	1.9	3.9	0.5	A-2	8-17
	AI-3	2.7	2.8	5.2	0.3	3.9	0.5	A-2	17-26
	4I-4	3.4	1.8	< 0.2	0.3	3.9	< 0.5	A-2	28-36
	AI-5	7.3	1.3	< 0.2	0.3	3.8	0.5	A-2	36-51
	9-IA	8.4	0.2	< 0.2	0.3	8.2	1.9	A-2	51-67
	AI4-1	28.5	19.7	< 0.2	0.3	5.2	< 0.5	A-4	0-20
	AI4-2	38.9	3.9	3.9	0.8	5.0	0.5	A-4	20-40
	AI4-3	36.3	4.5	1.3	1.9	2.5	< 0.5	A-4	09-07
	AI5-4	13.0	11.7	5.6	0.3	2.7	< 0.5	A-5	0-20
	AI5-5	18.1	2.6	ı	4.1	2.9	< 0.5	A-5	20-40
	AI5-6	23.3	9.4	< 0.2	0.3	2.0	< 0.5	A-5	09-07

Table 19 Nutrients in Interstitial Waters in Sediments from Dredging Channels

		+ HN-N	P-P04	S1-S1(OH) <sub>4</sub>		Sample Depth
	Sample	(µg-at N/R)	(µg-at P/k)	(µg-at S1/k)	Core	E
Corpus Christi	CCI-1	2460	3.3	345	CC-1	4-24
	CCI-2	2940	22.0	510	CC-1	24-44
	CCI-3	3720	1250	962	CC-1	79-77
	CCI-4	4120	1080	720	CC-1	78-49
Atchafalaya	IMC4-1	1020	59.8	96.3	MC-4	8-0
	IMC4-2	1490	197	143	MC-4	8-16
	IMC4-3	1540	85.0	146	MC-4	16-24
	IMC7-1	962	71.0	45	MC-7	8-0
	IMC7-2	1470	132	141	MC-7	8-16
	IMC7-3	1510	89.3	157	MC-7	16-24
Apalachicola	AI-1	889	17.6	760	A-2	8-0
	AI-2	1980	16.9	417	A-2	8-17
	AI-3	2820	18.8	397	A-2	17-26
	AI-4	3350	24.2	355	A-2	26-36
	AI-5	3750	21.5	312	A-2	36-51
	9-IA	4134	28.2	352	A-2	51-67
	AI4-1	2360	55.3	633	A-4	0-20
	AI4-2	2040	82.0	509	A-4	20-40
	AI4-3	5210	73.5	997	A-4	09-07
	AI5-4	1690	40.2	595	A-5	0-20
	AI5-5	4710	76.4	677	A-5	20-40
	AI5-6	4790	67.3	411	A-5	09-07

Table 20 Elutriate Test Results

A. Metals

Sample Depth (cm)	E WATER 10-55 55-100	E WATER 0-11 11-23 10-18	E WATER 0-64 0-72 0-70 0-64 0-72
			SITE 11 12 13 11 11 11 11 11 11 11 11 11 11 11 11
			<ul><li>0.3</li><li>1.4</li><li>1.7</li><li>0.7</li><li>0.7</li><li>0.7</li><li>0.7</li></ul>
Cd (μg/k)	32.2 38.3 6.5		A A A A A A A A A A A A A A A A A A A
Cr (µg/%)	0.5	2.0 9.1 5.1 0.4	0.00 0.00 0.00 0.00 0.00 0.00 0.00
Cu (μg/k)	19.2 4.8 2.4	37.8 15.3 14.0 18.0	2.2 0.7 1.2 1.2 1.2 1.0
			28.9 219 242 135 129 147 71.9
Fe (µg/ $\&$ )	105 105 252	105 105 210 105	98.5 26.9 9.0 17.9 53.7 53.7
Sample	CCEB CCE5-1 CCE5-2	MCEB MCE6-1 MCE6-2 MCE3	ASWET ASET-11 ASET-12 ASET-13 AMET-11 AMET-13
	Corpus Christi	Atchafalaya	Apalachicola

(continued)

Table 20 (concluded)

B. Nutrients

		N-NH <sup>+</sup>	P-P04	Si-Si(OH) <sub>4</sub>		Sample Depth
	Sample	(µg-at N/k)	(µg-at P/2)	(µg-at Si/k)	Core	(cm)
Corpus Christi	CCEB	18.6	1.8	142	SITE	WATER
	CCE5-1	162	4.2	166	CC-5	10-55
	CCE5-2	369	13.6	190	CC-5	55-100
Atchafalaya	MCEB	34.0	6.0	18.3	SITE	WATER
	MCE6-1	268	1.1	26.0	MC-6	0-11
	MCE6-2	192	1.1	20.0	MC-6	11-23
	MCE3	164	1.1	30.0	MC-3	10-18
Apalachicola	ASWET	3.7	0.1	25.3	SITE	WATER
	ASET-11	244	0.5	56.0	A-11	79-0
	ASET-12	192	9.0	57.8	A-12	0-72
	ASET-13	272	9.0	53.0	A-13	00
	AMET-11	262	9.0	53.2	A-11	79-0
	AMET-12	242	9.0	53.6	A-12	0-72
	AMET-13	260	9.0	56.9	A-13	0-70

Table 21 Grain Size\* of Sediments from Dredged Channels

Corpus Christi, TX, Atchafalaya, LA, Apalachicola, FL

Site	% Sand (> 62μ)	% Silt $(3.9-62\mu)$	% Clay (< 3.9μ)
Corpus Christi	0.7	19.8	79.4
Atchafalaya	7.07	16.1	13.2
Apalachicola	1.0	30.6	4.89

\* Grain size analysis was accomplished by conventional wet sieving and pipet analysis<sup>11</sup>.

Metals and Other Constituents in Sediments from Dredged Channels
Corpus Christi Bay and Apalachicola Bay

Site	Sample No.	Carbon (%) Total CO <sub>2</sub>	88	Fe (µg/mg)	Mn (µg/mg)	Cu (μg/g)	Pb (μg/g)
Corpus Christi Bay	00-1	10.8	1.2	10.5	0.394	18.9	11.8
Apalachicola Bay	A-I A-II	9.6	6 0.39	15.2	0.930	11.0	12.4

the 10-15 cm depth band. The sediment was predominantly sand with some silt and clay (Table 21) and had low water content (about 35% by wet mass). Core temperatures in October 1976 were all close to  $17.5^{\circ}$ C ( $\pm 0.5$ ).

Apalachicola Bay, Florida, sediment cores were brown from 0 to 35 cm and gray below 35 cm. Hydrogen sulfide odor was present. Sediments were predominantly clay and silt with a small amount of sand (Table 21). Water content was the highest of the three sites, approximately 70% by wet mass. Core temperatures for the April 1977 sampling period were 19.0 to 19.5°C.

### Dissolved Metals and Nutrients

Water samples were collected for determination of the levels of dissolved metals and nutrients in the discharge plume. To assess the short-term release or uptake of dissolved species, results of plume analyses were compared with ambient concentrations and, at Apalachicola Bay, with results of a pre-dredging survey.

#### Methods

Separate water samples for determination of metals, nutrients, and suspended solids were periodically collected at one or two depths in and around the disposal plumes at each of the three sites. A survey of ambient background concentrations of dissolved constituents was conducted prior to the beginning of dredging in Apalachicola Bay. At the other two sites background levels were assessed by determinations in the far-field because dredging had begun prior to sampling.

Samples for metals analyses were filtered immediately following collection and the dissolved metal sample (filtrate) was preserved by acidification with high purity nitric acid. These samples were analyzed for dissolved Fe, Mn, Zn, Cu, Cr, Cd and Pb by atomic absorption spectrometry following solvent extraction. Apalachicola Bay samples were analyzed for only Fe, Mn, Cu, and Cr.

Particulates were removed from water samples for determination of dissolved nutrients with in-line glass fiber filters. Water samples

were preserved by freezing immediately following collection. Nutrient analyses for all three sites were accomplished by conventional automated and manual methods for  $\mathrm{NH_4}^+$ ,  $\mathrm{Si(OH)_4}$ , and  $\mathrm{PO_4}^{-3}$  and, at Atchafalaya Bay and Corpus Christi Bay, for  $\mathrm{NO_2}^- + \mathrm{NO_3}^-$ .

Channel sediments obtained by coring were analyzed for interstitial water concentrations of metals and nutrients and for potential release or uptake of dissolved constituents during sediment disposal using the elutriate test. Descriptions of procedures are given in Appendix D.

### Dissolved metals

Results. No well-defined plume of dissolved metals (Table 23) was observed at any of the three sites although a small number of samples showed anomalously high levels of certain metals close to the discharge. No linear relationship of concentrations of dissolved metals with each other or with particle-associated metals was found. The few elevated concentrations of Mn in Atchafalaya Bay and Mn, Cu, and Cr in Apalachicola Bay were found near the discharge associated with concentrations of suspended solids near or exceeding 10<sup>3</sup> mg/L. Conversely, dissolved Fe concentrations were relatively low in these samples (see Tables 23, 27, 28).

Concentrations of dissolved metals (other than Fe and Mn) off the discharge were significantly higher in Corpus Christi Bay than at the other sites but no plume of dissolved metals was delineated. Concentrations of these metals in Atchafalaya Bay were usually below the detection limit of the analytical methods employed.

No significant increase in average dissolved metals concentrations was observed from samples collected before dredging compared with those collected from the plumes of suspended solids during dredging and disposal in Apalachicola Bay. In fact, analyses indicated a decrease in Fe from a mean of 674 ppb (samples A-1 to A-11) before dredging to a mean of 521 ppb\* (samples A-41 to A-80) in and near the plume during dredging

<sup>\*</sup> The decrease was not statistically significant because of the large variation in sample values both before and during dredging. (Standard deviations were 714 and 476, respectively).

Table 23
A. Corpus Christi Dissolved Metals\*

Station	Depth (m)	Fe	Mn	Zn	Cu	Cr	Cd	РЬ
CC 1	0.6	20.7	5.81	0.9	1.3	< 0.1	3.3	1.3
CC 1	2.1	25.2	7.56	5.2	5.1	< 0.1	2.2	< 0.1
CC 2	0.6	7.4	16.9	8.3	10.2	0.2	0.2	< 0.1
CC 2	2.1	32.6	20.3	5.2	5.1	< 0.1	2.7	1.3
CC 3	0.6	14.8	5.23	25	1.7	< 0.1	1.1	1.1
CC 3	2.1	20.7	6.39	0.2	2.7	< 0.1	0.4	< 0.1
CC 4	0.6	32.6	6.39	1.7	1.7	< 0.1	1.0	5.5
CC 4	2.1	45.9	8.72	2.0	3.4	< 0.1	2.8	< 0.1
CC 5	0.6	19.2	6.39	0.4	3.7	< 0.1	2.4	1.3
CC 5	2.1	53.3	7.56	34	18	1.2	0.7	3.6
CC 6	0.6	120	7.56	3.0	0.2	< 0.1	0.8	0.2
CC 6	2.1	203	66.9	1.5	3.1	< 0.1	2.3	0.2
CC 7	0.6	11.8	7.56	< 0.2	7.5	< 0.1	0.5	1.1
CC 7	2.1	38.5	37.8	12.0	2.8	< 0.1	1.3	0.8
CC 8	0.6	88.8	5.81	< 0.2	1.7	< 0.1	1.3	8.6
CC 8	2.1	105	9.30	< 0.2	3.4	1.2	1.9	< 0.1
CC 9	0.6	123	7.56	< 0.2	0.9	< 0.1	1.5	0.9
CC 9	2.1	149	5.81	< 0.2	0.7	< 0.1	1.1	1.1
CC10	0.6	126	5.81	< 0.2	1.4	< 0.1	1.1	< 0.1
CC10	2.1	194	11.0	3.0	1.2	< 0.1	0.8	3.4
CC11	0.6	11.8	4.65	35.0	1.7	1.0	0.8	1.8
CC11	2.1	25.2	8.14	3.0	1.7	1.1	0.3	< 0.1
CC12	0.6	66.6	10.5	< 0.2	1.4	1.1	0.7	< 0.1
CC12	2.1	81.4	4.07	2.4	12.6	< 0.1	0.4	< 0.1
CC13	0.6	51.8	6.98	20	7.8	0.8	1.0	4.6
CC13	2.1	167	13.4	12.0	24.0	< 0.1	0.2	3.2
CC14	0.6	72.5	9.88	< 0.2	1.0	0.9	0.9	< 0.1
CC14	2.1	90.3		73.0	0.9	< 0.1	0.2	0.4

Table 23 (continued)

Station	Depth (m)	Fe	Mn	_Zn_	_Cu_	Cr	Cd	Pb
CC15	0.6	72.5	9.30	< 0.2	0.8	< 0.1	0.4	1.0
CC15	2.1	161	11.0	5.0	12.0	0.2	1.1	2.9
CC16	0,6	11.8	5.81	6.1	25.0	< 0.1	0.2	5.1
CC16	2.1	10.4	4.65	< 0.2	2.7	0.4	< 0.1	< 0.1
CC17	0.6	11.8	7.56	< 0.2	6.1	2.1	0.2	0.3
CC17	2.1	32.6	9.30	0.9	2.7	0.2	1.0	1.0
CC18	0.6	13.3	8.14	< 0.2	0.7	< 0.1	0.7	1.1
CC18	2.1	14.8	6.97	6.7	4.8	< 0.1	0.3	0.6
CC19	0.6	25.2	9.30	< 0.2	35.0	< 0.1	0.8	7.8
CC19	2.1	29.6	9.30	< 0.2	8.1	< 0.1	0.1	0.2
CC20	0.6	34.0	9.30	< 0.2	3.1	< 0.1		1.3
CC20	2.1	22.2	29.1	< 0.2	3.1	< 0.1		1.3

<sup>\*</sup> All values are μg/l (ppb)

B. Atchafalaya Dissolved Metals\*

Station	Depth (m)	_Fe_	Mn	Zn	Cu	Cr	Cd	Pb
MC30	0.9	72.5	5.81	1.6	2.1	< 0.8	< 0.1	< 0.1
MC31	0.9	79.9	47.1	< 0.1	1.0	< 0.8	< 0.1	< 0.1
MC32	0.9	19.8	85.5	0.1	5.4	< 0.8	< 0.1	< 0.1
MC33	0.9	74.0	5.23	< 0.1	1.9	< 0.8	< 0.1	< 0.1
MC34	0.9	138	31.4	< 0.1	1.0	< 0.8	< 0.1	< 0.1
MC35	0.9	126	22.7	< 0.1	0.6	< 0.8	< 0.1	< 0.1
MC36	0.9	210	26.2	< 0.1	2.1	< 0.8	< 0.1	< 0.1
MC37	0.9	129	2.91	< 0.1	0.6	< 0.8	< 0.1	< 0.1
MC38	0.9	120	4.07	< 0.1	0.5	< 0.8	< 0.1	< 0.1
MC39	0.9	78.4	5.81	< 0.1	1.7	< 0.8	< 0.1	< 0.1

Table 23 (continued)

Station	Depth (m)	Fe_	Mn	Zn	Cu	Cr	Cd	Pb
MC40	0.9	155	4.65	< 0.1	0.5	< 0.8	< 0.1	< 0.1
MC41	0.9	54.8	2.91	< 0.1	0.2	< 0.8	< 0.1	< 0.1
MC42	0.9	87.3	10.5	< 0.1	0.2	< 0.8	0.1	< 0.1
MC43	0.9	101	3.49	< 0.1	1.0	< 0.8	< 0.1	< 0.1
MC44	0.9	110	5.23	< 0.1	0.2	< 0.8	< 0.1	< 0.1
MC45	0.9	66.6	3.49	< 0.1	1.4	< 0.8	0.1	< 0.1
MC46	0.9	53.3	6.39	< 0.1	0.5	< 0.8	0.3	< 0.1
MC47	0.9	56.2	47.1	< 0.1	0.3	< 0.8	1.9	< 0.1
MC48	0.9	134	41.9	< 0.1	0.2	< 0.8	0.1	< 0.1
MC49	0.9	105	14.0	< 0.1	1.0	< 0.8	< 0.1	< 0.1
MC50	0.9	79.9	4.07	< 0.1	3.0	< 0.8	0.1	< 0.1
MC51	0.9	104	6.39	< 0.1	0.2	< 0.8	0.6	< 0.1
MC52	0.9		36.0	< 0.1	2.5		0.5	< 0.1
MC53	0.9	101	21.5	< 0.1	1.7	< 0.8	0.2	< 0.1
MC54	0.9		9.88	< 0.1	1.5	< 0.8	< 0.1	< 0.1
MC55	0.9	136	15.1	< 0.1	3.8	< 0.8	0.1	< 0.1
MC56	0.9	60.7	5.81	< 0.1	1.2	< 0.8	< 0.1	< 0.1
MC57	0.9			< 0.1	2.7	< 0.8	< 0.1	< 0.1
MC58	0.9	88.8	9.30	< 0.1	1.7	< 0.8	< 0.1	< 0.1
MC59	0.9	68.1	4.65	< 0.1	0.8	< 0.8	0.2	< 0.1
MC60	0.9	59.2	5.23	< 0.1	0.8		< 0.1	0.8
MC61	0.9	70.0	9.88	< 0.1	5.7		< 0.1	< 0.1
MC62	0.9	74.0	5.23	< 0.1	2.7		0.4	< 0.1
MC63	0.9	37.0	3.49	< 0.1	3.0		0.1	< 0.1
MC64	0.9	39.9	3.49	< 0.1	2.3		< 0.1	< 0.1
MC65	0.9	75.5	3.49	< 0.1	1.7	< 0.8	< 0.1	< 0.1
MC66	0.9	66.6	3.49	< 0.1	1.9	< 0.1	< 0.1	< 0.1

<sup>\*</sup> All values are µg/l (ppb)

Table 23 (continued)
C. Apalachicola Dissolved Metals\*

Station	Depth (m)	Fe	Mn	Cu	C=
A 1	0.9	1330	92.9		Cr
				3.38	0.35
A 1	2.4	41.0	215	4.64	0.49
A 2	0.9	1210	29.7	2.71	< 0.06
A 2	2.4	48	101	0.77	0.06
A 3	0.9	315	20.8	1.93	< 0.06
A 3	2.4	82.0	11.9	0.39	0.06
A 4	0.9	1210	44.6	0.39	< 0.06
A 4	2.4	34.2	77.3	< 0.39	< 0.06
A 5	0.9	2730	62.4	1.93	0.49
A 5	2.4	61.5	125	< 0.39	< 0.06
A 6	0.9	1210	71.4	2.32	0.06
A 6	2.4	150	202	< 0.39	< 0.06
A 7	0.9	458	68.4	1.16	0.49
A 7	2.4	55.0	217	< 0.39	0.92
A 8	0.9	1180	74.3	0.39	0.20
A 8	2.4	1350	175	2.32	0.35
A 9	0.9	1300	41.6	1.55	0.20
A 9	2.4	68.4	360	< 0.39	0.06
A10	0.9	417	47.6	0.77	0.49
A10	2.4	41.0	407	< 0.39	0.06
A11	0.9	1250	80.5	0.39	< 0.06
A11	2.4	294	207	< 0.39	< 0.06
A41	0.6	376	28.8	0.77	0.20
A41	2.1	75.2	14.4	2.32	0.78
A43	0.6	1700	37.9	3.10	0.35
A43	2.1	273	60.4	12.0	0.49
		(cont	inued)		

Table 23 (continued)

Station	Depth (m)	_Fe_	Mn	Cu	Cr
A44	0.6	1320	31.6	1.16	0.35
A44	2.1	198	28.8	0.39	0.92
A45	0.6	451	25.9	0.39	0.64
A45	2.1	150	8.6	< 0.39	1.07
A46	0.6	1430	63.3	< 0.39	0.64
A46	2.1	205	14.4	1.93	1.21
A47	0.6	383	40.3	1.55	0.49
A47	2.1	212	17.3	< 0.39	1.21
A48	0.6	376	37.4	0.77	0.35
A48	2.1	123	5.75	0.39	1.21
A49	0.6	424	37.4	0.39	0.35
A49	2.1	137	8.63	< 0.39	0.92
A50	0.6	1180	20.1	2.71	0.64
A50	2.1	1890	685	1.55	0.20
A52	0.6	1180	34.5	4.25	0.35
A52	2.1	198	46.0	0.77	0.64
A53	0.6	397	71.9	0.39	0.29
A53	2.1	157	17.3	2.00	0.74
A54	0.6	431	63.3	0.39	0.31
A54	2.1	150	14.4	1.55	0.50
A55	0.6	465	28.8	4.61	1.41
A55	2.1	226	59.3	9.70	1.93
A56	0.6	1670	17.3	8.30	0.47
A56	2.1	232	549	16.0	7.57
A57	0.6	438	23.0	3.0	0.66
A57	2.1	171	28.8	1.84	0.47
A58	0.6	1210	37.4	3.00	0.38
A58	2.1	349	20.1	2.54	0.56

Table 23 (continued)

Station	Depth (m)	Fe	Mn	Cu	Cr
A59	0.6	1180	28.8	2.07	0.3
A59	2.1	98.5	11.5	2.07	0.3
A60	0.6	492	66.1	4.15	0.1
A60	2.1	215	20.1	1.15	0.4
A61	0.6	519	17.3	0.92	0.2
A61	2.1	116	17.3	2.77	0.4
A62	0.6	546	37.4	3.23	0.6
A62	2.1	134	14.4	1.84	0.4
A63	0.6	528	46.0	4.38	0.2
A63	2.1	161	.63	1.15	0.4
A64	0.6	824	25.9	1.15	0.2
A64	2.1	260	112	3.92	2.1
A65	0.6	1700	23.0	2.07	0.5
A65	2.1	206	14.4	1.84	0.4
A66	0.6	609	31.6	2.07	0.2
A66	2.1	143	11.5	1.84	0.4
A67	0.6	1230	20.1	1.15	0.3
A67	2.1	161	23.0	3.46	0.4
A68	0.6	403	28.8	1.84	0.4
A68	2.1	233	20.1	1.84	0.7
A69	1.6(a)	116	48.9	0.92	0.4
A69	0.6(b)	98.5	57.5	2.77	0.4
A69	0.6(c)	116	54.6	0.46	0.6
A69	0.6(d)	116	40.3	2.54	0.38
A69	2.1(a)	591	20.1	4.61	0.38
A69	2.1(b)	689	17.3	2.77	0.38
A69	2.1(c)	833	17.3	3.92	0.38
A69	2.1(d)	842	17.3	1.38	2.35

Table 23 (concluded)

Station A70 A70 A71 A71	(m) 0.6 2.1 0.6 2.1	Fe 1280 331 1960	Mn_ 25.9 69.0 34.5	2.07 0.46	0.47 0.94
A70 A71	2.1 0.6 2.1	331 1960	69.0	0.46	
	2.1	1960			
A71		260		3.23	0.56
		269	529	9.70	1.46
A73	0.6	376	20.1	1.84	0.66
A73	2.1	206	155	1.38	0.28
A74	0.3	331	101	1.45	0.55
A74	1.8	385	147	3.88	0.37
A75	0.3	448	74.8	3.15	0.37
A75	1.8	206	167	5.82	0.61
A76	0.3	430	31.6	0.97	0.37
A76	1.9	179	158	0.48	0.55
A77	0.3	501	23.0	1.21 .	0.37
A77	1.8	313	109	1.69	0.37
A78	0.3	671	28.8	1.45	0.37
A78	1.9	224	135	0.48	0.55
A79	0.3	394	94.9	3.39	0.37
A79	1.8	403	150	1.45	0.74
A80	0.3	627	63.3	1.45	0.37
A80	1.8	206	184	1.94	0.82

<sup>\*</sup> All values are µg/l (ppb)

Table 24

A. Corpus Christi Dissolved Nutrients

	Depth	N-NH <sub>4</sub> +	$N-NO_2+NO_3$	P-P0 <sub>4</sub>	Si-Si(OH)4
Station	(m)	(µg-at N/l)	(µg-at N/l)	(µg-at P/l)	(µg-at Si/l)
CC 1	0.6	3.46	0.10	0.92	98.4
CC 1	2.1	5.98	5.52	0.90	51.9
CC 2	0.6	4.93	0.38	0.83	49.6
CC 2	2.1	12.3	0.57	0.96	56.5
CC 3	0.6	3.67	0.32	0.77	51.3
CC 3	2.1	3.84	0.25	0.90	48.5
CC 4	0.6	5.63	0.15	0.83	50.3
CC 4	2.1	9.08	0.17	1.0	53.2
CC 5	0.6	12.1	0.15	1.3	55.9
CC 5	2.1	8.87	0.12	1.4	52.2
CC 6	0.6	9.77	0.29	1.0	53.2
CC 6	2.1	23.1	0.16	1.7	55.4
CC 7	0.6	8.01	0.14	0.98	51.7
CC 7	2.1	1.80	0.10	1.4	50.8
CC 8	0.6	6.24	0.10	1.2	55.9
CC 8	2.1	2.90	0.10	0.92	36.1
CC 9	0.6	3.59	0.08	1.1	53.2
CC 9	2.1	7.51	0.09	1.4	45.4
CC1.0	0.6	4.70	0.09	0.94	37.2
CC10	2.1	100	0.49	1.1	43.9
CC11	0.6	10.3	0.08	0.85	40.2
CC11	2.1	1.05	0.04	0.83	96.7
CC12	0.6	9.03	0.04	0.88	52.7
CC12	2.1	6.42	0.05	0.90	49.6
CC13	0.6	2.58	0.03	0.88	44.7
CC13	2.1	11.4	0.09	1.3	52.2
CC14	0.6	5.30	0.09	0.88	45.7
CC14	2.1	5.49	0.39	1.5	55.4

Table 24 (continued)

el Corte	Depth	N-NH <sub>4</sub> +	N-NO <sub>2</sub> +NO <sub>3</sub>	P-PO <sub>4</sub>	Si-Si(OH)4
Station	(m)	(µg-at N/L)	(µg-at N/l)	(µg-at P/l)	(µg-at Si/l)
CC15	0.6	1.81	0.08	1.1	52.7
CC15	2.1	9.97	0.08	1.5	51.8
CC16	0.6	3.91	0.05	0.75	40.2
CC16	2.1	1.69	0.03	1.2	51.7
CC17	0.6	1.42	0.03	0.92	65.1
CC17	2.1	1.08	0.04	0.94	52.2
CC18	0.6	1.98	1.14	0.98	42.9
CC18	2.1	3.10	0.04	1.0	52.2
CC19	0.6	1.27	0.14	0.96	57.5
CC19	2.1	4.02	0.03	1.2	55.4
CC20	0.6	2.71	0.03	0.77	57.0
CC20	2.1	0.81	0.03	0.90	55.9

B. Atchafalaya Dissolved Nutrients

	Depth	N-NH <sub>4</sub> +	N-NO <sub>2</sub> +NO <sub>3</sub>	P-PO <sub>4</sub>	Si-Si(OH)
Station	(m)	(µg-at N/l)	(µg-at N/l)	(µg-at P/l)	(µg-at Si/l)
MC30	0.9	13.9	9.90	0.71	17.6
MC31	0.9	22.4	7.57	0.92	24.7
MC32	0.9	20.7	7.81	1.3	21.4
MC33	0.9	3.35	6.11	0.83	15.4
MC34	0.9	10.2	8.31	0.85	21.0
MC35	0.9	5.75	6.28	0.75	20.6
MC36	0.9	3.30	7.04	0.88	20.9
MC37	0.9	20.4	1.87	0.83	11.1
MC38	0.9	14.2	5.93	0.77	17.6
MC39	0.9	22.9	7.01	0.86	20.7
MC40	0.9	17.0	5.41	0.75	15.3
MC41	0.9	232	1.49	0.90	13.1
			(continued)		

Table 24 (continued)

	Depth	N-NH <sub>4</sub> +	N-NO <sub>2</sub> +NO <sub>3</sub>	P-P0 <sub>4</sub>	Si-Si(OH)4
Station	(m)	(µg-at N/l)	(µg-at N/l)	(µg-at P/l)	(µg-at Si/l)
MC42	0.9	11.4	2.50	1.0	19.3
MC43	0.9	133	3.20	0.85	15.5
MC44	0.9	1.65	3.49	1.3	18.5
MC45	0.9	22.8	3.55	1.2	16.2
MC46	0.9	15.3	1.42	0.96	11.5
MC47	0.9	16.2	2.23	0.86	23.8
MC48	0.9	25.5	2.75	1.7	15.2
MC49	0.9	5.31	4.28	1.0	16.1
MC50	0.9	11.7	3.12	0.86	21.2
MC51	0.9	2.78	3.29	1.1	27.3
MC52	0.9	11.6	2.59	0.96	14.3
MC53	0.9	109	2.14	1.2	12.6
MC54	0.9	24.6	3.17	1.0	17.3
MC55	0.9	9.37	2.08	1.2	14.7
MC56	0.9	3.65	2.29	1.2	14.5
MC57	0.9	8.11	2.28	1.0	16.7
MC58	0.9	11.6	4.12	0.83	30.1
MC59	0.9	3.04	3.32	0.83	13.6
MC60	0.9	6.09	3.67	0.75	143
MC61	0.9	5.41	2.23	0.81	12.7
MC62	0.9	14.0	1.54	0.81	10.7
MC63	0.9	9.79	3.56	0.90	17.0
MC64	0.9	6.26	1.84		·
MC65	0.9	2.09	1.81	1.3	12.6
MC66	0.9	24.4	1.90	1.1	27.0

Table 24 (continued)
C. Apalachicola Dissolved Nutrients

	Depth	N_NU +	P. PO	C1_C1(OU)
C1		N-NH <sub>4</sub>	P-PO <sub>4</sub>	Si-Si(OH) <sub>4</sub>
Station	<u>(m)</u>	(µg-at N/l)	(µg-at P/l)	(µg-at Si/l)
A 1	2.4	14.5	0.9	63.8
A 1	0.9	2.3	0.8	20.2
A 2	2.4	17.7	0.7	43.1
A 2	0.9	3.0	0.8	18.8
A 3	2.4	4.9	0.3	17.6
A 3	0.9	2.8	0.3	13.6
A 4	2.4	15.8	<b></b> 12	
A 4	0.9	3.6	0.5	13.6
A 5	2.4	19.8	0.6	63.7
A 5	0.9	2.8	0.4	334
A 6	2.4	20.9	0.6	53.4
A 6	0.9	1.8	0.4	
A 7	2.4	20.5	0.8	72.3
A 7	0.9	2.8	0.2	18.7
A 8	2.4	4.6		028
A 8	0.9	3.5	0.3	17.1
A 9	2.4	24.2	0.7	73.1
A 9	0.9	3.2	0.2	19.4
A10	2.4	22.4	0.6	67.2
A10	0.9	3.4	0.3	17.2
A11	2.4	13.7	0.5	50.9
A11	0.9	1.5	0.6	31.6
A41	0.6	4.6	0.3	46.7
A41	2.1	8.2	0.3	37.9
A42	0.6			314
A42	2.1		11	-

Table 24 (continued)

	Depth	N-NH <sub>4</sub> +	P-PO <sub>4</sub>	Si-Si(OH)4
Station	<u>(m)</u>	(ug-at N/l)	(ug-at P/l)	(µg-at Si/l)
A43	0.6	0	L	
A43	2.1			13
A44	0.6	3.0	1.2	44.5
A44	2.1	3.2	0.4	44.3
A45	0.6	6.8	0.5	44.0
A45	2.1	27.4	0.4	40.0
A46	0.6	9.4	0.5	44.0
A46	2.1	9.2	0.4	38.8
A47	0.6	5.6	0.5	44.2
A47	2.1	7.7		A
A48	0.6	5.1	0.4	43.0
A48	2.1	6.5	0.4	38.0
A49	0.6	6.3	0.5	44.8
A49	2.1	6.6	0.4	40.8
A50	0.6	3.0	0.3	39.0
A50	2.1		+ 4 A	
A51	0.6	3 6 <del></del>	δε <del>-</del> ε	. Bosson 6.4
A51	2.1		5.03 1	<u>-</u> 11
A52	0.6	7.6	0.3	33.5
A52	2.1	9.2	1.1	49.7
A53	0.6	19.7	0.4	42.7
A53	2.1	8.2	0.3	47.0
A54	0.6	17.5	0.5	41.5
A54	2.1	8.3	0.2	23.4
A55	0.6	3.7	0.5	46.3
A55	2.1	6.05 - <del>-</del>	5.8 - 1	<del>-</del>
A56	0.6	2.9	0.5	44.0
A56	2.1	167	3	

Table 24 (continued)

	Depth	N-NH <sub>4</sub> <sup>+</sup>	P-PO <sub>4</sub>	Si-Si(OH)4
Station	<u>(m)</u>	(µg-at N/l)	(µg-at P/l)	(µg-at Si/l)
A57	0.6	6.6	0.4	45.8
A57	2.1	9.0	0.5	26.7
A58	0.6	7.9	0.4	44.3
A58	2.1	12.1	0.3	42.3
A59	0.6	8.2	0.4	44.4
A59	2.1	8.1	0.3	41.9
A60	0.6	4.6	0.4	48.7
A60	2.1	10.9	0.4	50.7
A61	0.6	2.2	0.4	44.0
A61	2.1	9.7	0.5	49.3
A62	0.6	6.7	0.5	41.8
A62	2.1	7.7	0.3	49.3
A63	0.6	4.4	0.5	42.8
A63	2.1	7.7	0.1	37.0
A64	0.6	4.2	0.7	45.6
A64	2.1	136	<del></del>	
A65	0.6	3.9	0.5	41.7
A65	2.1	8.4	0.4	48.9
A66	0.6	6.6	0.5	49.1
A66	2.1	6.7	0.2	52.5
A67	0.6	2.1	0.5	40.9
A67	2.1	8.7	0.3	47.0
A68	0.6	7.2	0.5	39.1
A68	2.1	-		
A69	0.6	2.6	0.8	43.2
A69	2.1	13.9	0.8	50.3
A70	0.6	5.8	0.6	43.4
A70	2.1	25.7	1.9	39.6

Table 24 (concluded)

	Depth	N-NH <sub>4</sub> +	P-PO <sub>4</sub>	Si-Si(OH)4
Station	(m)	(µg-at N/l)	(µg-at P/l)	(µg-at Si/l)
A71	0.6		<u></u>	
A71	2.1	<u></u>	<u></u>	
A72	0.6	<del></del>		
A72	2.1	<u></u>		
A73	0.6	2.9	0.4	42.4
A73	2.1	25.9	0.5	45.2
A74	0.3	6.3	0.4	44.2
A74	1.8	17.9	0.6	47.4
A75	0.3	4.4		41.7
A75	1.8	27.8	0.3	44.3
A76	0.3	5.6	0.3	37.9
A76	1.8	29.5	0.5	44.0
A77	0.3	4.3	0.3	40.2
A77	1.8	26.8	0.4	44.0
A78	0.3	29.4	0.3	39.7
A78	1.8	5.4	1.5	46.4
A79	0.3	29.1	0.4	42.4
A79	1.8	28.7	1.0	43.3
A80	0.3	29.4	0.3	40.9
A80	1.8	8.7	1.1	45.8

Summary of Data on Particle-Associated Metals in Suspended Sediment and in Channel Sediment Deposits

Site	Type	Fe (µg/g)	Mn (μg/g)	Zn (µg/g)	Cu (µg/g)	Cr (µg/g)	Cd (ng/g)	Cu Cr Cd Ph Hg (ug/g) (ug/g) (ug/g)	Hg (μg/g)
Corpus	Suspended*	$6.45 \times 10^{3}$	377		77.5	33.0	4.10	8.69	2.61
Atchafalaya	*Pepuded*	1.88 x 10 <sup>4</sup>	$1.47 \times 10^3$	200	32.5	23.1	1.61	2.03	0.409
Apalachicola	Suspended*	3.20 x 10 <sup>4</sup>	1.58 x 10 <sup>3</sup>	149	20.0	50.4	1.13	13.5	0.756
Corpus Christi	Bulk Sediment**	9.25 x 10 <sup>3</sup>	345	1	35.8	ı	ı	12.4	•
Apalachicola	Bulk Sediment**	1.38 × 10 <sup>4</sup>	830	4	14.6	1	1	12.7	1

\* Geometric mean of all values as  $\mu g/g$  suspended sediment (G.M.  $y = \sqrt{y_1 y_2 y_3 y_4 \cdots y_n}$ ).

Table 26
Particle-Associated Metals, Corpus Christi Bay (TX), 25 August 1976

Station	Depth (m)	Suspended Sediment*		Mn**		Cu**	Cr**	**P0	Pb**	H8**
CC 1	9.0		83.9	1.33	107	3.45	0.10	0.185	0.17	0.075
CC 1	2.1			5.17		1	0.61		0.61	1
CC 2	9.0			5.17		2.86	1.25	0.132	< 0.03	0.041
CC 2	2.1	16.2		35.9		5.12	0.33	0.132	1.22	0.125
CC 3	9.0			5.17		1.55	1.07		0.28	0.174
60 3	2.1			7.09		4.65	90.0 >	0.169	0.14	0.108
7 00	9.0			9.01		2.74	0.88	0.316	0.03	0.141
CC 4	2.1			28.2		1.67	0.42	0.106	0.14	0.148
CC 5	9.0			9.01		1.08	0.61	0.079	0.17	0.075
CC 5	2.1			12.8		5.25	2.26	0.527	0.32	0.108
9 00	9.0			24.4		1.79	1.25	0.158	< 0.03	0.174
9 00	2.1			109		11.8	3.82	0.185	< 0.03	0.158
00 7	9.0			1.33		1.07	0.00 >	< 0.027	0.10	0.125
CC 7	2.1			9.01		3.46	> 0.06	0.185	0.39	0.125
8 23	9.0			12.8		1.43	1.16	0.211	0.50	< 0.017
8 22	2.1			12.8		2.03	0.24	0.132	0.43	0.092
6 00	9.0			14.8		1.31	1.62	0.263	0.17	0.026
6 22	2.1			33.9		2.86	1.34	0.079	0.28	0.026

Table 26 (continued)

Station	Depth (m)	Suspended Sediment*	Fe*	Wn**	Zn**	Cu**	Cr**	**P2	Pb**	Hg**
0000	9.0	15.0		16.7	7.89	< 0.12	1.25	< 0.027	0.14	0.026
0100	2.1	13.9	484	35.9		4.29	1.16	0.106	0.21	0.026
CC11	9.0	12.6	87.3	3.25		3.94	0.00 >	0.106	0.21	0.125
CC11	2.1	13.6	484	5.17		5.84	1.53	0.079	•	0.108
CC12	9.0	15.3	111	5.17		< 0.12	0.61	0.290	0.68	< 0.017
CC12	2.1	17.4	182	10.9		5.49	1.62	0.474	0.72	0.042
CC13	9.0	14.8	328	20.5		2.27	1.07	0.342	0.10	0.141
CC13	2.1	32.4	522	41.6		3.70	1.16	0.053	0.24	0.059
CC14	9.0	27.0	169	16.7		< 0.12	0.70	0.027	0.10	< 0.017
CC14	2.1	130	321	20.5		2.63	2.08	0.290	0.43	< 0.017
CC15	9.0	ı	257	12.8		7.16	1.16	0.132	0.35	< 0.017
CC15	2.1	25.4	735	47.4		4.17	1.25	0.037	96.0	0.026
9100	9.0	6.94	67.0	3.25		0.12	0.52	0.158	0.35	0.026
9100	2.1	138	80.5	5.17		< 0.12	1.34	0.185	1.23	< 0.017
CC17	9.0	35.7	9.94	< 1.33		09.0	90.0	0.316	0.10	0.042
CC17	2.1	134	108	3.25		2.39	1.25	0.079	0.28	0.042
CC18	9.0	14.8	308	14.8		2.03	1.53	0.027	0.35	0.059
CC18	2.1	53.8	403	22.4		0.74	0.61	0.369	0.03	0.042
6100	9.0	23.4	220	9.01		3.10	0.42	0.027	0.14	0.108
6100	2.1	78.8	315	7		0.74	0.42	0.132	0.21	0.108
				(con	(continued)					

Table 26 (concluded)

Hg**	0.108	0.125
Pb**	98.0	0.28
**P0	0.079	0.053
Cr**	•	90.0
**n2	2.86	7.27
Zn**	72.5	101
Mn**	1.33	9.01
Fe *	63.6	196
Suspended Sediment*	18.3	87.3
Depth (m)	9.0	2.1
Station	0000	CC20

\* Values are mg/k (ppm)
\*\* Values are µg/k (ppb)

Table 27
Particle-Associated Metals, Atchafalaya Bay (LA), 21 October 1976

	Depth	Suspended	1	;	1	1	;		:	:
Station		Sediment	Fexx	Muxx	××u7	Cu**	Crww	× PO	PD**	HBKK
MC30	6.0	112	1860	254	18.9	3.55	2.31	0.10	0.11	0.069
MC31	6.0	189	6330	403	55.1	9.82	07.9	0.20	0.14	0.206
MC32	6.0	1104	2410	264	174	25.4	3.12	2.13	0.07	0.45
MC33	6.0	6.06	1860	174	25.4	3.12	2.13	0.07	0.42	0.183
MC34	6.0	317	0909	390	34.0	9.26	5.33	0.78	1.07	0.069
MC35	6.0	251	2060	333	31,3	8.54	5.33	1.00	0.35	< 0.008
MC36	6.0	313	2600	379	37.3	5.69	3.02	0.98	0.45	0.046
MC37	6.0	103	1770	179	44.3	1.55	1.95	0.02	0.11	0.069
MC38	6.0	121	2410	205	28.1	3.26	2.49	0.10	0.35	0.046
MC39	6.0	164	2770	238	24.4	6.54	00.9	0.15	0.25	0.069
MC40	6.0	95.4	2860	159	26.5	2.83	2.84	0.02	0.18	0.046
MC41	6.0	135	1860	170	28.6	3.26	2.10	0.07	0.32	< 0.008
MC42	6.0	1117	2410	234	24.3	3.69	2.67	0.17	0.32	0.069
MC43	6.0	130	2770	194	21.1	3.26	2.31	0.05	0.45	0.023
MC44	6.0	176	6240	419	51.9	11.8	8.71	0.45	0.25	0.114
MC45	6.0	131	2860	220	31.9	2.41	3.38	0.05	0.45	0.069
942W	6.0	95.1	1860	159	18.4	3.41	2.31	0.37	0.32	0.069
MC47	6.0	408	13,200	164	160	24.4	11.6	0.57	3.37	0.114
MC48	6.0	069	7230	452	48.2	15.7	8.04	0.37	0.35	0.387
				ဗ	(continued)					

179

Table 27 (concluded)

MC49         0.9         315         8750         55.3         65.2         16.7         9.72         3.84         1.07         0.15           MC50         0.9         212         4690         311         51.3         10.4         7.10         3.09         0.28           MC51         0.9         445         8980         566         12.3         18.2         9.78         0.42         1.17         0.069           MC52         0.9         425         8890         566         12.3         18.2         9.78         0.42         1.17         0.069           MC54         0.9         122         6240         391         529         9.52         4.89         0.20         0.04         0.04           MC54         0.9         122         6240         32         62.9         7.14         3.02         0.42         1.01         0.04           MC55         0.9         141         2210         160         26.5         7.14         3.02         0.42         0.28         0.040           MC54         0.9         124         250         26.5         3.74         3.74         3.74         0.25         0.25         0.20 <t< th=""><th>Station</th><th>Depth (m)</th><th>Suspended Sediment*</th><th>Fe**</th><th>Mn**</th><th>Zn**</th><th>Cu**</th><th>Cr**</th><th>** PO</th><th>Pb**</th><th>Hg**</th></t<>	Station	Depth (m)	Suspended Sediment*	Fe**	Mn**	Zn**	Cu**	Cr**	** PO	Pb**	Hg**
0.9         212         4690         311         51.3         10.4         7.10         3.09         0.28           0.9         445         8980         566         12.3         18.2         9.78         0.42         1.17           0.9         445         8980         566         12.3         18.2         9.78         0.42         1.17           0.9         125         6240         391         52.9         9.52         4.89         0.20         1.01           0.9         191         3960         262         26.5         7.14         3.02         0.72         0.28           0.9         141         2210         160         26.6         7.48         8.71         0.26         0.28           0.9         124         2210         160         26.6         7.48         8.71         0.26         0.28           0.9         124         273         25.9         3.75         5.53         1.55         0.28           0.9         124         125         27.8         3.74         3.14         0.05         0.28           0.9         10.7         1240         113         29.8         3.74         3.14	MC49	6.0	375	8750	553	65.2	16.7	9.72	3.84	1.07	0.157
0.9         445         8980         566         12.3         18.2         9.78         0.42         1.17           0.9         225         6240         391         52.9         9.52         4.89         0.70         1.01           0.9         192         3740         249         20.8         5.62         9.80         0.77         0.28           0.9         191         3960         262         26.5         7.14         3.02         0.77         0.28           0.9         141         2210         160         26.6         7.48         8.71         0.26         0.28           0.9         124         2650         273         25.9         3.75         5.53         1.55         0.28           0.9         124         2650         207         94.7         7.82         5.53         0.20         0.28           0.9         31.7         1240         113         27.6         2.98         2.99         0.05         0.44           0.9         31.7         11.9         3.83         2.31         0.07         0.28           0.9         37.7         14.0         11.9         3.83         2.13         1.00 <td>MC50</td> <td>6.0</td> <td>212</td> <td>0694</td> <td>311</td> <td>51.3</td> <td>10.4</td> <td>7.10</td> <td>3.09</td> <td>0.28</td> <td>0.092</td>	MC50	6.0	212	0694	311	51.3	10.4	7.10	3.09	0.28	0.092
0.9         225         6240         391         52.9         9.52         4.89         0.20         1.01           0.9         192         3740         249         20.8         5.62         9.80         0.77         0.28           0.9         191         3960         262         26.5         7.14         3.02         0.42         0.28           0.9         141         2210         160         26.6         7.48         8.71         0.26         0.28           0.9         124         2650         207         3.75         5.53         1.55         0.23           0.9         76.8         1450         113         27.6         2.98         2.99         0.05         0.44           0.9         76.8         1450         113         27.6         2.98         2.99         0.05         0.44           0.9         81.7         1240         113         29.8         3.74         3.14         0.07         0.28           0.9         87.3         1770         139         29.7         3.12         1.78         0.11         0.28           0.9         88.9         2130         174         1.41         1.44 <td>MC51</td> <td>6.0</td> <td>445</td> <td>8980</td> <td>999</td> <td>12.3</td> <td>18.2</td> <td>9.78</td> <td>0.42</td> <td>1.17</td> <td>0.069</td>	MC51	6.0	445	8980	999	12.3	18.2	9.78	0.42	1.17	0.069
0.9         192         3740         249         20.8         5.62         9.80         0.77         0.28           0.9         191         3960         262         26.5         7.14         3.02         0.42         0.25           0.9         191         3960         262         26.5         7.14         3.02         0.42         0.25           0.9         141         2210         160         26.6         7.48         8.71         0.26         0.28           0.9         124         2650         207         3.75         5.53         1.55         0.23           0.9         76.8         1450         113         27.6         2.98         2.99         0.05         0.44           0.9         81.7         1240         113         29.8         3.74         3.14         0.07         0.28           0.9         81.7         1680         121         11.9         3.83         2.31         0.50         0.28           0.9         87.3         1770         139         29.7         3.12         1.78         0.11         0.28           0.9         88.9         2130         174         124         0.42 <td>MC52</td> <td>6.0</td> <td>225</td> <td>6240</td> <td>391</td> <td>52.9</td> <td>9.52</td> <td>4.89</td> <td>0.20</td> <td>1.01</td> <td>0.046</td>	MC52	6.0	225	6240	391	52.9	9.52	4.89	0.20	1.01	0.046
0.9       191       3960       262       26.5       7.14       3.02       0.42       0.25       0.25         0.9       141       2210       160       26.6       7.48       8.71       0.26       0.28         0.9       120       3740       273       25.9       3.75       5.53       1.55       0.23         0.9       124       2650       207       94.7       7.82       5.53       1.55       0.23         0.9       76.8       1450       113       29.8       3.74       0.00       0.05       0.44         0.9       81.7       1240       113       29.8       3.74       0.07       0.05       0.44         0.9       10.7       1680       121       11.9       3.83       2.31       0.52       0.28         0.9       87.3       1770       1490       135       14.1       4.83       2.13       1.00       0.11          0.9       132       177       140       174       124       0.74       0.42       0.11          0.9       132       177       141       11.4       2.41       1.24       0.10       0.10       0.	MC53	6.0	192	3740	249	20.8	5.62	9.80	0.77	0.28	0,040
0.9         141         2210         160         26.6         7.48         8.71         0.26         0.28           0.9         220         3740         273         25.9         3.75         5.53         1.55         0.23           0.9         124         2650         207         94.7         7.82         5.53         0.20         0.56           0.9         76.8         1450         113         27.6         2.98         2.99         0.05         0.44           0.9         81.7         1240         113         29.8         3.74         3.14         0.07         0.28           0.9         107         1680         121         11.9         3.83         2.31         0.07         0.28           0.9         87.3         1770         1400         135         14.1         4.83         2.13         1.00         0.11         0.28           0.9         88.9         2130         176         16.8         3.26         0.70         0.50         0.11         0.4           0.9         88.6         1370         114         11.4         2.41         1.24         0.42         0.14         0.21           0.9 </th <td>MC54</td> <td>6.0</td> <td>191</td> <td>3960</td> <td>262</td> <td>26.5</td> <td>7.14</td> <td>3.02</td> <td>0.42</td> <td>0.25</td> <td>&lt; 0.008</td>	MC54	6.0	191	3960	262	26.5	7.14	3.02	0.42	0.25	< 0.008
0.9         220         3740         273         25.9         3.75         5.53         1.55         0.23           0.9         124         2650         207         94.7         7.82         5.53         0.20         0.56           0.9         76.8         1450         113         27.6         2.98         2.99         0.05         0.44           0.9         81.7         1240         113         29.8         3.74         3.14         0.07         0.28           0.9         107         1680         121         11.9         3.83         2.31         0.52         0.28           0.9         107         1680         121         11.9         3.12         1.78         0.11         0.28           0.9         77.7         1400         135         14.1         4.83         2.13         1.00         0.11         0.28           0.9         132         1770         141         11.4         2.41         1.24         0.42         0.14         0.14         0.10           0.9         89.6         2590         194         33.5         4.12         2.49         0.50         0.14         0.28           0.9 </th <td>MC55</td> <td>6.0</td> <td>141</td> <td>2210</td> <td>160</td> <td>56.6</td> <td>7.48</td> <td>8.71</td> <td>0.26</td> <td>0.28</td> <td>0,040</td>	MC55	6.0	141	2210	160	56.6	7.48	8.71	0.26	0.28	0,040
0.9       124       2650       207       94.7       7.82       5.53       0.20       0.56         0.9       76.8       1450       113       27.6       2.98       2.99       0.05       0.44         0.9       81.7       1240       113       29.8       3.74       3.14       0.07       0.28         0.9       107       1680       121       11.9       3.83       2.31       0.52       0.28         0.9       87.3       1770       139       29.7       3.12       1.78       0.11       0.28         0.9       87.3       1770       139       14.1       4.83       2.13       1.00       0.11          0.9       88.9       2130       176       16.8       3.26       0.70       0.50       0.11          0.9       89.6       2590       194       33.5       4.12       2.49       0.50       0.14          0.9       104       1680       152       15.7       1.98       2.49       0.50       0.28	MC56	6.0	220	3740	273	25.9	3.75	5.53	1.55	0.23	0.067
0.9       76.8       1450       113       27.6       2.98       2.99       0.05       0.04         0.9       81.7       1240       113       29.8       3.74       3.14       0.07       0.28         0.9       107       1680       121       11.9       3.83       2.31       0.52       0.28         0.9       87.3       1770       139       29.7       3.12       1.78       0.11       0.28         0.9       77.7       1400       135       14.1       4.83       2.13       1.00       0.11         0.9       88.9       2130       176       16.8       3.26       0.70       0.50       0.11         0.9       132       1770       141       11.4       2.41       1.24       0.42       0.14          0.9       89.6       2590       194       33.5       4.12       2.49       0.10       0.21         0.9       104       1680       152       15.7       1.98       2.49       0.50       0.28	MC57	6.0	124	2650	207	7.46	7.82	5.53	0.20	0.56	0.067
0.9       81.7       1240       113       29.8       3.74       3.14       0.07       0.28         0.9       107       1680       121       11.9       3.83       2.31       0.52       0.28         0.9       87.3       1770       139       29.7       3.12       1.78       0.11       0.28         0.9       77.7       1400       135       14.1       4.83       2.13       1.00       0.11         0.9       88.9       2130       176       16.8       3.26       0.70       0.50       0.11          0.9       132       1770       141       11.4       2.41       1.24       0.42       0.14          0.9       89.6       2590       194       33.5       4.12       2.49       0.10       0.21         0.9       104       1680       152       15.7       1.98       2.49       0.50       0.28	MC58	6.0	76.8	1450	113	27.6	2.98	2.99	0.05	0.44	0.023
0.9       107       1680       121       11.9       3.83       2.31       0.52       0.28         0.9       87.3       1770       139       29.7       3.12       1.78       0.11       0.28         0.9       77.7       1400       135       14.1       4.83       2.13       1.00       0.11       0.28         0.9       88.9       2130       176       16.8       3.26       0.70       0.50       0.11          0.9       132       1770       141       11.4       2.41       1.24       0.42       0.14          0.9       89.6       2590       194       33.5       4.12       2.49       0.10       0.21         0.9       104       1680       152       15.7       1.98       2.49       0.50       0.28	MC59	6.0	81.7	1240	113	29.8	3.74	3.14	0.07	0.28	0.016
0.9       87.3       1770       139       29.7       3.12       1.78       0.11       0.28         0.9       77.7       1400       135       14.1       4.83       2.13       1.00       0.11         0.9       88.9       2130       176       16.8       3.26       0.70       0.50       0.11          0.9       132       1770       141       11.4       2.41       1.24       0.42       0.14          0.9       89.6       2590       194       33.5       4.12       2.49       0.10       0.21         0.9       104       1680       152       15.7       1.98       2.49       0.50       0.28	MC60	6.0	107	1680	121	11.9	3.83	2.31	0.52	0.28	0.046
0.9       77.7       1400       135       14.1       4.83       2.13       1.00       0.11         0.9       88.9       2130       176       16.8       3.26       0.70       0.50       0.11          0.9       132       1770       141       11.4       2.41       1.24       0.42       0.14          0.9       89.6       2590       194       33.5       4.12       2.49       0.10       0.21         0.9       104       1680       152       15.7       1.98       2.49       0.50       0.28	MC61	6.0	87.3	1770	139	29.7	3.12	1.78	0.11	0.28	0.092
0.9       88.9       2130       176       16.8       3.26       0.70       0.50       0.11          0.9       132       1770       141       11.4       2.41       1.24       0.42       0.14          0.9       89.6       2590       194       33.5       4.12       2.49       0.10       0.21         0.9       104       1680       152       15.7       1.98       2.49       0.50       0.28	MC62	6.0	7.77	1400	135	14.1	4.83	2.13	1.00	0.11	0.046
0.9     132     1770     141     11.4     2.41     1.24     0.42     0.14        0.9     89.6     2590     194     33.5     4.12     2.49     0.10     0.21       0.9     104     1680     152     15.7     1.98     2.49     0.50     0.28	MC63	6.0	88.9	2130	176	16.8	3.26	0.70	0.50	0.11	< 0.008
0.9     89.6     2590     194     33.5     4.12     2.49     0.10     0.21       0.9     104     1680     152     15.7     1.98     2.49     0.50     0.28	MC64	6.0	132	1770	141	11.4	2.41	1.24	0.42	0.14	< 0.008
0.9 104 1680 152 15.7 1.98 2.49 0.50 0.28	MC65	6.0	9.68	2590	194	33.5	4.12	2.49	0.10	0.21	0.069
	990W	6.0	104	1680	152	15.7	1.98	2.49	0.50	0.28	0.046

\* Values in mg/& (ppm)
\*\* Values in µg/& (ppb)

Table 28
Particle-Associated Metals, Apalachicola (FL), 4-7 April 1976

Station	Depth (m)	Suspended Solids*	Fe**	Mn**	Zn**		Cr**	** PO	Pb**	Hg**
A 1	6.0	33.7	•	•	1		1		•	•
A 1	2.4	14.8	208	8.16	3.65	< 0.124	0.44 0.037	0.037	0.14	0.019
A 2	6.0	19.4	977	21.7	16.1		2.81	0.055	1.07	0.045
A 2	2.4	12.9	401	29.8	8.77		2.46	0.028	0.14	0.032
A 3	6.0	11.5	283	13.6	5.84		2.63	0.111	0.76	0.019
A 3	2.4	6.3	< 17.0	< 2.71	0.73		< 0.176 <	400.0	> 0.04	0.005
4 4	6.0	15.0	372	24.4	8.04		2.63	0.019	0.25	0.032
A 4	2.4	11.0	238	27.1	2.19		1.93	< 0.004	0.04	0.019
A 5	6.0	18.6	283	10.8	1.46		0.176	0.028	0.14	0.005
A 5	2.4	10.1	164	10.8	0.73		< 0.176 <	> 0.004	0.04	0.005
9 V	6.0	37.9	1040	62.4	6.57		3.06	0.023	96.0	0.032
9 V	2.4	14.5	206	35.3	< 0.73		2.28	0.009	0.14	0.045
A 7	6.0	18.4	178	8.13	0.73		0.527	< 0.004	0.04	0.005
A 7	2.4	7.6	356	36.1	68.9		0.379	0.124	0.14	0.054
8 W	6.0	18.8	535	35.3	2.19	< 0.124	2.46	0.056	0.25	0.019
8 W	2.4	17.9		1	ı	1	•	ı	1	1
6 V .	6.0	25.8	937	51.5	3.65	0.275	3.47	0.037	0.45	0.019
6 A	2.4	23.8	832	40.7	2.49	< 0.124	2.98	0.028	0.35	0.059

(continued)

Table 28 (continued)

Station	Depth (m)	Suspended Solids*	Fe**	Mn**	Zn**		Cr**	**P0	Pb**	Hg**
A10	6.0	22.5	595	40.7	2.92	< 0.124	2.11	0.019	0.35	0.032
A10	2.4	13.4	550	32.5	2.19		2.81	0.028	0.25	0.032
A11	6.0	6.04	729	32.5	4.38		0.702	0.084	0.35	0.019
A11	2.4	38.0	714	24.4	12.4		92.9	0.019	2.55	0.019
A41	9.0	17.5	253	10.8	3.65	< 0.124	0.176	0.019	0.04	< 0.005
A41	2.1	72.3	ı	1	1			1	1	
A43	9.0	20.2	253	19.0	4.38			0.004	0.14	0.032
A43	2.1	1270.4	1	1	•			1	1	1
A44	9.0	22.3	921	40.7	5.84			0.033	0.45	0.045
A44	2.1	51.7	1830	73.2	5.84			> 0.004	99.0	0.019
A45	9.0	15.1	1	1	1			1	1	ı
A45	2.1	13.5	ı	1	1			1	1	1
946	9.0	82.9	401	16.3	9.50	•		0.290	0.04	0.019
A46	2.1	38.3	134	10.8	1.46			< 0.004	0.04	< 0.005
A47	9.0	20.9	164	10.8	0.73		V	< 0.004	99.0	< 0.005
A47	2.1	78.6	1710	100	3.65			< 0.004	0.55	0.32
A48	9.0	34.3	520	16.3	1.46			< 0.004	0.14	0.005
A48	2.1	11.9	416	13.6	0.73			0.022	0.14	0.005

(continued)

Table 28 (continued)

401 10.8 2040 122 1 520 27.1 4.58 x 10 <sup>5</sup> 2.09 x 10 <sup>4</sup> 4.58 x 10 <sup>5</sup> 2.09 x 10 <sup>4</sup> 17480 322	Suspended	4	77.7	1	1	;	+:0	;	1
0.6 $28.5$ $401$ $10.8$ 2.1 $58.8$ $2040$ $122$ $1$ 0.6 $19.9$ $520$ $27.1$ 2.1 $ +.58 \times 10^5$ $2.09 \times 10^4$ 0.6 $22.84$ $ -$ 2.1 $63.36$ $7480$ $322$ 0.6 $24.81$ $ -$ 2.1 $17.80$ $1770$ $62.4$ 0.6 $22.97$ $ -$ 2.1 $4.34 \times 10^4$ $1.37 \times 10^6$ $5.92 \times 10^4$ 0.6 $16.22$ $ -$ 2.1 $4.34 \times 10^4$ $1.37 \times 10^6$ $5.92 \times 10^4$ 0.6 $18.95$ $535$ $24.4$ 2.1 $24.63$ $1550$ $65.1$ 0.6 $18.14$ $758$ $38.0$	TIDS*	Fexx	Mn××	Zuzz	Cu**	Crxx	× PO	Pb**	Hg**
2.1 $58.8$ $2040$ $122$ 1  0.6 $19.9$ $520$ $27.1$ 2.1 $ 4.58 \times 10^5$ $2.09 \times 10^4$ 0.6 $22.84$ $  -$ 2.1 $63.36$ $7480$ $322$ 0.6 $24.81$ $  -$ 2.1 $17.80$ $1770$ $62.4$ 0.6 $22.97$ $ -$ 2.1 $19.09$ $372$ $13.6$ 0.6 $16.22$ $ -$ 2.1 $19.09$ $372$ $13.6$ 0.6 $16.22$ $ -$ 2.1 $19.09$ $372$ $10^4$ 2.1 $19.09$ $372$ $10^6$ 2.1 $22.97$ $ -$ 2.1 $22.97$ $ -$ 2.1 $22.97$ $ -$ 2.1 $22.97$ $ -$ 2.1 $22.97$ $ -$ 2.1 $22.97$ $ -$ 2.1 $22.97$ $ -$ 2.1 $22.97$ $ -$ 2.1 $22.97$ $ -$ 2.1 $22.97$ $ -$ 2.1 $22.97$ $ -$ 2.1 $22.97$ $-$ 2.1 $22.97$ $-$ 2.1 $22.97$ $-$ 2.2 $22.7.1$ 2.1 $24.63$ $25.50$ $24.4$ 2.1 $24.63$ $25.50$ $25.50$ $24.4$ 2.1 $24.63$ $25.50$ $25.50$ $25.50$ 2.1 $24.63$ $25.50$ $25.50$ 2.1 $24.63$ $25.50$ $25.50$ 2.1 $24.63$ $25.50$ $25.50$ 2.1 $24.63$ $25.50$ $25.50$ 2.2 $24.4$ 2.1 $24.63$ $25.50$ $25.50$ 2.2 $24.4$ 2.1 $24.63$ $25.50$ $25.50$ 2.2 $24.4$ 2.3 $24.4$ 2.1 $24.63$ $25.50$ 2.4 $24.63$ $25.50$ 2.5 $25.50$ 2.7 $25.50$ 2.8 $25.50$ 2.9 $25.50$ 2.0 $25.50$	28.5	107		6.57	< 0.124	0.401	0.033	0.45	0.005
0.6 $19.9$ $520$ $27.1$ 2.1 $ 4.58 \times 10^5$ $2.09 \times 10^4$ 0.6 $22.84$ $  -$ 2.1 $63.36$ $7480$ $322$ 0.6 $24.81$ $  -$ 2.1 $17.80$ $1770$ $62.4$ 0.6 $22.97$ $  -$ 2.1 $19.09$ $372$ $13.6$ 0.6 $16.22$ $  -$ 2.1 $4.34 \times 10^4$ $1.37 \times 10^6$ $5.92 \times 10^4$ 0.6 $16.22$ $  -$ 2.1 $1030$ $9.97 \times 10^5$ $4.40 \times 10^4$ 0.6 $18.95$ $535$ $24.4$ 2.1 $24.63$ $1550$ $65.1$ 0.6 $18.14$ $758$ $38.0$	58.8	2040		12.4	0.824	3.81	0.011	99.0	0.032
2.1 - $4.58 \times 10^5$ 2.09 × $10^4$ 0.6	19.9	520		0.73	0.124	3.21	0.011	0.25	0.005
0.6 $22.84$ 2.1 $63.36$ $7480$ $322$ 0.6 $24.81$ 2.1 $17.80$ $1770$ $62.4$ 0.6 $22.97$ 2.1 $19.09$ $372$ $13.6$ 0.6 $16.22$ 2.1 $4.34 \times 10^4$ $1.37 \times 10^6$ $5.92 \times 10^4$ 0.6 $18.95$ $550$ $27.1$ 2.1 $1030$ $9.97 \times 10^5$ $4.40 \times 10^4$ 0.6 $18.95$ $535$ $24.4$ 2.1 $24.63$ $1550$ $65.1$ 0.6 $18.14$ $758$ $38.0$	•	4.58 x 10 <sup>5</sup>	7	869	134	707	4.61	217	1.58
0.6 $22.84$ 2.1 $63.36$ $7480$ $322$ 0.6 $24.81$ 2.1 $17.80$ $1770$ $62.4$ 0.6 $22.97$ 2.1 $19.09$ $372$ $13.6$ 0.6 $16.22$ 2.1 $4.34 \times 10^4$ $1.37 \times 10^6$ $5.92 \times 10^4$ 0.6 $5.57$ $550$ $27.1$ 2.1 $1030$ $9.97 \times 10^5$ $4.40 \times 10^4$ 0.6 $18.95$ $535$ $24.4$ 2.1 $24.63$ $1550$ $65.1$ 0.6 $18.14$ $758$ $38.0$									
2.1 $63.36$ $7480$ $322$ 0.6 $24.81$ 2.1 $17.80$ $1770$ $62.4$ 0.6 $22.97$ 2.1 $19.09$ $372$ $13.6$ 0.6 $16.22$ 2.1 $4.34 \times 10^4 1.37 \times 10^6$ $5.92 \times 10^4$ 0.6 $.5.57$ $550$ $27.1$ 2.1 $1030 9.97 \times 10^5$ $4.40 \times 10^4$ 0.6 $18.95$ $535$ $24.4$ 2.1 $24.63$ $1550$ $65.1$ 0.6 $18.14$ $758$ $38.0$	22.84		ſ	•	1	1	1	1	1
0.6 $24.81$ 2.1 $17.80$ $1770$ $62.4$ 0.6 $22.97$ 2.1 $19.09$ $372$ $13.6$ 0.6 $16.22$ 2.1 $4.34 \times 10^4$ $1.37 \times 10^6$ $5.92 \times 10^4$ 0.6 $5.57$ $550$ $27.1$ 2.1 $1030 \ 9.97 \times 10^5$ $4.40 \times 10^4$ 2.1 $24.63$ $1550$ $65.1$ 0.6 $18.14$ $758$ $38.0$	63.36		322	19.1	3.08	7.58	0.067	2.68	0.103
2.1 17.80 1770 62.4 0.6 22.97 2.1 19.09 372 13.6 0.6 $16.22$ 2.1 $4.34 \times 10^4 1.37 \times 10^6$ 5.92 $\times 10^4$ 0.6 $.5.57$ 550 $27.1$ 2.1 $1030 9.97 \times 10^5$ $4.40 \times 10^4$ 0.6 $18.95$ 535 $24.4$ 2.1 $24.63$ 1550 65.1 0.6 $18.14$ 758 38.0	24.81		•		1	1	1	ı	1
0.6 $22.97$ $19.09$ $372$ $13.6$ $0.6$ $16.22$ $ 16.22$ $ 0.6$ $4.34 \times 10^4$ $1.37 \times 10^6$ $5.92 \times 10^4$ $0.6$ $5.57$ $550$ $27.1$ $2.1$ $1030$ $9.97 \times 10^5$ $4.40 \times 10^4$ $0.6$ $18.95$ $535$ $24.4$ $2.1$ $24.63$ $1550$ $65.1$ $0.6$ $18.14$ $758$ $38.0$	17.80		62.4	6.57	0.550	3.61	0.011	96.0	0.045
2.1 $19.09$ 372 $13.6$ 0.6 $16.22$ 2.1 $4.34 \times 10^4 1.37 \times 10^6$ $5.92 \times 10^4$ 0.6 $5.57$ $550$ $27.1$ 2.1 $1030 9.97 \times 10^5$ $4.40 \times 10^4$ 0.6 $18.95$ $535$ $24.4$ 2.1 $24.63$ $1550$ $65.1$ 0.6 $18.14$ $758$ $38.0$	22.97		ı	•		1	1	1	1
0.6 $16.22$ $\frac{16.22}{2.1}$ $4.34 \times 10^4 1.37 \times 10^6$ $5.92 \times 10^4$ $0.6$ $5.57$ $550$ $27.1$ $2.1$ $1030 9.97 \times 10^5$ $4.40 \times 10^4$ $0.6$ $18.95$ $535$ $24.4$ $2.1$ $24.63$ $1550$ $65.1$ $0.6$ $18.14$ $758$ $38.0$	19.09		13.6	0.73	< 0.124	0.602	0.022	0.04	< 0.005
2.1 $4.34 \times 10^4 1.37 \times 10^6$ 5.92 × $10^4$ 0.6 $5.57$ 550 $27.1$ 2.1 $1030 9.97 \times 10^5$ $4.40 \times 10^4$ 0.6 $18.95$ 535 $24.4$ 2.1 $24.63$ 1550 $65.1$ 0.6 $18.14$ 758 $38.0$	16.22		1	1	1	1	1	1	•
0.6       .5.57       550       27.1         2.1       1030 9.97 x 10 <sup>5</sup> 4.40 x 10 <sup>4</sup> 0.6       18.95       535       24.4         2.1       24.63       1550       65.1         0.6       18.14       758       38.0	4 × 104	.37 x	$5.92 \times 10^4$	2110	426	1218	5.91	663	5.72
2.1 1030 9.97 x 10 <sup>5</sup> 4.40 x 10 <sup>4</sup> 0.6 18.95 535 24.4 2.1 24.63 1550 65.1 0.6 18.14 758 38.0	.5.57		27.1	5.11	0.275	2.61	> 0.004	0.14	0.019
0.6     18.95     535     24.4       2.1     24.63     1550     65.1       0.6     18.14     758     38.0	1030	.97	4.40 x 10 <sup>4</sup>	1240	287	847	3.27	419	3.44
2.1     24.63     1550     65.1       0.6     18.14     758     38.0	18.95		24.4	1.46	0.550	2.81	0.011	0.25	0.019
0.6 18.14 758 38.0	24.63		65.1	6.57	0.550	3.81	0.045	0.55	0.032
	18.14		38.0	8.04	0.275	3.21	0.022	0.25	0.019
2.1 24.98 505 16.3	24.98		16.3	2.92	0.275	1.20	0.011	0.14	0.019

(continued)

Table 28 (continued)

	Depth	Suspended								
Station	(B)	Solids*	Fe**	Mn**	Zn**	Cu**	Cr**	** PO	Pb**	Hg**
A59	9.0	16.49	193	8.13	2.19	0.824	< 0.176	< 0.004	0.14	< 0.005
A59	2.1	17.30	803	27.1	32.1	0.550	2.21	0.067	0.35	0.019
A60	9.0	16.8	535	29.8	8.77	0.550	3.21	0.056	0.55	0.032
A60	2.1	44.5	3740	170	22.2	2.59	5.85	2.89	1.3	0.069
A61	9.0	14.7	372	27.1	5.11	0.275	3.21	0.022	0.14	0.005
A61	2.1	17.71	1740	70.5	5.11	5.22	3.81	< 0.004	99.0	0.045
A62	9.0	21.7	1	1	1	ı	•	1		
A62	2.1	21.2	743	27.1	27.8	0.824	3.61	0.033	0.25	0.058
A63	9.0	19.9	557	33.1	2.12	0.124	0.947	0.020	0.29	0.014
A63	2.1	21.4	614	25.6	4.77	0.248	1.14	0.012	0.29	0.041
A64	9.0	19.0	591	43.7	3.71	0.248	0.947	0.012	0.44	0.014
<b>494</b>	2.1	2.19 x 10 <sup>4</sup>	8.77 x 10 <sup>4</sup>	3570	164	32.3	92.3	0.260	20.3	0.339
A65	9.0	16.1	379	28.6	2.65	0.497	0.568	0.012	0.07	0.034
A65	2.1	17.4	643	30.1	2.65	< 0.124	0.947	0.028	0.14	0.020
99Y	9.0	20.0	413	30.1	2.65	< 0.124	0.947	0.020	0.29	0.020
99Y	2.1	14.1	528	30.0	1.06	< 0.124	0.947	0.012	0.29	0.027
A67	9.0	15.9	384	31.6	3.18	0.124	0.758	0.012	0.87	0.020
A67	2.1	20.5	2010	57.2	0.530	< 0.124	0.473	0.013	0.36	0.014
89Y	9.0	18.0	579	34.6	3.18	0.124	0.947	0.049	0.51	0.027
A68	2.1	17.4	2780	99.2	5.42	0.706	2.26	0.076	0.82	0.077
				(continued	(pen					

Table 28 (continued)

Station	Depth (m)	Suspended Solids*	± 4 €	Mn**	20**	C11**	***	C3**	Ph**	Ho**
A69	(a)	17.6	4320	146	5.30	0.869		0.031	1.02	0.047
A69	0.6(b)	17.6	4320	151	7.42	1.12	3.60	0.040	0.87	0.047
99A	0.6(c)	17.6	4180	151	6.36	1.37		0.336	0.87	0.047
99A	0.6(d)	17.6	4460	151	7.95	1.24		0.013	0.87	0.077
A69	2.1(a)	1577	381	27.1	3.71	0.248		0.063	0.63	0.020
A69	2.1(b)	1577	419	30.1	1.06	0.124		0.040	0.29	0.014
469	2.1(c)	1577	425	30.1	2.65	0.124		0.049	0.14	0.014
469	2.1(d)	1577	430	31.6	2.12	0.124		0.058	0.14	0.020
A70	9.0	19.6	855	48.2	3.18	1.24		0.049	0.44	0.020
A70	2.1	-	2.01 × 10 <sup>4</sup>	867	82.7	7.64		0.850	7.04	0.115
A71	9.0	21.7	390	25.6	2.65	0.124		0.063	0.07	0.014
A71	2.1	5.42 x 104	1.35 x 10 <sup>6</sup>	2640	1880	373		380	626	4.24
A72	9.0	1	ı	1	•			1	1	
A72	2.1	1	ı	ı	•			•		
A73	9.0	14.9	390	22.6	3.18	0.497		0.040	0.04	0.027
A73		6.30 x 10 <sup>4</sup>	2.52 x 10 <sup>4</sup>	1240	44.2	10.1		0.246	67.6	0.248
A74	0.3	20.7	775	37.6	4.24	0.248		0.036	94.0	0.014
A74	1.8	111.1	1.32 x 10 <sup>4</sup>	049	38.9	6.77		0.276	5.72	0.134
A75	0.3	•	2450	91.8	4.77	0.745		0.013	0.73	0.014
A75	1.8	156.4	3.60 x 10 <sup>4</sup>	1390	50.4	9.94		0.123	10.3	0.153
				(continued	(pen					

		Depth	Suspended								
S	ation	(II)	Solids*	Fe**	Mn**	Zu**		Cr**	**PO	Pb**	Hg**
	A76	0.3	13.3	522	19.6	4.24		0.325	0.103	0.50	0.027
	A76	1.8	636.5	1.46 x 10 <sup>4</sup>	554	23.0		13.0	0.276	5.03	0.158
	A77	0.3	12.9	350	18.1	1.06		< 0.176	0.094	0.34	0.027
	A77	1.8	17.4	4320	188	10.6		3.57	0.085	1.68	0.054
	A78	0.3	12.8	396	16.6	1.59		0.217	0.058	0.59	< 0.005
	A78	1.8	71.2	3060	124	6.63	1.24	1.62	0.039	1.26	1.26 0.051
	479	0.3	48.0	1870	75.3	4.77		1.52	0.112	0.92	0.041
	479	1.9	551.5	1.10 x 10 <sup>4</sup>	767	16.8		7.58	0.276	4.19	0.068
100	A80	0.3	14.6	551	22.6	5.30		0.217	0.004	0.34	0.023
	A80	1.8	829.4	4.28 x 10 <sup>4</sup>	2100	6.89		35.7	0.302	17.4	0.286

\* Values in mg/& (ppm) \*\* Values in µg/& (ppb)

(Table 23). Similarly, the mean concentration of dissolved Mn decreased from 124 ppb to about 69 ppb\*. No substantial changes in concentrations of Cr and Cu were observed in Apalachicola Bay except in the immediate vicinity of the discharge.

Discussion. Comparison of samples collected from plumes with those taken in the far-field in Corpus Christi Bay and in Atchafalaya Bay showed no apparent differences in concentrations of dissolved metals. Relatively high ambient concentrations of Zn, Cu, Cd, and Pb in Corpus Christi Bay may be caused by local pollutant inputs to the Bay from Corpus Christi Harbor. Dissolved Zn and Cd concentrations in late summer (sampling period for this study) of up to 480 ppb and 78 ppb, respectively, have been documented by Holmes, et al. 2 in the inner harbor. Their reported values in the Bay are comparable to those determined for this study. No usable data were available for the Atchafalaya Bay site to permit comparison of dissolved metals concentrations observed in the suspended solids plume with those normally present in the local waters. However, the presence throughout our sampling area of very low concentrations (usually below the detection limit) for dissolved Zn, Cu, Cr, Cd, and Pb precludes any substantial release of these metals during dredging and disposal at Atchafalaya Bay.

Decreased levels of dissolved Fe and Mn in the discharge plume in Apalachicola Bay compared to their concentrations prior to dredging may be the result of scavenging by suspended matter and freshly formed Fe and Mn hydrous oxides. 12,13,14,15,16,17,18 Although scavenging by suspended matter occurs for the other dissolved metals as well 12,16 concentration reductions were not observed, possibly because these changes were within the sensitivity of the analytical methods.

Interstitial waters and elutriate tests. Results of elutriate tests (Tables 20A) were usually equivocal, however Mn release was indicated by the test results for all three sites.

For Apalachicola Bay, all elutriate tests indicated release of dissolved Mn and uptake of dissolved Fe and Cu by the suspended solids.

<sup>\*</sup> Significant at the 90% level.

AD-A058 507

STATE UNIV OF NEW YORK AT STONY BROOK MARINE SCIENCES--ETC F/6 13/2
FIELD INVESTIGATIONS OF THE NATURE, DEGREE, AND EXTENT OF TURBI--ETC(U)
JUL 78 J R SCHUBEL, H H CARTER, R E WILSON
WES-TR-D-78-30

NL

3 0F4

8 0F4

8 0F4

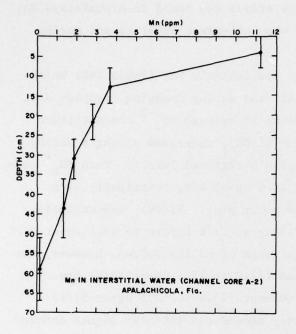
9 0

0

Sampling in the plume (Samples A-41 to A-80, Table 23) however, showed that mean Fe and Mn concentrations decreased relative to background levels (Samples A-1 to A-11). Except for a few elevated concentrations near the discharge, no substantial change in dissolved Cu concentrations was detected in Apalachicola Bay.

The elutriate test failed to predict metal behavior during dredging and disposal because it does not simulate the physico-chemical milieu of the disposal site. Disparity in dilution factor (water:sediment) and oxidation-reduction status between test and field are probably largely responsible for observed differences in the behavior of a given metal. Except where suspended sediment is particularly abundant, the dilution factor (water:sediment) in the discharge plume will be orders of magnitude greater than that in the elutriate test. Therefore, release of metals in sediment interstitial waters and from exchangeable sediment fractions, which may be detected by the elutriate test, can be masked at the disposal site by dilution and/or outweighed by removal processes such as scavenging of dissolved metals by suspended particles. Further, redox potential is not controlled during the elutriate test and must vary widely in the discharge plume during disposal of reducing sediments. Variations in redox potential can have an appreciable effect on release or uptake of dissolved metals by particles in sediment-water mixtures.

Although Fe and Mn followed similar trends in both the particulate and dissolved phases, some differences in their behavior were observed. Elutriate test results and dissolved metals analyses of plume samples associated with high suspended solids concentrations (> 10<sup>3</sup> mg/l) indicate somewhat divergent behavior of Fe and Mn. In addition, interstitial Fe and Mn at Apalachicola show different trends with depth in the sediment (Figure 88). Fe decreases and then increases with greater depth in the sediment while Mn concentrations continually decrease with depth. Different controls of Fe and Mn in interstitial waters of reducing sediments have been proposed in the literature. Berner<sup>19</sup> described sulfide phases as controlling Fe<sup>+2</sup> concentrations in interstitial waters of anoxic sediments. Holdren, Bricker, and Matisoff<sup>20</sup> cited carbonate (rhodocrosite) control of Mn<sup>+2</sup> concentration in pore waters under similar



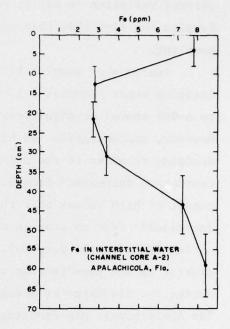


Figure 88. Fe and Mn in interstitial water, Apalachicola Bay.

conditions. These differences in behavior may be attributable to the accelerated oxidation of  ${\rm Fe}^{+2}\,{}_{1}{}^{4}$  and the greater stability of iron sulfides relative to  ${\rm Mn}^{+2}$  and  ${\rm MnCO}_3/{\rm MnS}$ , respectively.

### Dissolved nutrients

 $\frac{\text{Results.}}{3}$  No plumes of any of the nutrient species studied  $[\text{NH}_4^+, \text{PO}_4^{-3}, \text{Si(OH)}_4, \text{NO}_2^- + \text{NO}_3^-]$  were observed at any of the three disposal sites.

Orthophosphate  $(PO_4^{-3})$  concentrations were low, averaging 1 µg-at P/ $\ell$  or less for all three sites (Table 24). Dissolved ammonia species  $(NH_4^{-1})$  were at their greatest concentration in Atchafalaya Bay, followed by Apalachicola Bay and Corpus Christi Bay. Average concentrations were 23.8, 14.6, and 8.1 µg-at N/ $\ell$ , respectively. Average reactive silica  $[Si(OH_4)]$  concentrations in and around the plume exhibited the opposite order by site: Corpus Christi (51.6 µg-at Si/ $\ell$ ) > Apalachicola (43.1 µg-at Si/ $\ell$ ) > Atchafalaya (21.1 µg-at Si/ $\ell$ ). The latter is the same order as that for clay content of channel sediment (Table 21). The largest

percent variation in silica concentrations was found in Atchafalaya Bay despite the fact that this system was well-mixed prior to and during sampling.

Analysis of samples taken in Apalachicola Bay (Table 24C) before dredging began (Samples A-1 to A-11) and during dredging (Samples A-41 to A-80) showed no significant change in average  $PO_4^{-3}$  concentration. However, concentrations of  $NH_4^+$  and  $Si(OH)_4$  increased slightly during dredging relative to the pre-dredging background levels. Mean  $NH_4^+$  concentration increased\* from 9.5 to 14.6 µg-at N/ $\ell$ , principally as a result of high values near the discharge pipe.  $Si(OH)_4$  concentrations increased\*\* from an average of 37.5 µg-at  $Si/\ell$  before to 43.1 µg-at  $Si/\ell$  during dredging and disposal. The range of silica values, however, was greater in the pre-dredging samples (13.6 to 73.1 µg-at  $Si/\ell$ ) than during the discharge of dredged sediment (23.4 to 52.5 µg-at  $Si/\ell$ ). The Apalachicola pre-dredging survey showed consistently higher concentrations of dissolved silica at depth than near the surface. No such vertical gradient existed for silica in samples taken in the vicinity of the discharge during dredging and disposal.

Discussion. Although no well-defined plumes of dissolved nutrients were observed at any of the sites, comparison of mean concentrations of  $\mathrm{NH_4}^+$  and  $\mathrm{Si(OH)_4}$  before dredging began (Samples A-1 to A-11, Table 24C) with those in and around the discharge plume during dredging (Samples A-41 to A-80) at Apalachicola suggests that these nutrients were released to some extent during disposal. The predominant source of these nutrients was probably the interstitial waters. Pore water concentrations of  $\mathrm{NH_4}^+$  and  $\mathrm{Si(OH)_4}$  (Table 19) were greatly elevated over those present in the water column (Table 24).

The smaller range of Si(OH)<sub>4</sub> values at Apalachicola during disposal relative to the pre-dredging concentration range seems to indicate an equilibrium between silica associated with the suspended particles and dissolved silica present in the discharge plume.

\*\* Significant at the 90% level.

<sup>\*</sup> The increase was not statistically significant because of the large variation in sample values both before and during dredging (standard deviations were 8.26 and 25.7, respectively).

Although high concentrations of orthophosphate were found in interstitial waters of channel sediments (Table 19) no observable increase in concentrations of this nutrient was noted during dredging in Apalachicola Bay. This is probably the combined result of dilution by receiving waters, adsorption of  $PO_4^{-3}$  by suspended solids, 21 and precipitation with ferric iron in the water column. 22,23 Uptake of  $PO_4^{-3}$  by phytoplankton may also have had a significant effect.

Interstitial waters and elutriate tests. All elutriate tests (Table 20) indicated the release of NH<sub>4</sub><sup>+</sup> and Si(OH)<sub>4</sub> during mixing of sediments with disposal site water. These results are consistent with the increased levels of these nutrients in Apalachicola Bay samples taken during dredging as compared to pre-dredging samples. Since estuarine sediments and interstitial waters are generally rich in these constituents due to bacterial decomposition of organic matter (e.g. Table 19), it is expected that similar results would be obtained for most estuarine sediments.

The NH<sub>4</sub><sup>+</sup> and Si(OH)<sub>4</sub> concentrations measured in elutriates (Table 20) were variable and dependent upon the depth in the core from which the sediment was taken. This variation generally followed the gradients of these nutrients with sediment depth for a given site (Table 19). Since the elutriate test procedure<sup>24</sup> does not stipulate the depth at which a sediment sample should be collected, elutriate NH<sub>4</sub><sup>+</sup> and Si(OH)<sub>4</sub> concentrations will be a function of the investigator's sediment sampling method.

The elutriate tests and our observations indicate that dissolved orthophosphate, which is also usually present in relatively high concentration in interstitial waters of estuarine sediments (e.g. Table 19), is not significantly released to the waters at the disposal site. This is probably due to adsorption/coprecipitation reactions with suspended particles and ferric iron.<sup>25,26</sup>

#### Conclusions

- 1. No plumes with excess concentrations of dissolved metals were observed at any of the three sites.
- Dissolved metals concentrations in water samples obtained during dredging were generally comparable to available data

for normal conditions in Corpus Christi Bay and with results of surveys performed before dredging began in Apalachicola Bay. No data were available to permit comparison of metals concentrations observed during disposal operations at Atchafalaya Bay with those normally occurring in these waters.

- In Apalachicola Bay the mean levels of dissolved Fe and Mn were lower in the outfall plume than before disposal operations began.
- 4. Although field results of this study indicate generally similar behavior of Mn and Fe, apparent differences in the chemistries of these metals were indicated by elutriate tests, sediment interstitial waters, and samples from the discharge plume in which suspended sediment concentrations were particularly high (>  $10^3 \text{ mg/l}$ ).
- 5. Dissolved ammonia and silica species were released to a limited extent during disposal of dredged material while dissolved orthophosphate levels were unaffected.
- 6. The elutriate test is probably of limited utility in evaluating possible release of dissolved metals and nutrients from dredged sediments during open-water pipeline disposal operations. The test yields highly variable results and, for some constituents, results that are contrary to field observations.

#### Particle-Associated Metals

#### Methods

The research vessel followed ladder-type cruise tracks across plumes generated by the pipeline discharge of the hydraulic dredge. Continuous optical observations with nephelometers were converted to suspended solids concentrations and contoured. Paired water samples were periodically withdrawn from the system for analyses of metals and suspended solids. The time lag between samples averaged about fifteen seconds.

Samples of suspended solids for analyses of particle-associated metals were obtained by immediate filtration of water samples through glass fiber filters. Particle-associated metals concentrations were determined from the volume filtered as  $\mu g/\ell$ . The samples were analyzed for Fe, Mn, Zn, Cu, Cr, Cd, Pb, and Hg by atomic absorption spectrometry following acid digestion.

Water samples for suspended solids determinations were later foltered through membrane filters and weighed. To obtain precise Fe: suspended solids ratios (µg Fe/mg suspended sediment) necessary for development of the model described later, several of these samples were analyzed by atomic absorption for Fe. Fe:suspended solids ratios could not be determined from particle-associated metals samples with sufficient precision for use in the model since these samples were not weighed. Suspended solids samples for model calculations were selected from a single plume realization over a wide range of concentrations at each site. Concentrations of the other metals could not be determined on these samples because of contamination associated with the sampling system.

At Corpus Christi and Apalachicola Bays sediment samples from the channels were also collected and analyzed for several metals by atomic absorption spectrometry. Results are reported as µg metal/mg or g dry sediment. The procedures are described in detail in Appendix D. Results

Of the three sites Corpus Christi has significantly higher levels ( $\mu g$  metal/g suspended solids\*) of Zn, Cu, Cd, and Hg on suspended sediment particles in the disposal plume (Table 25). Comparison of Corpus Christi (Table 26), Atchafalaya (Table 27) and Apalachicola (Table 28) particle-associated metals ( $\mu g/k$ ) and suspended sediment (m g/k) concentrations in and around the dredge discharge plume shows that samples having the greatest concentrations of suspended solids also had the highest concentrations ( $\mu g/k$ ) of particle-associated metals regardless of site or sample position in the plume. Thus it appears, as one would expect, that variations in the concentration of suspended solids is the dominant control on the quantity of particle-associated metals in a given volume of water.

Examination of Figures 89, 90, 91 indicates general agreement between suspended solids concentrations determined gravimetrically and

<sup>\*</sup> Since particle-associated metals and suspended sediment samples were not taken at precisely the same time, µg metal/g dry suspended sediment values were generated by taking the geometric mean of metal/ suspended sediment concentration quotients for all samples.

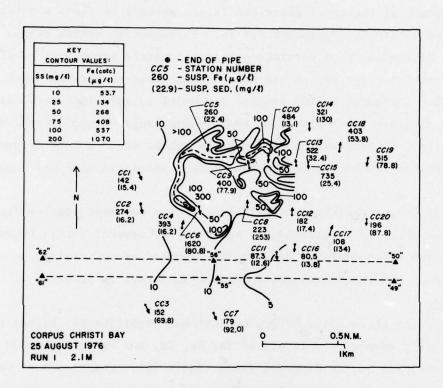


Figure 89. Comparison of turbidity plumes measured optically with concentrations of particle-associated Fe, Corpus Christi Bay.

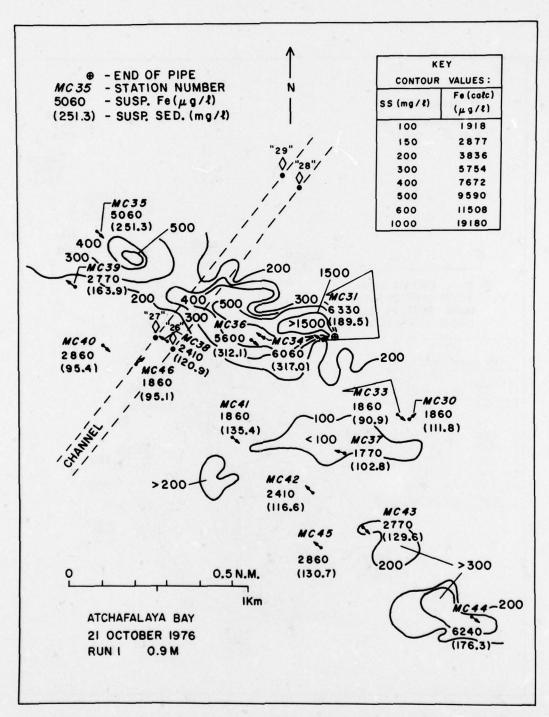


Figure 90a. Comparison of turbidity plumes measured optically with concentrations of particle-associated Fe, Atchafalaya Bay.

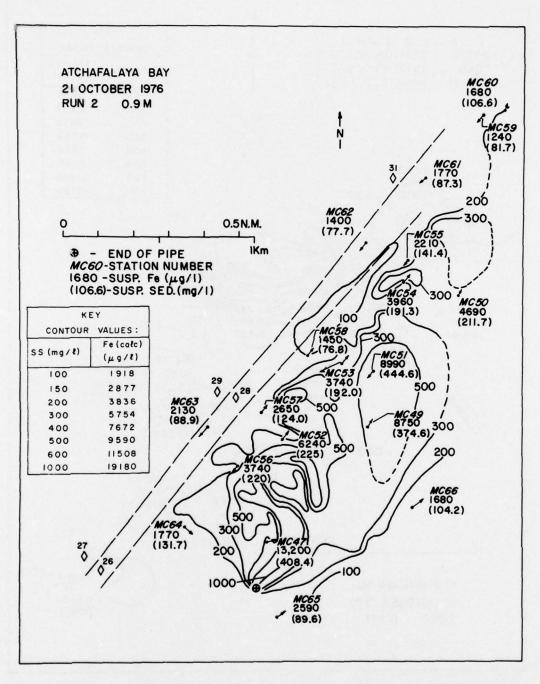


Figure 90b. Comparison of turbidity plumes measured optically with concentrations of particle-associated Fe, Atchafalaya Bay.

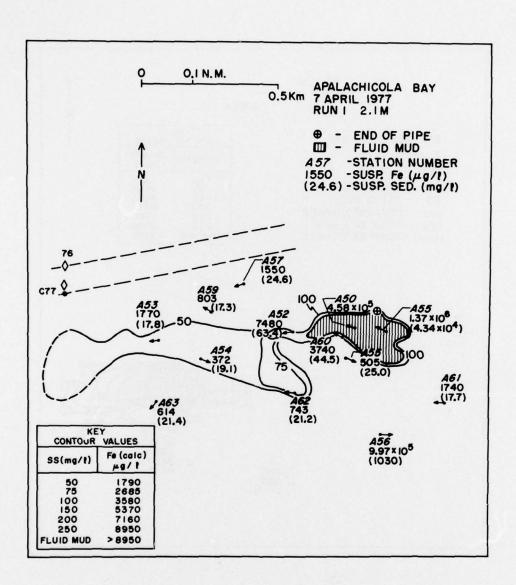


Figure 91a. Comparison of turbidity plumes measured optically with concentrations of particle-associated Fe, Apalachicola Bay.

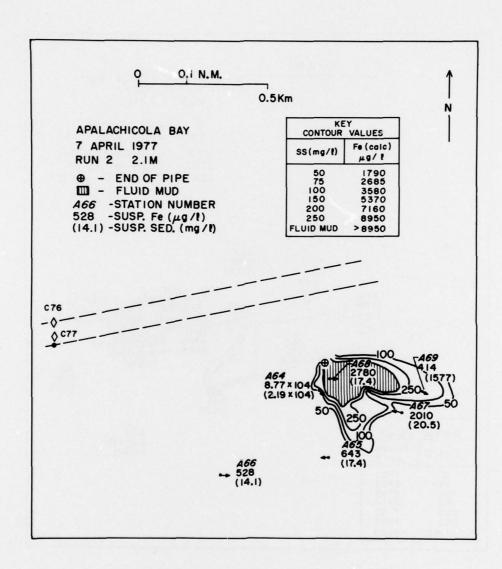


Figure 91b. Comparison of turbidity plumes measured optically with concentrations of particle-associated Fe, Apalachicola Bay.

those determined from nephelometry. Therefore, since the Fe:suspended sediment ratio for a given site and depth is relatively constant (coefficient of variation  $\leq$  about 10%, Table 29) optical data can be used to satisfactorily predict particle-associated Fe concentrations, as well as those of other particle constituents that behave similarly. These should include the other metals: Mn, Zn, Cu, Cr, Cd, Pb and Hg. The control of particle-associated metals concentrations ( $\mu g/\lambda$ ) by suspended solids abundance was used as the basis for the model described later.

Comparison of bulk metal analyses of channel sediment ( $\mu$ g metal/g sediment) and particle-associated metal data ( $\mu$ g metal/g suspended solids) from the discharge plume (Table 25) shows that for each site the corresponding metal values differ significantly and that no consistent relationships exist between the two groups of data.

These differences may be primarily attributable to two factors:

- Differences in composition between the natural background population of suspended particles and those particles introduced by dredging.
- 2. Differences in composition that result from particle size fractionation produced by settling.

Though the inorganic particles are probably of similar source and chemistry originally, compositional dissimilarity between channel deposits and ambient suspended particles in the water column may result from their divergent sedimentary histories. This effect will be most pronounced where concentrations of dredge-derived particles are low, i.e. near the edge and outside the plume of excess turbidity.

After discharge from the pipe, the dredged material will be fractionated to some extent by gravitational settling. Fine-grained sediments commonly contain greater quantities of organic matter<sup>27</sup> and trace metals, <sup>28,29,30,31</sup> than coarser materials. Because of their larger surface:volume ratio, smaller particles may during their sedimentary history undergo greater relative adsorption (mass of adsorbed constituent/mass of particle) of metals and organic matter than particles of larger radius. This can result in greater enrichment of the finer sediment fractions in metals and organic matter relative to coarser sediment

Table 29
Particle-Associated Iron on Suspended Solids Samples

	Sample	Depth (m)	Weight Sediment (mg)	Fe (µg/mg)	Coeff. of Variation
Corpus Christi	CC 2	0.6	3.38	4.29	
Bay, TX	CC14	0.6	6.75	5.37	
	CC16	0.6	11.58	5.32	
	CC17	0.6	8.75	4.76	
Mean		0.6		4.94*	10.35
	CC17	2.1	32.35	5.37	
	CC19	2.1	19.61	5.36	
	CC20	2.1	20.23	5.37	
Mean		2.1		5.37*	0.11
Atchafalaya	MC32	0.9	247.2	18.6	
Bay, LA	MC36	0.9	95.11	19.5	
	MC39	0.9	69.71	18.0	
	MC42	0.9	51.18	20.3	
	MC43	0.9	56.83	20.0	
	MC44	0.9	75.15	18.7	
Mean		0.9		19.2*	4.66
Apalachicola	A14	0.9	10.87	38.5	
Bay, FL	A15	0.9	8.83	-	
	A16	0.9	85.23	39.5	
Mean		0.9		39.0*	1.81
	A12	2.4	8.83	34.1	
	A13	2.4	44.47	37.8	
	A14	2.4	3.81	35.2	
	A15	2.4	63.86	35.9	
Mean		2.4		35.8*	4.34

<sup>\*</sup> Fe( $\mu$ g/mg Sediment) values used for calculation of Fe contours

fractions. Because of their lower density, particles composed primarily of organic matter remain suspended longer than inorganic particles of comparable physical size.

It is not possible to quantify the above effects or to generalize their relative significance with the data available for the three sites.

Predictive model for particle—
associated constituents

The objective was to develop a model to predict concentrations of particle-associated constituents in the discharge plume based on suspended solids concentrations and composition. If plume concentrations of particle-associated constituents, particularly heavy metals, could be predicted from a limited number of chemical analyses and inexpensive and easily-made optical measurements of suspended solids levels there would be substantial savings in time and money required for routine monitoring of open-water pipeline disposal operations.

There are three assumptions inherent in the model:

1. The composition of the material at the source, the discharge end of the pipe, is uniform over the lifetime of a given plume (≤ 10<sup>5</sup> seconds). This assumption appears to be justified, particularly with respect to the heavy metals composition of the discharge. In the Yukon and Amazon Rivers, Gibbs³² found that most of the Fe, Mm, Cu, Cr, Co, and Ni were transported in crystalline phases and as adsorbed/coprecipitated coatings of suspended particles. Assuming a relatively constant composition and source of materials discharged annually by rivers and from other suspended sediment inputs to an estuary, one would expect that the resulting estuarine sediments would be relatively homogeneous over limited areas of similar depositional characteristics, such as dredged navigation channels. Where significant local pollutant inputs occur, especially for the less prevalent trace metals, this may not be true.

With the possible exception noted, it is expected that sediment metal concentrations will be relatively uniform, particularly for channel sediments where mixing resulting from repeated dredging, slumping, and resedimentation should result in further homogeneity. Homogenization of channel sediments by the dredge should increase the compositional uniformity of sediments at the discharge source, the end of the pipe, to an even greater degree.

2. The composition of sediments suspended by disposal operations is relatively uniform over the particle size range so that particle size fractionation caused by differential settling rates does not significantly alter the metal:suspended solids ratio at a given depth in the plume. Direct analysis of suspended sediment samples for particle-associated Fe (Table 29) indicates that, for a particular depth in the disposal plume, Fe:suspended solids ratios ( $\mu g/mg$ ) were relatively constant (coefficient of variation  $\leq$  about 10%) and not substantially affected by variations in suspended solids levels. This should be true of any particle-associated constituents that behave similarly to Fe, including the other trace metals studied.

3. No substantial chemical changes occur to the suspended particles during dredging and disposal operations to add or remove measurable quantities of metals or other particle-associated constituents. Any alteration of sediment composition caused by trace metal uptake (precipitation or scavenging), redox effects, or other chemical processes during the relatively brief period of particle suspension by dredging and disposal should be minor since the preponderance of the heavy metals (and other constituents) in a given suspension will be associated with the particulate phase.

Separate samples were collected for determination of particle-associated metals and suspended solids concentrations. The attempt was made to collect these samples simultaneously but this could not be accomplished with precision with the plumbing system. Because of contamination problems only Fe could be determined on those samples collected for determination of suspended solids concentrations. The model was therefore constructed in two steps.

First, the particle-associated Fe concentrations in the plume were predicted from optically determined suspended solids concentrations and Fe:suspended solids ratios derived from Fe analysis of suspended solids samples. Second, the other particle-associated metals (Mn, Zn, Cu, Cr, Cd, Pb, Hg) were predicted from optically-determined suspended solids concentrations and regression equations generated from concentration plots of Fe vs. these metals.

For the model, suspended solids levels were determined optically by nephelometry. Good agreement was found between gravimetric and optical methods of measurement (except at low concentrations of suspended solids outside the plume).

## Predictions of particle-associated iron concentrations

Predicted particle-associated Fe concentrations (Fe<sub>calc</sub>) were calculated from the mean Fe:suspended solids ratios in Table 29 and the equivalent equations given in Table 30. These Fe<sub>calc</sub> concentrations, corresponding to optically determined suspended solids contours are listed on Figures 89, 90, 91. These figures were selected as representative examples. The remainder of the contours developed for this model are included in Appendix D (Figures D-4 through D-11). Directly determined Fe concentrations are plotted on the figures for comparison. Sampling locations are represented by arrows indicating the distance travelled by the research vessel during the modal sampling period (20 seconds).

Results. Examination of Figures 89, 90, 91 indicates that the model is relatively successful for predicting particle-associated Fe within the plume of excess turbidity for all three dredging operations. At near-background particle concentrations the predictions become less accurate, especially in Corpus Christi Bay. However, in Atchafalaya Bay Fe predictions were excellent for all values. Apalachicola Bay model results were generally good except where optically-determined suspended solids contours do not agree with gravimetrically-determined concentrations.

<u>Discussion.</u> Agreement between predicted and measured suspended Fe concentrations were best within the discharge plume where concentrations of excess suspended solids were high. In Atchafalaya and Apalachicola Bays the model also exhibited significant predictive success outside the plume. This was not the case in Corpus Christi Bay.

Compositional differences between dredged materials and the back-ground suspended matter may be a significant factor. River-derived sediment, organic matter, or resuspended bottom sediment may be the major suspended solids source locally. Composition of particles from these sources may differ from particles introduced by dredging and disposal operations. Where suspended solids concentrations are low, concentrations of particle-associated metals may be dominated by back-ground particles which are predominantly organic in origin.

Table 30
Predicted Particle-Associated Metal Concentrations

A. Corpus Christi, Tx (For Use With Figure 89)

	SS (mg/l)	Fe* calc (µg/l)	Mn calc (µg/l)	Zn** calc (µg/l)	Cu calc (µg/l)	Cr calc (µg/l)	Cd** calc (µg/l)	Pb calc (µg/l)	Hg** calc (μg/l)
	10	49.4	0.8		0.04	0.1			
	25	123	6.0		0.8	0.4		0.05	
	50	247	14.9		2.1	0.8		0.20	
0.6 m	75	370	23.7		3.5	1.1		0.35	
	100	494	32.5		4.8	1.5		0.50	
	200	987	67.7		10.1	3.1		1.1	
	10	53.7	1.1		0.1	0.1			
	25	134	6.8		0.9	0.4		0.06	
	50	268	16.4		2.4	0.8		0.23	
2.1 m	75	408	26.4		3.9	1.3		0.40	
	100	537	35.6		5.2	1.7		0.56	
	200	1070	73.6		10.9	3.4		1.2	

Metal	1926. 97 (ASSERTED	Regression Equation	
Mn:	${Fe} =$	14.0 {Mn} + 38.2	0.98
Cu:	${Fe} =$	93.53{Cu} + 46.0	0.52
Cr:	${Fe} =$	313{Cr} + 11.2	0.58
Pb:	${Fe} =$	820{Pb} + 82.0	0.48
Fe*(2):	${Fe(\mu g)} =$	4.94{suspended solids (mg)}	
Fe* <sub>(2)</sub> : Fe* <sub>(7)</sub> :	${Fe(\mu g)} =$	5.37{suspended solids (mg)}	

<sup>\*</sup> Derived from iron analysis of suspended solids (Table 29).

Equations used for calculation of predicted metal values derived from correlation plots of Fe vs. metal (Mn, Zn, Cu, Cr, Cd, Pb, Hg).

<sup>\*\*</sup> Zn, Hg, and Cd did not correlate with Fe. Large variation of Zn and Cd in Corpus Christi Bay sediments has been documented by Holmes et al.<sup>2</sup> Hg may be similarly variable.

Table 30 (continued)

#### B. Atchafalaya, LA (For Use With Figure 90)

									and the second second
		Fe*	Mn	Zn	Cu	Cr	Cď	Pb	Hg
	SS	calc	calc	calc	calc	calc	calc	calc	calc
	(mg/l)	$(\mu g/l)$	(μg/l)	(μg/l)	(µg/l)	(µg/l)	(μg/l)	(µg/l)	(µg/l)
	100	1920	169	<	2.17	1.73		0.01	6×10 <sup>-3</sup>
	200	3840	275	31.4	6.31	4.51		0.40	0.06
	300	5750	379	63.0	10.4	7.26		0.79	0.11
0.9 m	400	7650	484	94.8	14.6	10.0		1.18	0.16
	500	9590	` 589	127	18.7	12.8		1.56	0.21
	600	11500	694	158	22.8	15.6		1.95	0.26
	1000	19200	1120	286	39.4	26.7		3.51	0.47
<u>Metal</u>			]	Regress	ion Equ	ation**	6813 2181		r**
Mn:			${Fe} =$	18.26	(Mn) - :	1173			0.98
Zn:			${Fe} =$	60.4 {	$\{Z_n\}$ +	1945			0.45
Cu:			${Fe} =$	463.8 {	(Cu) +	912			0.85
Cr:			${Fe} =$	693{	(Cr) +	718			0.55
Pb:			${Fe} =$	4935{	Pb} + :	1867			0.50
Hg:			${Fe} =$	37527{	Hg} + 3	1699			0.28
Fe*:		{Fe	$(\mu g)$ =	19.18{	Suspend	ded solid	s (mg)]		

<sup>\*</sup> Derived from iron analysis of suspended solids (Table 29).

<sup>\*\*</sup> Equations used for calculation of predicted metal values derived from correlation plots of Fe vs. metal (Mn, Zn, Cu, Cr, Cd, Pb, Hg). Cd did not correlate with Fe.

Table 30 (concluded)

C. Apalachicola, FL
(For Use With Figure 91)

		Fe*	Mn	Zn	Cu	Cr	Cd**	Pb	Hg
	SS	calc	calc	calc	calc	calc	calc	calc	calc
	(mg/l)	(μg/l)	<u>(μg/l)</u>	(µg/l)	(μg/l)	(μg/l)	(µg/l)	(μg/l)	(µg/l)
	50	1950	80.6	7.3	1.0	2.8		0.8	0.03
	75	2925	125	8.8	1.3	3.6		1.2	0.04
0.3,	100	3900	169	10.3	1.5	4.5		1.6	0.04
0.6 m		5850	258	13.3	2.1	6.2		2.3	0.06
	200	7800	346	16.3	2.7	8.0		3.0	0.07
	250	9750	435	19.4	3.2	9.7		3.7	0.08
	50	1790	73.3	7.0	0.9	2.6		0.8	0.03
	75	2685	114	8.4	1.2	3.4		1.1	0.04
1.8,	100	3580	155	9.8	1.4	4.2		1.4	0.04
2.1 m		5370	236	12.6	2.0	5.8		2.1	0.05
	200	7160	317	15.4	2.5	7.4		2.8	0.06
	250	8950	398	18.1	3.0	9.0		3.4	0.08
F	luid Mud	8950	398	18.1	3.0	9.0		3.4	0.08
Metal Regression Equation †									
							, ,		
Mn:				Fe} =	22.02{Mr		4./		0.98
Zn:			{1	Fe =	653.7 {Zr	1) - 2	722		0.92
Cu:			{1	Fe =	3469{ Cu	1) - 1	443		0.94
Cr:			{1	Fe} =	1123{ Cr	} - 1	142		0.96
Pb:			{1	Fe} =	2706{ Pt	) - 32	6.3		0.96
Hg:			{1	Fe} =	157200{ Hg	g} - 3	013		0.85
	F	e*(1',2'	):{Fe(µg	g)} =	39.0 {Su	spende	d solids	(mg)}	

 $Fe*(6',7'):{Fe(\mu g)} = 35.8 {Suspended solids (mg)}$ 

<sup>\*</sup> Derived from iron analysis of suspended solids samples (Table 28).

<sup>\*\*</sup> Cd did not correlate with Fe.

<sup>†</sup> Equations used for calculation of predicted metal values. Derived from correlation plots of Fe vs. metals (Mn, Zn, Cu, Cr, Cd, Pb, Hg).

Background samples (< 25 mg/l) in Apalachicola Bay contained a substantially greater percentage of organic matter than samples from the plume (> 25 mg/l) which are characteristically low and relatively constant in combustible organics (see Figure 92). This parameter was not determined on suspended particles in Corpus Christi Bay, but similar results would be expected since phytoplankton biomass should be relatively high during August in this area. When suspended sediment levels fell

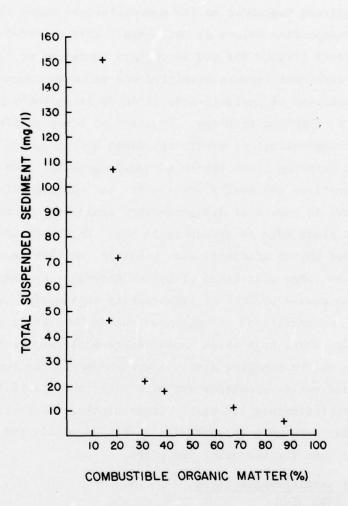


Figure 92. Concentration of total suspended solids versus combustible organic matter, Apalachicola Bay.

below 25 mg/ $\ell$  at a given depth in Apalachicola Bay the concentrations of Fe ( $\mu$ g/mg suspended sediment) were slightly lower than at higher concentrations of suspended sediment (Table 29). A similar relationship was observed in Corpus Christi Bay. Although these small differences may explain some of the difference between predicted and observed Fe values at these two sites, they are not sufficient to account for all of the discrepancies.

Examination of Figures 89 and 90 for agreement of measured and optically predicted suspended solids concentrations shows that in many cases the corresponding values do not agree. This occurred frequently at Corpus Christi (Figure 89) and in certain instances at Apalachicola. This lack of agreement between predicted and measured concentrations of suspended solids and of particle-associated Fe is probably largely attributable to sampling problems. In areas of steep gradients in suspended solids concentrations within the plume and along its edges the difference in sampling times (10-20 seconds) for water samples and optical observations can easily account for the observed discrepancies. Large gradients in levels of dredge-derived sediments occurred within and along the plume edge in Apalachicola Bay. In Corpus Christi Bay steep suspended solids gradients also resulted, in this case from local resuspension of large quantities of bottom material by shrimp trawlers.

Problems caused by lack of simultaneity in sampling, steep gradients and low concentrations of suspended solids were least pronounced in Atchafalaya Bay where high winds caused large-scale sediment resuspension over the entire sampling area. A well-mixed system resulted with small suspended solids gradients and high background particle concentrations of approximately 100~mg/l. Consequently, the predictions for Atchafalaya Bay were more accurate for suspended solids and particle-associated Fe than for the other two sites.

# Prediction of particle-associated metals other than iron

Since the model adequately predicts particle-associated Fe concentrations in the plume, the feasibility of extension of the model to

predicting concentrations of other particle-associated metals was evaluated. The data treatment which follows is based on the assumption that, due to their chemical similarity, concentrations of the metals studied (Fe, Mn, Zn, Cu, Cr, Cd, Pb, and Hg) are linearly related at a particular depth on particles suspended by dredging and disposal.

Linear least-square regression equations were obtained from individual correlation plots for particle-associated Fe versus Mn, Zn, Cu, Cr, Cd, Pb and Hg for each site. The plots were constructed using concentrations of particle-associated metals in samples collected within the plume where, by definition, suspended solids concentrations were above background. Background particle concentrations were estimated to be:

- 1. 10 mg/l for Corpus Christi Bay
- 2. 100 mg/l for Atchafalaya Bay
- 3. 25 mg/l for Apalachicola Bay.

Samples whose suspended solids concentrations fell below these values were excluded from the analysis. These plots are presented in Figures 93, 94, 95.

Regression equations were used to calculate predicted concentrations of Mn, Zn, Cu, Cr, Cd, Pb, and Hg corresponding to contour values of Fe (Fe calc) predicted earlier. For example:

$$\left[ \text{Fe}_{\text{calc}} \left( \mu g/\ell \right) \right] = m \left[ Mn_{\text{calc}} \left( \mu g/\ell \right) \right] + b$$
 (31)

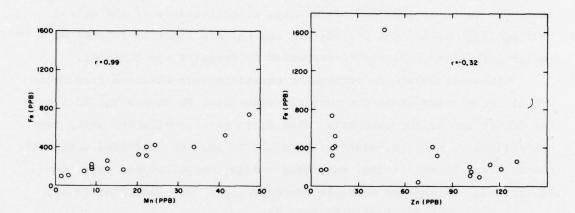
solving for Mn:

$$\left[\operatorname{Mn}_{\operatorname{calc}}(\mu g/\ell)\right] = \frac{\left[\operatorname{Fe}_{\operatorname{calc}}(\mu g/\ell)\right]}{m} - b \tag{32}$$

where m = slope

b = y-intercept

These predicted concentrations are listed in Table 30A, B, and C along with the regression equations used in the calculations. Also included in these tables are the coefficients of determination for each Fe vs. metal relationship. The coefficient of determination, r<sup>2</sup>, is



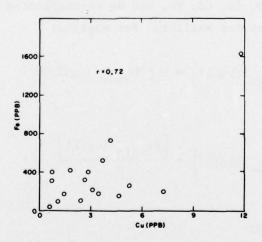


Figure 93. Correlations among particle-associated Fe and other metals on plume suspended solids, Corpus Christi Bay.

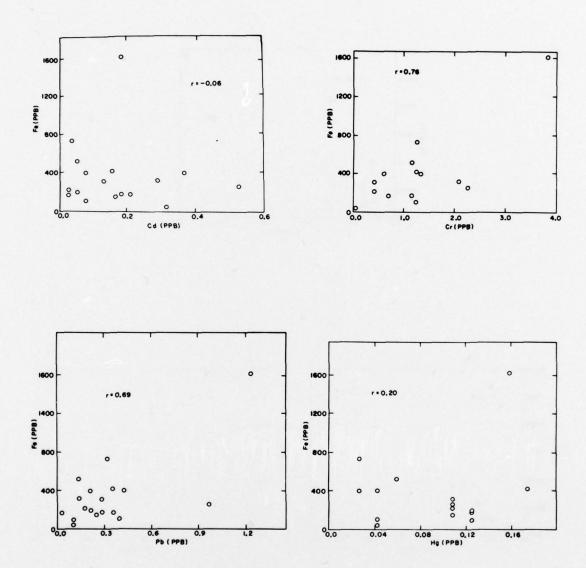
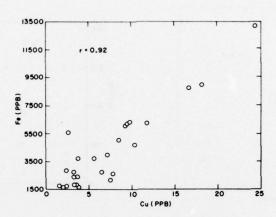


Figure 93. Correlations among particle-associated Fe and other metals on plume suspended solids, Corpus Christi Bay.



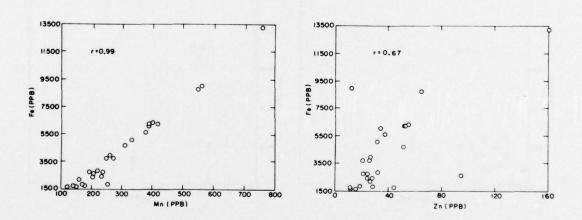
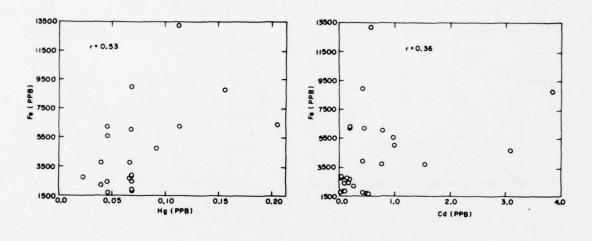


Figure 94. Correlations among particle-associated Fe and other metals on plume suspended solids, Atchafalaya Bay.



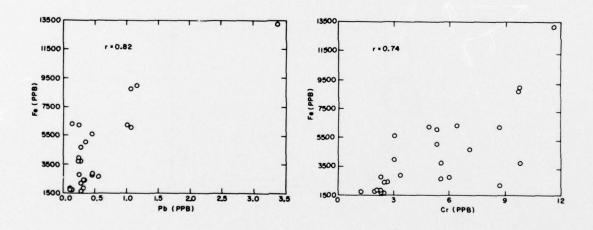
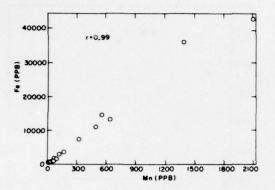
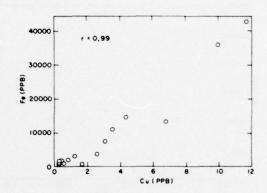


Figure 94. Correlations among particle-associated Fe and other metals on plume suspended solids, Atchafalaya Bay.





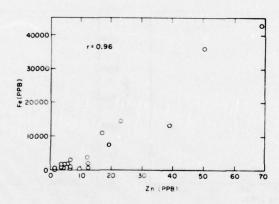
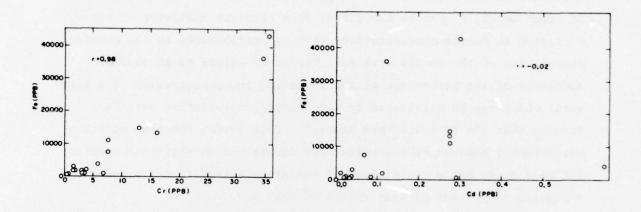


Figure 95. Correlations among particle-associated Fe and other metals on plume suspended solids, Apalachicola Bay.



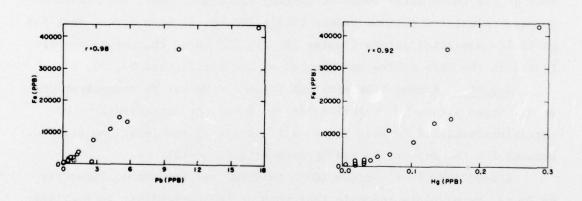


Figure 95. Correlations among particle-associated Fe and other metals on plume suspended solids, Apalachicola Bay.

generated by simply squaring the correlation coefficient, r. The coefficient of determination,  $r^2$ , was used in this study only as an indicator of the *relative* linearity of each metal with Fe at each site. In other words,  $r^2$  can be thought of as a relative indicator of the variation in metals concentrations that is attributable to the chemical association of the metals with Fe. Use of  $r^2$  values as an *absolute* indicator of the percentage of the variation in concentration of a given metal which can be attributed to its chemical association with Fe assumes that the Fe values are exact.<sup>33</sup> This is not the case with any measurement; however, Fe concentrations determined on replicate samples for this study had a coefficient of variation (standard deviation expressed as percent of mean value) of only 4.0.

The following evaluation of the feasibility of predicting concentrations of particulate metals other than Fe is based upon comparison of  $r^2$  values and visual inspection of the linearity of the Fe vs. metal plots (Figures 93, 94, 95) rather than the contours in Figures 89, 90, 91. Comparison of predicted and observed values for the seven metals at each of the three sites would be lengthy and cumbersome. The reader may compare calculated contour values (Tables 30A, B, C) with actual data for particle-associated metals (Tables 26, 27, 28) using the sample numbers listed in the data tables and plotted on contour Figures 89, 90, 91.

Results. Strong linearity was found for Mn vs. Fe concentrations at all three sites. No relationship was found for concentrations of particle-associated Cd with those of Fe at any of the locations studied. Results for Cu, Zn, Cr, Pb and Hg were site dependent.

Except for Cd, r<sup>2</sup> values (0.85 to 0.98) and the strong linearity of Fe vs. metal plots indicate that much of the variability in particle-associated metals concentrations can be accounted for by the chemical association of all heavy metals studied with Fe at Apalachicola Bay (Table 30C, Figure 95).

The strong linear relationship of the Fe vs. Mn plot  $(r^2 = 0.98)$  for Atchafalaya Bay indicates that chemical association with Fe accounts for nearly all the variability in Mn concentrations (Table 30B, Figure 94A). The linearity of Cu with Fe at this site was also good  $(r^2 = 0.85)$ .

For the remainder of the metals at Atchafalaya Bay (Table 30B, Figure 94) the Fe vs. metal fit was fair. Their  $r^2$  values ranged from 0.45 to 0.55. Exceptions were Cd and Hg where little or no linear fit was found.

Mn showed a strong linear relationship with Fe in Corpus Christi Bay ( $r^2 = 0.52$ , 0.58, 0.48, respectively) but no relationships were found between Fe concentrations and those of Zn, Hg, and Cd at Corpus Christi Bay (Table 30A, Figure 93).

<u>Discussion.</u> As indicated by the comparison of  $r^2$  values for a given metal and site, the adequacy of predictions based upon the regression equations varies widely among the three sites. Exceptions were Mn and Cd for which  $r^2$  values were consistently high and low, respectively. The departure from linear concentration relationships for the metals plotted against Fe was due to factors other than their chemical association with Fe. Principle influences that may be responsible for deviations from the expected linear relationships are:

1. Analytical error. Except for Fe and Mn, the detection limit of the analytical techniques employed was approached or reached when concentrations of suspended solids fell below roughly 200 mg/ $\ell$  (± about 100 mg/ $\ell$ ). This level of suspended solids necessary for accurate determinations of a given metal will be lower or higher depending upon (a) the quantity of the metal (µg metal/g suspended sediment) on the particles and (b) the sensitivity of the analysis for that metal. Analyses for this study indicate the order of "detectability" was: Cu > Zn > Cr > Pb > Cd. The relative  $r^2$  values of Fe vs. metal plots generally reflect this same order (Table 30).

The effect of analytical accuracy on linearity of regression plots can be evaluated to some extent by noting the greater relative scatter of data points at lower concentrations on these plots (Figures 93, 94, 95). This is demonstrated further by the fact that the highest  $\mathbf{r}^2$  values were found with data from Apalachicola Bay where the highest metal concentrations occurred. The plots for Apalachicola (Figure 95) and the regression equations are dominated by the high values. The  $\mathbf{r}^2$  values were lowest for Corpus Christi which also had the lowest concentrations of suspended solids, and therefore, metals. Atchafalaya Bay values for plume suspended solids, particle-associated metals, and  $\mathbf{r}^2$  were all intermediate between those for the other two sites.

Table D-3 (Appendix D) lists large coefficients of variation associated with sampling and analysis of the less prevalent

- metals. These are average values for high and low concentrations. Near the detection limits these values are considerably larger; often greater than 100%. With the exception of Cd, variability of this order could account for most of the scatter on even the least linear regression plots presented. For these reasons, analytical error is considered here to be the most significant factor responsible for the departure from the expected linear relationships between Fe and the other metals studied.
- Local sources of suspended solids and organic matter. Composition of background suspended matter, both organic and inorganic, may differ from that of the suspended dredged material and consequently alter particle-associated metal concentrations in and around the plume, especially where suspended solids concentrations are low. Since ambient suspended inorganic sediment and bottom sediment resuspended near the channel will probably be more similar in composition to disposed channel sediments than plankton, an increase in the relative abundance of organic matter would probably produce greater deviations in plume particle composition where suspended solids levels are low (see Figure 92). Table 29 indicates that Fe:suspended solids ratios are relatively constant at a given depth even where particle concentrations approach background levels. However, since the affinity of organic matter for the various trace metals differs34 there may be greater variation in concentration at low particulate levels for the other trace metals studied than for Fe. This could result in some loss of linearity and therefore predictive capability when the other metals are plotted against Fe. The greater scatter of data points at lower concentrations on Figures 93, 94, 95, supports this argument.
- 3. Inhomogeneity of dredged sediments. During the time, a few hours to perhaps a day, required to generate a turbidity plume the cutterhead may dredge sediments which differ in composition. This may have been a significant factor at Corpus Christi where Holmes et al.<sup>2</sup> documented substantial variability in Zn and Cd associated with Corpus Christi Bay surficial sediments. They attributed this variability to pollutant inputs to the Bay from Corpus Christi Harbor.
- 4. Grain size fractionation of sediments following discharge. Grain size fractionation of disposed sediments due to differential particle settling rates may result in differences in suspended solids composition vertically in the water column and longitudinally along the plume axis. The influence of differential particle settling velocities on particle composition within the plume depends on the distribution of particle-associated metals among the various size classes, on the intensity of water mixing, and on the particle size distribution of the dredged material at a particular site. At Apalachicola, and especially Corpus Christi, the channel

sediments were predominantly fine-grained and contained 1% by mass, or less, sand (Table 21). The median grain size of Corpus Christi and Apalachicola Channel sediments was less than 1 µm and approximately 1.3 µm, respectively. Therefore, little variation in particle settling rate and size for suspended solids in the disposal plume would be expected at these two sites. This is substantiated by suspended solids size data in Table 31 which shows small ranges in mean size (Stokes' diameter 3.2 to 4.1 μm at 2.1 m, 2.4 to 3.9 μm at 0.6 m depth) and settling velocity (9.4 x 10<sup>-4</sup> to  $1.5 \times 10^{-3}$  cm/sec at 2.1 m,  $5.2 \times 10^{-4}$  to  $1.4 \times 10^{-3}$  cm/sec at 0.6 m depth) for particles in the plume at Apalachicola Bay. Although a wide distribution in grain size was present in Atchafalaya channel sediments (Table 21), strong wind mixing at this site may have eliminated much of the effect of differential particle settling in segregating the different size fractions. This statement is confirmed by Table 31 which indicates little variation in mean grain size (Stokes' diameter 3.9 to 7.3  $\mu$ m) and settling velocity (1.4 x 10<sup>-3</sup> to 4.9 x 10<sup>-3</sup> cm/sec) for suspended solids samples along the axis of a plume at Atchafalaya Bay.

5. Chemical alteration of sediments during dredging and disposal. As discussed earlier it is considered unlikely that significant chemical changes in sediments occur during dredging and disposal. Any alteration of sediment composition during the brief period of particle suspension should be minor since the great majority of the heavy metals (and other constituents) in the turbid plume are associated with particulate phases.

For the purpose of estimating elevated levels of particulate metals caused by the discharge of dredged materials, predictions based on regression equations determined for a given site similar to those generated for this study will be sufficient for most purposes. This is especially true where concern is with high concentrations since these were the most linear with respect to Fe. The importance of increased analytical accuracy is illustrated by the strong linearity of Fe vs. metal regression plots for Apalachicola where large quantities of suspended solids were collected.

Since Cd did not show a linear relationship to Fe at any of the three sites studied, a brief assessment of the reasons for the difference in the behavior of Cd relative to the other metals is called for. Laboratory studies of the association of metals with different sediment phases under varied redox and pH conditions<sup>35</sup> showed that Cd was

Settling Velocity and Particle Size of Plume Suspended Solids Table 31

	Sample	Depth (m)	Mean Settling Velocity* (cm/sec)	Graphical Std. Dev.	Mean Equivalent Stokes' Diameter** (µm)	Suspended Solids Concentration (mg/l)
Apalachicola Bay	A39	2.1	9.4 x 10 <sup>-4</sup>	$2.7 \times 10^{-3}$	3.2	278.9
	A55	2.1	$1.4 \times 10^{-3}$	$5.6 \times 10^{-3}$	3.9	74.8
	A60	2.1	$1.5 \times 10^{-3}$	$8.4 \times 10^{-3}$	4.1	44.5
	A91	2.1	$1.2 \times 10^{-3}$	$7.2 \times 10^{-3}$	3.7	
	A56	9.0	1.4 × 10 <sup>-3</sup>	$6.1 \times 10^{-3}$	3.9	30.5
	A64	9.0	7.9 x 10 <sup>-4</sup>	1.6 x 10 <sup>-3</sup>	3.0	19.0
	A81	9.0	$5.2 \times 10^{-4}$	$7.9 \times 10^{-4}$	2.4	68.4
Atchafalaya Bay	MC32	6.0	$4.9 \times 10^{-3}$	$1.7 \times 10^{-2}$	7.3	1104
	MC35	6.0	$1.4 \times 10^{-3}$	$9.2 \times 10^{-4}$	3.9	251
	MC45	6.0	1.6 x 10 <sup>-3</sup>	$4.5 \times 10^{-3}$	4.2	131
	MC47	6.0	$2.3 \times 10^{-3}$	$7.0 \times 10^{-3}$	4.5	408
	MC57	6.0	$1.4 \times 10^{-3}$	3.3 × 10 <sup>-3</sup>	3.9	124

\* Particle settling velocities were determined with a Cahn Electrobalance Rodel DTL and Particle
 Sedimentation Accessory
 \*\* Calculated from mean settling velocity using Stokes' Law. 45

present in the readily bio-available soluble and exchangeable fractions to a greater degree than the other transition metals studied. Cd release to soluble forms was affected to a greater extent by redox potential increases, especially in sediment samples containing abundant organic matter. Differences in Cd behavior relative to Hg and Cu were observed in adsorption studies with sewage effluent containing 35 mg/\$\mu\$ of suspended solids. Hg and Cu adsorption onto particles increased with time while Cd was desorbed following rapid initial adsorption. In addition, Gambrell et al. 35 found Cd to be less associated with Fe and Mm oxides than other heavy metals. 37

Though it is unlikely that particulate/dissolved exchange due to the above factors would significantly affect particle-associated Cd concentrations during dredged material disposal, it is possible that the differences noted between Cd and other transition metals may result in variability and lack of correlation of Cd and Fe in sediments from the dredging channels studied.

#### Conclusions

- Particle-associated metals injected into the water during dredging and disposal operations tend to remain associated with suspended solids particles.
- Concentration ratios of particle-associated Fe:suspended solids were relatively constant in and near the disposal plume at a given site. Coefficients of variation were about 10% or less.
- 3. Particle-associated metals in the plumes were generally linearly related to particle-associated Fe; some differences were observed for particle-associated metals outside the plume of excess turbidity and in general, where suspended solids levels were sufficiently low to cause analytical problems.
- 4. Based on the above observations a model was developed with which particle-associated metals can be predicted from concentrations of suspended solids. The model and techniques employed are useful for:
  - a. Delineation of the extent of elevated levels of particle-associated constituents caused by suspended solids increases generated by dredging and disposal, and
  - b. The approximate prediction of concentrations of those particle-associated metals which are linearly related to suspended solids and Fe concentrations in the

turbidity plume of an open-water pipeline disposal operation. This is not the case for Cd and, in some instances, Zn and Hg for reasons given.

The model works best in a well-mixed system. The model does not accurately predict highly variable background concentrations of suspended metals where localized effects dominate.

# PART V: OPEN-WATER PIPELINE DISPOSAL AND DISSOLVED OXYGEN DEMAND

#### Introduction

Although considerable quantities of reduced particulate material with a high potential oxygen demand are introduced into the water column during open-water pipeline disposal of dredged material, only a small fraction of this material is reactive on a time scale comparable to that associated with settling of the bulk of the mass of particulate matter. Between 95-99% of dredged material is deposited close to the discharge structure and within a few tens to a few hundreds of seconds after discharge in shallow water. Most of the remaining 1-5% of the total mass of dredged material is deposited within a few hours of discharge. Thus, the "oxygen sag" resulting from open-water pipeline disposal of dredged material is smaller than would be predicted from either the organic carbon content or the total reducing capacity of the original in-place sediments.

The principal reduced species present in sediments capable of reacting with dissolved oxygen on a time scale of minutes to hours are present primarily in solution in the interstitial waters of the original sediment. The important species are reduced sulfur species (H<sub>2</sub>S, HS<sup>-</sup>, S<sup>-</sup>), reduced iron (Fe<sup>++</sup>) and reduced manganese (Mn<sup>++</sup>). While organic matter and sulfide minerals can be expected to exert an oxygen demand, most organic matter decomposition is bacterially-mediated and oxidation of sulfide minerals is initially limited to surfaces. These factors increase time scales for oxygen demand of the particulate matter to the point where these reactions should be important only in deposited material. Once dredged material is deposited, its oxygen demand on the overlying waters is initially dependent on the expulsion of interstitial water during compaction, and beyond this is diffusion-limited. Few actual measurements of the above species exist for channel sediments designated for dredging, but "worst case" estimates of oxygen demand

can be made using data from a variety of environments.

## Estimating Oxygen-Demand from Chemical Analyses

Estuarine sediments typically contain abundant detrital iron, which reacts with bacterially-produced sulfide species to form iron sulfide minerals and eventually pyrite. Berner<sup>38</sup> showed that organic carbon-rich sediments are a sink for sulfate and Goldhaber and Kaplan<sup>39</sup> summarized data that showed only about a third (7.4 mM) of the "closed system" sulfate available (25 mM) is actually present in sediments as dissolved sulfide species. Ferrous iron may reach millimolar concentrations but is usually present in much smaller concentrations. Holdren et al.<sup>20</sup> measured maximum reduced manganese concentrations of 0.7 mM in interstitial waters of Chesapeake Bay sediments.

Cline and Richards<sup>40</sup> studied the kinetics of hydrogen sulfide oxidation in seawater and showed that the major reaction products were thiosulfate and sulfate. Although they indicated the system is kinetically complex and very likely beyond simple or rigorous definition, their data and work by Ostlund and Alexander<sup>41</sup> indicate that sulfides have a half-life in oxygenated systems of between 17 min and 20 hr, depending on the O<sub>2</sub>:sulfide ratio. Kinetic studies of the oxidation of Fe<sup>++</sup> and Mn<sup>++</sup> solutions were not identified, but unpublished laboratory observations of the air oxidation of these solutions and the field studies of Bray et al.<sup>42</sup> suggest that these reactions must be rapid.

The predominant oxygen consuming reactions of the sulfide system are:

$$2HS^{-} + 2O_{2} -- \longrightarrow S_{2}O_{3}^{2-} + H_{2}O$$
 (33)

$$HS^- + 20_2 -- \rightarrow S0_4^{2-} + H^+$$
 (34)

For Fe<sup>++</sup> and Mn<sup>++</sup>, Stumm and Morgan<sup>43</sup> suggest the following as oxidation reactions:

$$4Fe^{++} + O_2 + 4H^{+} - - \rightarrow Fe^{3+} + 2H_2O$$
 (35)

$$Mn^{++} + \frac{1}{2} O_2 + H_2 O -- \rightarrow MnO_2 + 2H^+$$
 (36)

Considering the concentrations of the easily oxidized species and the stoichiometry of the oxidation reactions, reaction (34) must be the major reaction in causing an "oxygen sag" in the receiving waters of open-water pipeline dredged material disposal activities and will be considered in the estimate that follows.

It is difficult to accurately estimate "oxygen sags" because the concentrations of oxygen consuming species can be expected to vary with distance and location in a plume of suspended dredged material. Also, the species considered here are in solution and are not subject to sedimentation, so estimates of plume dilution derived from suspended sediment concentrations may not be the best indicators, Table 32.

Assuming 80% (by volume) water content, a cubic meter of in-place designated dredge material contains 800% of water and up to 5.9 moles of sulfide species. Oxidation of this by reaction (34) will require 11.8 moles of  $0_2$ . Saturated water with a chlorinity of 10%, and a temperature of 15°C has, at saturation, an oxygen content of 6.3 ml/l (9 mg/l, 563  $\mu$ mole/l, 563 m mole/m<sup>3</sup>)<sup>44</sup> so some 21 m<sup>3</sup> of water will be required to oxidize the sulfides in 1 m<sup>3</sup> of "typical" fine-grained dredged material. Using these data one can express the oxygen demand in terms of the mass of oxygen per mass of dry sediment. One obtains an estimated oxygen demand of about 0.4 mg  $0_2$ /g of dry sediment.

Accurate predictions of oxygen demands of dredged material require either detailed chemical analysis of the sediments and particularly of the interstitial waters, or direct determinations of the short-term oxygen consumption of samples of dredged materials and their interstitial waters. A direct method is desirable because of its simplicity.

Table 32

Summary of Oxygen Sags Expected for Different Dilutions

of Interstitial Water Released during

Dredging and Disposal

		Dilution	
	100:1	1000:1	100,000:1
Conc. Sulfide	0.074 mM	7.4 µM	0.074 μM
O <sub>2</sub> required to satisfy demand	0.148 mM	14.8 µM	0.148 μM
O, remaining	413 µM	548 µM	562.8 μM
	4.6 ml/l	6.1 ml/l	6.3 ml/l
% Sag (Below Saturation)	27%	3%	

## A Simple Method for Estimating Short-Term Oxygen Demand

A simple method can be used to estimate the short-term oxygendemand of dredged materials—the demand that can be expected to produce an oxygen sag during open-water pipeline disposal.

A plastic core liner is pre-drilled with a series of approximately 1.5 cm diameter holes at appropriate intervals along the length of the liner and covered with longitudinal strips of electrical tape. After a core is obtained, the tape is removed from the first hole below the sediment-water interface, a disposable 50 cc<sup>3</sup> syringe whose tip has been cut off is inserted, and a plug of sediment removed. As quickly as possible the syringe is inserted into the stopper of a modified 500 ml Erlemeyer flask (Figure 96) which has been filled with water from the disposal area whose 0<sub>2</sub> content has been determined. The sediment is expelled from the syringe into the flask and the overflow tube clamped off. A magnetic stirrer is activated and the rate of consumption of dissolved oxygen chronicled until no further change is observed over periods of a few minutes. The water in the flask is then transferred to a sample bottle for return to the laboratory where it will be evaporated

to dryness to determine the mass of sediment added to the flask.

Sample measurements from Apalachicola Bay sediments are presented in Figures 97, 98, 99. The data show the consumption of oxygen as a function of time for a series of samples from each of two cores, A6 and A7. The data show that:

- 1. the oxygen demands of the two cores were similar
- 2. the oxygen demand increased with depths in each core
- the short-term oxygen demand was largely satisfied within 10-15 min.

Using the data plotted in Figures 97, 98, 99 one can calculate the oxygen demand per unit mass of sediment for each of the sample depths, Table 33. The mean value was the same for each of the two cores, 1.2 mg  $^{\circ}$  per g of dry sediment.

Table 33
Short-Term Oxygen Demand of Apalachicola Bay Sediments

Station	Depth in Core (cm)	Oxygen Demand $(mg O_2/g dry sediment)$
A6	5	0.9
	15	0.7
	25	1.5
	35	1.4
	45	1.2
	75	1.3
		<1.2> mean
A7	12	1.2
	22	1.4
	42	1.2
	52	1.1
		<1.2> mean

This measured demand is attributable primarily to the sulfides in the interstitial water, but there may also be some oxidation of the surfaces of sulfide minerals. This estimate of oxygen demand is somewhat greater than that estimated previously from chemical analysis of interstitial waters from a variety of coastal environments.

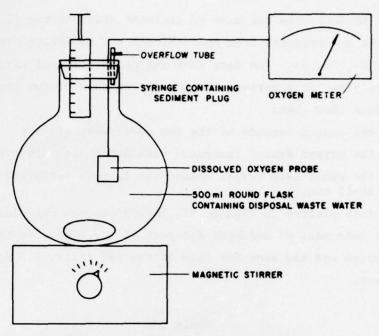


Figure 96. Sketch of apparatus used to measure short-term  $\ensuremath{\text{O}_2\text{--demand}}$  of sediments.

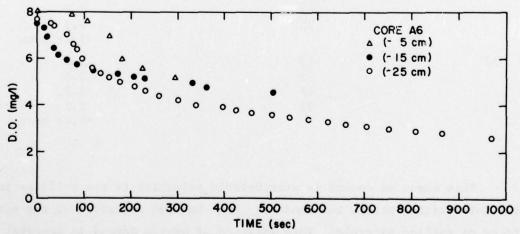


Figure 97. Depletion of dissolved oxygen versus time measured in the apparatus shown in Figure 96.

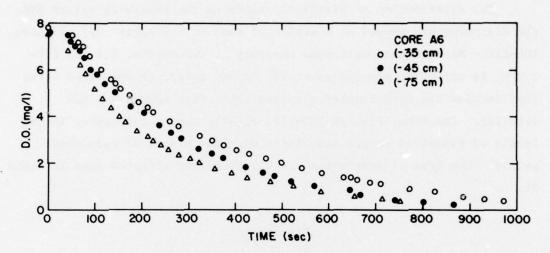


Figure 98. Depletion of dissolved oxygen versus time measured in the apparatus shown in Figure 96.

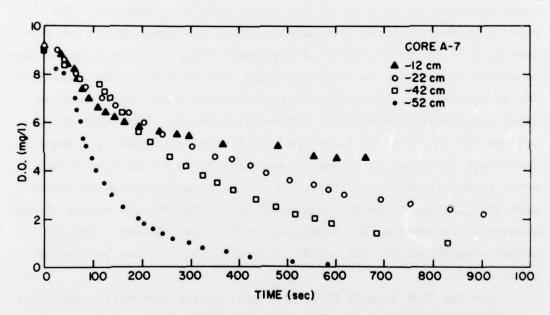


Figure 99. Depletion of dissolved oxygen versus time measured in the apparatus shown in Figure 96.

## Field Observations of Oxygen Sag in Apalachicola Bay

The distribution of dissolved oxygen in the receiving waters off the discharge was mapped on a series of runs on 7-8 April 1977, Figures 100-112. Measurements were made underway at two depths, 0.6 and 1.8-2.0 m, by attaching electrodes of YSI oxygen meters to the fixed strut that carried the nephelometer sampling tubes (see Appendix A for details). The maps, Figures 100-112, clearly show a depression in the levels of dissolved oxygen associated with the plumes of suspended solids. The area of depression are tabulated for selected runs in Table 34.

### Discussion

The total amount of oxygen consumed within the area of measured oxygen depression can be estimated for the water column above the lower sampling depth for each run if one makes certain assumptions. The authors assumed that the near-surface map of dissolved oxygen was representative of the distribution of dissolved oxygen from the water surface to midway between the two sampling depths for that run. The lower level map is assumed to represent the distribution from the lower sampling depth up to midway between the two sampling levels. Next, the areas between the isopleths of dissolved oxygen were determined by planimetry. These were converted to volumes by multiplication of the appropriate depth as described above. The total amount of oxygen consumed within each volume element was then estimated by multiplying the volume of the element by the mean oxygen depression within that element. The total oxygen consumption for the entire plume was then obtained by summing these values.

For Run 3 of 8 April 1977, the total oxygen consumption was about  $1 \times 10^9$  mg to a water depth of 1.8 m. Since the mean depth in the disposal area was about 2.4 m and since the oxygen depression increases with depth, the total oxygen consumption for the entire water column was significantly greater than this. If one considers a worst case and

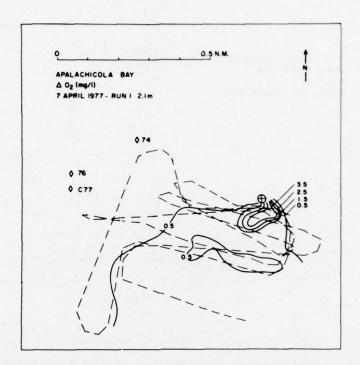


Figure 100. Distribution of dissolved oxygen depression  $(mg/\ell)$ .

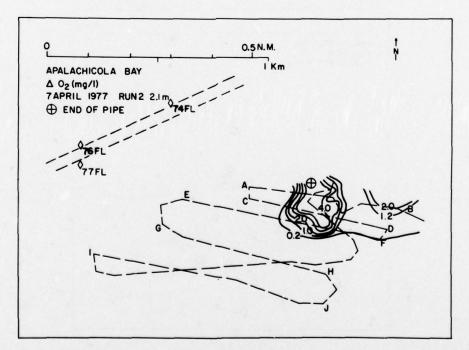


Figure 101. Distribution of dissolved oxygen depression (mg/l).

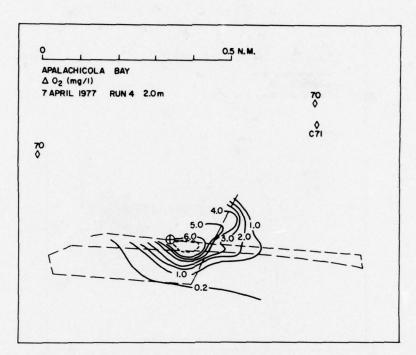


Figure 102. Distribution of dissolved oxygen depression ( $mg/\ell$ ).

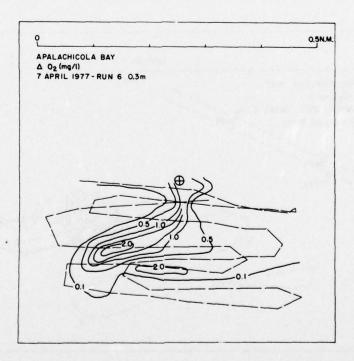


Figure 103. Distribution of dissolved oxygen depression ( $mg/\ell$ ).

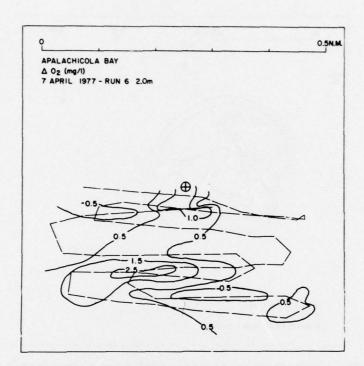


Figure 104. Distribution of dissolved oxygen depression (mg/l).

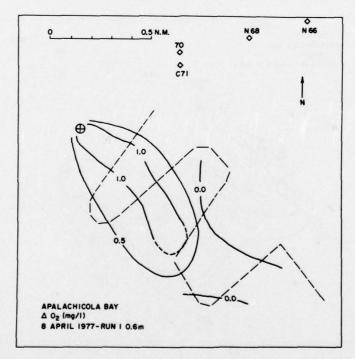


Figure 105. Distribution of dissolved oxygen depression (mg/l).

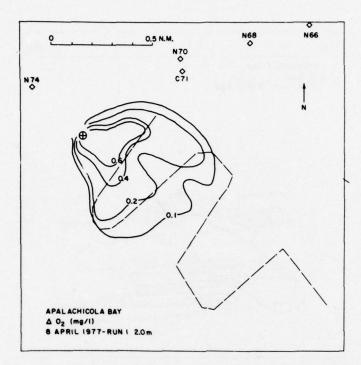


Figure 106. Distribution of dissolved oxygen depression (mg/ $\ell$ ).

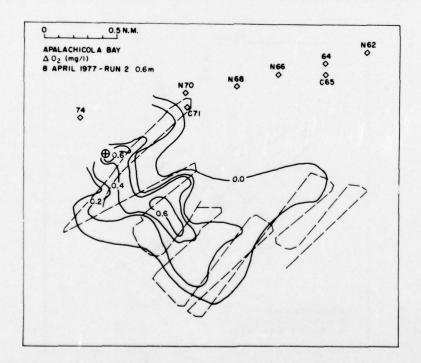


Figure 107. Distribution of dissolved oxygen depression (mg/l).

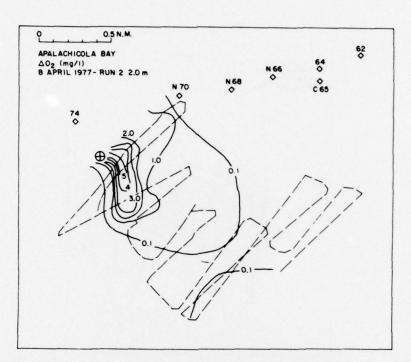


Figure 108. Distribution of dissolved oxygen depression (mg/l).

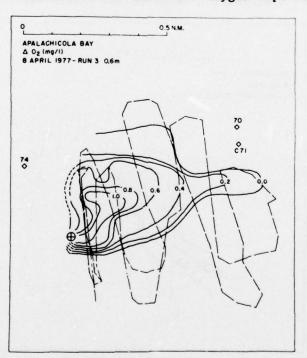


Figure 109. Distribution of dissolved oxygen depression (mg/l).

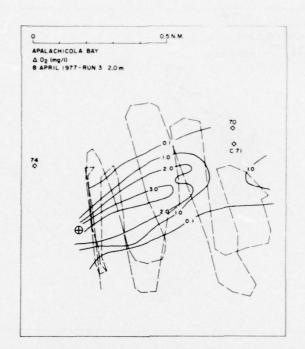


Figure 110. Distribution of dissolved oxygen depression (mg/l).

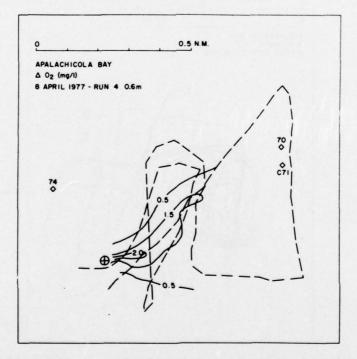


Figure 111. Distribution of dissolved oxygen depression (mg/l).

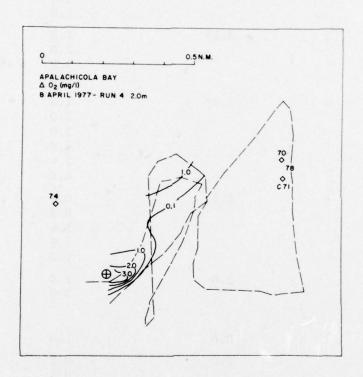


Figure 112. Distribution of dissolved oxygen depression (mg/l).

Table 34
Areas of Oxygen Depression in Apalachicola Bay

		Sampling	O <sub>2</sub> Depression	
		Depth	Ambient - Observed	Area
Date	Run #	<u>(m)</u>	(mg/l)	(km <sup>2</sup> )
7 Apr'77	1	2.1*	2.0 3.0 4.0	0.03 0.02 0.01
	2	2.1*	1.0 2.0 3.0 4.0	0.05 0.04 0.03 0.02
4	4	2.0*	1.0 2.0 3.0 4.0 5.0 6.0	0.13 0.09 0.07 0.05 0.03 0.01
	6	0.6	0.4 0.8 1.4 1.6 1.8	0.06 0.03 0.01 < 0.01 < 0.01
		2.0	2.0 3.0	0.04 0.01
8 Apr'77	1	0.6	1.0	0.15
		2.0	0.2 0.4 0.6	0.28 0.10 0.05
	2	0.6	0.2 0.4 0.6	1.49 0.52 0.11
		2.0	1 2 3 4 5	0.78 0.34 0.22 0.09 0.03

(continued)

Table 34 (concluded)

Date	Run #	Sampling Depth (m)	O <sub>2</sub> Depression  Ambient - Observed  (mg/l)	Area (km²)
8 Apr'77	3	0.6	0.2	
o Apr //	3	0.0		0.41
			0.4	0.34
			0.6	0.19
			0.8	0.09
			1.0	0.04
		2.0	1.0	0.35
			2.0	0.21
			3.0	0.04
	4	0.6	0.4	0.07
			0.8	0.01
	2.0	1.0	0.04	
		2.0	0.02	
			3.0	< 0.01

 $<sup>^{\</sup>star}$  Contours did not close, and as a result, areas of  $^{\rm 0}2^{\rm -depression}$  could not be planimetered.

assumes that below 1.8 m all the oxygen was depleted, the total oxygen consumption within the disposal area increases to about  $5 \times 10^9$  mg. One can relate this total oxygen consumption to the amount of dredged material discharged over the period required to produce the plume, approximately  $10^5$  sec. The rate of discharge of solid material was estimated at 0.13 metric tons/sec which results in a total daily discharge of about  $13 \times 10^9$  g. Using these values one obtains an Apparent Oxygen Demand of about 0.4 mg  $0_2$ /g sediment dredged. Estimates for other runs were comparable; the range was from about 0.3-0.6 mg  $0_2$ /g dry sediment.

It is instructive to compare this estimate of oxygen demand, the demand that was satisfied, with the potential oxygen-demand estimated from typical geochemical analyses of interstitial waters of estuarine sediments and with the author's measured oxygen demands for cores taken in the Apalachicola Bay channel. The oxygen demand estimated from chemical analyses of interstitial waters was about 0.4 mg  $0_2$ /g sediment. The oxygen demand measurements from actual cores was about 1.1 mg  $0_2$ /g sediment. While the excellent agreement between the oxygen demand calculated from observed oxygen depression and the oxygen demand estimated from interstitial water analyses is somewhat fortuitous, it supports the argument that observed oxygen sags are largely the result of oxidation of easily oxidized dissolved species in interstitial waters and perhaps to some extent to oxidation of the surfaces of sulfide minerals.

#### REFERENCES

- U. S. Army, "Final Environment Impact Statement: Maintenance Dredging Corpus Christi Channel, Texas," Nov 1975, U. S. Army Engineer District, Galveston, Texas.
- Holmes, C. W., Slade, E. A., and McLerran, C. J., "Migration and Redistribution of Zinc and Cadmium in Marine Estuarine System," Environmental Science and Technology, Vol 8, 1974, pp 255-259.
- Rusnak, G. A., "Sediments of Laguna Madre," In Shepard, F. P.,
   F. B. Phleger, and T. H. van Andel (ed.), Recent Sediments,
   Northwest Gulf of Mexico, Am. Assoc. Pet. Geol., Tulsa, Oklahoma,
   1960, pp 153-196.
- 4. Smith, N. P., "Meteorological and Tidal Exchanges between Corpus Christi Bay, Texas and Northwestern Gulf of Mexico," Est. Coast. Mar. Sci., Vol 4, No. 5, 1977, pp 511-520.
- Koefoed, J. W. and Gorsline, D. S., "Sedimentary Environments in Apalachicola Bay and Vicinity," Jour. Sed. Petrol., Vol 33, 1963, pp 205-223.
- 6. Hunt, J. N., "The Turbulent Transport of Suspended Sediment in Open Channels," *Proceedings of the Royal Society*, Series A, Vol 224, 1954, pp 322-335.
- Okubo, A., "A Review of Theoretical Models of Turbulent Diffusion in the Sea," Jour. Ocean. Soc. Japan, 20th Anniversary Volume, 1962, pp 286-320.
- 8. Carter, H. H. and Okubo, A., "Comments on Paper by G. T. Csanady, 'Accelerated Diffusion in the Skewed Shear Flow of Lake Currents'," Jour. Geophy. Res., Vol 71, 1966, pp 5012-5014.
- 9. Okubo, A., "Oceanic Diffusion Diagrams," Deep Sea Research, Vol 18, 1971, pp 789-802.
- 10. Biggs, R. B., "Gross Physical and Biological Effects of Overboard Spoil Disposal in Upper Chesapeake Bay; Project A-Geology and Hydrology," NRI Special Report No. 3, July 1970, Natural Resources Institute, Univ. of Md., Solomons, Maryland.
- 11. Folk, R. L., Petrology of Sedimentary Rocks, Hemphill's, Austin, Texas, 1964.
- Krauskopf, K. B., "Factors Controlling the Concentrations of Thirteen Rare Metals in Sea Water," Geochimica et Cosmochimica Acta, Vol 9, 1956, pp 1-32.
- 13. Stumm, W. and Lee, G. F., "Oxygenation of Ferrous Iron," Industrial and Engineering Chemistry, Vol 53, 1961, pp 143-146.
- Hem, J. D., "Deposition and Solution of Manganese Oxides," U.S.G.S. Water-Supply Paper 1667-8, 1964, U.S. Government Printing Office, Washington, D. C.

- Morgan, J. J. and Stumm, W., "Colloid Chemical Properties of Manganese Dioxide," Journal of Colloid Science, Vol 19, 1964, pp 347-359.
- 16. Jenne, E. A., "Controls on Mn, Fe, Co, Ni, Cu, and Zn Concentrations in Soils and Water: The Significant Role of Hydrous Mn and Fe Oxides," Trace Inorganics in Water, Advances in Chemistry Series, 73, American Chemical Society, Washington, D. C., 1968, pp 337-387.
- 17. Windom, H. L., "Environmental Aspects of Dredging in Estuaries,"

  Journal of the Waterways, Harbors and Coastal Engineering Division,

  Proceedings of the American Society of Civil Engineers, Vol 98,
  1972, pp 475-487.
- 18. Lee, G. F., "Role of Hydrous Metal Oxides in the Transport of Heavy Metals in the Environment," *Proceedings of the Symposium on Heavy Metals in the Environment*, Nashville, Tenn, 1973, pp 137-147.
- Berner, R. A., Principles of Chemical Sedimentology, McGraw Hill, New York, 1971.
- 20. Holdren, G. R., Bricker, O. P., and Matisoff, G., "A Model for the Control of Dissolved Manganese in the Interstitial Waters of Chesapeake Bay," In Church, T. M. (ed.), Marine Chemistry in the Coastal Environment, ACS Symposium Series 18, American Chemical Society, Washington, D. C., 1975, pp 364-381.
- Shulka, S. S., "Sorption of Inorganic Phosphate by Lake Sediments," Soil Science Society of America Proceedings, Vol 35, 1971, pp 361-365.
- 22. Chen, K. Y. et al., "Research Study of the Effect of Dispersion, Settling, and Resedimentation on Migration of Chemical Constituents During Open-water Disposal of Dredged Materials," Contract Report D-76-1, U. S. Army Engineer Waterways Experiment Station, Vicksburg, Miss, 1975.
- 23. Lee, G. F., "Factors Affecting the Transfer of Material Between Water and Sediments," Literature Review #1, Eutrophication Information Program, 1970, Water Resources Center, University of Wisconsin, Madison, Wisconsin.
- 24. Environmental Effects Laboratory, "Ecological Evaluation of Proposed Discharge of Dredged or Fill Material into Navigable Waters," Miscellaneous Paper D-76-17, U. S. Army Engineer Waterways Experiment Station, Vicksburg, Miss, 1976.
- 25. Lee, G. F. et al., "Research Study for the Development of Dredged Material Disposal Criteria," Contract Report D-75-4, U. S. Army Engineer Waterways Experiment Station, Vicksburg, Miss, 1975.
- Galal-Gorchev, H. and Stumm, W., "The Reaction of Ferric Iron with Orthophosphate," Journal of Inorganic and Nuclear Chemistry, Vol 25, 1963, pp 567-574.

- 27. Folger, D. W., "Texture and Organic Carbon Content of Bottom Sediments in Some Estuaries of the United States," In Nelson, B. W. (ed.), Environmental Framework of Coastal Plain Estuaries, Geological Society of America, Memoir 133, Boulder, Colorado, pp 391-408.
- 28. Rashid, M. A., "Role of Humic Acids of Marine Origin and Their Different Molecular Weight Fractions in Complexing Di- and Tri-Valent Metals," Soil Science, Vol 3, 1971, pp 298-306.
- 29. Rashid, M. A. and Leonard, J. D., "Modifications in the Solubility and Precipitation Behavior of Various Metals as Result of Their Interactions with Sedimentary Humic Acid," Chemical Geology, Vol 11, 1973, pp 89-97.
- Nissenbaum, A. and Snaine, D. J., "Organic Matter-Metal Interactions in Recent Sediments," Geochimica et Cosmochimica Acta, Vol 40, 1976, pp 809-816.
- 31. Bondarenko, G. P., "Stability of Soluble Coordination Compounds of Copper with Humic and Fulvic Acids, Geochemistry International, Vol 9, 1972, pp 702-711.
- 32. Gibbs, R. J., "Mechanisms of Trace Metal Transport in Rivers," Science, Vol 180, 1973, pp 71-73.
- 33. Kinsman, B., Unpublished Manuscript, Marine Sciences Research Center, State University of New York, Stony Brook, New York, 1977.
- 34. Schnitzer, M. and Skinner, S. I. M., "Organic-Metallic Interactions in Soils: 5. Stability Constants of Cu<sup>++</sup>, Fe<sup>++</sup> and Zn<sup>++</sup>-Fulvic Acid Complexes," Soil Science, Vol 102, 1966, pp 361-365.
- 35. Gambrell, R. P. et al., "Transformations of Heavy Metals and Plant Nutrients in Dredged Sediments as Affected by Oxidation-Reduction Potential and pH," Contract Report D-77-4, Office Chief of Engineers, Washington, D. C., 1977.
- 36. Gardiner, J., "The Chemistry of Cadmium in Natural Water-II, The Adsorption of Cadmium on River Muds and Naturally Occurring Solids," Water Research, Vol 8, 1974, pp 157-164.
- 37. Blom, B. E. et al., "Effect of Sediment Organic Matter on Migration of Various Chemical Constituents During Disposal of Dredged Material," Contract Report D-76-7, Environmental Effects Laboratory U. S. Army Corps of Engineers Waterways Experiment Station, Vicksburg, Miss, 1977.
- Berner, R. A., "Distribution and Diagenesis of Sulfur in Some Sediments from the Gulf of California," Mar. Geol., Vol 1, 1964, pp 117-140.
- Goldhaber, M. G. and Kaplan, I. R., "The Sulfur Cycle," In Goldberg, E. D. (ed.), The Sea, Vol 5, Wiley-Interscience, New York, 1974, pp 569-655.

- 40. Cline, J. D. and Richard, F. A., "Oxygenation of Hydrogen Sulfide in Seawater at Constant Salinity, Temperature and pH," Environmental Science and Technology, Vol 3, 1969, pp 838-843.
- Ostlund, H. G. and Alexander, J., "Oxidation Rate of Sulfide in Sea Water, a Preliminary Study," Jour. Geophys. Res., Vol 68, 1963, pp 3995-3997.
- 42. Bray, J. T., Bricker, O. P., and Troup, B. N., "Phosphate in Interstitial Water of Anoxic Sediments, Oxidation Effects During Sampling Procedure," *Science*, Vol 180, 1973, pp 1362-1364.
- 43. Stumm, W. and Morgan, J. J., Aquatic Chemistry, Wiley-Interscience, New York, 1970.
- 44. Carpenter, J. H., "New Measurements of Oxygen Solubility in Pure and Natural Water," Limnol. Oceanogr., Vol 11, 1966, pp 264-277.
- 45. Sverdrup, H. U., Johnson, M. W., and Fleming, R. H., *The Oceans*, Prentice-Hall, Englewood Cliffs, New Jersey, 1942.
- 46. Williams, J., "A Small Battery-operated Hydrophotometer," Technical Report 24, Mar 1961, Chesapeake Bay Institute, The Johns Hopkins University, Baltimore, Maryland.
- 47. Dayal, R. et al., "Water Column and Sediment Properties at the Eaton's Neck Disposal Site, L. I. Sound," 1976, U. S. Army Corps of Engineers, Waterways Experiment Station, Vicksburg, Miss.
- 48. Reeburgh, W. S., "An Improved Interstitial Water Sampler," Limnol. Oceanogr., Vol 12, 1967, pp 163-167.
- 49. Troup, B. N., Bricker, O. P., and Bray, J. T., "Oxidation Effect on the Analysis of Iron in Interstitial Water of Recent Anoxic Sediments," Nature, Vol 249, 1974, pp 237-239.
- Fanning, K. A. and Pilson, M. E. Q., "Interstitial Silica and pH in Marine Sediments: Some Effects of Sampling Procedures," Science, Vol 173, 1971, pp 1228-1231.
- 51. Degobbis, D., "On the Storage of Seawater Samples for Ammonia Determination," Limnol. Oceanogr., Vol 18, 1973, pp 605-610.
- 52. Thayer, G. W., "Comparison of Two Storage Methods for Analysis of Nitrogen and Phosphorus Fractions in Estuarine Water," *Chesapeake Science*, Vol 11, 1970, pp 155-158.
- 53. Black, C. A. et al., Methods of Soil Analysis, American Society of Agronomy, 1965, Pt. 2, pp 1387-1388.
- 54. Gross, M. G., "Carbon Determination," In Carver, R. E. (ed.), Procedures in Sedimentary Petrology, Wiley-Interscience, New York, 1971, pp 573-596.
- 55. Hawley, J. E. and Ingle, J. D., "Improvements in Cold Vapor Atomic Absorption Determination of Mercury," *Analytical Chemistry*, Vol 47, 1975, pp 719-723.

- 56. Nix, J. and Goodwin, T., "The Simultaneous Extraction of Iron, Manganese, Copper, Cobalt, Nickel, Chromium, Lead and Zinc from Natural Water for Determination by Atomic Absorption Spectroscopy," Atomic Absorption Newsletter, Vol 9, 1970, pp 119-122.
- 57. Kincade, J. D. and Van Loon, J. C., "Solvent Extraction for use with Flame Atomic Absorption Spectrometry," *Analytical Chemistry*, Vol 46, 1974, pp 1894-1898.
- 58. Segar, D. A., "The Determination of Trace Metals in Saline Waters and Biological Tissues Using the Heated Graphite Atomizer," Presented to the Joint Conference on Sensing Environmental Pollutants, Nov 8-10, 1971, Palo Alto, Calif.
- 59. Segar, D. A. and Gonzalez, J. G., "Evaluation of Atomic Absorption with a Heated Graphite Atomizer for the Direct Determination of Trace Transition Metals in Sea Water," *Anal. Chem. Act.*, Vol 58, 1972, pp 7-14.
- 60. Duchart, P., Calvert, S. E., and Price, N. B., "Distribution of Trace Metals in the Pore Waters of Shallow Water Marine Sediments," Limnol. Oceanogr., Vol 18, 1973, pp 605-618.
- 61. Boyle, E. A. and Edmond, J. A. "Determination of Trace Metals in Aqueous Solution by APDC Chelate Co-precipitation," Vol 6, Advances in Chemistry Series, #147, American Chemical Society, Washington, D. C., 1975.
- 62. Strickland, J. D. H. and Parsons, T. R., A Practical Handbook of Seawater Analysis, Bulletin 167 (2nd Edition), Fisheries Research Board of Canada, Ottawa, 1972.
- 63. Technicon Industrial Systems, "Nitrate and Nitrite in Water and Seawater," Industrial Method No. 158-71W, 1972, Technicon Instruments Corporation.
- 64. Technicon Industrial Systems, "Orthophosphate in Water and Seawater," Industrial Method No. 155-71W, 1973, Technicon Instruments Corporation.
- 65. Technicon Industrial Systems, "Silicates in Water and Seawater," Industrial Method No. 186-72W, 1973, Technicon Instruments Corporation.
- 66. Friederich, G. O. and Whitledge, T. E. "Autoanalyzer Procedures for Nutrients," In Pavlou, S. P. (ed.), Phytoplankton Growth Dynamics: Technical Series 1--Chemostat Methodology and Chemical Analyses, Special Report 52, Dept. of Oceanography, Univ. of Washington.

#### APPENDIX A: SUSPENDED SOLIDS MEASUREMENTS

## Nephelometry

Light is scattered in turbid sea water by suspended particles and the amount of light that is scattered has often been used as a measure of the amount of suspended material. The degree of scattering, however, depends not only on the quantity but also on the size, shape, and coefficient of reflection of the suspended particles. For a dilute solution, however, there is apparently a linear relationship between the amount of suspended material and the amount of light scattered.

A nephelometer is an instrument which measures the amount of light scattered at right angles to an incident beam by an extremely dilute suspension, and therefore, may be used to determine the relative quantity of suspended material in the water. In this study, a G.K. Turner Model 111 Fluorometer modified for use as a nephelometer was used. It was fitted with a UV general purpose fluorescent light source (Mercury lines at 365, 405, 436, 546, and 578 nm superimposed on a smooth broad curve centered at  $\sim$  380 nm), and a continuous flow, 1 cm square cross-section, borosilicate cuvette. A primary filter (Corning 7-60) with maximum transmission at  $\sim$  380 nm was placed in the incident light beam together with a 1% N.D. filter and a blue filter with maximum transmission at 415 nm (Corning 5-60) in the secondary reflected beam. Sea water was pumped through the cell at about 1-2  $\ell$ /min.

A Rustrak 100 mA recorder continuously monitored the instruments output. In general, two depths were sampled simultaneously ( $^{\sim}$  surface and  $^{\sim}$  bottom). A typical calibration curve is shown in Figure Al to demonstrate the linearity and sensitivity of the instruments used at one of the sites. From Figure Al it can be seen that the sensitivity of F\$\ell\$ 11 with the installed combination of light source, filters and cell was  $^{\sim}$  ±1 mg/ $^{\circ}$  for Apalachicola; F\$\ell\$ 10 was considerably more sensitive (±0.1 mg/ $^{\circ}$ ). However, background variations, of larger than these values, will determine the limiting value of sensitivity or detection for the various runs.

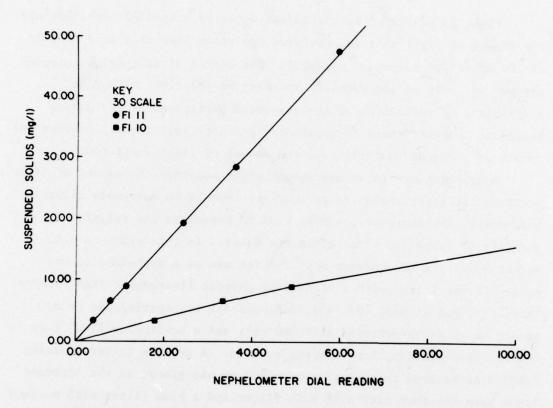


Figure Al. Typical nephelometer calibration curves from Apalachicola Bay suspended solids.

Figure A2 shows the sensitivity of one of the nephelometers relative to one of the transmissometers used during the study. It can be seen from this figure that the nephelometer provides considerably more sensitivity at both low and high suspended solids concentrations, i.e., transmission > 90% and < 10%. It should be pointed out, however, that the linear relationship shown in Figure Al holds only until such time as a significant fraction of the incident light is scattered more than twice. In addition, as the concentration increases the system will eventually go blind—the suspended solids concentrations are so high that light can not penetrate the sample.

# Transmissometry

Light transmission was measured using a modified William's transmissometer (Williams, 1961)<sup>46</sup>. The unit was redesigned to operate on 110 volts (AC) with a more powerful lamp source. Results were recorded on either a Leeds and Northerup Speedomax H Recorder or a Hewlett-Packard Mosley 7100 B Recorder. A sketch of the underwater unit of the transmissometer is shown in Figure A3.

Figure A4 shows the spectral response of the transmissometers used. A Schott VG9 color filter (green) was used in the receiver. The spectral response of the transmissometer peaks at approximately 522 nm. The coastal mean extinction coefficient reaches a minimum at about 540 nm in the green (Sverdrup, et al., 1946)<sup>45</sup>.

The two units employed during the study were calibrated shortly (within a few weeks) after each field deployment with sediment from the dredging area. Calibrations were conducted by placing the transmissometer head in a large plastic trash can filled with tap water that was continuously being mixed with a recirculating water pump. A small amount of pre-weighed sediment was added to the bath and when completely

<sup>\*</sup> Bulb #44, Chicago Minature Lamp Works, 4433 N. Ravenswood Avenue, Chicago IL 60640.

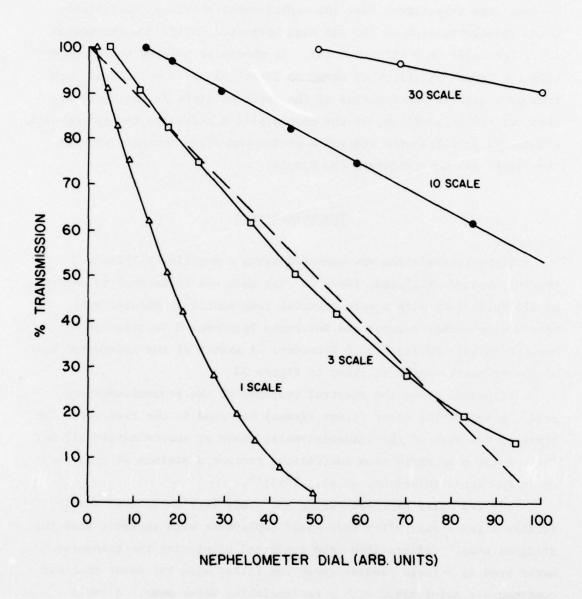


Figure A2. Comparison of sensitivities of transmissometer and nephelometer.

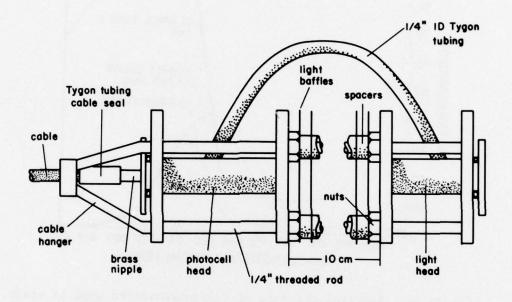


Figure A3. Sketch of underwater unit of transmissometer.

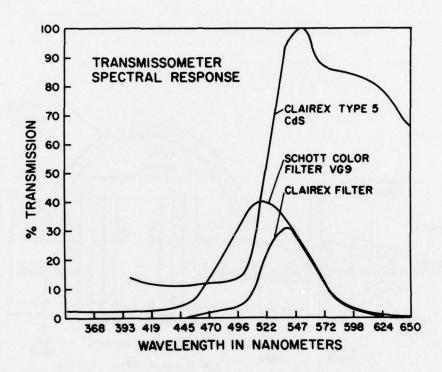


Figure A4. Spectral response of transmissometers used in study.

mixed, the transmission was recorded. A sample of the suspension was collected from the bath for gravimetric analysis. Another sample of sediment was added to the bath and the procedure repeated until a range of transmission values between 0 and 100% was obtained. Calibrations were run for the light path-lengths used in each of the field studies, 5 and/or 10 cm. The water samples were filtered through pre-weighed 47 mm, 0.6 µm APD Nuclepore filters, rinsed with distilled water, desiccated for at least 72 hours, reweighed, and the concentrations of total suspended solids calculated. All weighings were made to within ±0.03 mg.

The calibration data, sorted by site, were plotted and the points fitted by least-square regression with two straight lines—one line for the high values, the second for low to intermediate values. The boundary between intermediate and high values was selected by visual inspection. It is believed that this is the best method for predicting suspended solids concentrations from transmissometer data, and that higher order fits are not justified. This conclusion was supported by Professor Jerome Williams (personal communication) and Professor John Tyler (personal communication). A typical calibration curve is shown in Figure A5.

#### Converting Optical Measurements to Concentrations of Suspended Solids

The optical measurements have been converted to concentrations of total suspended solids using calibration curves determined as outlined previously from suspensions of different concentrations of sediment collected from the dredging area at each of the three sites. These "nominal" concentrations of suspended solids may differ from concentrations determined directly by filtration particularly outside the plume. Any discrepancies would probably be larger at low concentrations—near background levels—than at higher concentrations because the background population of suspended particles is derived primarily from a different source—primary production or river discharge, as opposed to resuspension of bottom sediments by the dredge, or by waves or currents.

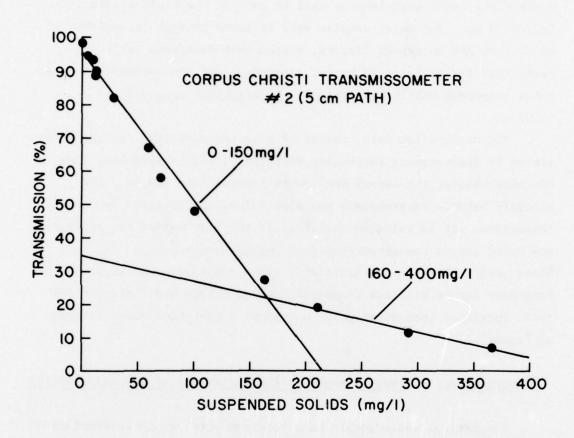


Figure A5. Typical transmissometer calibration curves used to predict concentrations of suspended solids.

Particles derived from different sources may have very different characteristic properties including: composition, density, size distribution, and index of refraction. Variations of these properties affect the optical properties of populations of these particles, sometimes dramatically, as noted earlier.

The background concentrations of suspended solids in Apalachicola Bay as determined gravimetrically were consistently lower (by about a factor of 1.5-2) than the nominal concentrations calculated from optical measurements at the same locations. It is believed that the higher nominal concentrations results from the increase in the relative abundance of low density suspended organic matter and perhaps to the presence of optically active dissolved and colloidal substances. These materials can have a marked effect on optical measurements but contribute little to the mass of suspended solids. As a result, use of these optical measurements with our calibration curves results in an over-estimate of the actual concentrations of suspended solids. The relative abundance of combustible organic matter increased with decreasing concentration of total suspended matter. At values of suspended solids from about 5-15 mg/& (background), combustible organic matter accounted for 50-87% of the total suspended matter; within the plume it accounted for < 20% of the total mass of suspended matter and decreased with increasing concentrations, Figure A6. Figure A6 shows variation in the relative abundance (%) of combustible organic matter with concentration of total suspended solids (mg/l) for Apalachicola Bay.

# Direct Determination of Concentrations of Suspended Solids

Suspended solids concentrations were determined by conventional gravimetric methods—filtering samples of measured volumes of sea water through pre-weighed filters. Water samples were collected from the shipboard pumping system on the downstream side of the nephelometers in 500 ml glass bottles. These samples were kept in the dark until they

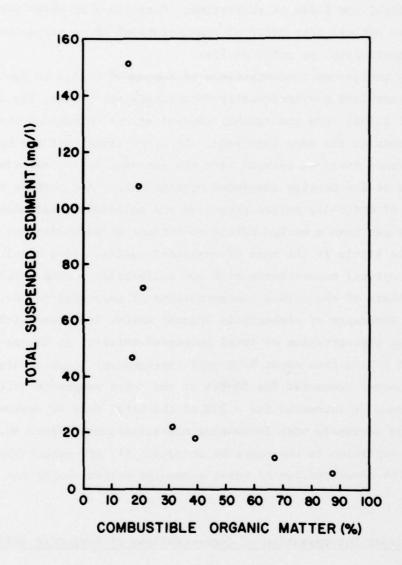


Figure A6. Total suspended solids  $(mg/\ell)$  versus combustible organic matter (%) for samples from Apalachicola Bay.

were filtered through preweighed, 47 mm diameter, 0.6 µm APD Nucleopore filters\*. The filters and their suspended loads were washed with distilled water to remove any sea salt and stored in individual dessicators at ambient temperature for a minimum of 72 hours before reweighing. The individual dessicators consist of small, wide-mouth, squat-form jars partially filled with silica gel into which is stuck a short, 30 mm, length of glass or plastic pipe (40 mm outer diameter). The weighed filter rests on top of this pipe. The membrane filters employed are susceptible to electrostatic charges and thus were weighed under an alpha-emitting source\*\*. All filter weights were determined to ±0.03 mg using a Mettler HE 20 balance.

# Particle Size Distributions of Suspended Solids

The mass-settling (size) distribution of suspended particles in the dredge discharge areas was determined by the cumulative method with a Cahn Electrobalance R Model DTL and Particle Sedimentation Accessory. This system measures the total mass of a sample settled from an initially homogenous suspension. The suspension undergoes size differentiation by gravity settling,

Samples of suspended solids to be analyzed for the size distribution of suspended particles were collected from the shipboard pumping system on the downstream side of the nephelometers in 1.0 liter plastic bottles. These samples were kept in the dark until the completion of each field study and then stored in a refrigerator (approximately 4°C) in the laboratory until ready for analysis.

Samples were concentrated prior to analysis because the samples typically contained less than 100 mg/ $\ell$  of suspended solids and only a 20-25 m $\ell$  aliquot from each sample is used to determine the size

<sup>\*</sup> Available from Arthur H. Thomas Company, Philadelphia, PA. \*\* The Staticmaster Ionizing Unit, Model No. 2U500 mounted on a Flexible Arm Staticmaster Positioner BFL available from Nuclear Products Co., 10173 E. Rush Street, El Monte, CA.

distribution of the particles. At such low levels, the detection level of the Cahn system is approached, yielding ambiguous results. To avoid this problem, the samples were concentrated either by centrifugation or by settling and decantation.

Analysis for size distribution was performed according to the method described in the Cahn instruction manual for the Particle Sedimentation Accessory. A sample is shaken vigorously by hand and a 20 to 25 ml aliquot is drawn out of the bottle with a 35 cm<sup>3</sup> syringe equipped with a short piece of glass tubing (1.5 mm inner diameter). This slurry is carefully added to the top of the sedimentation column and thoroughly dispersed through the column with a plunger. As the particles settle, the output of the instrument is recorded on a strip chart as a data curve of mass settled vs. time. For complete details of the Cahn electrobalance the reader is referred to the manufacturer's manual.

The data were presented on log-probability paper, and statistics of the particle size distributions were estimated by graphical methods.

In accordance with letter from DAEN-RDC, DAEN-ASI dated 22 July 1977, Subject: Facsimile Catalog Cards for Laboratory Technical Publications, a facsimile catalog card in Library of Congress MARC format is reproduced below.

Schubel, J I

Field investigations of the nature, degree, and extent of turbidity generated by open-water pipeline disposal operations / by J. R. Schubel ... cet ala, Marine Sciences Research Center, State University of New York at Stony Brook, Stony Brook, N. Y. Vicksburg, Miss.: U. S. Waterways Experiment Station; Springfield, Va.: available from National Technical Information Service, 1978.

245, c 52 pp.: ill.; 27 cm. (Technical report - U. S. Army Engineer Waterways Experiment Station; D-78-30)

Prepared for Office, Chief of Engineers, U. S. Army, Washington, D. C., under Contract No. DACW39-76-C-0129 (DMRP Work Unit No. 6C02)

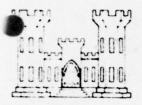
Appendices B, C and D on microfiche in pocket. References: p. 241-245.

1. Dredged material. 2. Dredged material disposal. 3. Environmental effects. 4. Field investigations. 5. Open water dis-

(Continued on next card)

Schubel, J R
Field investigations of the nature, degree, and extent of turbidity generated by open-water pipeline disposal operations ... 1978. (Card 2)

posal. 6. Plumes. 7. Suspended solids. 8. Turbidity. I. New York (State). State University at Stony Brook. Marine Sciences Research Center. II. United States. Army. Corps of Engineers. III. Series: United States. Waterways Experiment Station, Vicksburg, Miss. Technical report; D-78-30. TA7.W34 no.D-78-30



# Dredged Material Research Program



Technical Report D-78-30

FIELD INVESTIGATIONS OF THE NATURE, DEGREE, AND EXTENT OF
TURBIDITY GENERATED BY OPEN-WATER PIPELINE DISPOSAL OPERATIONS

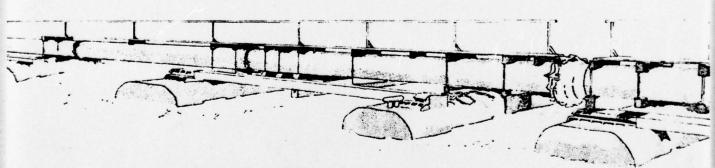
by

J. R. Schubel, H. H. Carter, R. E. Wilson, W. M. Wise, M. G. Heaton, M. G. Gross

Marine Sciences Research Center State University of New York at Stony Brook Stony Brook, N. Y. 11794

> July 1978 Final Report

APPROVED FOR PUBLIC RELEASE; DISTRIBUTION UNLIMITED



Prepared for Office, Chief of Engineers, U. S. Army Washington, D. C. 20314

Under Contract No. DACW39-76-C-0129
(DMRP Work Unit No. 6C02)

Monitored by Environmental Laboratory

U. S. Army Engineer Waterways Experiment Station

P. O. Box 631, Vicksburg, Miss. 39180

APPENDIX B: GRAIN-SIZE ANALYSIS OF BOTTOM SEDIMENTS

The cores were cut into 5-10 cm lengths and a wet subsample of approximately 5 grams (dry) drawn from each. Each subsample was then analyzed in accordance with the following procedure.

# Preparation of Samples

Each sample was transferred to a clean, dry 250 ml beaker. To the beaker were added 100 ml distilled water, exactly 40 ml 1% Calgon solution (dispersant), and 20 ml 30% hydrogen peroxide for removal of organic material. Preparation and standardization of the dispersant solution are described at the end of the method section. The sample was allowed to stand overnight and then placed in a hot water bath at 90°C for 3 hours to remove residual peroxide, which can inhibit complete dispersion.

# Wet Sieving

The sample was then wet-sieved through a 63 µm mesh screen to separate the sand fraction from the mud fraction (silt and clay). A squeeze bottle filled with distilled water was used to wash the sediment on the screen. The mud fraction was washed through the screen directly into a clean, dry 1000 ml graduated cylinder. The sand fraction remaining on the screen was washed into a clean, dry, pre-weighed 50 ml beaker. The beaker was then placed in a drying oven (LabLine Imperial "D" radiant heater), dried overnight at 100°C, cooled and reweighed the following morning. The weight of sand in the sample was computed.

The mud fraction in the cylinder was made up to approximately 950 ml with distilled water. The suspension in the cylinder was then stirred with a plexiglass stirring rod and allowed to stand for 2 hours to check for flocculation of the sediment. An additional 5 ml dispersant solution was then pipetted into the cylinder as a precautionary measure. The cylinder was then filled to exactly 1000 ml with distilled water.

# Pipette Analysis

A pipetting schedule was prepared showing  $\phi$  diameters,\* withdrawal depths, and withdrawal times for several samples.

The sample in the cylinder was stirred vigorously until all the sediment was uniformly distributed throughout the column. An electric timer was started as the bottom plate of the stirring rod broke the surface on the final upward stirring stroke. Exactly 20 seconds later a 20 ml aliquot was withdrawn by pipette from a depth of 20 cm below the surface. This aliquot was emptied into a pre-weighed 50 ml beaker. Pipette withdrawals were continued at the times and depths specified in the pipetting schedule. Between withdrawals, where time allowed, the pipette was washed with 20 ml distilled water.

Upon completion of the 9  $\phi$  withdrawal, late in the afternoon, the sample was restirred and the 10  $\phi$  withdrawal was made early the following morning. The 50 ml beakers from the withdrawals were placed in the drying oven at 100°C for 24 hours. The beakers were then removed from the oven, allowed to cool and their contents allowed to equilibrate with atmospheric moisture, and then weighed to 0.001 grams.

#### Computations

The weight of mud and Calgon in each pipette withdrawal was computed by subtracting the weight of the clean, dry 50 ml beaker from the weight of the beaker plus mud and Calgon. The weight of Calgon in a 20 ml aliquot from the sample suspension was computed by dividing the total weight of Calgon added to the cylinder by 50 (20 ml = 1/50 of 1000 ml). The section on preparation and standardization of dispersant solution gives the total weight of Calgon added to each cylinder. The weight of Calgon in a 20 ml aliquot was then subtracted from the weight of mud plus Calgon to give the weight of mud in the 20 ml aliquot. This weight multiplied by 50 to give the weight of sample finer than a

<sup>\*</sup>  $\phi = -\log_2$  (diameter of grain measured in mm).

particular  $\phi$  unit in the entire cylinder. The above computation for the 4  $\phi$  withdrawal represents the entire weight of mud in the sample. The weight of the sand fraction was added to this 4  $\phi$  weight to obtain the total sample weight.

Cumulative percentages of the total sample were obtained from pipette withdrawal data using the equation:

cumulative percent coarser =  $\frac{100 \text{ (S+F-P)}}{\text{S+F}}$ 

where S = weight of sand fraction

F = weight of mud fraction

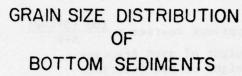
P = weight of mud fraction finer than a certain φ diameter (obtained by multiplying pipetted sample weight minus Calgon by 50)

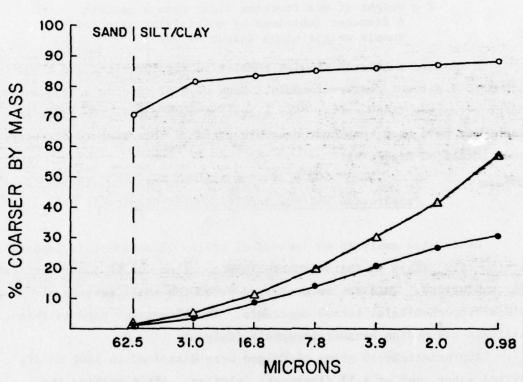
Data were tabulated showing cumulative sample weight and a cumulative percent coarser formula. Data were plotted on a "cumulative percent coarser than" curve. For illustrative purposes, the data for each site have been combined, ensemble averaged according to diameter, and plotted on Figure B1.

# Preparation and Standardization of Dispersant

Grain-size analysis on individual grains of sediment is impossible if the clay flakes in the sediment clump together due to ionic attraction (flocculation). This can be prevented by adding small amounts of dispersing chemicals, termed peptisers. The dispersant used in this analysis was sodium hexametaphosphate (Calgon).

Approximately 10 grams of Calgon were dissolved in 1000 m² distilled water, making a 1% dispersant solution. After shaking the dispersant solution well 20 m² was pipetted into each of five pre-weighed aluminum dishes. The dishes were placed in a drying oven overnight at 100°C. The dishes were then removed from the oven, allowed to cool and the Calgon allowed to equilibrate with atmospheric moisture, and reweighed. The weight of Calgon in each dish was computed and a mean value was taken. This value represents the weight of Calgon in a 20 m² aliquot of dispersant solution. By noting the exact amount of dispersant





- ATCHAFALAYA BAY 12 cm CORE (6cm INTERVAL)
- . CORPUS CHRISTI BAY 85cm CORE (5cm INTERVAL)
- APALACHICOLA BAY 65cm CORE (IOcm INTERVAL)

Figure B1. Particle size distributions of channel sediments.

solution added to the sample it was therefore possible to calculate exactly how much Calgon had been added. In fact, all samples received the same amount of dispersant solution and, hence, the same amount of Calgon.

#### APPENDIX C: INSTRUMENTATION

#### Navigation

Two different electronic positioning systems were used during the project. For the Corpus Christi study, a Decca Hi-Fix system was employed; at Atchafalaya Bay and Apalachicola Bay, a Motorola Mini-Ranger system was used.

Decca Hi-Fix employs either hyperbolic or circular (range-range) geometry and in both cases compares the phases of two transmission waves which are of the 2 MHz band. In our case, the circular mode was employed. The two lane readings were displayed on the research vessel to the closest one-hundredth of a lane\*. A track plotter was also employed to maintain a continuous visual record of the research vessel's track during sampling runs. Instrument accuracy is reported to be ±0.01 lane, which at 2 MHz is equavalent to ±0.8 meters. High local atmospheric noise, due to local late afternoon thunderstorms, caused severe problems in reception such that the system, as installed on the R/V S.W. RESEARCHER, was occasionally rendered unusable (~ 1400 on both 23 and 26 August, 1976).

The Motorola Mini-Ranger is a pulse radar type system using circular geometry operating in the C-band (5400 to 5600 MHz). In the version of this system used, (Mini-Ranger III), a range console, a receiver-transmitter and omni-directional antenna were installed on the research vessel with a pair of reference stations located at known points ashore. Measured ranges to the two reference stations from the research vessel were continuously displayed on the range console to ±0.9 meter and also recorded on a printer together with time. Positions at one minute intervals were plotted by computer from these range data using a simple trigonometric algorithm. The system is essentially line-of-sight with reported accuracy of ±3 meters.

<sup>\*</sup> It can be shown that in phase comparison systems, a lane is approximately 1/2 of the wavelength ( $\sim 150$  m at 2 MHz).

#### Currents

Currents were measured during all three study periods with ENDECO Type 105 current meters. The Type 105 meter is a horizontally-moored, ducted-impeller recording current meter, and is specially suited to minimize wave contamination of the current record in shallow, nearshore zones.

Advertised specifications are as follows:

power	4 "D" cells (62 days)
velocity range	$\sim 2.3-87.2 \text{ cm s}^{-1}$
threshold	∿ 2.3 cm s <sup>-1</sup>
resolution	∿ 2.3 cm s <sup>-1</sup>
accuracy	±3% of full scale
magnetic compass direction	0°-360°
compass accuracy {	±5° at 2.3 cm s <sup>-1</sup>
	±4° above 2.3 cm s <sup>-1</sup>

Data are recorded on a standard 16 mm 50 ft film cartridge with a shutterless camera. The film is exposed by light-emitting diodes which illuminate speed and direction sensors. A small drive motor advances the film at precise (±1.5 seconds/day) 30 minute intervals so that a direct recording of time is not necessary.

The speed sensing system consists of an eight blade propeller which is magnetically coupled through the PVC meter housing to a 5750:1 reduction gear. The output of the reduction gear drives a drum on which is inscribed a transparent helical line. Inside the drum is a light-emitting diode. The camera views this diode through the helical line and through a plate with a narrow slit parallel to the drum axis. The illumination thus appears as a dot of light moving up the slit, disappearing at the top of the slit and simultaneously reappearing at at the bottom, as the drum turns. Over the 30 minute recording period between film advances, the "moving" light will expose a line on the film the length of which is proportional to the number of revolutions of the impeller and, therefore, proportional to the average horizontal current

speed over the 30 minutes.

The direction sensor is a magnetic compass with an illuminated spiral directly etched on the compass card. The camera views the compass spiral through a slit via a small mirror which reflects the image alongside the speed slit. The top and bottom of the compass slit correspond to North and the center of the slit corresponds to South. Should the current change direction during the exposure interval, the compass reading is taken as the mid-point of the resulting line.

The ENDECO current meter has lead weights attached to the lower fin. These weights serve two purposes: first, they provide a means to adjust the meter buoyancy and, second, they keep the direction compass disc horizontal.

Additionally there is a threaded rod running along the bottom of the meter from the lower fin to the nose cap. On this rod are two lead weights which can be moved fore or aft to precisely level the instrument.

The current meter is moored to a vertical wire by a "Cook" clamp which permits the meter to move about the wire in the horizontal plane. A 1.5 m rope tether connects the clamp to the meter nose cap. This mooring system allows the meter to move more freely with the oscillatory currents characteristic of surface gravity waves. The effect of wave induced currents on the film record is, therefore, greatly reduced.

## Conductivity and Temperature

Temperature and conductivity (salinity) were measured at the three sites by means of a Beckman Model RS-5 Portable Salinometer. This instrument is portable, battery operated, and designed to make in-situ measurements of electrical conductivity and temperature to depths of  $\sim$  120 m. The instrument measures the electrical conductivity of sea water by an inductive or electrodeless method which utilizes two toroidally wound coils located in a submersible transducer. Temperature is measured with a thermistor also located in the transducer. Salinity is calculated to  $\pm 0.3$  % automatically from these measurements by means of a computing

bridge circuit. The instrument is used by lowering the transducer to the desired depth and directly reading on appropriate counters the values of temperature, conductivity, and salinity. Reported accuracies are  $\pm 0.5$  mS per cm in the range 0-60 mS per cm for conductivity and  $\pm 0.5$ °C in the range 0-40°C for temperature. The instrument is quite stable, however, and may be calibrated to 0.1% of full scale.

# Dissolved Oxygen

Oxygen measurements were made with YSI Model 51A oxygen meters. According to the manufacturer these units have a range of from 0-15 ppm in dissolved oxygen, an accuracy (with direct calibration) of ±0.25 ppm and repeatability (precision) of ±0.1 ppm. The unit uses a Clarktype oxygen sensor which measures the pressure drop across a membrane. Inside the membrane next to the cathode the oxygen pressure is zero because the oxygen is consumed as it reaches the cathode; outside the membrane the oxygen pressure is the ambient pressure to be measured. Oxygen flows or diffuses through the membrane because of the pressure differential. The flow of oxygen through the membrane is directly proportional to the differential oxygen pressure across the membrane (since the oxygen pressure is zero on the cathode side of the membrane the flow is proportional to the absolute oxygen pressure on the outside of the membrane). The chemical reaction within the sensor produces a current which is in direct stiochiometrical relation to the amount of oxygen being consumed. Hence, the cell current is directly proportional to the oxygen pressure to which the sensor is exposed,

The meters were calibrated in air and in freshwater saturated with air several times each day. Underway measurements of dissolved oxygen were made by attaching oxygen sensors to the rigid sampling strut that carried the nephelometer sampling tubes. Measurements were made at two depths every few minutes.



#### APPENDIX D: CHEMICAL ANALYTICAL METHODS AND MODEL CONTOURS

Interstitial water receiving bottles and dissolved metal bottles (250 ml polypropylene (Nalgene) bottles) were extracted with concentrated HC1, rinsed twice with Super Q deionized distilled water, and filled with 1% (v/v)\* concentrated HNO3 in deionized water. Before collection of the filtered sample, the bottles were emptied and rinsed twice with deionized water on board ship<sup>47</sup>. Nutrient samples were collected in 125 ml polypropylene (Nalgene) bottles for PO $_4^{-3}$  and Si(OH) $_4$ , and 25x150 mm screw cap glass test tubes for NH $_4^{+4}$ . These containers and 48 mm disposable petri dishes for particle-associated metal samples were soaked in 20% (v/v) HC1 in distilled deionized water for at least six hours, rinsed twice with distilled deionized water and air dried<sup>47</sup>.

Benthos core liners (6.5 cm i.d.) and caps were rinsed with 20% (v/v) concentrated HCl in distilled deionized water and rinsed twice with deionized water.

Reeburgh-type sediment squeezers were soaked for one hour in 10% (v/v) concentrated HCl, rinsed twice with distilled deionized water and air dried. All glass apparatus for elutriate tests were soaked in 20% (v/v) concentrated HCl in distilled deionized water for one hour, rinsed twice with distilled deionized water and oven dried. Membrane filters (47 mm Gelman Metricel GA-6, 0.45 µ pore size) were soaked in 10% (v/v) concentrated HCl in distilled deionized water for one hour and rinsed with distilled deionized water before and after mounting in the filtration apparatus. Site water for the elutriate test was collected in a five gallon polypropylene (Nalgene) carboy which was soaked with 20% (v/v) concentrated HCl in distilled deionized water, rinsed twice with distilled deionized water and allowed to air dry.

All glass millipore filter heads and receiving flasks for on board filtration of metal samples were soaked for one hour in 20% (v/v) concentrated HCl in distilled deionized water, rinsed twice with distilled deionized water and allowed to air dry before use.

<sup>\*</sup> v/v indicates a concentration by volume.

# The Sample Collection System

All samples were taken simultaneously while underway. Samples were pumped aboard via an over-the-side aluminum strut with depth-adjustable sampling ports situated in front of the strut to avoid contamination. Samples at Corpus Christi Bay and Apalachicola Bay were taken at two depths, while at Atchafalaya Bay samples were collected at one depth only due to the limited water depth.

Poly-flo tubing (1/2 i.d.) and all-plastic valves and connectors were used in the continuous-flow sampling system on the upstream side of the point where heavy metals samples were drawn to avoid contamination (see Figure A5). Using a Millipore vacuum pump, metal samples were drawn from the main sampling line before the nephelometers and nutrient sampling ports. One-liter Erlenmeyer sidearm flasks were rinsed twice with sample before collection; on collection, 250 ml of the water sample was transferred to a graduated cylinder. The graduated cylinder was also rinsed twice with sample before filling. This sample was immediately filtered using all glass Millipore filter heads supporting Gelman Type A.E, 47 mm (0.45  $\mu$  average pore size) glass fiber filters. All parts of the filtration system, including filters, were rinsed twice with distilled deionized water between samples.

The dissolved metal samples were collected in 250 ml Nalgene bottles. The filters and their suspended metal samples were placed in 48 mm Millipore disposable petri dishes.

Nutrient samples were collected simultaneously with metal samples at the nutrient sampling ports shown in Figure D1. After passage of the sample through the nephelometers and Whatman Gamma-12-80 (8  $\mu$  pore size) in-line glass fiber filters, they were collected in glass test tubes for NH<sub>4</sub><sup>+</sup>, and in 125 ml Nalgene bottles for PO<sub>4</sub><sup>-3</sup> and Si(OH)4. Containers were rinsed with sample before collection.

Suspended solids samples were also taken simultaneously with metals and nutrient samples at the sampling ports shown in Figure D1.

These unfiltered samples were collected in 500 ml glass bottles. After collection they were filtered volumetrically onto preweighed Nucleopore

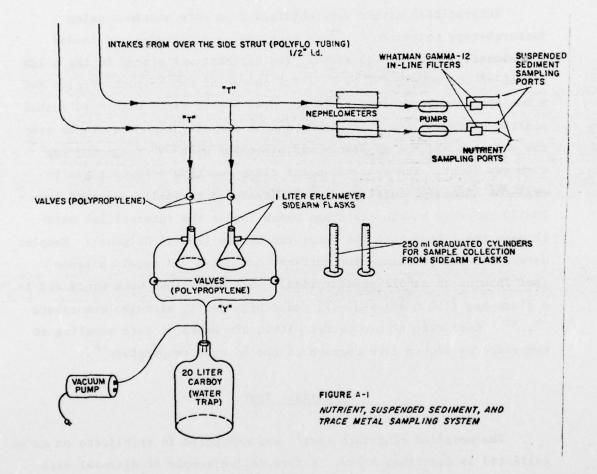


Figure D1. Sketch of sampling system for analyses of nutrients, suspended solids, and metals.

APD filters (47 mm, 0.45  $\mu$  pore size) and washed with distilled water to remove salts. Following dessication for at least 72 hours, weights were determined to the nearest 0.03 mg.

# Core Sampling

Cores were taken at selected sites in that part of the channel about to be dredged with a non-contaminating Benthos gravity corer. Six to nine core samples were taken at each project site.

Interstitial waters were obtained from core sections using Reeburgh-type squeezers 48. Core sections were extruded and loaded individually into the squeezers. The sediment was placed in the nylon barrel of the squeezer (7.3 cm i.d.) on top of two support screens and a Nuclepore membrane filter (90 mm, 0.45 µ pore size) with acid washed plastic spatulas. An acid-rinsed dental dam diaphragm was placed atop the sediment and the apparatus was assembled with "O" rings and cap with gas inlet. The external metal clamp was then screwed tight to seal the assembly. Nitrogen gas at pressures gradually elevated from 10-150 psi acts on the diaphragm which forces the interstitial water through the filter into the receiving bottle (250 ml Nalgene). Samples were split and preserved for nutrient and dissolved metal analyses (see section on sample preservation). All operations were conducted in a glove bag (IZR model x-37-37) under high purity nitrogen atmosphere 49, 42. Core extrusion occurred within six hours of core sampling at temperatures within five degrees of the in situ temperature 50.

# Elutriate Test

The modified elutriate test  $^{25}$  was conducted in triplicate on cores collected as described above. A five gallon sample of disposal site water was collected from just below the surface; 250 ml of this water was filtered through an acid soaked Gelman Metricel membrane filter (0.45  $\mu$  pore size) and analyzed to obtain background concentrations of dissolved metals and nutrients. All-glass Millipore filter heads were

used as filter supports for vacuum filtration of all elutriate test samples.

The test consisted of four steps: (1) 75 m2 of sediment, determined by volume displacement, was combined with a total of 1425 m2 of unfiltered site water in a 3 liter Erlenmeyer flask (5% (v/v) sediment to site water), (2) High purity compressed air was first passed through a deionized water trap and then bubbled vigorously through the sediment-site water slurry to agitate this mixture for thirty minutes, (3) The slurry was then allowed to settle for one hour, followed by (4) vacuum filtration of the supernatant as above. The standard elutriate test, which substitutes mechanical shaking for air agitation, was also performed on sediments from the Apalachicola Bay dredging site (Environmental Effects Laboratory, 1976)<sup>24</sup>. The filtrate was split for NH<sub>4</sub>, PO<sub>4</sub> and Si(OH)<sub>4</sub>, and dissolved metals. These samples were contained and stored as described in the following sections dealing with materials preparation and sample preservation.

# Sample Preservation

All dissolved nutrient samples were frozen immediately after collection to fix nutrient concentrations 1, 52 until analysis. Dissolved metal samples were acidified below pH 2 (one ml per 250 ml sample) with Ultrex concentrated HNO3 to maintain ions in solution. Particulate metal samples were placed in petri dishes and refrigerated or kept on ice. Sediment cores were sealed at both ends with core caps held by hose clamps. Interstitial waters were squeezed from core sections within six hours of coring as noted previously. These samples were split for nutrient and metal analyses. The nutrient portion was frozen immediately. The metal portion was acidified below pH 2 with Ultrex concentrated HNO3. For the elutriate test several cores were kept on ice or refrigerated before analysis (4-7 days). All cores were wrapped in large plastic bags to avoid contact with sunlight. Cores for interstitial waters were kept upright. Elutriate test site water was kept on ice or refrigerated before use 25.

# Carbon Analysis of Channel Sediments

Sediment samples taken from the channels to be dredged were analyzed for carbonate carbon and total carbon. Homogenized sediment samples were freeze-dried for another 12 hours prior to analysis.

Carbonate carbon was determined by a titrimetric method 53 as follows:

- 1. 50 ml of standardized (0.4995 N) HCl was added to an accurately weighed sediment sample (1-2 g) and heated for 20 minutes at 90°C.
- 2. Four drops of phenophthalein (0.1% in ethanol) were added and the excess acid was titrated with standardized (0.2442 N) NaOH to the indicator endpoint.
- 3. Percent carbonate carbon was calculated using the following equation:

$$% C_{CO_3} = \frac{(ml \ HC1 \times N_{HC1}) - (ml \ N_{NaOH})}{\text{weight sediment (S)}} (0.006) (100)$$

Reagent grade CaCO<sub>3</sub> was run through the analysis as a check on the method which was found to be accurate. All titrations were performed in triplicate.

Total carbon analyses were made on the same samples using a carbon-hydrogen-nitrogen analyzer (Hewlett Packard Model 185)<sup>54</sup>. Sample analyses were performed in triplicate.

# Heavy Metals Analyses

#### Instrumentation

- Perkin-Elmer model # 403 atomic adsorption spectrophotometer equipped with a deuterium arc background corrector and a Hewlett/Packard model # 7100B strip chart recorder.
- Perkin-Elmer model # HGA-70 graphite furnace and power source.
- Modified Perkin-Elmer mercury analysis system (see Figure 2) adapted from Hawley and Ingle (1975)<sup>55</sup>.
- 4. Perkin-Elmer single element, hollow cathode lamps.

#### Reagents

 Super-Q ultrapure water; deionization to 18 megaohmcm resistivity, absolute filtration at a 0.22 to 1.2 μm level. (Millipore Corporation: Bedford Massachusetts).

THIS PAGE IS BEST QUALITY FRACTICABLE.

D6

- Concentrated (70% wt/wt) HNO<sub>3</sub> A.C.S. reagent grade. (Fisher Scientific Corporation: Fair Lawn, New Jersey).
- 4-methyl-2-pentanol (methyl isobutyl carbinol) (CH<sub>3</sub>)2 CHCH<sub>2</sub>CHOHCH<sub>3</sub> (Eastman Kodak Corporation: Rochester, New York).
- 4. 20% (wt/v) sodium diethyldithiocarbamate solution in Super-Q (CH<sub>2</sub>CH<sub>2</sub>)2 NCSSNa.3H<sub>2</sub>O (certified A.C.S. salt) triple extracted with methyl isobutyl carbinol (MIBC) (Fisher Scientific Corporation: Fair Lawn, New Jersey).
- 5. 1.0% (wt/v) SnCl + 1.0% (v/v) HCl in Super Q (certified A.C.S. salt). (Fisher Scientific Corporation: Fair Lawn, New Jersey).
- 6. Standard stock solutions of 1000 µg ml<sup>-1</sup> of each; Cu, Cd, Cr, Pb, Fe, Mn, and Zn + 1.0% HNO<sub>3</sub> in Super-Q prepared using A.C.S. certified metal salts or foils as described in the "standard conditions" section of Analytical Methods for Atomic Absorption Spectrophotometry Perkin-Elmer Corporation: Norwalk, Connecticut.

#### Preparation of glassware

All glassware and digestion bottles used for metals analyses were cleaned in the following manner:

- 1. scrub with soap and tap water.
- 2. rinse with demineralized water.
- 3. rinse with Super-Q.
- 4. rinse with conc. HNO2.
- 5. rinse with Super-Q.
- 6. rinse with conc. HNO2.
- 7. rinse with Super-Q.
- 8. store filled with Super-Q.

In addition, the digestion bottles were pre-extracted for metals in the polymer lattice by heating them with a hot plate at  $85^{\circ}$ C while they contained 10 ml of conc.  $\text{HNO}_3$ . This was done for a minimum of 3 hours and was followed by two rinses with Super-Q.

THIS PAGE IS BEST QUALITY PRACTICABLE FROM COPY FURNISHED TO DDC

# Particle-Associated Metals Analysis

Suspended metal samples were analyzed in the following manner. The glass fiber filter\* containing the filtered solids was placed in a 1 oz. wide-mouth bottle\*\*, after which 5 ml of conc. HNO<sub>3</sub> was added. The bottles were tightly capped and placed on a sand bath at 85°C for two hours to acheive a gentle reflux action. Intermittantly, the bottles were vigorously shaken to destroy the structural integrity of the filters. While still warm, the digest solution was filtered through another glass filter using a filtering apparatus † adapated to a 125 ml separatory funnel evacuation system (see Figure D2). The filtering apparatus was cleaned in the following manner:

- 1. insert new glass fiber filter.
- 2. one rinse with 75 ml of Super-Q.
- 3. one rinse with 50 ml of conc. HNO3.
- 4. one rinse with 75 ml of Super-Q.

The suspended load-acid digest was then poured onto the filter head of the evacuated chamber and aliquots of the filtrate were drawn off into a 25 ml volumetric flask. The digest bottles were rinsed with 10 ml of Super-Q and the rinse water was sent through the filtering apparatus. Additional aliquots of Super-Q used to rinse the filtering apparatus were drawn off and added to the sample in the 25 ml volumetric flask. Super-Q was added directly to the flask to bring the volume to 25 ml. The glass fiber filter in the filtering apparatus was replaced and the cleaning procedure was repeated for the next sample.

Clean filters were subjected to the digestion and filtering procedures and served as blanks. The filtered samples were analyzed for Fe, Mn, and Zn using an atomic absorption spectrophotometer equipped

<sup>\*</sup> Gelman type A glass fiber filter (47 mm) pre-rinsed with Super Q. Gelman Instrument Company: Anne Arbor, Michigan.

<sup>\*\*</sup> Nalgene, 1 oz., linear polyethylene, wide mouth, screw cap bottle.

<sup>†</sup> Gelman type A glass fiber filter (25 mm) Gelman Instrument Company: Anne Arbor, Michigan.

<sup>††</sup> Pyrex Microanalysis system (25 mm) with fritted glass head Millipore Corporation: Bedford, Massachusetts.

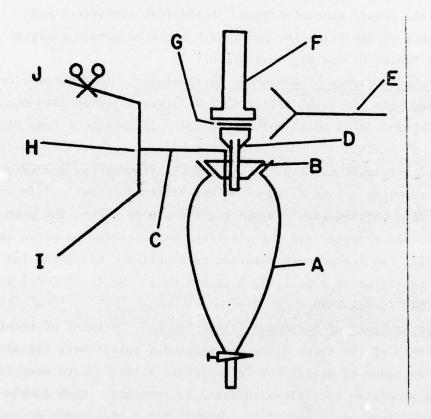


Figure D2. Sketch of microfiltration system: A. 125 ml separatory funnel, B. rubber stopper, C. 90° glass elbow, D. Pyrex microanalysis filter head with fritted glass (25 mm), E. Millipore filtering apparatus clamp, F. Pyrex filter funnel, G. Gelman type A glass fiber filter (25 mm), H. Polyethylene T, I. Vacuum hose leading to water aspirator, J. Vacuum release valve consisting of polyethylene tubing and pinch clamp.

with a deuterium arc background corrector and an air/acetylene flame. Cd, Cu, Cr, and Pb were analyzed using flameless atomic absorption, employing a graphite furnace. Analytical parameters for these analyses can be found In Table D1.

Mixed standard solutions were prepared using Super-Q as the dilutant and contained 1.0, 10, 40, 100, 400  $\mu/\ell^{-1}$ , and 1.0, 2.0, and 10 mg/ $\ell^{-1}$  of each metal, respectively. The concentrations of the standards used to construct the Beer's law plot were dependent on the range of the sample concentrations. Analytical parameters and coefficients of variation for particle-associated metals analyses are listed in Tables D1 and D3, respectively.

Mercury Analysis of Suspended Particulates. To determine Hg, 3 ml of reducing solution (1.0%  $\rm SnCl_2 + 1.0\%$  HCl) was injected into the reaction chamber of a small volume, Hg analysis apparatus (see Figure D3) using a Plastipak\* 10 ml syringe equipped with a modified, disposable, micropipette tip. After the air flow purged contaminants from the reducing solution, 10 ml of the filtered digest sample was pipetted into the reaction chamber via the sample port. The peak absorbance was recorded and the air flow was continued to purge the system until the strip chart returned to baseline. Standards for the analysis consisted of 0.5, 1, 2, 3, and 4  $\mu g/l^{-1}$  Hg in 5% (v/v) conc. HNO<sub>3</sub> + 0.01% (wt/v) KMnO<sub>4</sub>.

Iron Analysis of Suspended Solids Samples. A total of twenty samples taken at the three sites for suspended solids were digested and analyzed in order to obtain the Fe/suspended solids ratios used in computing predicted particle-associated Fe contours. Each sample set was selected from one plume at two depths with a wide range of suspended solids values. Samples were collected on 47 mm Nucleopore filters as described in the sections on suspended solids sampling.

The samples were desiccated and weighed to 0.01 mg and placed in hot acid soaked and Super-Q rinsed one ounce Nalgene (LLP) bottles. Ten ml concentrated HNO, were added followed by heating on a sand bath

<sup>\*</sup> Becton-Dickinson and Company: Rutherford, New Jersey.

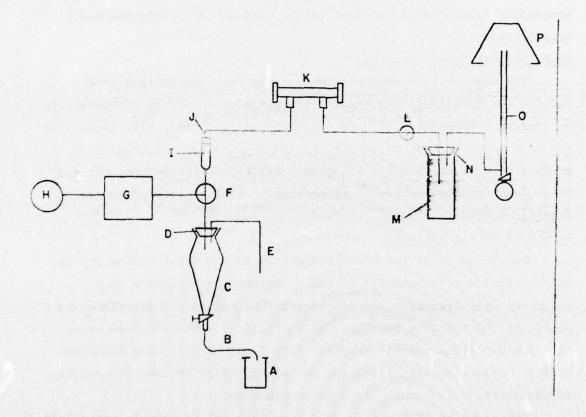


Figure D3. Sketch of mercury analysis system: A. Atchment, B. Drain tube, C. 250 ml separatory funnel, D. Rubber stopper, E. Vacuum hose, F. 3-way valve, G. Perkin-Elmer air compressor from mercury analysis system, H. Variac (used to control flow rate) I. Medium porosity sintered glass funnel with rubber stopper (used as the reaction chamber), J. Rubber septum inserted in a glass tube (sample port), K. Hg optical absorption tube, L. 3-way valve, M. Hg vapor absorbing trap, N. Rubber stopper, O. Bubble burette, P. Fume hood exhaust

at 85°C for four hours.

The hot digests were filtered through acid and deionized waterrinsed 24 mm glass fiber filters as with the suspended metal samples. Filtrates and Super-Q rinses were made up to volume with deionized water in volumetric flasks of varying capacity, depending on the weight of the original sample.

Iron concentrations were determined by atomic absorption as µg metal/mg suspended solids. It is from these analyses that particle-associated Fe/suspended sediment ratios used in the predictive model were derived.

# Bulk Sediment Metals Analysis

Two samples from each site were taken from homogenized grab samples for total sediment metals determination in the ship channels to be dredged. These samples were (1) dried at 85°C for twelve hours, (2) ground with mortar and pastle, (3) dried at 60°C for six hours, (4) weighed to 0.01 mg, and (5) digested and analyzed for Fe, Mn, Cu, and Pb as described in the preceding section. Results are reported as µg metal/g or mg dry sediment.

#### Dissolved Metals Analyses

Sample analyses for dissolved metals in the water column and in interstitial waters entailed either an extraction procedure or a selective volatilization process in order to remove the interferences caused by the sea salt matrix. The extractions were performed using ammonium pyrollidinedithiocarbamate (APDC) and methylisobutylcarbinol (MIBC). Selective volatilization was accomplished by careful charring in the graphite (furnace) prior to atomization.

Since the Fe-APDC and Mn-APDC complexes are relatively unstable  $^{56}$ ,  $^{57}$  these metals were analyzed by the selective volatilization process which has been demonstrated to be reliable for these metals  $^{58}$ ,  $^{59}$ . In this latter method, 20  $\mu\ell$  of sample is injected directly into the graphite furnace and dried at 100°C for 30 seconds, followed by ashing at 1150°C for 60 seconds. The sample was then atomized at 2500°C for 6 seconds and the peak absorbance was noted on a strip chart recorder.

Standards were made according to the methods of standard additions.

Small aliquots of stock solutions of Fe and Mn were added to Sargasso seawater\* such that the solutions contained an additional 10, 20, 30, 40, 100, 500, 1000, and 2000  $\mu g/l^{-1}$  of Fe and 10, 20, 30, 40, 100, 200, 400 and 1000  $\mu g/l^{-1}$  of Mn. The appropriate standards were used to bracket the samples analyzed. The extraction was used for Cu, Cr, Cd, Pb and Zn, and the procedure was taken from the work of Duchart et al., (1973)60. A 100 ml aliquot of sample was poured into a calibrated 125 ml separatory funnel. The pH of the sample was adjusted to 6 using NH<sub>4</sub>OH after which 4 ml of a 20% (w/v) sodium diethyldithiocarbamate solution was added. Five ml of MIBC was added and the funnels were mechanically shaken for 15 minutes. The organic and aqueous phases were allowed to separate for 20 minutes. The aqueous layer was then drained and the organic layer collected in a 1 oz. LPE bottle.

Aliquots of Super-Q and previously extracted water samples served as reagent blacks. Atomic absorption standards were prepared by the method of standard additions. In this method, minute quantities of mixed standard were added to four composite samples of site water resulting in standards containing an additional 1.0, 5.0, 10, and 20  $\mu g/\ell^{-1}$  of each metal, respectively.

Cd, Cu, Cr, and Pb were determined by flameless atomic absorption on a graphite furnace. Zn was determined by aspiration into an air/acetylene flame. Analytical parameters and coefficients of variation for the analyses of dissolved metals are given in Tables D2 and D3.

Determination of Interstitial and Elutriate Cadmium and Lead. Since difficulty was incurred in obtaining satisfactory standards for Cd and Pb following extraction for dissolved metals in interstitial waters and elutriates, a modification of the method of Boyle and Edmond (1975) 61 was employed for preparation of these samples.

Prior to addition of samples, beakers were (1) washed with laboratory soap and water, (2) heated at 90°C while containing 40 ml of

<sup>\*</sup> Collected aboard the R/V Colombus Iselin, 25 January, 1977 at 12°45'01" N, 60°35'01" W.

Table D1 Analytical Parameters for Suspend | Metals\*

					FURNAC	FURNACE PARAMETERS	
Element	Mode	Slit	HC1 current	Sample	Dry	Ash time/temp	Atomize time/temp
ъ	air/ace. flame	3(0.2 nm)	30 ma	N/A	•	i dom:	•
W.	air/ace. flame	3(0.2 nm)	20 ma	N/A			ecció
Zu	air/ace. flame	4(0.7 nm)	15 ma	N/A	i f	i luz Or ex stouts	1
25	furnace	4(0.7 nm)	15 ma	50 µ&	50 sec 100°C	50 sec 1100°C	10 sec 2700°C
Pb	furnace	4(0.7 nm)	8 ma	20 µ&	30 sec 100°C	50 sec 490°C	10 sec 2300°C
PO	furnace	4(0.7 nm)	8 ша	10 με	30 sec 100°C	30 sec 1100°C	10 sec 2700°C
Cr	furnace	4(0.7 nm)	25 ma	20 µR	30 sec 1.00°C	50 sec 1100°C	10 sec 2700°C
Hg	cold	4(0.7 nm)	10 ma	10 mL	1	plin 8 I lie n Act 8	See y <b>L</b> s Sees S

Analytical lines used for the analyses were those recommended in Analytical Methods for Atomic Absorption Spectrophotometry for maximum sensitivity.

Table D2

Analytical Parameters for Dissolved Metals\*

					FURNAC	FURNACE PARAMETERS	
Element	Mode	Slit	HC1 current	Sample	Dry cime/temp	Ash time/temp	Atomize time/temp
F e	sel. vol. furnace	(0.2 nm)	30 та	20 m2	30 sec 100°C	60 sec 1150°C	6 sec 2700°C
Mn	sel. vol. furnace	3(0.2 nm)	20 ma	20 m2	30 sec 100°C	60 sec 1150°C	6 sec 2700°C
Cu	extraction furnace	4(0.7 nm)	15 ma	20 mL	30 sec 100°C	40 sec	6 sec 2700°C
Pb	extraction furnace	4(0.7 nm)	8 ma	20 m2	30 sec 100°C	40 sec 490°C	6 sec 2300°C
PO	extraction furnace	4(0.7 nm)	8 ma	20 m&	30 sec 100°C	50 sec 330°C	6 sec 1800°C
Cr	extraction furnace	4(0.7 nm)	25 ma	20 m%	30 sec 100°C	50 sec 330°C	6 sec 2700°C

\* Analytical lines used for the analyses were those recommended in Analytical Methods for Atomic Absorption Spectrophotometry for maximum sensitivity.

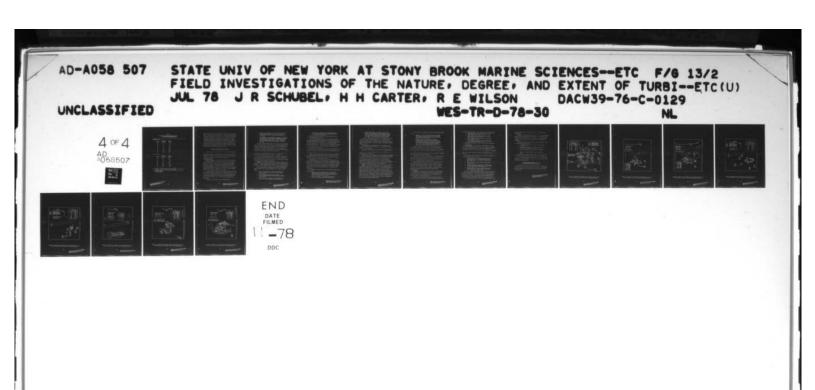


Table D3 Analytical Coefficients of Variation for Dissolved and Suspended Metals

Instrument C of V*	Total C of V**	
1.3	4.0	
1.7	4.1	
2.1	35.7	
5.3	29.0	
6.7	25.6	
37.0	83.2	
30.0	27.1	
N.D.	24.0	
Instrument C of V*	Total C of V**	
10.2	12.1	
11.4	11.4	
5.2	N.D. <sup>†</sup>	
23.7	56.6	
11.3	66.0	Tie.
23.3	N.D. <sup>†</sup>	
	C of V*  1.3  1.7  2.1  5.3  6.7  37.0  30.0  N.D.  Instrument C of V*  10.2  11.4  5.2  23.7  11.3	C of V*       C of V**         1.3       4.0         1.7       4.1         2.1       35.7         5.3       29.0         6.7       25.6         37.0       83.2         30.0       27.1         N.D. †       24.0         Instrument C of V*       C of V**         10.2       12.1         11.4       11.4         5.2       N.D. †         23.7       56.6         11.3       66.0

21.2

\* Based on 4 replicate analyses of two samples.
\*\* Based on 2 sets of 4 replicate samples taken at one station, different depths.

N.D.

† Not determined.

Pb

HNO<sub>3</sub> for four hours, (4) rinsed three times with Super-Q, and (5) oven dried. A measured volume of each sample was added to a 50 ml beaker and evaporated to dryness in an oven at 85°C. To the evaporated samples 25 drops of 60% perchloric acid were added and the samples were again evaporated to dryness. The residue was dissolved in 5 ml of Ultrex concentrated HNO<sub>3</sub>, transferred to an acid washed volumetric flask, and made up to 10 ml with rinses of deionized water. This solution was analyzed for Cd and Pb by injection into the graphite furnace of the atomic absorption spectrometer as described above. Standard additions and blanks were taken through the same procedure.

## Analysis of Dissolved Nutrient Samples

Nutrient samples from Atchafalaya Bay and Corpus Christi Bay were analyzed using a Tachnic m Autoanalyzer II. Analyses of Apalachicola Bay samples were performed using standard manual methods as described in Strickland and Parsons (1972)<sup>62</sup>. Absorbance for the manual methods was measured on a Beckman Acta II UV-VIS spectrophotometer.

Automated Procedures

Nitrate + Nitrite. The automated procedure used  $^{6.3}$  determines the sum of nitrate and nitrite in water samples as  $\mu g$ -at  $N/\ell$  through the reduction of nitrate to nitrite by a cadmium-copper reductor column. The nitrite ion reacts with sulfanilamide under acidic conditions to form a diazo compound. This diazo compound then couples with N-1-naphthylethylenediamine to form the colorimetrically (550 nm) determined reddish-purple azo dye. Samples were run at a rate of twenty samples per hour. All chemicals used were reagent grade.

The cadmium-copper column was prepared using cadmium powder which was rinsed with 1N HCl and deionized water and allowed to air dry. 10 g of this powder was washed well with 10 m $^2$  of 2% (w/v) CuSO $_4$  and rinsed with distilled deionized water. The column was then packed with the metal in distilled deionized water making sure no air bubbles were incorporated.

The reagents were introduced in the following order:

- 1. Ammonium chloride (NH<sub>4</sub>Cl)- 10 g NH<sub>4</sub>Cl and 0.5 ml Brij-35 (wetting agent) diluted to one liter with distilled deionized water the pH of which had been adjusted to 8.5 with NH<sub>4</sub>OH.
- 2. Color reagent -20 g sulfanilamide (C,H<sub>8</sub>N<sub>2</sub>O<sub>2</sub>S), 200 ml H<sub>3</sub>PO (concentrated), 1.0 g N-1-naphthylethylenediamine dihydro-chloride (C<sub>12</sub>H<sub>14</sub>N<sub>2</sub> 2HC1), and 1.0 ml Brij-35 diluted to two liters with distilled-deionized water. Wash water was distilled deionized water containing 2.0 ml Brij-35 per liter.

The stock standard (1000 µg-at N/L) was prepared from 0.101 g  $\rm KNO_3$  and 1.0 ml  $\rm CHCl_3$  diluted to one liter with distilled deionized water. A secondary standard (50 µg-at N/L) was prepared by 20:1 dilution of the stock  $\rm KNO_3$  with distilled deionized water. Four or five working standards were prepared by further dilutions of this secondary standard. Standards were run before, during, and after samples.

The range of the method is 0 to 5  $\mu g-at$  N/2. Out of range samples were diluted with distilled deionized water. The coefficient of variation of the method is given as 0.59% at 2.5  $\mu g-at$  N/2.

Sample tubes and glassware were soaked in 20% (v/v) concentrated HCl in distilled deionized water for at least six hours, rinsed twice with distilled deionized water and allowed to air dry before use. Sample tubes were rinsed with sample before filling.

<u>Phosphate</u>. The automated orthophosphate method<sup>64</sup> is based on the formation of a phosphomolybdenum blue complex determined colorimetrically at 800 nm. A single combined working reagent is used. Samples were run at a rate of thirty samples per hour. All chemicals were reagent grade.

The procedure utilizes a relatively unstable (8 hours) working reagent composed of four solutions combined in the amounts and order given:

- 50 ml 4.9N sulfuric acid 136 ml concentrated H<sub>2</sub>SO<sub>4</sub> (sp. gr. 1.84) diluted to one liter with distilled deionized water.
- 2. 15 ml ammonium molubdate ((NH<sub>4</sub>)<sub>6</sub>Mo<sub>7</sub>O<sub>24</sub>4H<sub>2</sub>O) 4.0 g ammonium molybdate diluted to one liter with distilled deionized water.
- 3. 30 ml ascorbic acid (C<sub>6</sub>H<sub>8</sub>O<sub>6</sub>) 18.0 g ascorbic acid diluted to one liter with distilled deionized water.

4. 5 ml antimony potassium tartrate (K(SbO)C<sub>4</sub>H<sub>4</sub>O<sub>6</sub>·½H<sub>2</sub>O)-3.0 g antimony potassium tartrate diluted to one liter with distilled deionized water.

Wash water was distilled deionized water containing 2.0 m $\ell$  of Levor IV (wetting agent) per liter.

The stock standard (1000  $\mu g$ -at P/ $\ell$ ) was prepared with 0.136 g anyhydrous potassium dihydrogen phosphate and 1.0 m $\ell$  CHCl $_3$  made up to one liter with distilled deionized water. A secondary standard (40  $\mu g$ -at P/ $\ell$ ) was prepared by 25:1 dilution of the stock standard with distilled deionized water. Four or five working standards were prepared by further dilutions of the secondary standard. Standards were run before, during and after samples.

The range of the method is 0 to 4  $\mu g$ -at P/ $\ell$ . Samples found to be outside this range were diluted with distilled deionized water. The coefficient of variation of the method is given as 1.98% at 2  $\mu g$ -at P/ $\ell$ . The detection limit is 0.8  $\mu g$ -at P/ $\ell$ .

Sample tubes and glassware were soaked in 20% (v/v) concentrated HCl in distilled deionized water for six hours, rinsed twice with distilled deionized water and allowed to air dry before use. Sample tubes were rinsed with sample prior to filling.

Reactive Silica. The automated silicate method<sup>65</sup> utilizes the reduction of a silicomolybdate in acid solution to molybdenum blue by ascorbic acid. Concentrations are determined colorimetrically at 660 nm. The introduction of oxalic acid into the sample stream before addition of the ascorbic acid eliminates interference from phosphate. Samples were run at a rate of thirty samples per hour. All chemicals were reagent grade.

The procedure involves the use of three reagents introduced in the following order:

- Ammonium molybdate (NH<sub>4</sub>) Mo<sub>7</sub>O<sub>2</sub> H<sub>2</sub>O)- 10 g ammonium molybdate made up to one liter with 0.1 N H<sub>2</sub>SO<sub>4</sub> (2.8 ml concentrated H<sub>2</sub>SO<sub>4</sub> (sp. gr. 184) diluted to one liter with fresh distilled deionized water.
- 0xalic acid (H<sub>2</sub>C<sub>2</sub>O<sub>4</sub>) 50 g oxalic acid diluted to one liter with fresh distilled deionized water.

THIS PAGE IS BEST QUALITY PRACTICABLE FROM COPY FURNISHED TO DDC 3. Ascorbic acid (C<sub>6</sub>H<sub>8</sub>O<sub>5</sub>) - 17.6 ascorbic acid, 50 ml acetone, and 0.5 ml Levor IV (wetting agent) diluted to one liter with fresh distilled deionized water. Wash water was synthetic seawater prepared with 31.0 g NaCl, 10.0 g MgSO<sub>4</sub> - 7H<sub>2</sub>O, 0.041 g NaHCO<sub>3</sub>, and 2.0 ml Levor IV in one liter of fresh distilled deionized water.

The stock standard (10,000  $\mu g$ -at Si/ $\ell$ ) was prepared from 1.88 g sodium flourosilicate (Na $_2$ SiF $_6$ ) made up to one liter with fresh distilled deionized water. A secondary standard (1000  $\mu g$ -at Si/ $\ell$ ) was prepared by 10:1 dilution of the stock standard with synthetic seawater prepared as above.

Working standards were prepared by further dilutions of the secondary standard with synthetic seawater. Standards were run before, during, and after samples.

The range of the method is 0 to 50  $\mu$ g-at Si/ $\ell$ . Samples found to be outside this range were diluted with synthetic seawater. The coefficient of variation at 25  $\mu$ g-at Si/ $\ell$  is given as 0.95%. The detection limit is 1  $\mu$ g-at Si/ $\ell$ .

Sample tubes, plastic containers, and glassware-were (1) seaked-in 20% (v/v) concentrated HCl in fresh distilled deionized water prepared in a polypropylene (Nalgene) carboy, (2) rinsed twice with fresh distilled deionized water, and (3) allowed to air dry before use. Sample tubes were rinsed with sample prior to filling. All reagents were stored in polypropylene (Nalgene) bottles and contact with glass was minimized throughout analysis to avoid contamination.

Ammonia. The automated ammonia method used is a modification of the Berthelot reaction based on the formation of a compound closely related to indophenol from the reaction of an ammonium salt with sodium phenoxide and sodium hypochlorite. Precipitation of calcium and magnesium hydroxides is prevented by addition of sodium citrate to the sample stream. The sample is run through a ten minute coil submerged in an 80°C oil bath for development of the blue color characteristic of the indophenol compound. Concentrations are determined colorimetrically at 640 nm. Samples were run at twenty samples per hour. All chemicals were reagent grade unless otherwise noted.

The two reagents were added to the sample stream in the following order:

- 1. Reagent A- 35.0 g of analytical grade phenol (C<sub>6</sub>H<sub>5</sub>OH) and 0.400 g of sodium nitroprusside dihydrate (Na<sub>2</sub>Fe (CN)<sub>5</sub>NO·2H<sub>2</sub>O) were dissolved and diluted to one liter with distilled deionized water.
- 2. Reagent B- 280 g of sodium citrate (HOC(COONa) (CH<sub>2</sub>COONa)<sub>2</sub>:H<sub>2</sub>O) and 1.50 g NaOH were dissolved in distilled deionized water 35 ml of commercial bleach (5.25% sodium hypochlorite) was added and the solution was diluted to one liter with distilled deionized water. Wash water was distilled deionized water with 2.0 ml Brij-33 (wetting agent) added per liter.

The stock standard (2000 ug-at N/ $\ell$ ) was prepared with 0.107 g NH $_4$ Cl dissolved and diluted to one liter with distilled deionized water. A few drops of CHCl $_3$  were added as a preservative. A secondary standard (50 µg-at N/ $\ell$ ) was prepared by 40:1 dilution of the stock standard with distilled deconized water. Four or five working standards were prepared by further dilutions of the secondary standard. Standards were run before, during, and after samples.

The range of the method is 0 to 20 µg-at  $N/\lambda$ . Samples found to be outside this range were diluted with distilled deionized water. The coefficient of variation, determined over several days is 6.0% at 1.0 µg-at  $N/\lambda$ . The detection limit is 0.1 µg-at  $N/\lambda$ .

Sample tubes and glassware were soaked in 20% (v/v) concentrated HCl in distilled deionized water for six hours, rinsed twice with distilled deionized water and allowed to air dry before use. Sample tubes were rinsed with sample prior to filling. Care was taken to eliminate contact of reagents, water, standards, and samples with the atmosphere to minimize alteration of ammonia concentrations.

Manual Procedures

Phosphate. The procedure given in Strickland and Parsons (1972, p. 49)<sup>59</sup> is similar to the automated procedure discussed above with minor modifications. The extinction of the phosphomolybdenum blue complex is measured at 885 nm (10 cm cell).

Five ml of the combined working reagent, composed of the four solutions given below, is added to 50 ml distilled deionized water and

5 ml of the combined reagent. All chemicals used were reagent grade.

- 200 ml ammonium molybdate- 15 g (NH<sub>4</sub>)<sub>6</sub>Mo<sub>7</sub>O<sub>24</sub>·4H<sub>2</sub>O in 500 ml distilled deionized water.
- 2. 500 ml sulfuric acid- 140 ml concentrated  ${\rm H_2SO_4}$  in 900 ml distilled deionized water.
- 200 ml ascorbic acid- 27 g ascorbic acid in 500 ml distilled deionized water.
- 4. 100 ml antimonyl tartrate- 0.34 g K(Sb0)C4H4O6·3H2O in 250 ml distilled deionized water.

Standards were prepared as before. The range of the methods is 0.03 to 5  $\mu g$ -at P/ $\ell$ .

Reactive Silica. Reactive silica was determined by the method given in Strickland and Parsons (1972, p. 65)<sup>59</sup>. Again, the chemistry is similar to the automated method. Absorbance measurements were accomplished using a 1 cm cell at 810 nm. All glassware was washed with chromic acid and rinsed tell with distilled delanized water. Precautions were taken to limit contact of solutions and standards with glass surfaces.

The reagents and their composition are listed below followed by a brief description of the procedure:

- 1. Ammonium molybdate- 80 g (NH<sub>4</sub>) $_6$ Mo $_7$ 0 $_2$ 4 $^{\bullet}$ 4H $_2$ 0 and 24 ml concentrated HCl in 1  $^{\circ}$ 2 distilled deionized water. The solution is filtered through #1 Whatman filter paper before use.
- Cxalic acid- 50 g (COOH)<sub>2</sub>·2·H<sub>2</sub>O in 50 ml distilled deionized water.
- 3. Sulfuric acid (50%)- 250 ml concentrated H<sub>2</sub>SO<sub>4</sub> added to 250 ml distilled deionized water. Cool<sup>2</sup> and dilute to 500 ml with distilled deionized water.
- Reducing reagent- 333.3 ml of metol/sulfite reagent, 200 ml oxalic acid, 200 ml 50% H<sub>2</sub>SO<sub>4</sub> diluted to 1 l with distilled deionized water.

Ten ml of the ammonium molybdate reagent was pipetted into a 125 ml flask to which 25 ml of the sample was added, mixed and allowed to stand for 10-30 minutes. Fifteen ml of the combined reducing reagent was added and the solution was allowed to stand for three hours to allow the color to develop before analysis on the spectrophotometer.

The standards were prepared as for the automated procedure. The

range of this method is 0.1 to 140  $\mu g-at$  Si/ $\lambda$ . All chemicals were reagent grade.

Ammonia. The manual ammonia determination <sup>59</sup>, as with the automated method, involves the formation of blue indophenol. The absorbance was measured at 640 nm using a 5 cm cell. Samples and reagents were kept covered to avoid incorporation of any ammonia from the laboratory atmosphere.

Reagents were added, with mixing following each addition, to 25 m $\ell$  of the nutrient sample as follows:

- 1 ml Phenol solution- 20 g crystalling phenol in 200 ml 95% ethanol.
- 1 ml Sodium nitroprusside solution- l g Na<sub>2</sub>Fe(CN)<sub>5</sub> NO•2H<sub>2</sub>O in 200 ml distilled deionized water.
- 3. 2.4 ml Oxidizing solution- this solution consisted of 100 ml of fresh chlorox (1.5% sodium hypothlorite) and 400 ml of sodium citrate solution (1.0 g Naccitrate and 5 g NaOH in 500 ml distilled deionized water).

The mixture was allowed to stand for one hour, upon which color development is complete, before solution absorbance was measured.

The standard solutions were prepared as for the automated method. The range of the method using 5 cm cells is 0.2 to 20  $\mu$ g-at N/ $\ell$ . All chemicals were reagent grade.

## Contours-Model for Prediction of Particle-Associated Chemical Constituents

The model for prediction of particle-associated constituents is described in section IV of the main body of the report. Several model contours not incorporated in that section are included here (Figures D4 through D11).

THIS PAGE IS BEST QUALITY PRACTICABLE FROM COPY FURNISHED TO DDC

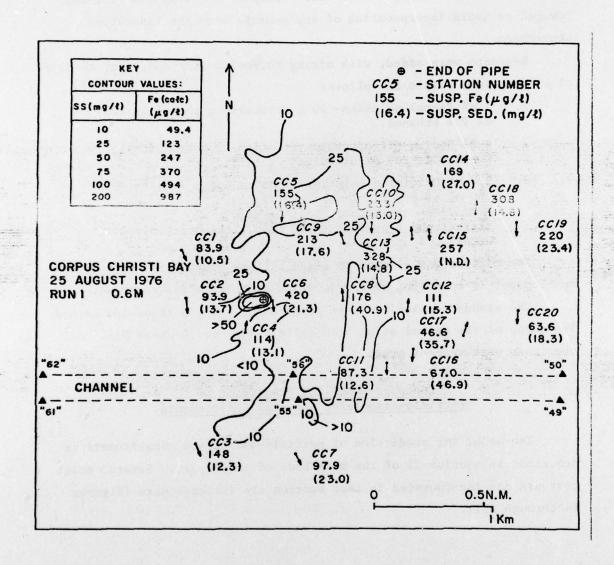


Figure D4. Comparison of turbidity plumes measured optically with concentrations of particle-associated Fe, Corpus Christi Bay.

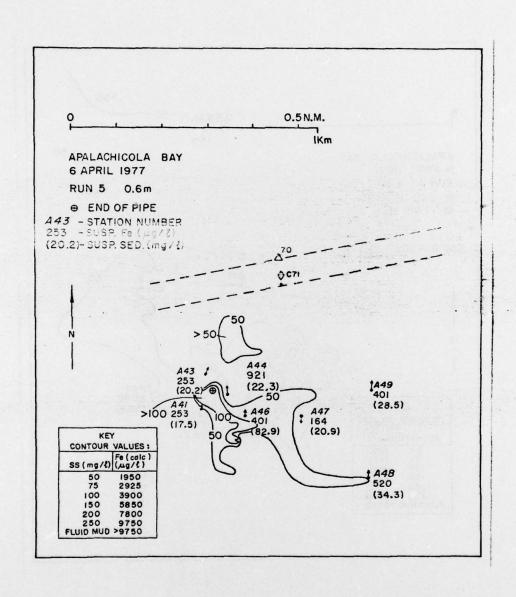


Figure D5. Comparison of turbidity plumes measured optically with concentrations of particle-associated Fe, Apalachicola Bay.

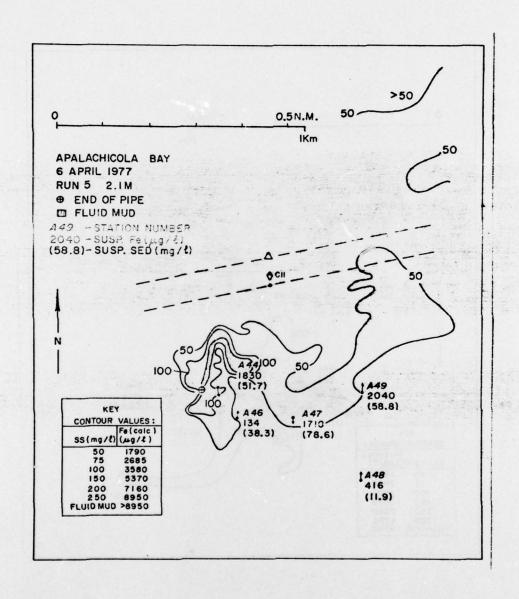


Figure D6. Comparison of turbidity plumes measured optically with concentrations of particle-associated Fe, Apalachicola Bay.

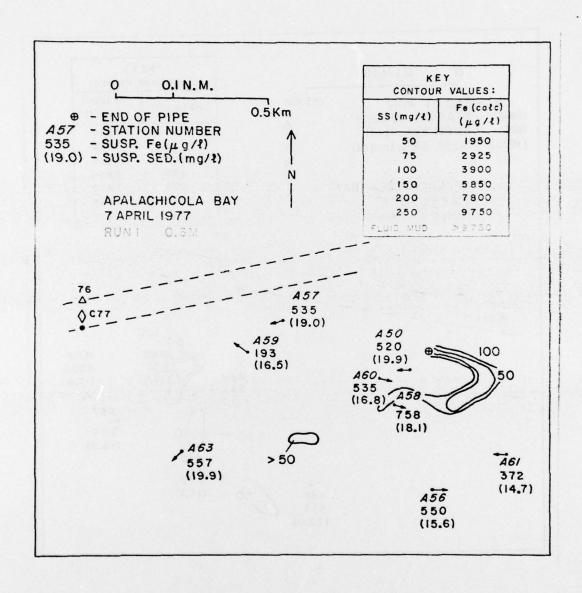


Figure D7. Comparison of turbidity plumes measured optically with concentrations of particle-associated Fe, Apalachicola Bay.

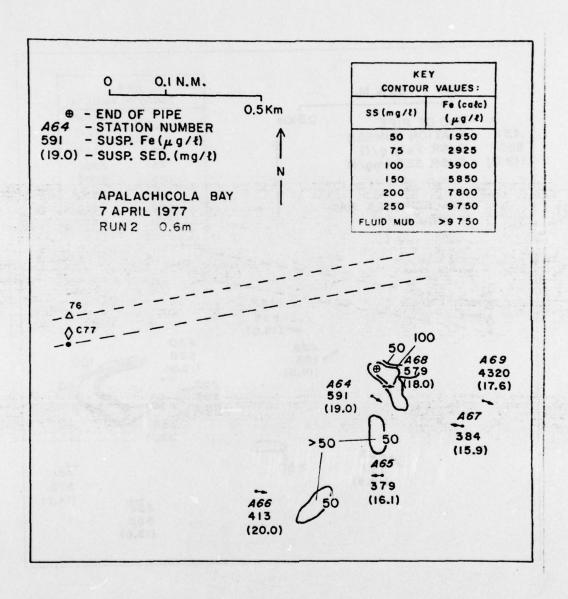


Figure D8. Comparison of turbidity plumes measured optically with concentrations of particle-associated Fe, Apalachicola Bay.

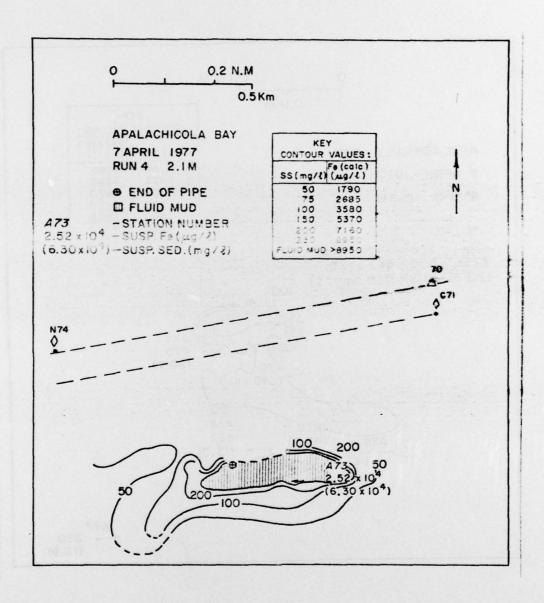


Figure D9. Comparison of turbidity plumes measured optically with concentrations of particle-associated Fe, Apalachicola Bay.

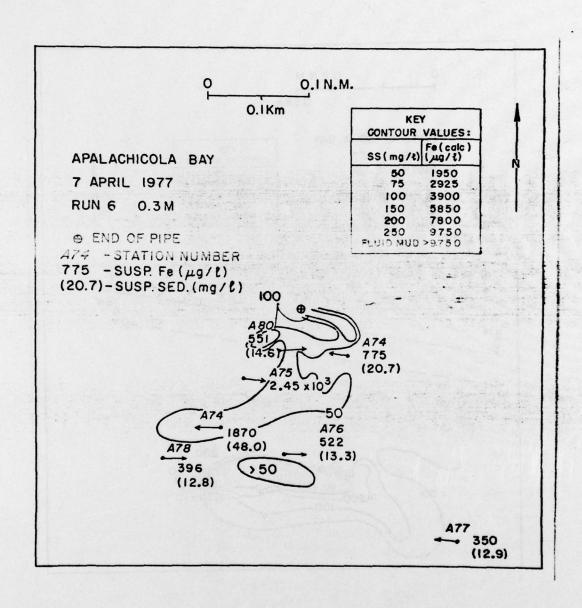


Figure D10. Comparison of turbidity plumes measured optically with concentrations of particle-associated Fe, Apalachicola Bay.

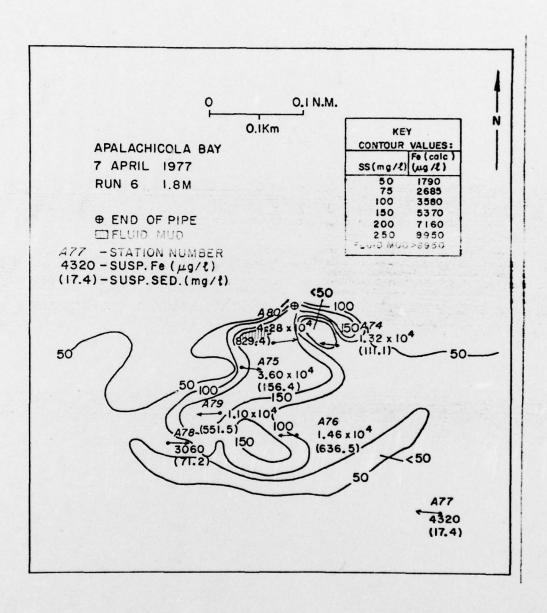


Figure Dll. Comparison of turbidity plumes measured optically with concentrations of particle-associated Fe, Apalachicola Bay.